VIETNAM ATOMIC ENERGY COMMISSION

The ANNUAL REPORT for 2007

SCIENCE AND TECHNICS PUBLISHING HOUSE

VIETNAM ATOMIC ENERGY COMMISSION

The ANNUAL REPORT for 2007

Editorial board:

Porf. Vuong Huu Tan, Chief Editor
Dr. Le Van Hong
Mr. Nguyen Hoang Anh
Ms. Dang Thi Hong
Mr. Nguyen Trong Trang

Hanoi, 11 - 2008

The VAEC Annual Report for 2007 has been prepared as an account of works carried out at VAEC for the period 2007. Many results presented in the report have been obtained in collaboration with scientists from national and overseas universities and research institutions.

The ANNUAL REPORT for 2007
Edited by
Vietnam Atomic Energy Commission
59 Ly Thuong Kiet, Hanoi
Vietnam
Chairman: Prof. Dr Vuong Huu Tan
Tel: +84-4-39422756
Fax: +84-4-39424133

This report is available from:

Training and Information Division
Dept. of Planning and R&D Management
Vietnam Atomic Energy Commission
59 Ly Thuong Kiet, Hanoi,Vietnam
Tel: +84-4-39423591
Fax: +84-4-39424133
E-mail: hq.vaec@hn.vnn.vn
infor.vaec@hn.vnn.vn

Contents

Preface **11**

1. CONTRIBUTIONS **13**

1.1 - NUCLEAR PHYSICS **15**

Study on Neutron Capture Cross Sections Using The Filtered Neutron Beams of 55keV and 144keV at The Dalat Reactor and Related Applications. **17**

Vuong Huu Tan, Nguyen Canh Hai, Pham Ngoc Son and Tran Tuan Anh

On The Phase Transition in Stable Quark Matter. **27**

Tran Huu Phat, Nguyen Tuan Anh, Nguyen Van Long and Le Viet Hoa.

Development of a Method for Measurement of Total Neutron Cross Sections Based on The Neutron Transmission Method Using a He-3 Counter on Filtered Neutron Beams at Dalat Research Reactor. **33**

Tran Tuan Anh, Dang Lanh, Nguyen Canh Hai, Nguyen Xuan Hai, Pham Kien, Nguyen Thuy Nham, Pham Ngoc Son and Ho Huu Thang.

Microscopic Study of Elastic and Inelastic Alpha-Nucleus Scattering at Medium Energies. **38**

Dao Tien Khoa, Hoang Si Than, Do Cong Cuong, Ngo Van Luyen, Nguyen Ngoc Quynh and Nguyen Tuan Anh.

1.2 - REACTOR PHYSICS, REACTORS AND NUCLEAR POWER **43**

Conceptual Nuclear Design of Two Models of Research Reactor Proposed for Vietnam. **45**

Nguyen Nhi Dien, Huynh Ton Nghiem, Le Vinh Vinh and Vo Doan Hai Dang.

Evaluations of Physical Parameters of Heu and Leu Fuel Assemblies Used in Dalat Nuclear Research Reactor Using MVP Code. **55**

Le Dai Dien and Hoang Minh Giang.

Investigation of The Thermal Hydraulics Safety Characteristic Parameters on The Dalat Research Reactor as Inserting Additional Fresh Fuel Assemblies with High Enriched Uranium or Fuel Assemblies with Low Enriched Uranium. **59**

Luu Anh Tuan, Tran Van Hien and Hoang Duc Huynh..

1.3 - INSTRUMENTATION **67**

Experimental Evaluation of Systematic Errors of Gamma Spectrometer for Assay of Radioactive Waste Drums. **69**

Tran Quoc Dung, Nguyen Duc Thanh, Luu Anh Tuyen, Lo Thai Son and Phan Dinh Phuc.

Develop The Spectrometer Systems to Measure Gamma Cascade, Nuclear Data and Other Applications on The Neutron Beam. **75**

Vuong Huu Tan, Pham Dinh Khang, Nguyen Xuan Hai, Pham Ngoc Son, Tran Tuan Anh, Ho Huu Thang, Nguyen Canh Hai, Pham Ngoc Tuan and Nguyen Thi Thuy Nham.

Study of Beam Dynamics in Cyclotron. **81**

Nguyen Tien Dung, Trinh Dinh Truong, Nguyen Manh Hung, Pham Dinh Khang and Others.

Standardization of Irradiation Values at The Radiation Calibration Laboratory. **85**

Pham Van Dung, Hoang Van Nguyen, Phan Van Toan, Phan Dinh Sinh, Tran Thi Tuyet and Do Thi Phuong.

Design and Construction of The 8K Multi-Channel Gamma Spectrometer Module (AMPLIFIER+ADC+MCD). **88**

Truong Van Dat, Hoang Thi Ngoc Bich, Pham Ngoc Tuan, Dang Lanh, Tuong Thi Thu Huong and Vu Xuan Cach.

Design and Construct an Interface Card for Spectroscopy of Amplitude of Coincident Pulses. **93**

Nguyen Xuan Hai, Pham Ngoc Tuan, Pham Dinh Khang, Vu Xuan Cach, Ho Huu Thang, Tran Tuan Anh, Hoang Thi Ngoc Bich, Nguyen Canh Hai, Nguyen Thi Thuy Nham, Tuong Thi Thu Huong, Pham Ngoc Son and Pham Duy Tung.

Design and Construction of The Ethanol-Chlorobenzene Dosimetry System Using Oscillometric Method. **97**

Nguyen Duc Hoa, Tran Khac An, Huynh Dong Phuong, Bui Phi Khanh, Chau Le Ha, et al.

Improvement of Quality of Radiation Indicator Used for Food Irradiation in Dose Range of 3-10 kGy **103**

Hoang Hoa Mai, Pham Duy Duong and Nguyen Dinh Duong.

Thyroid Uptake Measurement System. **107**

Nguyen Duc Tuan, Nguyen Thi Bao My and Nguyen Van Sy.

1.4 - INDUSTRIAL APPLICATIONS **113**

Establishment of Tracer Technologies in Gas Phase. **115**

Nguyen Huu Quang, Bui Quang Tri, Huynh Thai Kim Ngan, Dang Nguyen The Duy, Tran Tri Hai, Pham Hoang Ha, To Ba Cuong, Bui Trong Duy and Phan Thanh Khoa.

Building of Training Program of Non-Destructive Testing for Concrete Structures (Part 1: Radiographic Testing; Ultrasonic Pulse Velocity Measurement;nuclear Moisture-density Gauge). **125**

Nguyen Le Son, Phan Chanh Vu, Pham The Hung and Vu Huy Thuc.

1.5 - ECOLOGY, ENVIRONMENT AND GEOLOGY **129**

Study of Isotopic Technical Application to Estimate Origin of Nitrogen Composision of Groundwater in Hanoi Area. **131**

Trinh Van Giap, Dinh Bich Lieu, Dang Anh Minh, Vo Thi Anh, Bui Dac Dung, Nguyen Thi Hong Thinh, Nguyen Manh Hung, Nguyen Van Hoan and Nguyen Van Hai.

Biodegradation of Organ Chlorine Pesticides in Contaminated Soil Collected from Yen Tap, Cam Khe, Phu Tho. **135**

Nguyen Thuy Binh, Nguyen Van Toan, Pham Thi Thai and Dinh Thi Thu Hang.

Studying on The Contaminative Determination of Existing Forms of As^{3+}, As^{5+}, Sb^{3+} and Sb^{5+} in Ground Water at Lamdong Province. **140**

Nguyen Giang, Nguyen Thanh Tam, Truong Phuong Mai, Ho Tran The Huu and Nguyen Van Minh.

Combined Use of Cs-137 and Be-7 to Assess The Effectiveness of Soil Conservation for Vetiver Grass Strips in Coffee Crop Lands in The Central Highlands. **146**

Phan Son Hai, Nguyen Dao, Tran Van Hoa, Tran Dinh Khoa, Nguyen Thi Mui and Trinh Cong Tu.

Determination of 22 Elements in Marine Environmental Samples in Special Areas at The South of Vietnam. **152**

Nguyen Ngoc Tuan, Nguyen Giang, Nguyen Thanh Tam and Truong Phuong Mai.

1.6 - BIOLOGY, AGRICULTURE AND MEDICINE **161**

Study on The Procedures for Determining of Pesticide Residues in Green Vegetables. **163**

Le Tat Mua, Nguyen Tien Ẹat, Nguyen Van Minh, Nguyen Ngoc Tuan, Le Thi Ngoc Trinh, Ta Thi Tuyet Nhung, Truong Van Tai, Tran Thanh Nha and Nguyen Thi Hong Tham.

Study on The Application of Nutrient Immobilized Hydrogel as a Substrate for Hydroponics Culture. **176**

Vo Thi Thu Ha, Le Quang Luan, Nguyen Thi Nu, Nguyen Thi Vang, Phan Dinh Thai Son and Nguyen Quang Khanh.

Study on Procedure for Determination of Cr, As, Se, Cd, Hg, Pb in Some Kinds of Herb Products Such as: Kind of Fungus, Philamin... by ICP-MS". **183**

Pham Ngoc Khai, Do Van Thuan, Nguyen Thi Kim Dung and Nguyen Hong Minh.

Study on Application of Molecular Techniques (RAPD–PCR and RAMP-PCR) to Detect Mutation in Rice Breeding. **189**

Hoang Thi My Linh, Phan D. T. Son, N. T.vang, Nguyen T. T. Hien and Le Xuan Tham.

1.7 - RADIATION PROTECTION AND RADIOACTIVE WASTE MANAGEMENT **197**

Study on Technology for Radioactive Waste Treatment and Management from Uranium Production. **199**

Vu Hung Trieu, Vu Thanh Quang, Nguyen Duc Thanh, Trinh Giang Huong, Tran Van Hoa, Hoang Minh Chau, Ngo Van Tuyen, Nguyen Hoang Lan and Vuong Huu Anh.

Study of Exposure Dose in Some Serious Hypothesis Accidents of SVST-CO60/B Irradiator for Planning Accident Responses. **207**

*Tran Van Hung, Tran Khac An, Cao Van Chun and Nguyen Anh Tuan***.**

1.8 - RADIATION TECHNOLOGY **213**

Study on The Synthesis of Colloidal Silver Nanoparticles by γ-Irradiation for Using as An Antimicrobial Substance. **215**

Dang Van Phu, Bui Duy Du, Nguyen Trieu, Vo Thi Kim Lang, Doan Thi The and Nguyen Quoc Hien.

Study of Gamma Radiation Effect on Natural Polymer of Extracted Peat HUMIC/HUMATE to Apply in Agriculture. **221**

Le Huu Tu, Le Hai, Nguyen Tan Man, Tran Thi Tam, Tran Thu Hong, Pham Thi Sam, Nguyen Tuong Ly Lan and Le Van Toan.

1.9 - RADIOCHEMISTRY AND MATERIALS SCIENCE **225**

Study on Preparing Porous Hydroxyapatite Ceramic for Born Replacement in Animal. **227**

Do Ngoc Lien, Nguyen Duc Kim, Dang Ngoc Thang, Cao Phuong Anh, Tran Thi Thanh Hien, Trinh Binh, Ngo Duy Thin and Luu Dinh Mui.

Processing Pa Lua Uranium Ore by Mixing and Curing with Sulfuric Acid on a Scale of 500 Kg/Batch to Recover Yellowcake. **231**

Le Quang Thai, Cao Hung Thai, Le Thi Kim Dung, Phung Vu Phong, Tran Van Son,

Doan Thi Mo, Hoang Bich Ngoc, Nguyen Hong Ha, Vu Khac Tuan, Vu Hung Trieu, Tran Van Hoa, Nguyen Duy Phap, Doan Thanh Son and Pham Quang Minh.

Study on Precipitation of Amoni Diuranate - $(NH_4)_3U_2O_7$ from UO_2F_2- HF Solution for Fuel Ceramic UO_2 Powder Preparation. **240**

Dang Ngoc Thang, Pham Danh Khanh, Ha Dinh Khai, Nguyen Van Doan, Tran Thi Hong Thai and Pham Hung Vuong.

Study on The Synthesis of Disida Derivatives for Labeling with ^{99m}Tc. **243**

Pham Ngoc Dien, Duong Van Dong, Nguyen Thi Thu, Bui Van Cuong, Mai Phuoc Tho and Vo Cam Hoa.

Designing, Making Apparatus and Study on Technology of Forming Ceramics by Extrusion Method. **250**

Dao Truong Giang, Nguyen Duc Kim, Ngo Quang Hien, Cao Phuong Anh and Ha Dinh Khai.

Study on Technology for Manufacturing Alloy (Lead – Tin – Bismuth – Cadmium) Having Low Melting Temperature (≤ 80^0C) Used to Shield Radioactive Rays for Treating Cancer. **253**

Ngo Xuan Hung, Pham Duc Thai, Nguyen The Khanh, Vu Quang Chat, Nguyen Huu Quyet

Research on The Recovery of Neodymium and Iron from NdFeB Permanent Magnet Scraps. **260**

Hoang Nhuan, Tran Ngoc Ha, Nguyen Thuc Phuong, Hoang Van Duc and Nguyen Thi Thanh Thuy.

Study on Preparation of Zinc Oxide Catalyst for Removing Hydrogen Sulfide from Gas Material of Urea Plant. **265**

Vu Thanh Quang, Ngo Van Tuyen, Trinh Giang Huong and Vuong Huu Anh.

Study on The Preparation of Titanium Dioxide Powder for Producing Pigment from 85% Synthetic Rutile (TiO_2). **270**

Tran Van Son, Cao Hung Thai, Than Van Lien, Nguyen Dinh Van, Doan Thi Mo and Hoang Bich Ngoc.

Investigating The Application of The ISP Technology for Producing Zinc Metal from Galvanizing Zinc Dust. **276**

Pham Quang Trung, Pham Minh Tuan, Le Minh Tuan, Tuong Duy Nhan, Ngo Trong Hiep and Tran The Dinh.

Synthesis and Study on Complexes of Some Lanthanides to L-Isoleucine. **280**

Le Minh Tuan, Pham Minh Tuan and Tran The Dinh.

Preparation of High Quality Zirconium Oxychloride from Zircon of Vietnam. **286**

Ngo Van Tuyen, Vu Thanh Quang, Trinh Giang Huong and Vuong Huu Anh.

1.10 - COMPUTATION AND OTHER RELATED TOPICS **293**

Development of a Graphical Interface Computer Code for Reactor Fuel Reloading Optimization. **295**

Do Quang Binh, Nguyen Phuoc Lan and Bui Xuan Huy.

2. IAEA TC PROJECTS AND RESEARCH CONTRACTS **303**

2.1- List of VIE Projects Implementing in 2007 **305**

2.2- List of RAS Projects Implementing in 2007 **307**

2.3- International Research Contracts in 2007 **310**

3. SCIENTIFIC PAPERS PUBLISHED ABROAD AND IN VIETNAM **313**

3.1- Scientific Papers Published Abroad. **315**

3.2- Scientific Papers Published in Vietnam. **316**

3.3- Scientific Papers Presented in International Conferences. **318**

3.4- Scientific Papers Presented in National Conferences. **320**

Preface

The research activities of the Vietnam Atomic Energy Commission (VAEC) during the period from 1 January to 31 December 2007 are presented in this Report. The research activities are focused on the following fields:

1. Nuclear Physics;
2. Reactor Physics, Reactors and Nuclear Power;
3. Instrumentation;
4. Industrial Applications;
5. Applications in Ecology, Environment and Geology;
6. Applications in Biology, Agriculture and Medicine;
7. Radiation Protection and Radioactive Waste Management;
8. Radiation Technology;
9. Radiochemistry and Materials Science;
10. Computation and Other Related Topics.

The total number of permanent staff working at the VAEC as December 31, 2007 was 721 including the clerical service staff. The VAEC was funded from the Government with the amount to 71.196 billion VN Dong for FY 2007. The fund for the research contracts is 12.770 billion VN Dong in FY 2007. The international support for the VAEC activities is committed to over 1 million USD including equipment, staff training and expert services.

Main results of fundamental and applied research implemented in the year were presented in 166 scientific articles, reports and contributions published in many journals, proceedings of conferences, etc. These results were obtained on the basic of the technical cooperation projects (18 VIE projects, 37 RAS projects), the research contracts with the IAEA (13 RCs), the research contracts with the Government, the Ministry of Science, Technology, Vietnam Atomic Energy Commission and the National Program for Fundamental Research (totally 56).

During the time of year 2007, in the VAEC there were 2 graduated in Ph.D. courses; about 200 people have been trained abroad in the fields of nuclear science and technology.

Prof. Dr. Vuong Huu Tan

Chairman, VAEC

1. Contributions

1.1 - Nuclear Physics

STUDY ON NEUTRON CAPTURE CROSS SECTIONS USING THE FILTERED NEUTRON BEAMS OF 55KEV AND 144KEV AT THE DALAT REACTOR AND RELATED APPLICATIONS

Vuong Huu Tan, Nguyen Canh Hai, Pham Ngoc Son and Tran Tuan Anh

Vietnam Atomic Energy Commission (VAEC)

ABSTRACT: In this fundamental research project on nuclear physics in period of 2007, the neutron capture cross sections for the reactions of ^{146}Nd(n, γ)^{147}Nd, ^{148}Nd(n, γ)^{149}Nd, ^{150}Nd(n, γ)^{151}Nd, ^{154}Sm(n, γ)^{155}Sm, ^{181}Ta(n, γ)^{182}Ta and total neutron cross section of ^{181}Ta have been measured at the filtered neutron beams of 54keV and 148keV of the Dalat nuclear research reactor. The present results were compared with the previous measurements from EXFOR-2003, and the evaluated values of JENDL 3.3 and ENDF/B-6.8. Beside that development computer codes for exact analysis of the buildup and decay of fission products for time following a fission burst, for determination of correction parameters to improve the accuracy in measurements of the neutron capture cross-section on filtered neutron beams and for determination of characteristic parameters of monoenergetic neutron beams were also carried out.

I. Introduction

Accurate measurements of neutron capture cross sections for most of nuclides are currently necessary for the calculations of neutron transport, the assessments of the reactor safety, the investigations of high-burn-up core characteristics, the decay heat power predictions and for the nuclear transmutation study. In keV energy region, the (n,γ) cross sections are special important for the study on the s-process reaction chain for nucleosynthesis. However, the present status of experimental data for capture cross sections is still inadequate both in quality and in quantity. Therefore, it is important to perform the precisely measurements of capture cross sections for those nuclides, particular in keV energy region.

In the present experiment, we performed the measurements of capture cross section of ^{146}Nd(n, γ)^{147}Nd, ^{148}Nd(n, γ)^{149}Nd, ^{150}Nd(n, γ)^{151}Nd, ^{154}Sm(n, γ)^{155}Sm and ^{181}Ta(n, γ)^{182}Ta on the filtered neutron beams of 54keV and 148keV, relative to the standard capture cross section of ^{197}Au by the activation method. The neutron beams were derived from the horizontal channel No.4 of the research reactor at the Dalat Nuclear Research Institute (DNRI), by using the filtered compositions of 98cmSi + 35g/cm^{2}S + 0.2g/cm^{2}B^{10} and 98cmSi + 1cmTi + 0.2g/cm^{2}B^{10} for 54keV and 148keV respectively. The neutron energy resolution, FWHM, is 8keV at 54keV peak, and 22keV at 148keV peak.

Determination of total neutron cross sections and average resonance parameters in the energy range from tens keV to hundreds keV is important for fast reactors calculations and designs because this energy range gives the most output of all neutron induced reactions in the spectrum of fast reactors. Besides, the total neutron cross section measurement is also one of the methods for determination of s, p and d-wave

neutron strength functions. The average total neutron cross sections of ^{181}Ta were obtained from neutron transmission measurements using ^{3}He counter on filtered neutron beams of 54keV and 148keV at the horizontal channel No.4 of the Dalat research reactor. The neutron counting system is also served for determination of hydrogen index, for neutron flux monitoring and for neutron physics experiments at the Dalat reactor.

Precise information of the variation of fission product concentration for time after a fission burst is necessary for safety designs and operations of nuclear power reactors, fuel storage, transport flasks, and for spent fuel management and processing. In this study, a computer code has been developed for exact analysis of the buildup and decay of fission products for time following a fission burst. In which, a new numerical measure to solve the linear and nonlinear decay chains was introduced. The analytical data of fission product concentration, obtained by using the present code, was applied to calculate aggregate fission product decay heat form neutron fission of U-235, U-238, U-233, Pu-239, Pu-241 and Th-232.

Determination of correction parameters to improve the accuracy in measurements of the neutron capture cross-section on filtered neutron beams at Dalat nuclear research reactor. Computer codes to calculate these factors for effect of resonance capture at low energy background, multi scattering, and shelf shielding have been developed based on the methods of Monte Carlo, neutron transmission and unfolding. The calculated and experimental results of neutron background spectra for 54keV and 148keV filtered neutron beams and the correction factors for nuclei of Au-197, ^{146}Nd, ^{148}Nd, ^{150}Nd, ^{154}Sm, ^{181}Ta were reported.

The characteristic parameters of monoenergetic neutron beams are neutron spectra, relative intensity, energy resolution, dimension of filters, and suitable composition of materials. These parameters have been calculated to create the neutron beams with mono-energies of 1.9keV, 24.3 keV, 53.9keV, 58.8keV 133 keV and 148.3keV, at the horizontal channel No.4 of the Dalat research reactor. In which, the two available filtered neutron beams of 55keV and 144keV were recalculated with resulting that the beam energies should be 53.9 and 148.3keV, respectively. The results of calculated parameters in the present work are useful for the development of new filtered neutron beams in the near future at the Dalat research reactor.

II. Objective

The project have been implemented in order to push up the activities of fundamental research on nuclear physics, and to use effectively the research reactor and neutron facilities. In addition, these studies play an important role in process of education and development of human resource.

III. Contents

The main contents of the project are as following: (i) Implementation of measurement of average neutron capture cross section of ^{146}Nd, ^{148}Nd, ^{150}Nd, ^{154}Sm, ^{181}Ta at energies of 54keV and 148keV, (ii) Evaluation and discussion on present results in comparison with previous ones, (iii) Development computer codes for: exact analysis of the buildup and decay of fission products for time following a fission burst, determination of correction parameters to improve the accuracy in measurements of the neutron capture cross-section on filtered neutron beams and determination of

characteristic parameters of monoenergetic neutron beams are neutron spectra, relative intensity, energy resolution, dimension of filters, and suitable composition of materials.

IV. Method

In the current study, the radiactive neutron capture cross section for the reactions of $^{146}Nd(n,\gamma)^{147}Nd$, $^{148}Nd(n,\gamma)^{149}Nd$, $^{150}Nd(n,\gamma)^{151}Nd$, $^{154}Sm(n,\gamma)^{155}Sm$ and $^{181}Ta(n,\gamma)^{182}Ta$ at energies of 54 keV and 148 keV have been measured by the activation method on the filtered neutron beams. The capture cross sections were obtained relative to the standard capture cross sections of ^{197}Au. Specific activities of irradiated samples were measured by using a high quality gamma spectroscopy and HPGe detector with relative efficiency of 58%.

A computer code has been developed calculating the decay and buildup of FPs following time after a fission burst or a fission process. The method used in the program is numerical analysis, in which the buildup and decay of FP nuclides are analyzed by introduce a new algorithm for exactly analysis of the general solutions of the Bateman's Equations. Based upon the input data including nuclear decay data and fission yield from JENDL3.3, ENDF/B-6 or JEFF3.0, the concentration of each FP nuclide as a function of cooling time is determined. The algorithm made it possible to overcome the difficulties of the solution for a complex decay-net system. Moreover, all of decay modes, excepted for spontaneous fission, are taken into analyze automatically in the program.

Monte Carlo method was used to determine correction parameters to improve the accuracy in measurements of the neutron capture cross-section: factors for effect of resonance capture at low energy background, multi scattering, and shelf shielding.

V. Results and discussion

In the present work, the new values of average neutron capture cross sections of ^{146}Nd, ^{148}Nd, ^{150}Nd, ^{154}Sm, ^{181}Ta and of total neutron cross sections of ^{181}Ta at incident neutron energies of 54keV and 148keV are reported with errors about 5-6.5%. The results are given in Table 1. The uncertainties in the present measurements are mainly due to the statistical errors (0.1-2%), the uncertainties of γ-ray detection efficiency (3.5%), the reference cross section (~3%) and the correction factors for neutron resonance capture, self-shielding and multi-scattering effects (~3%) (Table 2). In comparisons with the previous measurements and the evaluated data, the present results are in good agreement with the previous measurements and with the evaluated data of JENDL3.3 and ENDF/B-6.8 within the experimental uncertainties. The comparisons results are shown in Figs.1-6.

Table 1: The neutron capture cross sections of ^{146}Nd, ^{148}Nd, ^{150}Nd, ^{154}Sm, ^{181}Ta

Average neutron energy [Energy range] (keV)	**$\langle\sigma_a\rangle^{Nd-146}$ (barn)**	**$\langle\sigma_a\rangle^{Nd-148}$ (barn)**	**$\langle\sigma_a\rangle^{Nd-150}$ (barn)**	**$\langle\sigma_a\rangle^{Sm-154}$ (barn)**	**$\langle\sigma_a\rangle^{Ta-181}$ (barn)**	**$\langle\sigma_{tot}\rangle^{Ta-181}$ (barn)**
54 [51-59]	0.0883 ± 0.0058	0.1189 ± 0.0094	0.0849 ± 0.0132	0.1521 ± 0.0106	0.3707 ± 0.0094	10.34 ± 0.25
148 [133-155]	0.0642 ± 0.0045	0.0936 ± 0.0066	0.0636 ± 0.0045	0.0841 ± 0.0059	0.2516 ± 0.0189	7.61 ± 0.27

Table 2: Correction factors for multi-scattering, self-shielding and background resonance capture of neutron in the samples

Nuclides	54 keV				148 keV			
	SSF	MSF	Res.	Total.	SSF	MSF	Res	Total.
Au-197	0.9985	0.9901	0.4269		0.9988	0.9929	0.5338	
Nd-146	0.9961	0.9719	0.6674	1.5385 ± 0.0462	0.9973	0.9856	0.9300	1.7321 ± 0.0519
Nd-148	0.9982	1.0000	0.6688	1.5830 ± 0.0474	0.9984	1.0000	0.9307	1.7566 ± 0.0527
Nd-150	0.9981	1.0000	0.6495	1.5374 ± 0.0461	0.9984	1.0000	0.8824	1.6655 ± 0.0499
Sm-154	0.9869	0.9639	0.6095	1.4064 ± 0.0422	0.9561	0.8238	0.8087	1.3131 ± 0.0394
Ta-181	0.9559	0.8905	0.4046	0.8905 ± 0.0267	0.9652	0.9156	0.7121	1.2731 ± 0.0382

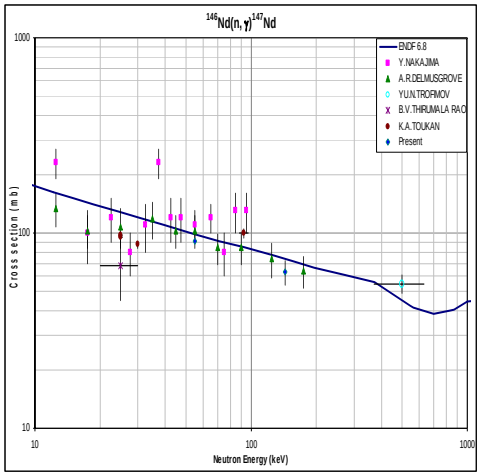

Fig. 1: Neutron capture cross section of ^{146}Nd in keV region

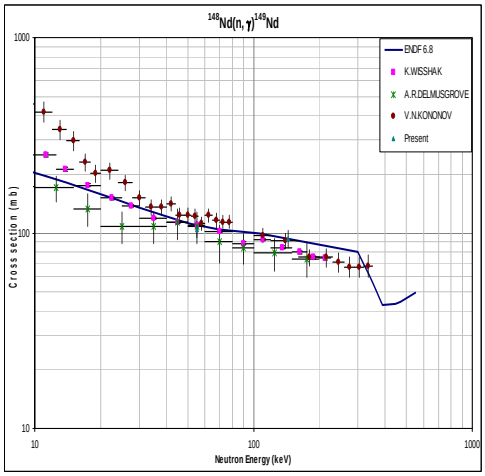

Fig. 2: Neutron capture cross section of ^{148}Nd in keV region

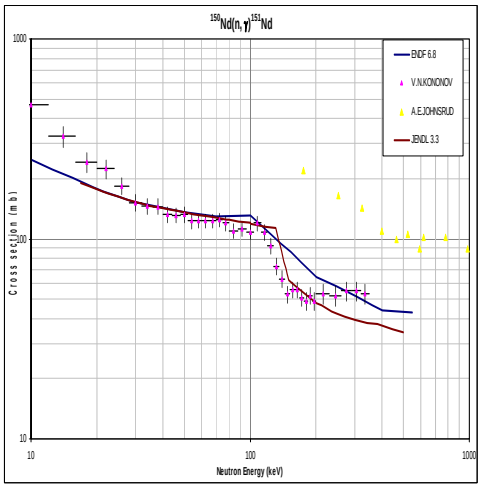

Fig. 3: Neutron capture cross section of ^{150}Nd in keV region

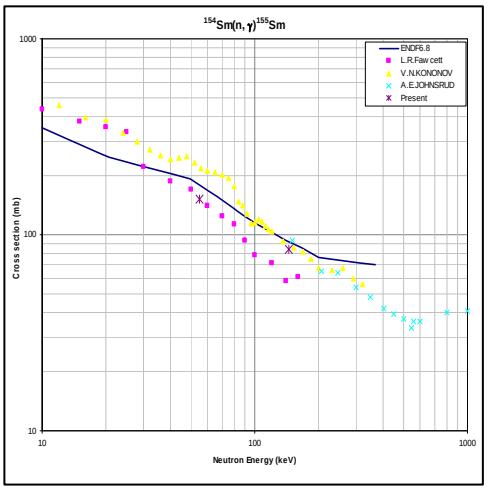

Fig. 4: Neutron capture cross section of ^{154}Sm in keV region

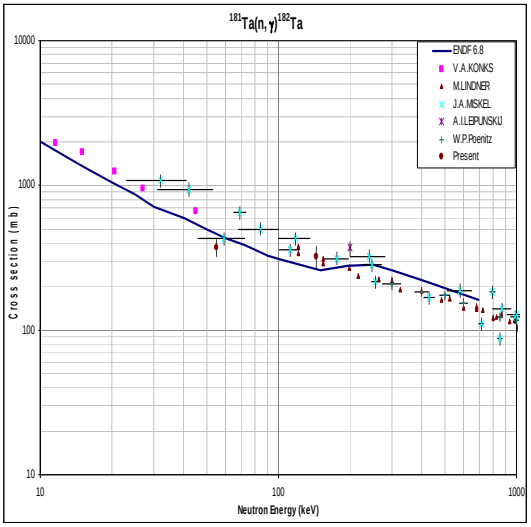

Fig. 5: Neutron capture cross section of ^{181}Ta in keV region

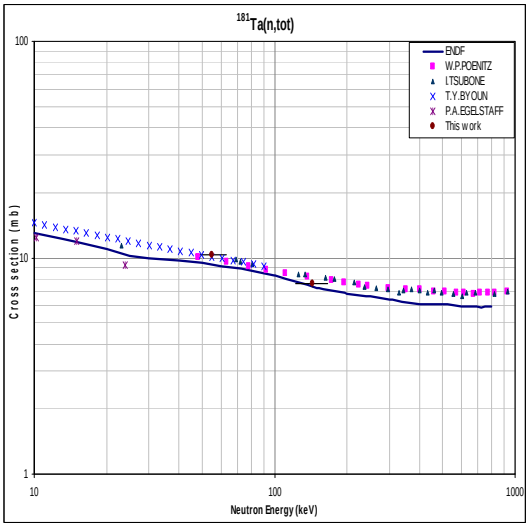

Fig. 6: Total neutron cross section of ^{181}Ta in keV region

In the present work a computer code has been developed for calculation the decay and growth of FP concentrations. The data calculated from this program have been introduce into summation calculation of FP total decay heat for several fissile nuclides such as ^{235}U, ^{238}U, ^{233}U, ^{239}Pu, ^{241}Pu and ^{232}Th, using the decay data and fission yield from JENDL3.3. The present results are shown in Figures 1-6, in comparison with the experimental values measured by the University of Tokyo (YAYOI) and the Oak Ridge National Laboratory (ORNL). As shown in the Figures 7-12, the agreements between the present calculation results and measured data say that the present computer code would qualify for applications related to FP concentrations data.

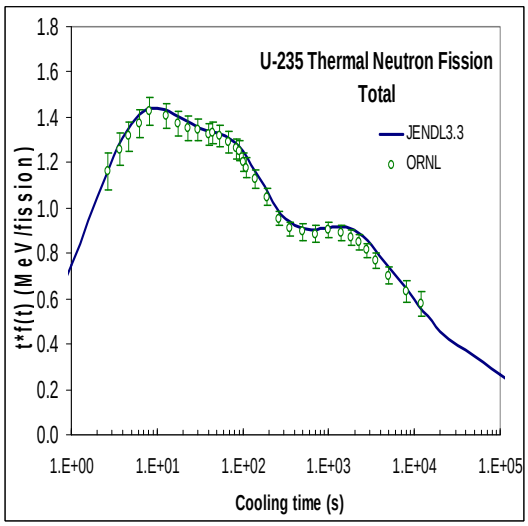

Fig. 7: Calculated total decay heat from FPs after a thermal neutron fission burst of ^{235}U

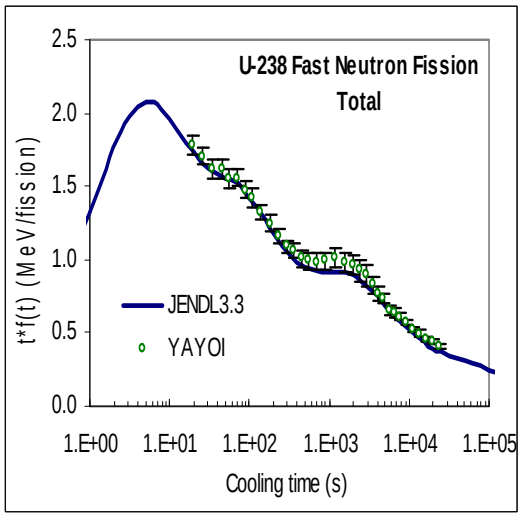

Fig. 8: Calculated total decay heat from FPs after fast neutron fission burst of ^{238}U

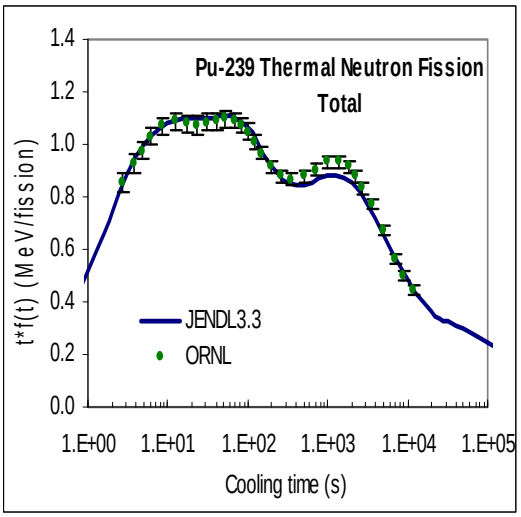

Fig. 9: Calculated total decay heat from FPs after a thermal neutron fission burst of ^{239}Pu

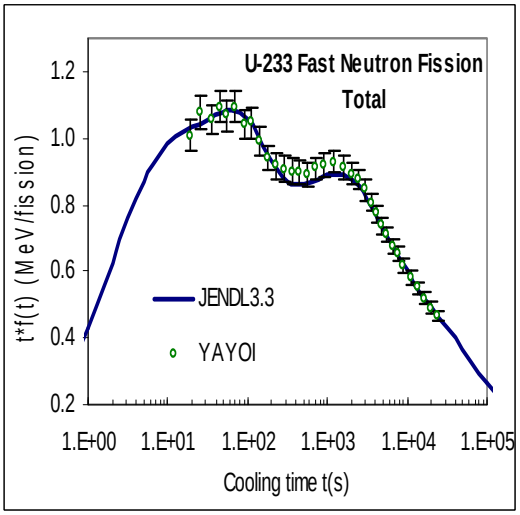

Fig. 10: Calculated total decay heat from FPs after fast neutron fission burst of ^{233}U

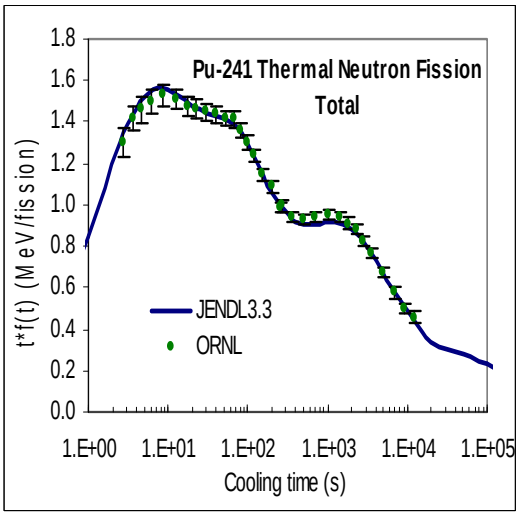

Fig. 11: Calculated total decay heat from FPs after a thermal neutron fission burst of ^{241}Pu

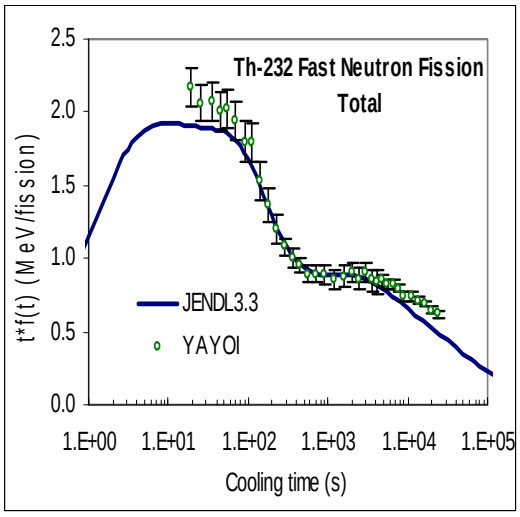

Fig. 12: Calculated total decay heat from FPs after fast neutron fission burst of ^{232}Th

The characteristic parameters of monoenergetic neutron beams are neutron spectra, relative intensity, energy resolution, dimension of filters, and suitable composition of materials have been calculated to create the neutron beams with mono-energies of 1.8keV, 24.3keV, 53.9keV, 58.8keV 133keV and 148.3keV at the horizontal channel No.4 of the Dalat research reactor. The properties of the filtered neutron beams are given in Table 3 and neutron spectra with necessary energy are shown in Fig. 13-18.

Table 3: The properties of the filtered neutron beams

E_n *keV*	ΔE_n *keV*	Φ x10^5 *n/cm^2/s*	I *(%)*	**Filter combination**
1.8	1.5	24.0	95.79	0.2g/cm^2 **^{10}B** + 200g/cm^2 **Sc** + 1cm **Ti**
24.3	1.8	2.6	96.72	0.2g/cm^2 **^{10}B** + 20cm **Fe** + 30cm **Al** + 35g/cm^2 **S**
53.9	1.5	1.7	78.05	0.2g/cm^2 **^{10}B** + 98cm **Si** + 35g/cm^2 **S**
58.8	2.7	1.1	92.28	0.2g/cm^2 **^{10}B** + 10cm **Ni** + 11g/cm^2 **V** + 10cm **Al** + 35g/cm^2 **S**
133	3.0	0.5	92.89	0.2g/cm^2 **^{10}B** + 50g/cm^2 **Cr** + 10cm **Ni** + 60cm **Si**
148.3	14.8	7.2	95.78	0.2g/cm^2 **^{10}B** + 98cm **Si** + 2cm **Ti**

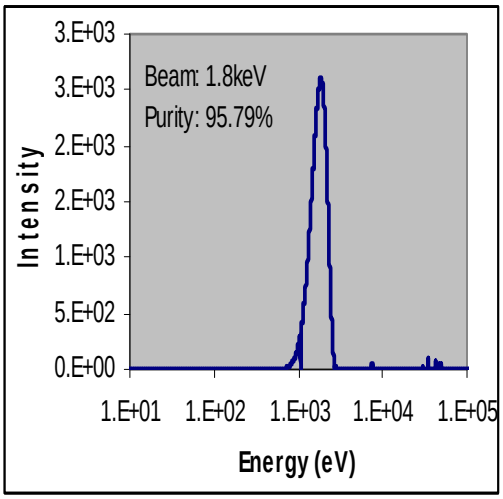

Fig. 13: Neutron filter for energy 1.8keV

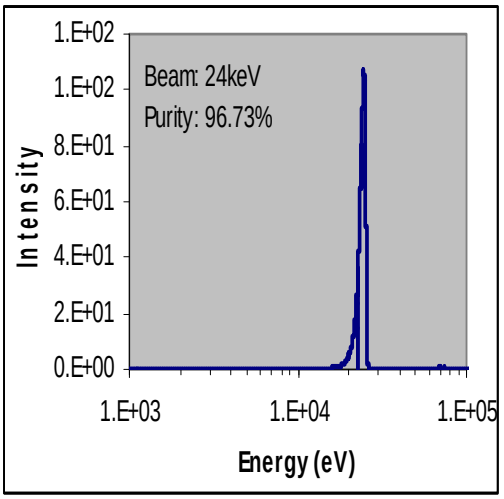

Fig. 14: Neutron filter for energy 24keV

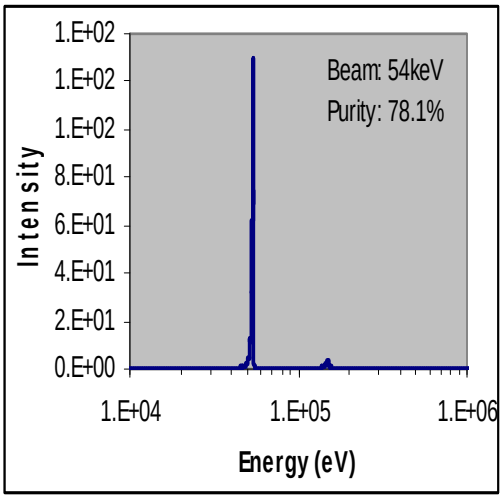

Fig. 15: Neutron filter for energy 54keV

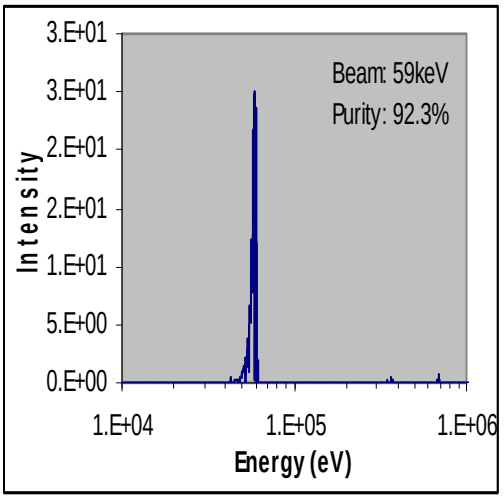

Fig.16: Neutron filter for energy 59keV

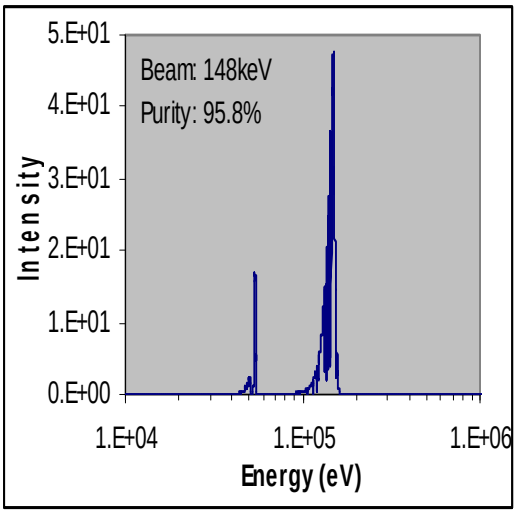

Fig. 17: Neutron filter for energy 148keV

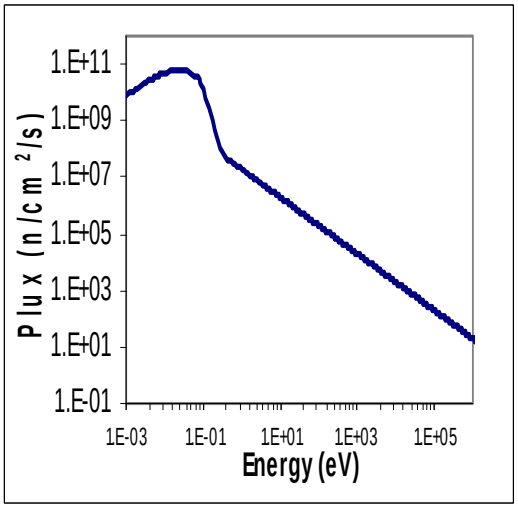

Fig. 18: Neutron spectrum at the before neutron filter

Acknowledgments

The authors would like to express our thanks to the Vietnam Atomic Energy Commission (VAEC) and the Dalat Nuclear Research Institute (DNRI) for their great encouragement and helpful in creating an advantage research condition for this work. The present study was sponsored by the Fundamental Research Program of VAEC under the subproject No. 409706. The advanced gamma-ray spectroscopy system used in the experiments was supported by IAEA. We also wish to express our deep gratitude to the members of the Nuclear Data Center of JAEA for helpful reference data and materials.

REFERENCES

[1] K. H. Guber, et al., Neutron Cross Section Measurements at the Spallation Neutron Source, Int. Conf. on Nuclear Data for Science and Technology, Tsukuba (JP), 7-12, P. 281, Oct. 2001.

[2] Stefano Marrone, Measurement of the ^{139}La(n,γ) Cross Section at n_TOF, 12th Conference on Capture Gamma-Ray Spectroscopy and Related Topics, CGS12, 4-9 (2005).

[3] S. O'Brien et al., Neutron capture cross section of ^{139}La, Phy. Rev. C68, 035801 (2003).

[4] Z. Y. Bao, H. Beer, F. Kappeler, F. Voss, And K. Wisshak, Neutron Cross Sections for Nucleosynthesis Studies, Atomic Data and Nuclear Data Tables 76**,** 70–154 (2000).

[5] Kazuya OHGAMA, et al., Measurement of keV-Neutron Capture Cross Sections and Capture Gamma-Ray Spectra of ^{91,92}Zr, J. Nuclear Science and Technology, Vol. 42, P. 333 (April 2005).

[6] A. R. de L. Musgrove, B. J. Allen, R. L. Macklin, Resonance Neutron Capture in ^{139}La, Aust. J. Phys., 30, 599-604 (1977).

[7] K. Wisshak, et al., Neutron Capture in ^{148,150}Sm: A Sensitive Probe of the S-Process Neutron Density, Phy. Rev. C48, 3, (1993).

[8] B. Duamet, et al. Measurement of keV-Neutron Capture Cross Sections and Capture Gamma-Ray Spectra of ^{147,148,149,150,152,154}Sm, J. Nucl. Sci. Tech., Vol. 36, p. 865-876 1999).

[9] R. L. Macklin, D. M. Darke and J. J. Malanify, Fast Neutron Capture Cross Section of ^{169}Tm, ^{191}Ir, ^{193}Ir, ^{175}Lu for En from 3-2000 keV, LA-7479-MS, Aug. 1978.

[10] K. Oyamatsu, "Easy-To-Use Application Programs to Calculate Aggregate Fission Product Properties on Personal Computers", JEARI-Conf 99-002 (1999).

[11] A.L. Nichols, Nuclear Data Requirements for Decay Heat Calculations, *Lectures given at the Workshop on Nuclear Reaction Data and Nuclear Reactors: Physics, Design and Safety, Trieste, 25 February – 28 March 2002.*

[12] J. Katakura, T. Yoshida, K. Oyamatsu and T. Tachibana, JENDL FP Data File 2000, JAERI-1343 (2001).

[13] K. Tasaka, J. Katakura and T. Yoshida, "Recommend Values of Decay Heat Power and Method to Utilize The Data", JEARI-M-91-034, (1991).

[14] M. Akiyama and S. An, " Measurement of fission products decay heat for fast reactor", Proc. of Int. Conf. on Nucl. Data for Science and Techno., Antwerp, Belgium, P.237 (1982).

[15] J. K. Dickens et al., "Fission Products Energy Release for Time following Thermal Neutron Fission of ^{235}U between 2 and 14000 seconds", ORNL/NUREG-14 (1977); Nucl. Sci. Eng., 74, 106 (1980).

[16] J. K. Dickens et al., "Fission Products Energy Release for Time following Thermal Neutron Fission of ^{239}Pu between 2 and 14000 seconds", ORNL/NUREG-34 (1978); Nucl. Sci. Eng., 78, 126 (1981).

[17] R. C. Greenwood and R. E. Chrien, Filtered Reactor Beams For Fast Neutron Capture γ-Ray Experiments, Nucl. Instr. and Meth. 138 (1976), pp. 125-143.

[18] O. D. Simpson and L. G. Miller, A Technique To Measure Neutron Cross Sections in The Low keV Energy Region, Nucl. Instr. and Meth. 61 (1968), pp. 245-250.

[19] O. O. Gritzay, V. V. Kolotyi and O. I. Kaltchenko, Neutron Filters at Kyiv Research Reactor, Preprint KINR-01-6 (2001).

[20] Block R.C., Brugger R.M., "Filtered Neutron Beams", Neutron Sources for Basic Physics and Applications, OECD/NEA Report, Pergamon Press, (1983), P. 177.

[21] Vertebnyi V.P., Murzin A.V., Pshenychnyi V.A. et al. Filtered medium and thermal neutron beams and their use, "Properties of Neutron Sources", IAEA – TECDOC-410, Vienna, IAEA, (1987), P. 257.

[22] Wolfgang G. Alberts, Calibration of Neutron Monitors for Radiation Protection at 24.5 keV And 2 keV**,** Nucl. Instr. and Meth. 155 (1978), pp. 307-308.

[23] O.O. Gritzay and A.V. Murzin, Analysis of the Possibility of Using the Reactor Filtered Neutron Beam Formed by Ni-60 Filter for BNCT, "Current status of neutron capture therapy", IAEA-TECHDOC-1223, May 2001, pp.147-151.

[24] R. Moreha, R.C. Block and Y. Danon, Generating a multi-line neutron beam using an electron Linac and a U-filter, Nucl. Instr. and Meth. 562 (2006), pp. 401-406.

[25] K. Shibata, et al., "Japanese Evaluated Nuclear Data Library Version 3 Revision-3: JENDL-3.3," J. Nucl. Sci. Technol. **39**, 1125 (2002).

PAPERS PUBLISHED IN RELATION TO THE PROJECT

1. V. H. Tan, T. T. Anh, N. C. Hai, P. N. Son and T. Fukahori, *Measurement of Neutron Capture Cross Section of ^{139}La, ^{152}Sm and ^{191,193}Ir at 55keV and 144keV*, SND2006-V.02-1, Proceeding of 2006 Symposium on Nuclear Data, Jan. 25-26, 2007, RICOTTI, Tokai, Ibaraki, Japan, ISBN978-4-89047-138-6, [CD], 2007.
2. V.H.Tan, N.C.Hai, P.N.Son, T.T.Anh, *Measurement of Neutron Capture Cross Sections of ^{191}Ir and ^{193}Ir at 55 keV and 144 keV*, Journal of Nuclear Science and Technology, Vol. 5, No.1 (2007), VAEC, ISSN 1810-5408, June 2007, pp. 13-20.
3. Vuong Huu Tan, Pham Ngoc Son, *A computer code for calculation of fission product concentrations for time following fission burst*, Dự kiến đăng trên Tuyển tập Báo cáo Hội nghị Khoa học và Công nghệ Hạt nhân lần thứ 7, Đà Nẵng và Tạp chí Khoa học và Công nghệ Hạt nhân, VAEC, ISSN.
4. Vương Hữu Tấn, Phạm Ngọc Sơn, Trần Tuấn Anh, Hồ Hữu Thắng, Nguyễn Cảnh Hải, *Tính toán các thông số đặc trưng phục vụ phát triển các dòng nơtron* phin *lọc mới tại lò phản ứng Đà Lạt*, Dự kiến đăng trên Tuyển tập Báo cáo Hội nghị Khoa học và Công nghệ Hạt nhân lần thứ 7, Đà Nẵng và Tạp chí Khoa học và Công nghệ Hạt nhân, VAEC, ISSN.
5. Vương Hữu Tấn, Nguyễn Cảnh Hải, Phạm Ngọc Sơn, Trần Tuấn Anh, Trịnh Thị Tú Anh, Mai Xuân Trung, *Nghiên cứu xác định hệ số hiệu chỉnh trong phép đo tiết diện bắt bức xạ neutron,* Dự kiến đăng trên Tuyển tập Báo cáo Hội nghị Khoa học và Công nghệ Hạt nhân toàn quốc lần thứ 7, Đà Nẵng.
6. V. H. Tan, N. C. Hai, P. N. Son, T. T. Anh, *Neutron capture cross section measurements of ^{69}Ga, ^{71}Ga and ^{160}Gd on filtered neutron beams of 55keV and 144keV*, Proceedings of the 6th National Conference on Nuclear Science and Technology, Dalat, Vietnam, Published June 2007, pp. 46-50.
7. V. H. Tấn, T. T. Anh, N. C. Hải, P. N. Sơn, N. X. Hải, H. H Thắng, Đ.Lành, *Xác định cường độ tương đối của các tia gamma tức thời từ phản ứng ^{35}Cl(n, γ)^{36}Cl và ^{48}Ti(n, γ)^{49}Ti trên dòng nơtron nhiệt*, Tuyển tập Báo cáo Hội nghị Khoa học và Công nghệ Hạt nhân toàn quốc lần thứ VI, Xuất bản 6/2007, trang 160-164.
8. N. N. Dien, P. N. Son, N. C. Hai, T. T. Anh and V. H. Tan, *Differential neutron energy spectrum measurement at the horizontal channel No.4 of the Dalat reactor*, Proceedings of the 6th National Conference on Nuclear Science and Technology, Dalat, Vietnam, Published June 2007, pp. 177-183.
9. N. C. Hai, N. N. Dien, P. N. Son, T. T. Anh, P. N. Tuan, D. V. Khiem, L. B. Vien, N. X. Hai, H. H Thang. *Innovation of prompt gamma neutron activation analysis facility at the Dalat reactor*. Proceedings of the 6th National Conference on Nuclear Science and Technology, Dalat, Vietnam, Published June 2007, pp. 627-631.

ON THE PHASE TRANSITION IN STABLE QUARK MATTER

Tran Huu Phat [(1)]***, Nguyen Tuan Anh*** [(2)]***, Nguyen Van Long*** [(3)] ***and Le Viet Hoa*** [(4)]

[(1)] *Vietnam Atomic Energy Commission, Vietnam.*

[(2)] *Institute for Nuclear Science and Technique, VAEC, Vietnam.*

[(3)] *Gialai Teacher College, Vietnam.*

[(4)] *Hanoi University of Education, Vietnam.*

ABSTRACT: Within the framework of the Cornwall - Jackiw - Tomboulis (CJT) effective action approach we consider phase transition in the four-fermion model, which gives rise to the saturation property of quark matter. It is shown that in the Hartree-Fock (HF) approximation a first order phase transition occurs at zero and low temperature, while a second-order phase transition exists at higher temperature.

Keywords: phase transition, saturation property, effective action, Hartree-Fock approximation.

1. INTRODUCTION

It is known that understanding the phase transition between different thermodynamical states of strongly interacting matter at finite temperature and density turns out to be of great significance in modern physics. Until now we have known only two points in T-ρ plane, namely, the vacuum ($T = 0$, $\rho = 0$) and the nuclear matter ($T = 0$, $\rho = 0.17$ fm^{-3}). It is expected that the transition from the hadronic to the quark-gluon phase would be observed in heavy ion collisions. The lattice QCD calculations indicates that quark matter does undergo both chiral phase transition and confinement - deconfinement phase transition at the same temperature $T = 150$ MeV [1]. However, the lattice calculations have been carried out only at zero density. In this respect, investigating effective models, which provide with the saturation property, is very useful for understanding the matter states under different conditions. As was well known, in several chiral models, e.g., the Nambu-Jona-Lasinio (NJL) model and the linear sigma model, the saturation property is absent not only in the mean field approximation [2, 3], but also in the HF approximation [4, 5]. The saturation mechanism is only restored in their extended versions [6].

In this paper, following [7] we consider the quark model which scalar and vector-isoscalar, through which two condensates $\langle\bar{\mathbf{q}}\mathbf{q}\rangle$ and $\langle\bar{\mathbf{q}}\boldsymbol{\gamma}_{\mu}\mathbf{q}\rangle$ are formed. The saturation of quark matter appears as the compensation of these two condensations. Section 2 deals with the CJT effective action at finite temperature and density. In Section 3 the numerical calculations are presented in detail. The conclusion and discussion are given in Section 4.

2. CJT EFFECTIVE ACTION AT FINITE T AND ρ

Let us begin with the stable quark matter modeled by $N_f = 1$ Lagrangian density

$$L = \bar{\mathbf{q}}(i\gamma^{\mu}\partial_{\mu} - M)\mathbf{q} + \frac{G_s}{2}(\bar{\mathbf{q}}\mathbf{q})^2 - \frac{G_v}{2}(\bar{\mathbf{q}}\gamma_{\mu}\mathbf{q})^2$$

where M is the quark mass, G_s and G_v coupling constants. Performing the bosonization

$$\boldsymbol{\sigma} = \frac{g_s}{m_\sigma^2}\,\bar{\mathbf{q}}\mathbf{q}, \qquad \boldsymbol{\omega}_\mu = \frac{g_v}{m_\omega^2}\,\bar{\mathbf{q}}\gamma_\mu\mathbf{q}.$$

we are led to

$$L = \bar{\mathbf{q}}(i\gamma^\mu\partial_\mu - M)\mathbf{q} + g_s\bar{\mathbf{q}}\boldsymbol{\sigma}\mathbf{q} - g_v\bar{\mathbf{q}}\gamma^\mu\boldsymbol{\omega}_\mu\mathbf{q} - \frac{m_\sigma^2}{2}\boldsymbol{\sigma}^2 + \frac{m_\omega^2}{2}\boldsymbol{\omega}^2 \qquad (2.1)$$

in which $G_{s,v} = g_{s,v}^2/m_{\sigma,\omega}^2$, m_σ and m_ω are respectively the masses of scalar and vector mesons. (2.1) clearly resembles the QHD-I Lagrangian of the Walecka model [8] without the kinetic terms for bosons, which describes the symmetric nuclear matter. According to [7] the expression for the CJT effective potential reads

$$\begin{aligned} V = {} & \frac{m_\sigma^2}{2}\sigma^2 - \frac{m_\omega^2}{2}\omega^\mu\omega_\mu - i\int\frac{d^4p}{(2\pi)^4}\,tr\left[\ln S_0^{-1}(p)S(p) - S_0^{-1}(p;\sigma,\omega)S(p) + 1\right] \\ & + \frac{i}{2}\int\frac{d^4p}{(2\pi)^4}\,tr\left[\ln C_0^{-1}(p)C(p) - C_0^{-1}(p)C(p) + 1\right] \quad + \frac{i}{2}\int\frac{d^4p}{(2\pi)^4}\,tr\left[\ln D_0^{\mu\nu\,-1}(p)D_{\mu\nu}(p) - D_0^{\mu\nu\,-1}(p)D_{\mu\nu}(p) + 1\right] \\ & - \frac{i}{2}g_s\int\frac{d^4p}{(2\pi)^4}\frac{d^4k}{(2\pi)^4}\,tr\left[S(p)\Gamma(p,k-p)S(k)C(k-p)\right] \\ & + \frac{i}{2}g_v\int\frac{d^4p}{(2\pi)^4}\frac{d^4k}{(2\pi)^4}\,tr\left[\gamma^\mu S(p)\Gamma^\nu(p,k-p)S(k)D_{\mu\nu}(k-p)\right], \end{aligned} \qquad (2.2)$$

here

$$iS_0^{-1}(p) = \hat{p} - M, \quad iS_0^{-1}(p;\sigma,\omega) = iS_0^{-1}(p) + g_s\sigma - g_v\gamma^0\omega, \quad iC_0^{-1} = -m_\sigma^2, \quad iD_0^{\mu\nu-1} = g^{\mu\nu}m_\omega^2;$$

S, C, $D_{\mu\nu}$ are the propagators of quark, sigma and omega mesons, respectively;

$$\sigma = \langle\boldsymbol{\sigma}\rangle = const., \quad \langle\boldsymbol{\omega}_\mu\rangle = \omega\delta_{0\mu} = const.$$

are the expectation values of the field operators in the ground state of quark matter.

The configuration of the ground state corresponds to

$$\frac{\delta V}{\delta F} = 0, \quad F = \{\sigma,\omega\} \qquad (2.3)$$

$$\frac{\delta V}{\delta G} = 0, \quad G = \{S, C, D_{\mu\nu}\} \qquad (2.4)$$

(2.3) is the gap equation for quark matter and (2.4) is the Schwinger-Dyson (SD) equation for propagator G. Inserting (2.2) into (2.3) yields the gap equations for σ and ω, respectively

$$\sigma = -\frac{g_s}{m_\sigma^2}\int\frac{d^4p}{(2\pi)^4}\,tr[S(p)] = g_s\rho_s, \qquad \omega = -\frac{g_v}{m_\omega^2}\int\frac{d^4p}{(2\pi)^4}\,tr[\gamma^0 S(p)] = g_v\rho. \qquad (2.5)$$

where ρ_s and ρ are the scalar and quark density, respectively.

The SD equations for the propagators S, C and $D_{\mu\nu}$ are obtained by substituting (2.2) into (2.4) accordingly,

$$iS^{-1}(k) = iS_0^{-1}(k) - \Sigma(k), \tag{2.6}$$

$$\Sigma(k) = -g_s\sigma + ig_s\int\frac{d^4p}{(2\pi)^4}\left[S(p)\Gamma(p,p+k)C(p+k)\right] + g_v\gamma^0\omega_0 - ig_v\int\frac{d^4p}{(2\pi)^4}\left[\gamma^\mu S(p)\Gamma^\nu(p,p+k)D_{\mu\nu}(p+k)\right]$$

$$iC^{-1}(k) = -m_\sigma^2 - \Pi_\sigma(k), \qquad \Pi_\sigma(k) = -ig_s\int\frac{d^4p}{(2\pi)^4}\,\mathrm{tr}\left[S(p)\Gamma(p,p+k)S(p+k)\right] \tag{2.7}$$

$$iD_{\mu\nu}^{-1}(k) = m_\omega^2 g_{\mu\nu} + \Pi_{\mu\nu}(k), \qquad \Pi_{\mu\nu}(k) = -ig_v\int\frac{d^4p}{(2\pi)^4}\,\mathrm{tr}\left[\gamma_\mu S(p)\Gamma_\nu(p,p+k)S(p+k)\right] \tag{2.8}$$

Σ, Π_σ and $\Pi_{\mu\nu}$ are self energies of quark, sigma and omega mesons, respectively. Next let us consider the CJT effective potential V in the bare vertex approximation (BVA), in which $\Gamma = g_s, \Gamma^\mu = g_v\gamma^\mu$. To this end, let us first express Σ in term of its Dirac components

$$\Sigma(k) = \gamma_0\Sigma_0(k) - \vec{\gamma}.\vec{k}\Sigma_v(k) - \Sigma_s(k)$$

Due to (2.7a) the quark propagator $S(k)$ is then rewritten as

$$iS^{-1}(k) = iS_0^{-1}(k) - \Sigma(k) = \gamma_0 k_0 - \Sigma_0(k) - \vec{\gamma}.\vec{k}(1-\Sigma_v(k)) - (M + \Sigma_s(k))$$

Introducing the effective quantities

$$k_0^* = k_0 - \Sigma_0(k), \quad \vec{k}^* = \vec{k}\,[1-\Sigma_v(k)], \quad M_k^* = M + \Sigma_s(k) \tag{2.9}$$

we arrive at

$$S(k) = (\hat{k}^* + M_k^*)G_k, \quad G_k = G_k^F + G_k^D = \frac{i}{\hat{k}^{*2} - M_k^{*2} + i\varepsilon} - 2\pi\delta(k^{*2} - M_k^{*2})n_k, \tag{2.10}$$

with n_k the Fermi distribution function, $n_k^{*\pm} = (e^{(E_k^*\pm\mu)/T} + 1)^{-1}, E_k^* = (\vec{k}^{*2} + M_k^{*2})^{1/2}$.

Substituting (2.10) respectively to (2.7), (2.8) and (2.9) we get the following equations in the HF approximation

$$\mu^* = \mu - \Sigma_0 = \mu - \frac{1}{4\pi^2}\left[-\frac{g_s^2}{m_\sigma^2} + 2\frac{g_v^2}{m_\omega^2}(2N_cN_f + 1)\right]\int_0^\Lambda p^2dp\,(n_p^{*-} - n_p^{*+}), \tag{2.11}$$

$$M^* = M + \Sigma_s = M + \frac{1}{4\pi^2}\left[\frac{g_s^2}{m_\sigma^2}(4N_cN_f + 1) + 4\frac{g_v^2}{m_\omega^2}\right]\int_0^\Lambda p^2dp\,\frac{M^*}{E_p^*}(1 - n_p^{*-} - n_p^{*+}), \tag{2.12}$$

where Λ is the cutoff in 3-dimensional momentum space. Finally, we obtain the formulae for thermodynamic potential

$$V(M^*,\mu,T) = \frac{2N_cN_f(M-M^*)^2}{(4N_cN_f+1)G_s + 4G_v} - \frac{2N_cN_f(\mu-\mu^*)^2}{2(2N_cN_f+1)G_v - G_s} - \frac{m_\omega^2}{2} + \frac{N_cN_f}{\pi^2}\int_0^\Lambda p^2dp\left[E_p^* + T\ln(n_p^{*-}n_p^{*+})\right]$$

$$\Omega = V - V_{vac}, \quad V_{vac} = V(M_{vac}, \mu = 0, T = 0). \tag{2.13}$$

3. NUMERICAL CALCULATION IN HF APPROXIMATION

Now the numerical calculations are carried out for different cases in the HF approximation.

3.1 Zero temperature

The masses of quark is fixed to be $M = 5.6$ MeV. We then solve the integral equation (2.12) and substitute the found values of $M^*(k_F)$ into the expression for binding energy $\in_{bind}$ to be defined as $\in_{bind} = -M_{vac} + \varepsilon/\rho N_c$, where $\varepsilon = \Omega + \mu N_c \rho$. The two parameters g_s and g_v are adjusted to reproduce the saturation point, which is determined by demanding that the binding energy per three quarks takes the minimum value $\in_{bind} = -15.8$ MeV at the normal density $k_F = 1.42$ fm^{-1}. Consequently, the corresponding values of G_s and G_v are fixed to be $G_s = 4.957/\Lambda^2$, $G_v = 0.3G_s$ and $\Lambda = 404$ MeV. In Fig.1 it is shown the saturation curve with these value of G_s, G_v and Λ. Next the $\mu-$dependence of M^* is considered by means of Eqs.(2.11), (2.12).

A first-order phase transition shown up in Fig.2. A better understanding of phase transition is highlighted in Fig.3, where the M^* dependence of Ω is plotted for several value of μ.

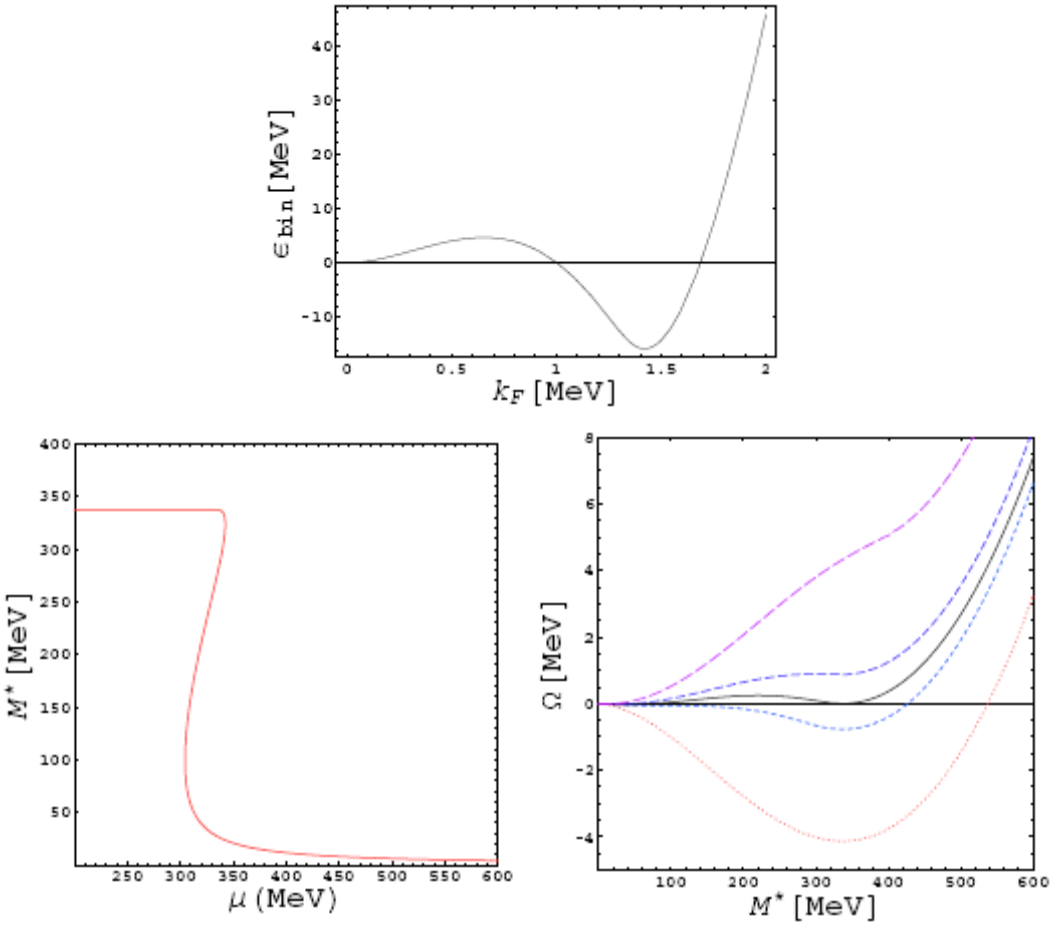

Fig. 1: Density dependence of binding energy.

Fig. 2: μ dependence of M^*.

Fig.3: $\Omega[\times 10^8]$ as a function of M^*.

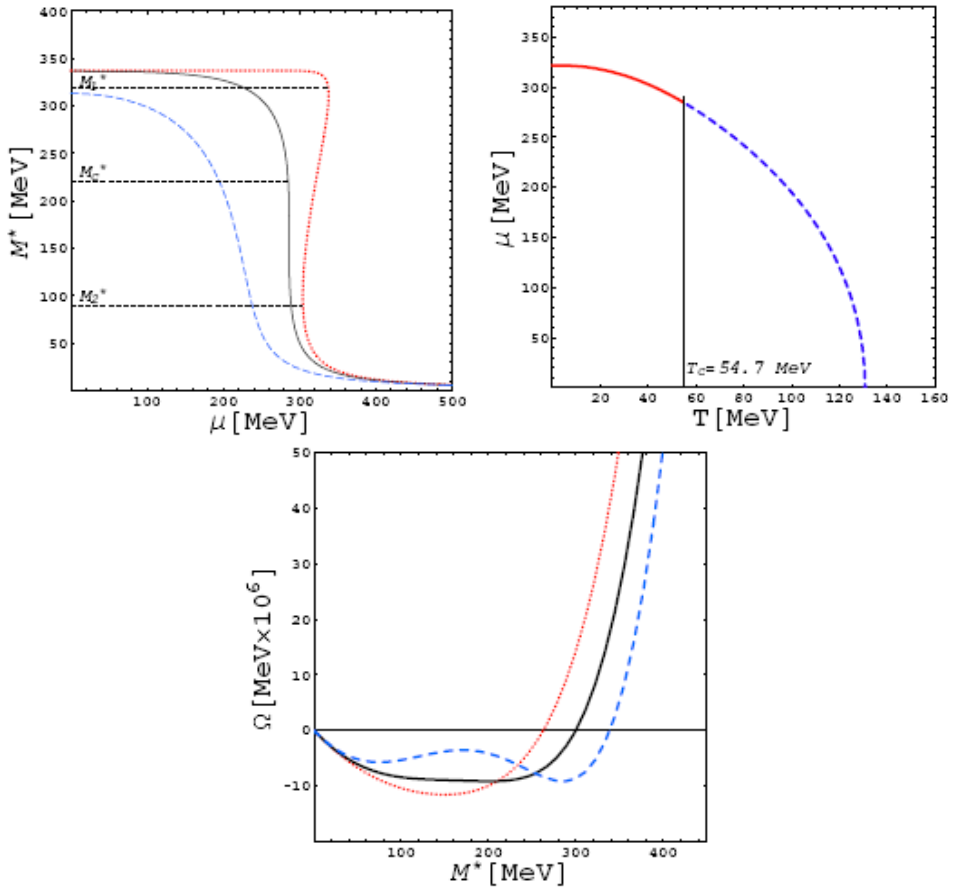

Fig. 4: Quark mass as a function of the chemical potential μ at $T \neq 0$. Red dotted line (at $T = 10$ MeV) is the first transition, blue dashed line (at $T = 100$ MeV) is the second transition, black solid line is at $T_c = 54.7$ MeV (when $\mu_c = 284.8$ MeV and $M_c^* = 220$ MeV).

Fig. 5: Curve of μ and T. At $T < 54.7$ MeV, first-order phase transition

Fig. 6: Error! Objects cannot be created from editing field codes. as a function of M^* at $T =$ 40 MeV, μ = 300 MeV (dashed line), T_c = 54.7 MeV, μ_c = 290 MeV (solid line) and $T =$ 70 MeV, μ = 280 MeV (dotted line).

3.2 Finite Temperature and chemical potential.

Eqs.(2.11) and (2.12) determined the μ dependence of M^* at $T \neq 0$. This dependence is given by several graphs in Fig.4, which correspond respectively to $T = 10$ MeV, 54.7 MeV and 100 MeV. It is clear that a first-order phase transition occurs for low temperature, $T < 54.7$ MeV, and begin to smear out at $T = 54.7$ MeV. For $T > 54.7$ MeV a second-order phase transition emerges. It is observed that for T raising from low to sufficiently high temperature the pair of points M_1^*, M_2^* will move to a point, where the first-order phase transition comes to disappear. These points are close to $M_C^*(M_C, \mu_C)$. Therefore, basing on this observation and adopting the definition of critical points proposed by [9] we assume that the critical line in the $T - \mu$ plane is

defined by the equation $M^*(\mu_C, T_C) = M_C$, the graph of which is depicted in Fig.5, where solid line corresponds to first-order transition and dashed line second-order phase transition. More detailed information on phase transitions is obtained in Fig.6, where the M^* dependence of Ω for different temperatures is given.

4. CONCLUSION AND DISCUSSION

The stable quark matter, which has the saturation property, has been studied in this paper by means of the CJT effective action. The Lagrangian of our model in the bosonized form is similar to that of QHD-I. In the HF approximation it is shown that a first-order phase transition is present at zero and low temperature. But at sufficiently high temperature the first-order phase transition is smeared out and then disappears; instead, a second-order phase transition comes to emerge. This result is quite different from those obtained when the symmetric nuclear matter, described by QHD-I, was considered in the mean-field approximation [10], where only the first-order phase transition exhibits. This distinction arises due to the fact that the vicinity of the critical point the fluctuation of the order parameter is very large, while in the mean-field approximation this quantity is neglected.

ACKNOWLEDGMENT

This paper is supported by the Vietnam National Science Foundation.

REFERENCES

[1]. F. Karsch, in "Quark-Gluon Plasma", ed. R.C. Hwa, World Scientific, Singapore, 1990.

[2]. V. Koch, T.S. Biro, J. Kunz and U. Mosel, Phys. Lett. **B185** (1987) 1.

[3]. M. Buballa, Nucl. Phys. **A611** (1996) 393.

[4]. L.G. Liu, W. Benz and A. Arima, Ann.Phys. **194** (1989) 387.

[5]. Tran Huu Phat, Nguyen Tuan Anh and Le Viet Hoa, Adv. Natur. Sci. **5** (2004) 33.

[6]. J. Boguta, Phys. Lett. **B120** (1983) 34; **B128** (1983) 19; Y. Ogawa et al, nucl-th/0312042; nucl-th/0307063; I. N. Mishustin et al, hep-ph/0304296; S. A. Moszkow et al, nucl-th/0204047.

[7]. Tran Huu Phat, Nguyen Tuan Anh and Le Viet Hoa, Nucl. Phys. **A722** (2003) 548c.

[8]. P. D. Serot and J. D. Walecka, Adv. Nucl. Phys. **16** (1985) 1; Int. J. Mod. Phys. **E6** (1997) 515.

[9]. M. Asakawa and K. Yazaki, Nucl. Phys. **A504** (1989) 668.

[10]. M. Müller and B. D. Serot, Phys. Rev. **C52** (1995) 2072.

PAPERS PUBLISHED IN RELATION TO THE PROJECT:

1. On the phase transition in stable quark matter, báo cáo tại Hội nghị Khoa học và Công nghệ Hạt nhân, tổ chức ở Đà Nẵng, 30-31/08/2007.
2. Phase transitions of nuclear matter beyond mean field theory, Physical Review C(76), 10/2007.

DEVELOPMENT OF A METHOD FOR MEASUREMENT OF TOTAL NEUTRON CROSS SECTIONS BASED ON THE NEUTRON TRANSMISSION METHOD USING A He-3 COUNTER ON FILTERED NEUTRON BEAMS AT DALAT RESEARCH REACTOR

Tran Tuan Anh, Dang Lanh, Nguyen Canh Hai, Nguyen Xuan Hai, Pham Kien Nguyen Thuy Nham, Pham Ngoc Son and Ho Huu Thang

Nuclear Research Institute, VAEC, Vietnam

ABSTRACT: Determination of total neutron cross sections and average resonance parameters in the energy range from tens keV to hundreds keV is important for fast reactors calculations and designs because this energy range gives the most output of all neutron induced reactions in the spectrum of fast reactors. Besides, the total neutron cross section measurement is also one of the methods for determination of s, p and d-wave neutron strength functions. The purpose of this project is to develop a method for measurement of total neutron cross sections based on the neutron transmission technique using a He-3 counter. The average total neutron cross sections of ^{238}U were obtained from neutron transmission measurements on filtered neutron beams of 55 keV and 144 keV at the horizontal channel No.4 of the Dalat research reactor. The present results have been compared with the previous measurements, and the evaluated data from ENDF/B-6.8 library.

1. INTRODUCTION

Determination of total neutron cross sections in the energy range from tens keV to hundreds keV is important for fast reactors calculations and designs because this energy range gives the most output of all neutron induced reactions in the spectrum of fast reactor. Besides, the total neutron cross section measurement is also one of the methods for determination of s, p and d-wave neutron strength functions. However, it is well known that most neutron data were obtained in neutron physics experiments at pulse neutron sources, where intensity of neutron beams in this energy region is not high enough. At the present time one of the most intensive neutron sources in this energy region is filtered neutron beams at steady-state atomic reactor. By using differential neutron filters at the Dalat research reactor, some monoenergetic neutron beams such as 55 keV and 144 keV neutron beams with high enough intensity have been received. The neutron counting system based on μP which is able to interface to PC through USB V2.0 using ^{3}He counter is designed and constructed in NRI, Dalat, and served for measurement of total neutron cross sections, for determination of hydrogen index, for neutron flux monitoring and for neutron physics experiments at the Dalat reactor.

2. DESIGN AND CONSTRUCTION OF NEUTRON COUNTING SYSTEM

The electronic modules were designed and constructed for the neutron counting system including: Preamplifier, High Voltage Power Supply (HVPS), Amplifier, TSCA and interface to PC through USB V2.0 (Fig. 2.1).

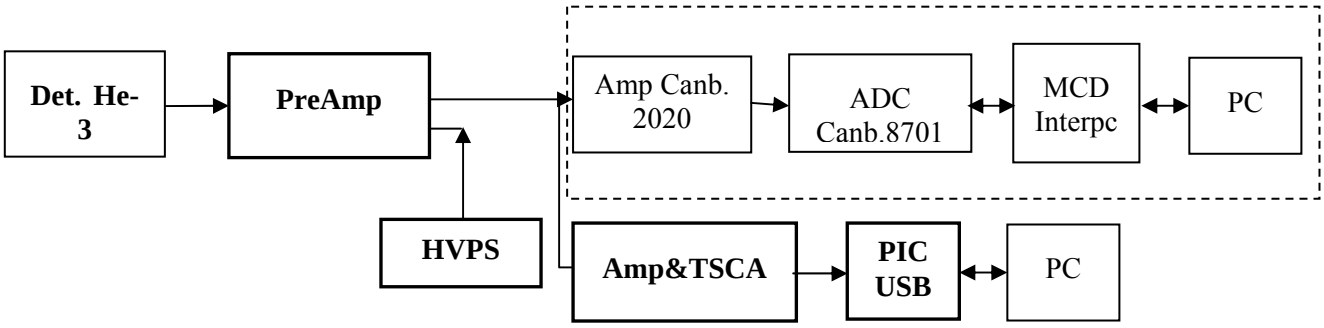

Fig. 2.1: Electronic modules

The typical performance characteristics of these modules:

+ Low voltage power supply: +5V (1A); +15V (1A); -15V (1A).

+ HVPS (High Voltage Power Supply): 2000V (1mA).

+ Preamp: charge sensitive, Output polarity: negative

+ Amplifier: Input polarity: negative or positive; Output polarity: positive; Amplifier gains: x10, x20, x30.

+ TSCA: output pulse in TTL LLD and ULD windows

+ Interface to PC through USB V2.0; microcontroller PIC18F4550 is programmed on PICBasicPRO; application software programmed by VB6 in Windows XP.

3. EXPERIMENTS

3.1. Experimental arrangement

The measurements for total neutron cross sections of ^{238}U at the energies of 55 keV and 144 keV were performed on filtered neutron beams of DNRI. The neutron beams were collimated to 3 cm in diameter by using the usual materials of LiF, Cd, B_4C, Pb and borated paraffin. The physical properties of these beams are given in Table 3.1. The ^{3}He counter was properly shielded with lead and borated paraffin against scattered neutrons and prompt gamma-rays. The samples were prepared from standard Uranium foils with 2.54 cm in diameter and 0.1mm in thickness.

Table 3.1: Filtered neutron beam characteristics

Neutron Energy	Filter combination	Neutron Flux ($n.cm^{-2}.s^{-1}$)	R_{cd} or FWHM
Thermal	98 cm Si +1,0 cm Ti +35 g/cm^2 S	1,81 × 10^7	143
144 keV	98 cm Si +1,0 cm Ti + 0,2 g/cm^2 B-10	2,14 × 10^6	22 keV
55 keV	98 cm Si + 35 g/cm^2 S + 0,2 g/cm^2 B-10	5,61 × 10^5	8 keV

3.2. Data processing

The total neutron cross sections were measured by neutron transmission technique. For a target of thickness x, the experimental total neutron cross section is determined by the formula:

$$\sigma_t = \frac{1}{\rho x} \ln \frac{1}{T} \tag{3.1}$$

where ρ is the concentration of the target nuclei and T is the neutron transmission ratio defined experimentally as:

$$T = \frac{a - a^b}{a_0 - a_0^b} \tag{3.2}$$

where a_0 and a are the neutron count rates of the transmitted and incident beams, a_0^b and a^b are the corresponding backgrounds.

In the experiments, the incident and transmitted neutron fluxes a_0 and a were measured by a proportional counter of ^{3}He. The backgrounds a_0^b and a^b were determined by intercepting the neutron beams by a 10 cm long polyethylene.

In the case of ^{238}U, the experimental cross sections defined by Eq.(3.l) are not identical to the average total neutron cross section and slightly vary with the thickness of the target due to the self-shielding effect. In Fig.3.1 the experimental cross sections were presented versus the target thicknesses for 55 keV and 144 keV neutron energies. At these energies, the self-shielding effect is rather weak, and the thickness dependence of the experimental cross sections can be expressed by a linear function:

$$\sigma_t = \langle\sigma_t\rangle - ax \tag{3.3}$$

The averaged total neutron cross sections $\langle\sigma_t\rangle$ can be obtained by extrapolating the experimental cross sections to zero target thickness.

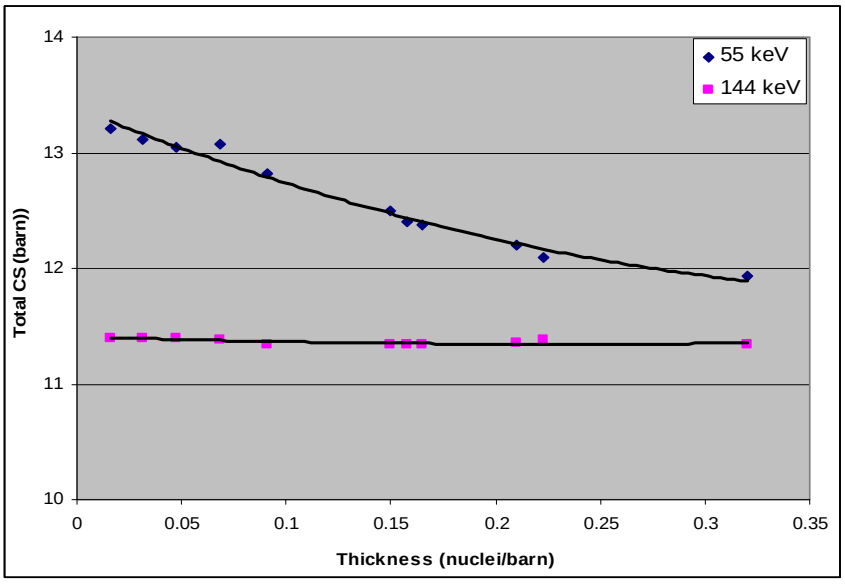

Fig. 3.1: Thickness dependence of the experimental cross section

3.2.3. Results and discussions

By using this neutron counting system, we carried out to measure the total neutron cross sections of ^{238}U at incident neutron energies of 55 keV and 144 keV. The fitting procedure has yielded the results in Table 3.2. The present results are in very good agreement with the results obtained in the previous measurements Ref. [11]. The experimental errors are about 3% and could be further reduced by increasing the number of measuring cycles.

Table 3.2: Total neutron cross sections of ^{238}U in keV region

Neutron energy	ENDF B6.8	L. L. Litvinski et al	V. V. Filipov et al	P. D Hien et al	This work
55 keV	12.97	13.343 ± 0.051	12.95 ± 0.2	13.31 ± 0.11	13.14 ± 0.31
144 keV	11.44	11.55 ± 0.022	11.7 ± 0.15	11.52 ± 0.10	11.61 ± 0.37

Table 3.3: Sources of error

Sources of error	Error (%)
Total cross section of U	0.1(th), 0.38(55keV), 0.19(144keV)
Statitics	<=2
Correction for scattering and attenuation	<0.5
Background	<1
Weighting error of sample	<0.05

For comparison, the total neutron cross sections of ^{238}U obtained in this work are plotted together with data of other authors from EXFOR-2003 and ENDF/B6.8 libraries. (see Fig. 3.2)

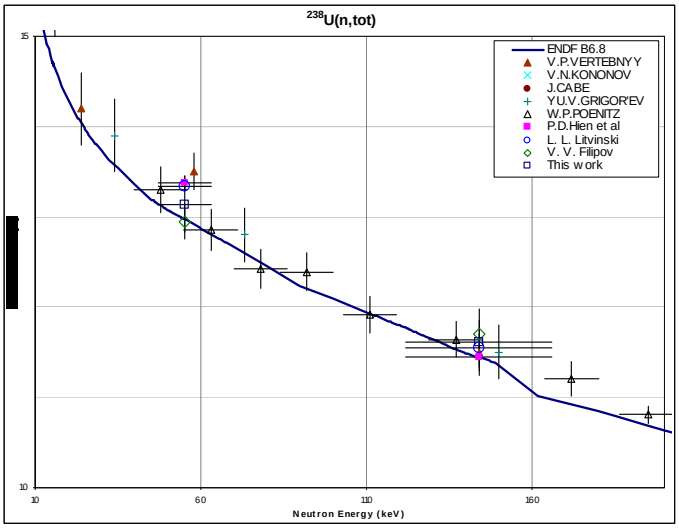

Fig. 3.2: Total neutron cross section of ^{238}U in keV region

REFERENCE

[1]. Vương Hữu Tấn và cộng sự, *Nghiên cứu ứng dụng các hiệu ứng tương tác của nơtron, gamma và các hạt mang điện được tạo ra trên các thiết bị đã có sẵn ở Việt Nam*, Đề tài cấp nhà nước KC-09-08,1995.

[2]. *^{3}He Proportional Counters*. http://www.centronic.co.uk

[3]. T. W. Crane et al. *Neutron Detectors*. www.fas.org/sgp/othergov/doe/lanl/lib-www/la-pubs/00326408.pdf

[4]. *Janis 2.2*, OEDC Nuclear Energy Agency, http://www.nea.fr/janis/ June 2005.

[5]. Handbook on Nuclear Activation Data, Technical Reports Series No. 273, International Atomic Energy Agency, Vienna, 1987.

[6]. Nguyễn Cảnh Hải và cộng sự, *Xây dựng thiết bị kiểm soát dòng nơtron dùng ống đếm BF3*, Đề tài cấp Bộ 2003-2005.

[7]. Nguyễn Cảnh Hải và cộng sự, *Xây dựng quy trình phân tích định lượng các nguyên tố B, H, N, S, C, P, Si, Cd, Gd trong mẫu đất đá và mẫu sinh học sử dụng thiết bị phân tích kích hoạt nơtron gamma tức thời (PGNAA) mới được nâng cấp tại lò phản ứng hạt nhân Đà Lạt*. Báo cáo tổng kết đề tài KHCN cấp cơ sở 2005.

[8]. Herve DERRIEN et al, *Average Total Neutron Cross Section of ^{233}U, ^{235}U and ^{239}Pu from ORELA Transmission Measurements and Statistical Analysis of the Data,* Oak Ridge National Laboratory, Oak Ridge, TN 37831, USA

[9]. L. L. Litvinski, V. A. Libman, A. V. Murzin, Preprint, Kiev, Inst. of Nucl. Phys., 85-35, 1985.

[10]. V. V. Filipov, in INDC (CCP)-335, p.45, IAEA, August 1991.

[11]. Pham Zuy Hien et al, *Total neutron cross-section of U-238 as measured with filtered neutrons of 55 keV and 144 keV*, INDC(NDS)-0256, Vienna, 1992.

[12]. High Voltage Power Supply Model 201, MoKSp, IAEA, 1986.

[13]. SCA / TECDOC-563 / IAEA, 1989.

[14]. PIC 18F4550, Microchip Technology, http://www.digchip.com.

MICROSCOPIC STUDY OF ELASTIC AND INELASTIC ALPHA-NUCLEUS SCATTERING AT MEDIUM ENERGIES

Dao Tien Khoa, Hoang Si Than, Do Cong Cuong, Ngo Van Luyen
Nguyen Ngoc Quynh and Nguyen Tuan Anh

Institute for Nuclear Science and Technology, VAEC, Vietnam.

ABSTRACT: Analyses of the inelastic $\alpha+^{12}C$ scattering at medium energies have indicated that the strength of the Hoyle state (the isoscalar 0_2^+ excitation at 7.65 MeV in ^{12}C) seems to exhaust only 7 to 9% of the monopole energy weighted sum rule (EWSR), compared to about 15% of the EWSR extracted from inelastic electron scattering data. The full monopole transition strength predicted by realistic microscopic α-cluster models of the Hoyle state can be shown to exhaust up to 22% of the EWSR. To explore the missing monopole strength in the inelastic $\alpha+^{12}C$ scattering, we have performed a fully microscopic folding model analysis of the inelastic $\alpha+^{12}C$ scattering at E_{lab}=104 to 240 MeV using the 3-α resonating group wave function of the Hoyle state obtained by Kamimura, and a complex density-dependent M3Y interaction newly parametrized based on the Brueckner Hartree Fock results for nuclear matter. Our folding model analysis has shown consistently that the missing monopole strength of the Hoyle state is not associated with the uncertainties in the analysis of the $\alpha+^{12}C$ scattering, but is most likely due to the short lifetime and weakly bound structure of this state which significantly enhances absorption in the exit $\alpha+^{12}C^*\left(0_2^+\right)$ channel.

Given a vital role in the stellar synthesis of Carbon, the isoscalar 0^+_2 state at 7.65 MeV in ^{12}C (known as the Hoyle state) has been studied over the years in numerous experiments. Although this state was clearly identified long ago on the inelastic $\alpha+^{12}C$ scattering at medium energies [1-4] and inelastic electron scattering [5] as an isoscalar E0, our knowledge about its unique structure is still far from complete [6]. To investigate the missing monopole strength of the Hoyle state, we have performed a consistent folding model analysis of the inelastic $\alpha+^{12}C$ scattering at E_{lab}=104 to 240 MeV using microscopic nuclear densities obtained from the 3-α RGM wave functions by Kamimura [7], and a new complex density-dependent M3Y interaction. Excepting the early work by Bauhoff [8] where a density independent Gaussian has been used as αN interaction in the single-folding calculation, other studies mentioned here have used the well-known DDM3Y [9] interaction in the double-folding calculation of the $\alpha+^{12}C$ potentials. Since the DDM3Y interaction is real, the imaginary parts of both the optical potential (OP) and inelastic FF were chosen phenomenologically in these studies. For example, in the CC analysis of the $\alpha+^{12}C$ scattering by Ohkubo and Hirabayashi [10,11] the imaginary inelastic FF was neglected and parameters of the Woods-Saxon imaginary OP were adjusted separately for each exit channel to obtain a good CC fit to the measured cross sections. Although one could achieve a reasonable description of the inelastic $\alpha+^{12}C$ scattering data in such a CC analysis, an arbitrary choice of the imaginary potentials makes it difficult to estimate accurately the absolute E0 transition strength. Up to now, the E0 strength of the Hoyle state has been deduced from the DWBA or CC analyses of the inelastic ^{3,4}He,^{6}Li + ^{12}C scattering [12-13] using the breathing mode (BM) model [16] for the nuclear transition density.

$$\rho_{0_1^+\to 0_2^+}(r) = -\beta\left[3\rho_0(r) + r\frac{d\rho_0(r)}{dr}\right], \qquad (1)$$

where $\rho_0(r)$ is the ground-state (g.s.) density of ^{12}C. In this case, $S_0 = [\beta/\beta_{\max}]^2$, where $\beta_{\max}$ is the deformation parameter required for a monopole excitation to exhaust 100% of the EWSR (see Eq. (3.5) in Ref.[14]). The inelastic scattering FF is then obtained by (double) folding the transition density (1) with the effective nucleon-nucleon (*NN*) interaction and projectile g.s. density [15,16]. The CDJLM interaction was used to calculate the complex OP and inelastic FF for the microscopic DWBA and CC analyses of the elastic and inelastic $\alpha+^{12}C$ scattering data at E_{lab}=104 [1,2], 139 [3], 172.5 [4] , and 240 MeV [13]. The generalized double-folding method [16] was used to calculate the complex $\alpha-nucleus$ potential as the following HF-type matrix element of the CDJLM interaction.

$$U_F = \sum_{i\in a, j\in A, j'\in A'}\left[\langle ij'|u_D|ij'\rangle + \langle ij'|u_{EX}|j'i\rangle\right] \qquad (2)$$

where A and A* are states of the target in the entrance- and exit channel of the $\alpha-nucleus$ scattering, respectively. Thus, Eq.(2) gives the elastic (diagonal) OP if A*=A and inelastic (transition) FF if otherwise.

The OM and CC descriptions of the elastic $\alpha+^{12}C$ scattering at the considered energies are shown in Fig.1. The DWBA results obtained with the complex folded OP and inelastic folded FF are compared with the measured cross section for inelastic $\alpha+^{12}C$ scattering to the Hoyle state in Figs. 2. We found that the calculated DWBA cross sections systematically overestimate data at all energies if the inelastic folded FF is obtained with

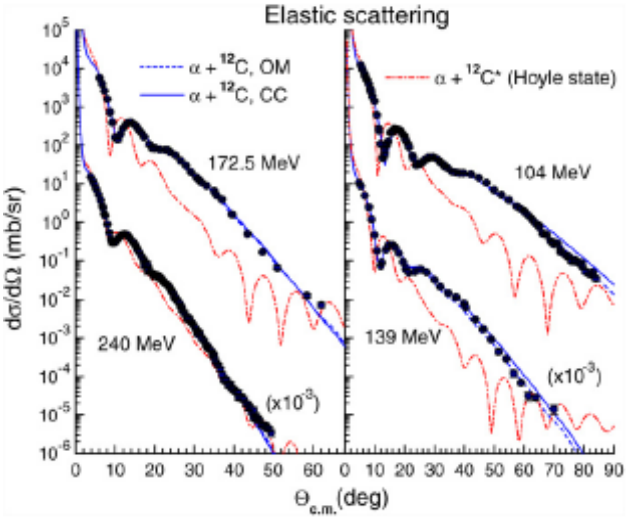

Fig. 1: Elastic $\alpha+^{12}C$ scattering data measured at Elab=104[1,2], 139[3], 172.5 [4] and 240 MeV [13] in comparison with the OM and CC results given by the complex folded OP. The elastic α scattering on the Hoyle state is predicted by the OM calculation using the diagonal.

The *unrenormalized* RGM transition density [7]. Given the accurate choice of the density dependent *NN* interaction and nuclear densities, this discrepancy is clearly

not associated with usual uncertainties of the folding model analysis of $\alpha - nucleus$ scattering [17]. Since the RGM transition density has been proven to reproduce nicely the (**e,e'**) data [7,18], the folding + DWBA results shown in Figs.2 might indicate a ``suppression" of the monopole E0 strength occurred in the inelastic $\alpha+^{12}C$ scattering. To further probe this effect, we have used a realistic Fermi distribution for the g.s. density of ^{12}C [19] to generate the BM transition density (1) for the DWBA analysis of inelastic scattering to the Hoyle state. We have fixed the monopole deformation parameter β so that (1) gives exactly the same E0 transition strength as that given by the RGM transition density and, hence, exhausts 22.8% of the isoscalar monopole EWSR as discussed above. As can be seen from Figs.2, the DWBA cross sections given by the inelastic FF folded with the BM transition density for the Hoyle state are very close to those given by the RGM transition density.

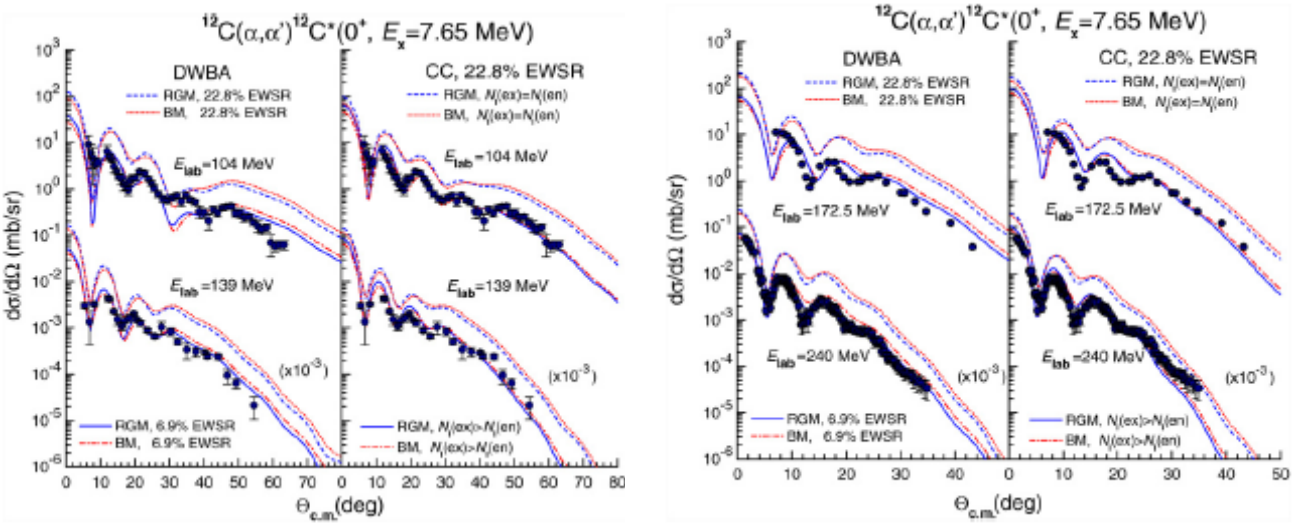

Fig. 2: Inelastic $\alpha+^{12}C$ scattering data at E_{lab}=104 [1,2], 139 [3], 172.5 [4], and 240 [13] MeV for the 0_2^+ state of ^{12}C in comparison with the DWBA and CC results given by the complex folded OP and inelastic FF obtained with two choices of the transition density for the 0_2^+ state. A good DWBA description of the data is reached only if the the transition densities are scaled by a factor of 0.55 which reduces E0 sum rule strength to S_0=6.9% of the monopole EWSR.

To match the calculated DWBA cross section to the data points, we need to scale both transition densities by a factor of 0.55 which reduces the sum rule strength of the Hoyle state to S_0= 6.9% of the EWSR. Such a small sum rule strength is significantly below the empirical range of 15 - 20% of the EWSR discussed above. Given an accurate energy dependence of the CDJLM interaction, with its density dependence carefully calibrated against the BHF results at each energy, the RGM and BM transition densities scaled by the same factor of 0.55 give reasonable DWBA descriptions of the data at four considered energies. The sum rule strength of the Hoyle state found in our DWBA analysis is comparable to that (7.6± 0.9%) found in the folding + DWBA analysis of the inelastic $\alpha+^{12}C$ scattering at 240 MeV [15], where a Gaussian has been used for the αN interaction in the folding calculation of the OP and inelastic FF.

In conclusion, a realistic (complex) density dependence was introduced into the M3Y-Paris interaction, based on the Brueckner Hartree Fock calculation of nuclear matter, for the folding model study of the $\alpha+^{12}C$ scattering at E_{lab}=104 to 240 MeV. Given an accurate estimation of the bare $\alpha+^{12}C$ optical potential, our folding model analysis has shown consistently that there should be an enhancement of absorption in the exit $\alpha+^{12}C^{*}$ (0^{+}_{2}) channel due to the short lifetime and weakly bound structure of the Hoyle state, which accounts for the ``missing" monopole strength of the Hoyle state observed earlier in the DWBA analysis of inelastic $\alpha+^{12}C$ scattering.

REFERENCES

[1]. G. Hauser, R. Lohken, H. Rebel, G. Schatz, G.W. Schweimer, and J. Specht, Nucl. Phys. A 128 (1969) 81.

[2]. J. Specht, G.W. Schweimer, H. Rebel, G. Schatz, R. Lohken, G. Hauser, Nucl. Phys. A 171 (1971) 65.

[3]. S.M. Smith, G. Tibell, A.A. Cowley, D.A. Goldberg, H.G. Pugh, W. Reichart, N.S. Wall, Nucl. Phys. A 207 (1973) 273.

[4]. S. Wiktor, C. Mayer-B\"oricke, A. Kiss, M. Rogge, P. Turek, and H. Dabrowski, Acta Phys. Pol. B 12 (1981) 491;

A. Kiss, C. Mayer-B\"oricke, M. Rogge, P. Turek, and S. Wiktor, J. Phys. G 13 (1987) 1067.

[5]. P. Strehl, Z. Phys. 234 (1970) 416.

[6]. M. Freer, J. Phys. G 34 (2007) 789;
M. Freer, to appear in Proceedings of Intern. Symp. on Physics of Unstable Nuclei (ISPUN07) (World Scientific: Singapore).

[7]. M. Kamimura, Nucl. Phys. A 351 (1981) 456; M. Kamimura, private communication.

[8]. W. Bauhoff, Phys. Lett. 139 B (1984) 223.

[9]. A.M. Kobos, B.A. Brown, P.E. Hodgson, G.R. Satchler, A. Budzanowski, Nucl. Phys. A 384 (1982) 65.

[10]. Y. Hirabayashi, S. Ohkubo, Phys. At. Nuclei 65 (2002) 683.

[11]. S. Ohkubo, Y. Hirabayashi, Phys. Rev. C 70 (2004) 041602(R).

[12]. D. Lebrun, M. Buenerd, P. Martin, P. de Saintignon, G. Perrin, Phys. Lett. 97 B (1980) 358.

[13]. B. John, Y. Tokimoto, Y.W. Lui, H.L. Clark, X. Chen, D.H. Youngblood, Phys. Rev. C 68 (2003) 014305.

[14]. D.J. Horen, J.R. Beene, G.R. Satchler, Phys. Rev. C 52 (1995) 1554.

[15]. D.T. Khoa, G.R. Satchler, W. von Oertzen, Phys. Rev. C 56 (1997) 954.

[16]. D.T. Khoa, G.R. Satchler, Nucl. Phys. A 668 (2000) 3.

[17]. G.R. Satchler, D.T. Khoa, Phys. Rev. C 55 (1997) 285.

[18]. Y. Funaki, A. Tohsaki, H. Horiuchi, P. Schuck, G. Ropke, Eur. Phys. J. A 28 (2006) 259.

[19]. D.T. Khoa, Phys. Rev. C 63 (2001) 034007.

PAPERS PUBLISHED IN RELATION TO THE PROJECT

1. Hoang Sy Than, Dao Tien Khoa, Nguyen Van Giai, Elias Khan, "Continuum properties of the Hartree-Fock mean field with finite-range interactions.- Báo cáo tại Intern. Symposium on Physics of Unstable Nuclei (ISPUN2007) tổ chức tại Hội An (http://www.inst.gov.vn/ispun07/).
2. Do Cong Cuong and Dao Tien Khoa, "Microscopic study of the inelastic alpha+^{12}C scattering.- Báo cáo tại Intern. Symposium on Physics of Unstable Nuclei (ISPUN2007) (http://www.inst.gov.vn/ispun07/).
3. Đào Tiến Khoa, "Nghiên cứu phương trình trạng thái của vật chất hạt nhân qua phản ứng tán xạ hạt nhân.- Báo cáo mời tại phiên toàn thể của Hội nghị Khoa học và Công nghệ Hạt nhân toàn quốc lần thứ 7, Đà Nẵng, tháng 8/2007.
4. Hoàng Sỹ Thân, Đỗ Công Cương, Đào Tiến Khoa, "Nghiên cứu vi mô những kích hoạt hạt nhân tương tự đồng khối và hiệu ứng liên quan trong vật lý thiên văn..- Báo cáo tại hội nghị khoa học và công nghệ hạt nhân toàn quốc lần thứ 7, Đà Nẵng, tháng 8/2007.
5. Đỗ Công Cương, Đào Tiến Khoa, Nguyễn Ngọc Quỳnh. Tương tác Nucleon-Nucleon hiệu dụng phức từ tính toán Brueckner Hartree-Fock.- Báo cáo tại Hội nghị Khoa học và Công nghệ Hạt nhân toàn quốc lần thứ 7, Đà Nẵng, tháng 8/2007.

1.2 - Reactor Physics, Reactors and Nuclear

CONCEPTUAL NUCLEAR DESIGN OF TWO MODELS OF RESEARCH REACTOR PROPOSED FOR VIETNAM

Nguyen Nhi Dien, Huynh Ton Nghiem, Le Vinh Vinh and Vo Doan Hai Dang

Nuclear Research Institute, VAEC, Vietnam.

ABSTRCT: The joint study on the development of a new research reactor model for Vietnam was done. The KAERI (Korea Atomic Energy Research Institute) experts and DNRI (Dalat Nuclear Research Institute) researchers developed an advanced HANARO reactor (AHR), a 20-MW open-tank-in-pool type reactor, upward cooled and moderated by light water, reflected by heavy water and rod type fuel assemblies used. Based on the AHR model, a MTR reactor with plate fuel assemblies was developed.

Computer codes named MCNP and MVP/BURN were used. Major analyses have been done for the relevant nuclear design parameters such as the neutron flux and power distributions, reactivity coefficients, control rod worth, etc. in both with clean, unperturbed core and equilibrium core condition.

In case of AHR model, calculation results using MVP/BURN and MCNP codes were compared with the results using HELIOS and MCNP codes by KAERI experts and they are in a good agreement.

1. Introduction

A research reactor is designed in conformity with user's requirements; especially the reactor type, power, and core configuration, systems and the installed experimental facilities depend on the application purposes of a research reactor. Hence, a flexible design is an indispensable feature when considering a future expansion of its experimental facilities.

The major basic principles to develop a reference model of AHR and MTR reactors are as follows:

1) Multipurpose research reactor with a medium power
2) Application of the HANARO concepts
3) High ratio of flux to power
4) High Safety and Economics
5) Sufficient spaces and expandability of the facility for various experiments.

The detailed nuclear design requirements for the AHR and MTR are considered in two parts, functional and performance requirements. The functional requirements are:

1) The overall power coefficient of the reactivity shall be negative for all operational and accident conditions.

2) Temperature and void coefficients of the reactivity associated with the fuel and core shall be negative for all operational states and accidents conditions.

3) The shutdown margin should be at least 1% $\Delta k/k$ regardless of any changes in the reactor condition, by taking into account the worst set of reactivity effects from

experiments and irradiations, and with the most reactive control assembly stuck in its most reactive position.

4) The second reactor shutdown system should be prepared to improve the reactor safety and its shutdown reactivity margin should be at least 1% Δk/k for shutting down the reactor for all relevant design basis fault sequences.

5) The excess reactivity for conducting experiments should be at least 10 mk at the EOC of the reactor.

6) A reactivity of 15 mk for the Xe override should be reserved.

7) The shutdown system should maintain the reactor in a sub-critical condition.

Performance requirements are as below:

1) The maximum unperturbed thermal neutron flux at an irradiation site inside the core and reflector region should be greater than $4.0x10^{14}$ and $4.0x10^{14}$ n/cm^2.s, respectively. The maximum unperturbed fast neutron flux at an irradiation site inside the core should be $1.3x10^{14}$ n/cm^2.s.

2) The maximum local power peaking factor should be less than 3.0.

3) The average discharge burn-up of the fuel assembly should be higher than 50% of the initial fissile heavy material, U-235.

4) The reactor operating cycle should be longer than 30 days.

5) The axial neutron flux gradient in the reflector region should be within ±20% over a length of 50 cm.

2. Structure of the proposed reactors

The reactor core is composed of 23 hexagonal lattices (4.48 cm in side) for AHR and square lattices (8.15 cm in side) for MTR, and their active length is 70 cm. The heavy water reflector tank of 200 cm in diameter and 120 cm in height surrounds the core. The nominal core consists of 16 standard fuel assemblies, 4 control fuel assemblies and 3 in-core irradiation sites. 4 control rods are used for both reactor control system and reactor protection system. The active volumes are 1199.5 x 70 cm^3 for AHR and 1527.7 x 70 cm^3 for MTR, the amount of U-235 is 9,87 kg for AHR and 10,12 kg for MTR. Figure 1a and Figure 1b show a horizontal cross sectional view of the AHR and MTR cores, respectively. Table 1 summarizes the main characteristics of the AHR and MTR cores.

Table 1: Main characteristics of the AHR and MTR core

No.	Characteristics	AHR reactor	MTR reactor
1	Core volume, cm^3	1199.5 x 70	1527.7 x 70
2	Number of fuel assemblies	16 + 4	16 + 4
3	Number of control rods	4	4
4	Absorb material of CR	Hf	Hf
5	Amount of U-235, kg	9,87	10,12

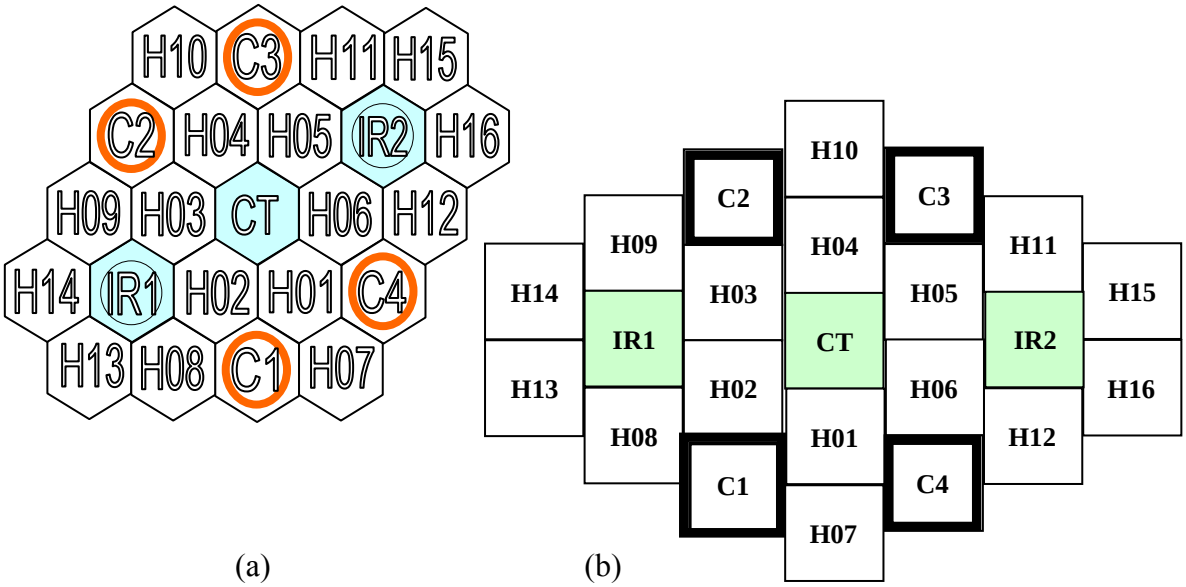

Fig. 1: Cross section view of the AHR core (a) and MTR core (b)

Fuel assemblies of AHR are similar of HANARO reactor in geometry, but with higher Uranium density. Fuel assemblies of MTR are similar of OPAL reactor, but with longer length. Fuel type is U_3Si_2-Al with enrichment of 19.75 % U^{235}.

For AHR, 2 kinds of fuel assemblies are used. A standard fuel assembly is composed of 36 fuel rods and loaded into the hexagonal flow tubes. A control fuel assembly consists of 18 fuel rods and is loaded into the cylindrical flow tubes. Control and shut-off rods of a tubular type are inserted into or withdrawn from the core by moving the surrounding cylindrical flow tubes up and down.

For MTR, 2 kinds of fuel assemblies are used, standard and following control rod fuel assemblies. Each fuel assembly has 8 cm x 8 cm in square section for standard and 6.8 cm x 6.8 cm for following control rod fuel assemblies, and more than 1 m in length. In each fuel assembly there are 21 fuel plates for standard and 17 fuel plates for following control rod fuel assemblies. The Cd wires with 0.04 cm in diameter are sticked on two edges of each fuel assembly as burnable poisoning material for reactivity control.

A Control Absorber Rod (CAR) is a hollow cylinder type with 0.4 cm thickness for AHR and a square cylinder type with a 0.5 cm thickness for MTR. They are made of natural Hf with a 70 cm in length. In a case of AHR, CAR moves up and down while embracing an 18-elements fuel assembly and in a case of MTR, CAR is connected above following fuel assembly in aluminum square cylinder type with a 2.95 cm thickness. When CAR moves up, following fuel assembly moves up to fill up the place of CAR went out.

The concept of using control rods sharing for both the Reactor Protection System (RPS) and the Reactivity Control System (RCS) is adopted. Even with this common control rods concept, the RPS and RCS are independently separated from each other in terms of an instrumentation and control.

The heavy water reflector tank provides 4 tangential beam tubes and a total of 18 vertical irradiation holes with different diameters. Thus 10 holes are selected for a radioisotope production (RI), 3 holes for a neutron activation analysis (NAA), 2 holes for hydraulic transfer system (HTS), 3 holes for a neutron transmutation doping (NTD). There are 4 beam tubes, including 2 for thermal neutron, 1 for cold neutron (CN) and 1 for neutron radiography (NR).

I. 3. Results of calculation and nuclear analysis

For AHR, MVP/BURN and MCNP computer codes were used. Calculation results were compared with the results of KAERI experts using HELIOS and MCNP codes and in a good agreement. It shows that MVP/BURN and MCNP codes are suitable for reactor design calculation. For MTR, only MVP/BURN and MCNP codes were used. The analysis results are described for both a fresh core and an equilibrium core. A fresh core is a core loaded with all new fuels which can not be configured practically. An equilibrium core is dependant on the choice of the reactor owner, and it can be configured differently according to its operation policy.

3.1. Fresh core

Neutron flux distribution. The neutron fluxes were calculated for an unperturbed clean core by the MCNPX code using a mesh tally. The neutron flux is grouped into fast and thermal groups, whose cut-off energies for each of them are above 1MeV and below 0.625eV, respectively. The position of the peak thermal flux in the reflector is predicted to be about 28 cm from the core center, and the fast flux reduces exponentially from the core.

Reactivity of control rods and reactivity effect of irradiation facilities. The calculation results shown in Table 2. The total control rods worth is 178.5 mk and 182.4 mk for AHR and 217.3 mk and 217.7 mk for MTR with and without irradiation facilities in the reflector, respectively. Reactivity effect of irradiation facilities are about 20.2 mk for AHR and 28.9 mk for MTR in case of control rods withdrawn.

Table 2: Reactivity of irradiation facilities and control rods

Reactor type	**Irradiation facility**	**Position of CAR**	**k-eff**	**Reactivity (mk)**	
				CAR	Irradiation facilities
AHR	Non	Full out	1.2570	178.5	20.2
		Full in	1.0266		
	Yes	Full out	1.2259	182.4	
		Full in	1.0019		
MTR	Non	Full out	1.1296	217.3	28.9
		Full in	0.9070		
	Yes	Full out	1.0939	217.7	
		Full in	0.8835		

Neutron flux distribution at irradiation facilities. Table 3 shows that the neutron fluxes at irradiation holes of AHR and MTR are satisfied with application purposes.

Table 3: Neutron flux at irradiation holes

Position	AHR reactor				MTR reactor			
	Maximum		Average		Maximum		Average	
	Thermal	Fast	Thermal	Fast	Thermal	Fast	Thermal	Fast
CT	4.46E+14	1.46E+14	3.04E+14	9.80E+13	4.01E+14	1.13E+14	2.87E+14	8.06E+13
IR1	3.21E+14	1.18E+14	2.23E+14	8.29E+13	3.37E+14	9.31E+13	2.49E+14	6.76E+13
IR2	3.16E+14	1.20E+14	2.23E+14	8.26E+13	3.33E+14	9.16E+13	2.46E+14	6.65E+13
CNS	8.71E+13	1.15E+12	7.01E+13	8.76E+11	8.49E+13	1.69E+12	6.48E+13	1.24E+12
ST1	1.37E+14	1.96E+12	-	-	1.40E+14	3.23E+12	-	-
ST2	2.40E+14	3.47E+12	-	-	1.79E+14	1.01E+13	-	-
NR	1.28E+14	3.20E+11	-	-	1.28E+14	1.32E+12	-	-
NTD1	4.74E+13	1.13E+11	4.31E+13	8.12E+10	4.93E+13	4.19E+11	4.26E+13	3.19E+11
NTD2	4.63E+13	9.91E+10	4.24E+13	7.60E+10	5.29E+13	4.84E+11	4.57E+13	3.56E+11
NTD3	5.16E+13	2.43E+11	4.70E+13	2.04E+11	4.64E+13	5.21E+11	3.93E+13	3.78E+11
HTS1	6.96E+13	3.42E+11	5.96E+13	2.71E+11	7.02E+13	6.30E+11	5.79E+13	5.03E+11
HTS2	2.23E+13	2.07E+10	1.93E+13	1.39E+10	2.25E+13	2.81E+10	1.97E+13	2.29E+10
NAA1	1.39E+14	4.96E+11	1.20E+14	3.88E+11	1.22E+14	8.15E+11	1.05E+14	6.27E+11
NAA2	4.11E+13	-	3.59E+13	-	4.00E+13	-	3.55E+13	-
NAA3	1.74E+13	-	1.52E+13	-	1.53E+13	-	1.35E+13	-
RI1	3.53E+14	1.47E+13	2.60E+14	9.05E+12	2.31E+14	1.49E+13	1.69E+14	9.28E+12
RI2	3.44E+14	1.42E+13	2.57E+14	8.91E+12	2.18E+14	1.47E+13	1.58E+14	9.13E+12
RI3	2.46E+14	4.03E+12	1.85E+14	2.54E+12	2.10E+14	1.53E+13	1.58E+14	9.56E+12
RI4	2.48E+14	4.23E+12	1.86E+14	2.82E+12	2.03E+14	1.45E+13	1.52E+14	8.92E+12
RI5	2.24E+14	3.12E+12	1.67E+14	2.10E+12	2.15E+14	1.55E+13	1.58E+14	9.51E+12

Power distribution and power peaking factors. Table 4 shows the maximum power peaking factors and linear power following the control rods position of AHR. Such values at position of 300 mm are 2.33 and 96.5 kW/m, respectively. In case of MTR, such values at position of 300 mm are 2.82 and 187.7 kW/m, respectively.

Table 4: Maximum peaking factors and maximum linear power of AHR

Position of control rods (mm)	Maximum peaking factors (Fq)	Maximum linear power (kW/m)
550	2.02	83.8
500	2.10	87.1
450	2.14	88.8
400	2.26	93.6

350	2.29	94.9
300	2.33	96.5
250	2.28	94.4
0	2.04	84.5

Table 5 shows the power distribution and peaking factors for each fuel assembly with the control rods position at 300 mm. Results show that maximum peaking factors of MTR are even still less than 3.0 but relatively high as 2.82.

Table 5: Power distribution and peaking factors (position of control rods at 300 mm)

Position	AHR reactor			MTR reactor			
	Power	Fr	Fq	Power	Fr	Fq	*
H01	1085	0.98	2.11	1086	1.04	2.80	2.37
H02	1188	1.07	2.13	1117	1.07	1.94	1.89
H03	1193	1.07	2.13	1118	1.07	1.95	1.89
H04	1101	0.99	2.12	1089	1.04	2.82	2.37
H05	1194	1.07	2.16	1129	1.08	1.98	1.91
H06	1193	1.07	2.15	1125	1.08	1.96	1.90
H07	988	0.89	1.90	940	0.90	2.16	1.84
H08	1090	0.98	2.00	1089	1.04	2.35	1.97
H09	1130	1.02	2.10	1088	1.04	2.37	1.99
H10	1054	0.95	2.05	945	0.90	2.20	1.87
H11	1127	1.01	2.03	1125	1.08	2.42	2.04
H12	1099	0.99	1.98	1100	1.05	2.39	2.01
H13	1103	0.99	1.79	1024	0.98	1.87	1.60
H14	1137	1.02	1.83	1017	0.97	1.86	1.60
H15	1136	1.02	1.78	1076	1.03	2.03	1.74
H16	1120	1.01	1.83	1057	1.01	1.82	1.59
C1	506	0.91	2.16	714	0.84	2.04	1.80
C2	524	0.94	2.33	714	0.84	2.04	1.81
C3	520	0.94	2.30	729	0.86	2.10	1.85
C4	510	0.92	2.23	717	0.85	2.03	1.80

Reactivity Coefficients. An isothermal temperature coefficient can be defined as a reactivity effect by the temperature and density changes of all the reactor components such as its coolant, reflector, fuel, etc. In this calculation, it was calculated for temperature changes at every 5 degree in the range of 20 to 50 degree. Table 6 shows the isothermal temperature coefficient. From Table 6, a power defect of -3.0 mk should be considered for AHR and -6.0 mk for MTR.

Table 6: Isothermal temperature coefficient

Temperature [^oC]	H_2O density [gm/cc]	D_2O density [gm/cc]	Reactivity defect [mk]		Coefficient [mk/^oC]	
			AHR	MTR	AHR	MTR
20	0.9983	1.1053	0	0		
25	0.9971	1.1045	-0.2893	-0.8715	-0.0579	-0.1743
30	0.9957	1.1033	-0.6361	-1.7882	-0.0694	-0.1833
35	0.9940	1.1017	-1.0421	-2.7322	-0.0812	-0.1888
40	0.9923	1.1000	-1.5089	-3.7200	-0.0934	-0.1976
45	0.9902	1.0979	-2.0381	-4.7665	-0.1058	-0.2093
50	0.9880	1.0957	-2.6315	-5.8550	-0.1187	-0.2177

Prediction of excess reactivity of the equilibrium core. The reactivity for the equilibrium core should be evaluated to meet the reactivity requirements for an equilibrium core. The expected excess reactivity to compensate the effects for fuel burnup, power defect, Xe accumulation, Xe override and irradiation targets at the beginning of a cycle in an equilibrium state is presented in Table 7. The maximum excess reactivity at the beginning of a cycle (BOC) is expected to be 113 mk for AHR and 93 mk for MTR.

Table 7: Reactivity demands for an equilibrium core

Items	Excess reactivity (mk)	
	AHR reactor	MTR reactor
Fuel burnup	35~40	15~20
Power and temperature defect	3	6
Xe accumulation	35~40	33~38
Xe override	15	15
Irradiation targets	5~15	5~15
Total	93~113	74-94

3.2. Equilibrium Core

Fuel management. A candidate model for an equilibrium core can be easily obtained by considering a target discharge burnup, a cycle length and an excess reactivity at a BOC and an EOC. There may be many candidate models according to the number of reloaded fuel assemblies and the loading pattern.

Table 8: Burnup and reactivity for the equilibrium cores of AHR

Parameter	6-batch core (day)			9-batch core (day)		
Cycle (day)	36	37	38	26	27	28
Average Burnup (%U-235)						
- BOC	24.1	24.6	25.2	26.8	27.7	28.5
- EOC	32.7	33.5	34.3	33.0	34.2	35.2
- Discharge	51.9	53.2	54.6	55.4	57.4	59.2
Reactivity (mk)						
- BOC (eq. Xe)	69.43	67.72	65.80	60.55	57.57	54.77
- EOC (eq. Xe)	29.43	26.72	23.30	28.29	23.60	19.58

Burnups and reactivities of an equilibrium core. Table 9 shows the results of burnups and reactivities with different cycles. It shows that the 36-day cycle for AHR and 34-day cycle for MTR are satisfied with the purpose that average burnup of discharged fuel assemblies are more than 50%, using reactivity is about 30 mk and the working cycle is more than 30 days.

Table 9: Burnups and reactivities of an equilibrium core with different cycles

Parameter	AHR reactor			MTR reactor		
Cycle (day)	35	36	37	33	34	35
Average Burnup (%U-235)						
- BOC	23.43	24.02	24.61	22.38	23.04	23.70
- EOC	31.82	32.65	33.47	29.08	29.94	30.81
- Discharge	50.35	51.77	53.18	48.65	49.91	51.17
Excess Reactivity(mk)						
- BOC (no Xe)	111.9	109.9	107.8	87.8	85.8	83.6
- Fuel Depletion	37.5	38.7	39.9	15.1	16.7	18.3
- Xenon buildup	38.1	38.1	38	36.2	36.3	36.3
- Power coefficient	3.0	3.0	3.0	3.0	3.0	3.0
- EOC (eq. Xe)	33.4	30.1	26.9	33.5	29.8	26.0
- Shutdown margin	15.0	17.1	19.6	22.2	24.2	26.4

Power distribution. Power distributions for the equilibrium core of 6 cycles were evaluated and shown in Table 10. The maximum total peaking factor Fq of AHR was 2.56. This value is higher than of fresh core as of 2.33. For MTR this value was 2.79 and 2.82, respectively.

Table 10: Maximum peaking factors of the equilibrium cores

Reactor type	Parameters	Cycle					
		1	2	3	4	5	6
AHR	FA position	H02	C2	H01	H03	C3	H04
	Fq	2.47	2.56	2.50	2.46	2.56	2.49
MTR	FA position	H09	H04	H01	H11	H04	H01
	Fq	2.69	2.77	2.74	2.76	2.76	2.79

Reactivity Coefficients.

+ The fuel temperature coefficient is estimated as being negative and about -0.002 mk/K and -0.001 mk/K for AHR and MTR, respectively. However, this effect is so small that it can be negligible.

+ The coolant temperature coefficient is negative in the temperature range from 293 to 400K and about 0.059mk/K and 0.11 mk/K for AHR and MTR, respectively.

+ The void coefficients for the coolant are negative and about 1.23, 1.37 and 1.48 mk/% for the ranges of 0~5%, 5~10% and 10~20%, respectively for AHR. For MTR, these coefficients are negative and about 1.79, 1.97 and 2.25 mk/% for the ranges of 0~5%, 5~10% and 10~20%, respectively

+ The temperature coefficient for the heavy water due to a density decrease is negative and about 1.26 and 0.79 mk/% in the range of 0~5% for AHR and MTR, respectively. Table 11 summarizes the above-mentioned values.

Table 11: Temperature coefficients

Parameter	AHR reactor	MTR reactor
Fuel temperature coefficient (mk/K)	<-0.002	<-0.001
Light water temperature coefficient (mk/K)		
- Coolant	-0.059	-0.11
- Moderator	0.060	
Density coefficient for light water (mk/%)		
0 - 5 %	-1.23	-1.79
5 - 10 %	-1.37	-1.97
10 - 20 %	-1.48	-2.25
Density coefficient for heavy water (mk/%)		
0 - 5 %	-1.26	-0.79

4. Conclusion

Major analyses have been done for the relevant nuclear design parameters such as the neutron flux and power distributions, reactivity coefficients, control rod worth, etc. using MCNP, MVP/BURN codes.

For a clean, unperturbed core condition such that the fuels are all fresh and there are no irradiation holes in the reflector region, the fast neutron flux ($E_n \geq 1.0$ MeV) reaches more than 1.0×10^{14} n/cm^{2}s and the maximum thermal neutron flux ($E_n \leq 0.625$ eV) reaches more than 4.0×10^{14} n/cm^{2}s in the core region. In the reflector region, the thermal neutron peak occurs about 28 cm far from the core center and the maximum thermal neutron flux is estimated to be 4.0×10^{14} n/cm^{2}s.

The cycle length was estimated more than 30 days long with a refueling scheme for 6-cycle equilibrium core. The excess reactivities at a BOC and an EOC are satisfied to user's requirements. The assembly average discharge burnup is more than 50% of initial U-235 loading. For the proposed fuel management scheme, the maximum peaking factor Fq was calculated less than 3.0. The shutdown margins by the 1st and 2nd shutdown systems were estimated more than 1%. Both the isothermal temperature coefficient and the power coefficient were negative, so the AHR and MTR cores are characterized as being inherently safe.

It was shown that AHR model is better than MTR model in the economic aspect, but the inherent safety of MTR model is higher than of AHR model.

REFERENCES

[1]. Safety of Research Reactors, Safety Requirements, No. NS-R-4, IAEA, 2005.

[2]. B. C. Lee et al., A Study on the Configuration of Irradiation Holes in the AHR, Technical report, KAERI/TR-3302/2007, Jan., 2007.

[3]. C. Park et al., "Design Approach to the Development of an Advanced HANARO Research Reactor", HANARO Symposium, Daejeon, Korea, April, 2005.

[4]. J. F. Briesmeister (Editor), "MCNP-A General Monte Carlo N-Particle Transport Code", LA-12625-M, Los Alamos National Lab., 1993.

[5]. Denise B. Pelowitz (Editor), "MCNPX User's Manual", LA-CP-05-0369, Los Alamos National Lab., 2005.

PAPERS PUBLISHED IN RELATION TO THE PROJECT

1. Seo ChulGyo, Kim Hak Sung, Park Cheol, Huynh Ton Nghiem, Le Vinh Vinh, Vo Doan Hai Dang, Conceptual Nuclear Design of a 20 MW Multipurpose Research Reactor; KAERI/VAEC joint study on a new research reactor for Vietnam, KAERI/TR-3444/2007, 8/2007.
2. Chae Heetaek, Seo ChulGyo, Park JongHark, Park Cheol. Le Vinh Vinh, Huynh Ton Nghiem, Vo Doan Hai Dang, Conceptual Thermal Hydraulic Design of a 20MW Multipurpose Research Reactor; KAERI/VAEC joint study on a new research reactor for Vietnam, KAERI/TR-3443/2007, 8/2007.
3. Huỳnh Tôn Nghiêm, Lê Vĩnh Vinh, Nguyễn Nhị Điền, Võ Đoàn Hải Đăng, Tính toán thiết kế hạt nhân cơ bản với hai loại lò phản ứng nghiên cứu mới đề xuất cho Việt Nam; Thông tin KH&CNHN, Viện NLNTVN (đã gửi bài tháng 8/2008).

EVALUATIONS OF PHYSICAL PARAMETERS OF HEU AND LEU FUEL ASSEMBLIES USED IN DALAT NUCLEAR RESEARCH REACTOR USING MVP CODE

Le Dai Dien [(1)]***, Hoang Minh Giang*** [(1)] ***and Dang Minh Hue*** [(2)]

[(1)] Institute for Nuclear Science and Technology, VAEC, Vietnam.

[(2)] Computational and Fundamental Research Center, INST, Vietnam.

ABSTRACT: Lattice cell calculations for VVR-M2 fuel assemblies of DaLat Nuclear Research reactor were performed using Monte Carlo code MVP. The physical parameters like infinite multiplication factors, few group constants, neutron flux distributions and temperature effects were investigated for both HEU and LEU configurations. The infinite multiplication factor and thermal neutron flux for LEU fuel are lower than HEU one. In order to effectively use Monte Carlo codes the high performance computing with cluster technique is proposed for large problems.

Content

In the framework of RERTR program, the fresh nuclear fuel assemblies left in DaLat Nuclear Research Reactor have been replaced by new design fuels. The enrichment of U235 in the VVR-M2 fuel is decreased from HEU(36%) to LEU (19,75%). In order to use the new fuel type in the reactor core without modification, the geometry design and dimension of the fuel assembly are kept unchanged. The HEU fuel content is uranium and aluminium with uranium density of 1.4 g/cm^3 and for the LEU fuel the fuel meat consists of UO_2 and aluminium with uranium density of 2.5 g/cm^3. There are also some changes in the thickness of fuel meat and cladding. The fuel assemblies are manufactured and supplied by JSC TVEL, Russia.

There have been several studies for using LEU VVR-M2 fuel in Dalat Research Reactor. These studies have been carried out by Argone National Lab., United State and by researchers from DaLat Nuclear Research Institute. All of these calculations were performed for global reactor core to investigate the safety features of the core like criticality, burnup, excess reactivity and thermal hydraulics characteristics. The computer codes like WIMS-ANL, REBUS-PC, MCNP4C2, ORIGEN and RELAP5 have been extensively used. The use of LEU fuels in Dalat Research Reactor has been confirmed and it has been already put in the reactor core since 2007. Now Dalat Research Reactor is operating with mixed core (HEU and LEU fuels).

From the point of view of reactor physics calculation, it is very useful to perform the lattice calculations for HEU and LEU fuel assemblies, so that we can compare the lattice parameters of these fuels. By using Monte Carlo code, namely MVP/GMVP supplied from JAEA, Japan, we have performed the lattice cell calculations for HEU and LEU VVR-M2 fuel configurations. The main results of our study are as follows:

- Calculations of infinite multiplication factor K_{inf} for both cell lattices are carried out. The K_{inf} of LEU is smaller than HEU's in the range of 5-6 mk (see table 2).

Table 1: Infinite multiplication factors for HEU fuel assembly.

$K_{inf}(27^oC)$			
TRIPOLI*	APOLLO2*	MCNP4C2*	MVP
1.64727	1.64486	1.64463	1.64317
± 0.00025	± 0.000007	± 0.00009	± 0.00016

- Investigations of neutron flux distribution in the fuel assembly regions as well as energy spectrum of neutron flux are performed. For thermal range, the neutron flux in LEU is lower than HEU. The LEU/HEU ratio in neutron flux is about 0.94 in accordance with experiments carried out by manufacturer.

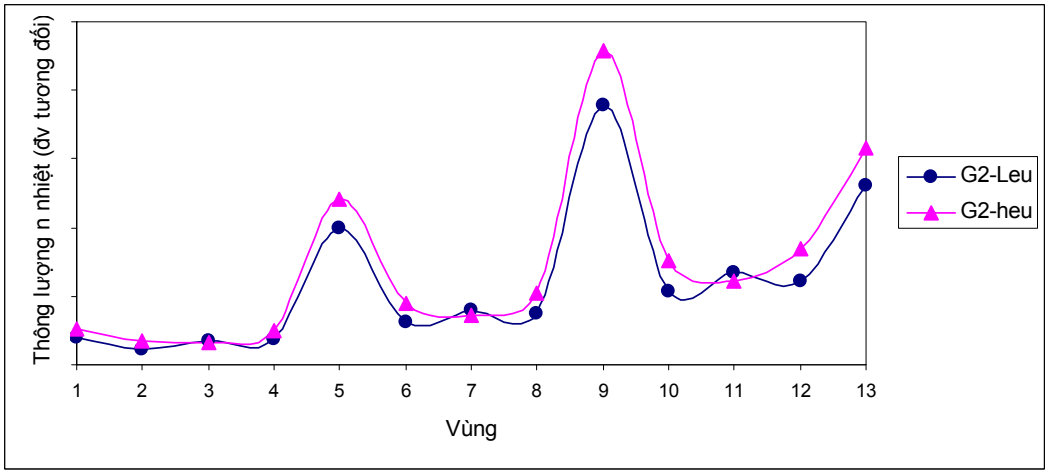

Fig. 1: Thermal neutron flux distribution in 13 zone lattice cell VVR-M2

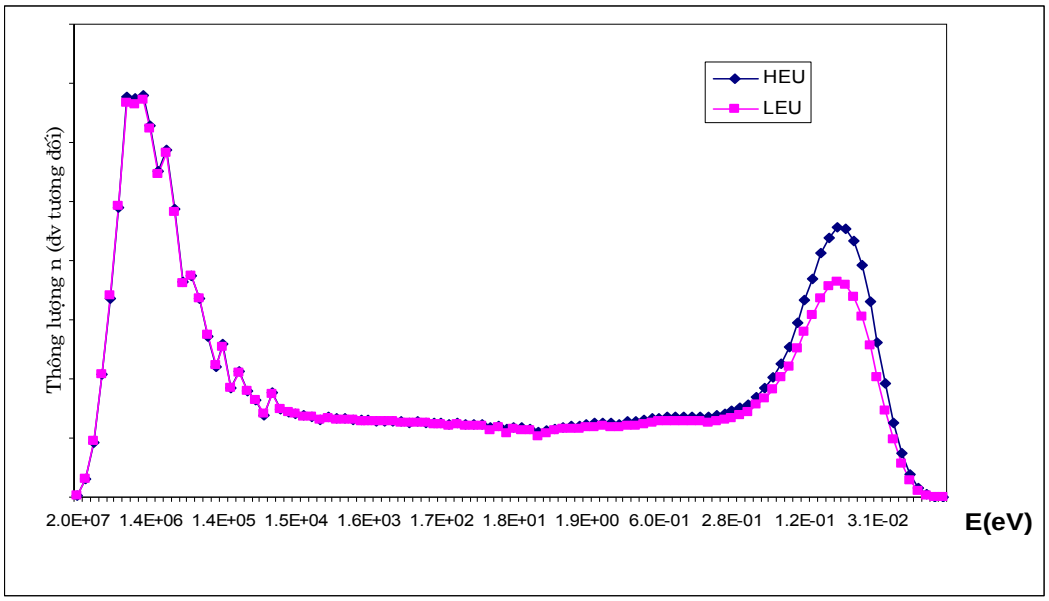

Fig. 2: Energy spectrum of neutron flux for HEU and LEU fuel assemblies.

- Few group constants are also given.

- The temprature effects like isothermal temprature coefficient (ITC), doppler effect and void effect in the assumption of boiling water are discussed.

Table 2: Multiplication factors and temperature effect in HEU and LEU fuels.

	23^{o}C	**43^{o}C**	**(pcm/^{o}C)**
HEU	1.64267 ± 0.00016	1.64227 ± 0.00015	-2
LEU	1.63597 ± 0.00021	1.63507 ± 0.00020	-4.5

+ The outer hexagonal fuel layer of VVR-M2 is modified to circle form to investigate the effect of boundary condition.

+ The MVP code is also compiled in LINUX platform. The high performance computing (HPC) on LINUX platform with cluster technique as the solution for using Monte Carlo codes for large problem is proposed.

From this study it is concluded that it is quite satisfactory to use LEU fuel assemblies in DaLat Reactor core and the safety characteristics of the LEU fuel are better than HEU fuel.

REFERENCES

[1]. Analyses for Inserting Fresh LEU Fuel Assemblies Instead of Fresh HEU Fuel Assemblies in the Dalat Nuclear Research Reactor in Vietnam N. A. Hanan, J.R. Deen, and J. E. Matos. Presented at the 2004 International Meeting on RERTR. November 7-12, 2004, IAEA, Vienna, Austria.

[2]. Báo cáo các phân tích an toàn để so sánh cho trường hợp nạp vào vùng hoạt các bó nhiên liệu có độ giàu thấp thay vì các bó nhiên liệu có độ giàu cao hiện có ở lò phản ứng hạt nhân Đà Lạt. Phạm Văn Làm, Huỳnh Tôn Nghiêm, Lương Bá Viên, Lê Vĩnh Vinh (Viện NCHN), J. Liaw và J.E. Matos (ANL). Đà Lạt, 9-2005.

[3]. Các bó nhiên liệu VVR-M2. Mô tả theo danh mục.0001.04.00.000 ?KO. 2006.

[4]. Accuracy of VVR-M Criticality Calculations with Code MCU-RFFI. Y.V.Petrov, A.N.Erykalov, M.S.Onegin. Presented at the 1999 International Meeting on RERTR. October 2-9, 1999, Budapest, Hungary.

[5]. Method and Codes for Neutronic Calculations of the MARIA Research Reactor. K. Andrzejewski and T. Kulikowska (Institute of Atomic Energy, Poland) , M.M. Bretscher, N.A. Hanan, and J.E. Matos (ANL). Presented at the 1998 International Meeting on RERTR. October 18-23, 1998, Sao Paulo, Brazil.

[6]. Neutronic Performance of the WWR-M Research Reactor in Ukraine. R. B. Pond, N.A. Hanan and J. E. Matos (ANL),Y. Mahlers and A. Dyakov (Kiev Institute for Nuclear Research). Presented at the 2002 International Meeting on RERTR, November 3 – 8, 2002 San Carlos de Bariloche, Argentina.

[7]. Calculation of Temperature Reactivity Coefficients in KRITZ-2 Critical Experiments Using WIMS. D.J. Powney, AEA Technology.

[8]. NRC Inspection Manual : Inspection Procedure 61708 – 1985.

[9]. Isothermal Temperature Reactivity Coefficient Measurement in TRIGA Reactor. T.Zagar, M.Ravnik and A.Trkov. International Conference “Nuclear Energy for New Europe 2002, Slovenia, September 9-12, 2002.

[10]. Comparisons of Diffusion Theorry and Monte Carlo Burnup. N. A. Hanan, R. B. Pond, M. M. Bretscher, and J. E. Matos. Presented at the 2002 International Meeting on RERTR, November 3 – 8, 2002 San Carlos de Bariloche, Argentina.

[11]. Y. Nagaya, K. Okumura, T. Mori , M. Nakagawa : MVP/GMVP II : General Purpose Monte Carlo Codes for Neutron and Photon Transport Calculations based on Continuous Energy and Multigroup Methods , JAERI-1348 (2005).

[12]. Methods of Steady-State Reactor Physics in Nuclear design. Rudi J.J. Stamm'ler and Maximo J. Abbate. 1983 Academic Press.

INVESTIGATION OF THE THERMAL HYDRAULICS SAFETY CHARACTERISTIC PARAMETERS ON THE DALAT RESEARCH REACTOR AS INSERTING ADDITIONAL FRESH FUEL ASSEMBLIES WITH HIGH ENRICHED URANIUM OR FUEL ASSEMBLIES WITH LOW ENRICHED URANIUM

Luu Anh Tuan, Tran Van Hien and Hoang Duc Huynh

Institute for Nuclear Science and Technology, VAEC, Vietnam.

ABSTRACT: To prepare inserting additional reactivity for Dalat Nuclear Research Reactor, it is necessary a research to calculate for defining Thermal hydraulic Safety characteristic parameters such as the maximal values of the fuel surface temperature in active zone, minimal values of the temperature of Onset of Nucleate Boiling in different operating regimes of Nominal and Limited powers. They are the important part in the process of Safety Analyses for the reactor. The strategy of loading 36 fresh fuel assemblies of HEU or 36 fresh fuel assemblies of LEU is divided into four cycles to remove the highest burnup assembiles and insert fresh ones as following: 8; 8; 10 and 10 with the current operating core configuration of 104 VVR- M2 fuel assemblies is used. The results calculated by using Computer code COOLOD-N2 are compared with experimental data received on the DNRR[11] and other data [12] are given.

Keywords: Thermal Hydraulics Safety Analysis, COOLOD-N2 computer code; Core configuration; Physics cell, Modeled cell for calculation; ínsert reactivity; Fuel with High Enriched Uranium HEU; Fuel with Low Enriched Uranium LEU; Nominal Power; Limited Power; Maximal Temperature of Cladding; Onset of Nucleate Boiling ONB.

1. Introduction

For preparation of inserting additional fresh fuel in DNRR, there are two variants: The first is using fresh fuel with high enriched Uranium HEU; The second one is using fresh fuel with low enriched Uranium LEU. The second one is very important to bring security and safety on research reactor.

It is necessary to investigate the thermal hydraulic safety characteristic parameters such as maximal surface fuel cladding temperatures and ONB temperature in the reactor active zone.

II. Structural features of Dalat Nuclear Research Reactor [8]

The reactor core and components have being coolled by natural convection circulation.

In order to intensify heat transfer in the reactor based on natural convection circulation, aim to double power to 500 kW, an extract well a new structure was designed to connect above on the reactor core zone.

The cooling water flow rate in primary loop is 50 m3/h.

The suction of cooling water is performed on the up part of the reactor vessel. One part of cooling water flows through the active zone, the rest part flows in space between the reactor wall and extract well then mix with each other and is extracted out by pump.

The cooling water flow rate in secondary loop is 90 m3/h.

The moving force of the cooling water is determined by the following formula:

$$H_{CĐ} = \Delta P_{MS}$$

Where $H_{CĐ} = H \Delta\gamma_1 + h_{VH} \Delta\gamma_2$

Heat distribution law [12] is up on the reactor design and operational diapasone.

The hydraulics resistance:

$$\Delta P_{MS} = (\Sigma \xi_M + \lambda_{MS} l / d_r) V^2 \gamma / 2g$$

III. Modeled cell for calculation

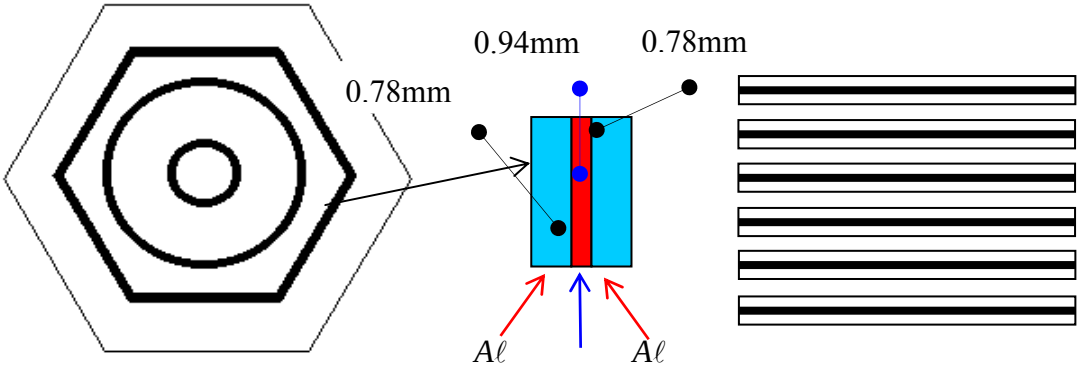

2a. Physics cell

2b. Modeled cell for calculation

Fig. 1: Dalat reactor cell

Table 1: Characteristics of fuel assembly VVR-M2 [5] and modeled cell for calculation. [6].

Parameter	Physical cell	Modeled cell	Physical cell	Modeled cell
Number of fuel elements in an assembly	3		3	1
Number of fuel plates in an assembly		6		6
With hexagonal shape (outermost element)	1		1	
With circular shape (inner elements)	2		2	
Thickness, mm				
Fuel element (fuel meat and cladding)	2.5	2.5	2.5	2.5
Fuel meat (UO_2+ Al)	0.70	0.70	0.94	0.94
Cladding (Al alloy)	0.90	0.90	0.78	0.78
Space for water flow	2.5 - 3.	3.	2.5 - 3.	3.

Cross section area, cm^2				
Fuel cell	10.61	10.61	10.61	10.61
Water flow	5.85	5.85	5.85	5.85
Length, mm				
Total fuel assembly	865	865	865	865
Active height (fueled part)	600	600	600	600
U-235 content				
Enrichment, %	36	36	19.75	19.75
Weight, g	40.00	40.00	49.70	49.70

III. Calculation results

The heat flux in the configuration of 104 fuel assemblies and average cooling flow rate appeared in active zone:

Power, kW	Heat flux, W/m2	Average cooling flow rate, m^3/h
P= 500 kW	q = 2,11 10^4. W/m2	G= 23,67 m^3/h
P= 550 kW	q = 2,34 10^4 W/m2	G= 24,33 m^3/h

Table 2: The data and calculated results of the thermal hydraulic safety characteristic parameters in average channel

Parameter	**End-104 HEU**		**36- Assemblies HEU**		**36- Assemblies LEU**	
Power, kW	500	550	500	550	500	550
Core inlet temperature, ^oC	32.0	32.4	32.0	32.4	32.0	32.4
Core outlet temperature, ^oC	51.25	53.0	51.21	52.95	51.21	52.95
ONB temperature, ^oC	107	107	107	107	107	107
Temperature difference, Δt, ^oC	55.75	54	55.79	54.05	55.79	54.05
Maximal cladding temperature, ^oC	69.20	72.22	69.16	72.18	69.16	72.18
Heat flux, W/m^2	21100	23400	21100	23400	21100	23400

Table 3: The data and calculated results of the thermal hydraulic characteristic safety parameters in hot channel

Parameter	**End 104-Assemblies HEU**		**36- Assemblies HEU**		**36- Assemblies LEU**	
Power, kW	500	550	500	550	500	550
Core inlet temperature, ^oC	32.0	32.4	32.0	32.4	32.0	32.4
Core outlet temperature, ^oC	64.91	67.61	69.42	72.44	68.08	71.01

ONB temperature, ^oC	107.38	107.49	107.54	107.65	107.49	107.61
Temperature difference Δt, ^oC	15.12	10.59	7.81	2.74	9.94	5.06
Maximal cladding temperature, ^oC	92.26	96.90	99.73	104.91	97.55	102.55
Heat flux, W/m^2	33100	36400	37800	41600	36400	40100
Maximal cladding temperature, ^oC (*)	101.6	105.5	98.7	102.4	96.9	100.6

Table 4: The data and calculated results of the thermal hydraulic characteristic safety parameters in hot channel in different cycles adding fuel assemblies HEU or LEU

Parameter	**Cycle I (Add 8 Assemblies)**				**Cycle II (Add 8 Assemblies)**			
Power, 500 kW	HEU F: 1.32; 2.08		LEU F: 1.32; 2.06		HEU F: 1.32; 2.04		LEU F: 1.32; 2.00	
Cooling water temperature ^oC	60.08	71.92	59.81	71.53	59.55	71.15	59.01	70.38
Maximal cladding temperature, ^oC : 1;2	100.73	103.81	100.15	103.18	99.58	102.56	98.43	101.31
ONB temperature ^oC	108.91	107.62	108.39	107.61	108.38	107.59	108.35	107.57
Heat flux, W/m^2	52600	40300	52100	39900	51600	39500	50500	38800

Parameter	**Cycle III (Add 10 Assemblies)**				**Cycle IV (Add 10 Assemblies)**			
Power, 500 kW	HEU F: 1.32; 1.99		LEU F: 1.32; 1.94		HEU F: 1.32; 1.95		LEU F: 1.32; 1.88	
Cooling water temperature ^oC	58.87	70.19	58.29	69.23	58.33	65.42	57.39	68.08
Maximal cladding temperature, ^oC : 1;2	98.15	101.00	96.70	99.43	97.00	99.73	94.97	97.55

ONB temperature ^oC	108.35	107.56	108.31	107.53	108.32	107.54	108.27	107.49
Heat flux, W/m^2	50300	38600	49000	37600	49300	3780	47500	36400

Parameter	**Cycle I (Add 8 Assemblies)**				**Cycle II (Add 8 Assemblies)**			
Power, 550 kW	HEU F: 1.32; 2.08		LEU F: 1.32; 2.06		HEU F: 1.32; 2.04		LEU F: 1.32; 2.00	
Cooling water temperature ^oC	62.45	75.11	62.16	74.70	61.88	74.29	61.30	73.47
Maximal cladding temperature, ^oC : 1;2	105.84	106.97	105.35	106.76	104.73	106.52	103.49	105.97
ONB temperature ^oC	108.54	107.63	108.53	107.64	108.51	107.65	108.48	107.66
Heat flux, W/m^2	57800	44300	57300	43900	56700	43500	55600	42600

Parameter	**Cycle III (Add 10 Assemblies)**				**Cycle IV (Add 10 Assemblies)**			
Power, 550 kW	HEU F: 1.32; 1.99		LEU F: 1.32; 1.94		HEU F: 1.32; 1.95		LEU F: 1.32; 1.88	
Cooling water temperature ^oC	61.15	73.26	60.43	72.24	60.58	72.44	59.57	71.01
Maximal cladding temperature, ^oC : 1;2	103.18	105.86	101.63	104.57	101.94	104.91	99.75	102.55
ONB temperature ^oC	108.48	107.66	108.44	107.65	108.95	107.65	108.40	107.61
Heat flux, W/m^2	55300	42400	53900	41300	54200	41600	52300	40100

2. Comparison of calculated results with experimental and other data

Table 5: Data and calculated results of maximal cladding temperature parameters as used total 36 fuel assemblies of HEU or LEU and calculated results in Argonne National Laboratory , USA(*) [10]

Parameter	**End 104 - Assemblies HEU**		**36 - Assemblies HEU**		**36 - Assemblies LEU**	
Power, kW	500	550	500	550	500	550
Maximal cladding temperature, ^{o}C,	92.26	96.90	99.73	104.91	97.55	102.55
Maximal cladding temperature, ^{o}C, (*)[10]	101.6	105.5	98.7	102.4	96.9	100.6

Table 6: The maximal fuel cladding temperature measured in the reactor active zone (**)[11] and the design data calculated by Russian (***)[12]

Parameter	**89- Assemblies HEU**		**94- Assemblies HEU**		**94- Assemblies HEU**	
Power, kW	500		500		550	
Maximal cladding temperature,^{o}C; 1(**)[11]	99.30					
Maximal cladding temperature, ^{o}C 1; 2(***)[12]			93.60	96.10	97.50	100.10

The received results on the tables 6,7,8, the charateristic safety thermal hydraulic values lie within the specified range [7].

3. Discussion.

To pay attention on the table 7, the reactor operating at the cycle end of 104 HEU fuel assemblies, there is a difference in comparison with the values of [10], because, in this period the maximal surface cladding temperature must be lower than that when inserting additional fresh fuels.

4. Conclusion

In this work show the results of the investigation of Safety condition of the reactor as inserting additionally new fresh fuel assemblies of high enriched Uranium HEU or lowed enriched Uranium LEU.

The calculation for defining the values of thermal hydraulic safety characteristic parameters such as maximal temperature on the fuel surface in the active zone and Onset of Nucleate Boiling temperature (ONB) at power level of 500; 550 kW for the core configuration of 104 fuel assemblies of the DNRR using the COOLOD-N2 code[5]

has been carried out. The comparison of the received results with other data calculated by Soviet experts [11], and experimental data [12] received on the DNRR is reasonable.

REFERENCES

[1]. Jordi Roglans, Nuclear Engineering, Research and Test Reactor Conversion, Argonne National Laboratory, USA.

[2]. Research Reactors & Security, IAEA Promotes Research Reactor Safety, Staff Report, 8 March 2004.

[3]. Lưu Anh Tuấn, Trần Văn Hiển và những người khác. "Sử dụng chương trình Coolod- N2 để nghiên cứu tính toán phân bố nhiệt độ trên bề mặt nhiên liệu theo chiều cao vùng hoạt lò phản ứng nghiên cứu Đà Lạt". Báo cáo tổng kết Đề tài khoa học công nghệ cấp cơ sở năm 2005. Mã số CS/05/04-05. Tháng 12/2005.

[4]. Masanori Kaminaga, COOLOD-N2, a computer code for the Analyses of steady- state Thermal Hydraulics in Research Reactors, JAERI, 1984.

[5]. Safety Analysis Report, Nuclear Research Institute, Chapter 1, Page 3; Chapter 5, Page 1-3, Vietnam, 2002.

[6]. Safety Assessment of Research Reactors and Preparation of the Safety Analysis Report, Safety Series No. 35-G1 IAEA, Vienna, 1994.

[7]. Technical Project, Rebuilding and Extending of the Research Reactor in Dalat City. Vol. 3, 651-0-3. AtomEnergoExport USSR (form.). Tom 3, Page 63-64, Reactor IVV-9.00.000 PZ Explanation Text. (in Russian).

[8]. V.M. Liatcher, A.M. Prudovski, Hydraulics Modeling, Moscow, Atomic Energy Publisher, 1984.(in Russian).

[9]. P.V.Lam, H.T.Nghiem, .L.B.Vien and L.V.Vinh, Dalat Nuclear Research Institute, Vietnam, J.Liaw, J.E.Matos, Argonne National Laboratory, USA, Analyses for inserting fresh LEU fuel assemblies instead of fresh HEU fuel assemblies in the Dalat Nuclear Research Reactor, September, 2005.

[10]. Database for the Operation of the Dalat Nuclear Research Reactor, period 1983- 2003, Page 159, Dalat City October 2004.

[11]. Additional Physical and Hydraulics Data of IVV-9, Federal Export and Import Consortium. (done according to the Report confirming of Reactor Technical Project from October 1, 1979 in Hanoi.(in Russian).

1.3 - Instrumentation

EXPERIMENTAL EVALUATION OF SYSTEMATIC ERRORS OF GAMMA SPECTROMETER FOR ASSAY OF RADIOACTIVE WASTE DRUMS

Tran Quoc Dung [(1)], Nguyen Duc Thanh [(1)], Luu Anh Tuyen [(1)], Lo Thai Son [(1)]
Phan Dinh Phuc [(1)], Nguyen Canh Hai [(2)] and Ngo Minh Triet [(3)]

[(1)] Centre for Nuclear Techniques, VAEC, Vietnam.

[(2)] Nuclear Research Institute,VAEC, Vietnam.

[(3)] Dalat University, Vietnam.

ABSTRACT: To develop the gamma technique to measure the activity of the radioactive waste drums released during operation of Dalat Research Reactor, Dalat City, the experimental study are carried out to confirm the calculation results of the systematic errors and evaluate the performance of the technique using two identical detectors in practice. In this paper, the results are presented. The results are also basic for establishment of measuring procedure for assay of the radwaste drums. The radioactive isotopes and activity of some real radwaste of of Dalat Research Reactor, which were measured by this technique, are also given.

Keyword: Gamma techniques, radwaste, NDT.

I. INTRODUCTION

During twenty-four-year operation,Dalat Research Reactor has released about 200 low radioactive waste packages which have both cylindrical and cubic shapes. The waste is sandwiched by concrete at the ends of the packages, therefore the waste packages usually weigh from 250 to 400 kg. The waste must be checked to satisfy regulations of radioactive waste management.

Segmented Gamma Scanner (SGS) is a traditional tool for the isotopic composition measurement and for determination of the activity level in gamma contaminated waste drums [1,2]. At present, there is not any SGS system in Vietnam. If there were, it could not be used. Because the weight of the packages SGS can not move them upward.

The other measuring technique has been studied [9] for assay of the drums containing low density waste, mainly consisting of organic materials such as contaminated paper, rags, protective clothing, shoes, etc. The measuring arrangement consists two identical detectors set at equal distances from two bases of drum.The error is still very large (223 %) if the activity is distributed in the vertical large region. In this measurement the drum must lie down and two identical detectors set at equal distances from two bases of drum. It is practically impossible for assay of the packages because very small sensitivity of the measurements caused by the concrete lyer at the end of the drums.

In order to sholve this problem an other method, which was proposed [10,11], has been developed. Experimental studies are carried out to confirm the calculation results of the systematic errors and evaluate the performance of this technique in practice. The affect of factors, such as distribution of sources, attenuation coefficients

and homogeneity of matrix, on the measuring results were also investigated. The results are also basic for establishment of measuring procedure for assay the radwaste drums. In this paper, the results of homogenous matrix and point source in different positions in the drum are presented.

II. MEASURING PRINCIPLE

The measuring principle of the proposed technique can be seen in the published papers [9,10]. Two identical detectors are set at the same distance from the middle of the drum (see Figure 1.) If this distance is large enough the detector size and the height of the drum can be neglected.

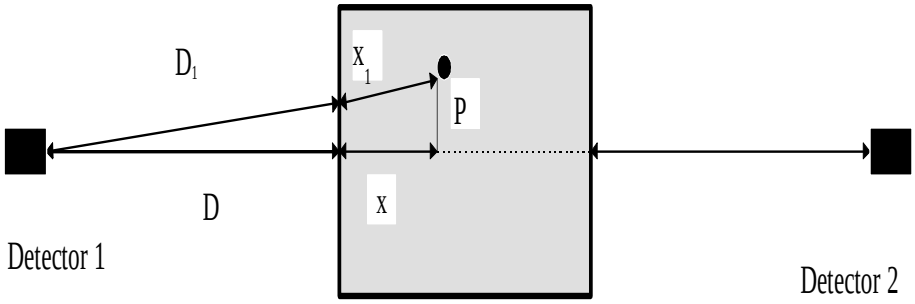

Fig. 1: Waste drum counting geometry. Two identical detectors set to the drum at its middle point at equal distances.

Since the detectors view the curved surface of drum, a "mean thickness" of the drum is assumed to equal to 0.823.d, where d is the diameter of the drum. The constant of 0.823 is the geometrical coefficient [2,12]. In other word, the drum is assumed to be a rectangular prism whose thickness is equal to 0.823d. The activity I concentrates in the drum can be determined by

$$I = \frac{(C_1 C_2)^{1/2}}{G} \tag{1}$$

$$G = \frac{\alpha}{S^2} \exp -(\mu_1 \times 0.832 \times R) \tag{2}$$

Where C_1, C_2 are the count rates of two the detector 1 and 2, respectively. S=K-0.823.R , K- distance from detector to the center of the drum. This distance is larger the diameter of the drum several times; α- coefficient, that is a function of the gamma-ray energy, intrinsic efficiency of detector and the effective distance K. R- radius of drum, and μ_1=2/S+μ, μ - the linear attenuation coefficient in the waste mixture.

Before estimate of the total activity the values of G in equation (2) must be determined. The values of α / D^2 versus gamma ray energy can be determined by using appropriate standard source. The attenuation coefficient can be evaluated by computation based on the fact that the mass attenuation coefficients of most organic materials are nearly equal to that of water μ_H. Thus the linear attenuation coefficients can be determined by the expression $\mu_H = \mu.\rho$, where ρ is the density of the waste assayed. The value of G is also determined directly by experiment by using a calibrated source placed next to one base of the drum.

III. EXPERIMENTAL STUDY AND DISCUSSION

In principle, the measurement using two identical detectors at the same distances from the detectors to get count rate C_1(of detector 1) and C_2 of (of detector 2) as given above is the same as two measurements with one detector: first measurement gives C_1, second measurement gives C_2 after turning the drum 180^o. Hence, when having only one detector the drum can be measured two times in two directions opposite each other at the same distances from the detector.

The measuring arrangement is given in Figure 2. A detector sets perpendicularly to the drum axis at its middle point at equal distances from the curve face of drum.

In the experiments, a standard drum was used. Two point sources Co-60 of 0.36 MBq and two point sources Cs-137 of 0.64 MBq were located at four specified radial positions in the different measurements as in Figure 2. Many pieces of matrix with various shapes and densities are made from clothing materials. A High-purity germanium detector-Gem 50P4, and a standard digital spectrometer, model DSPEC.JR-312-Ortec, with GAMMAVISION 32 version 6.1 were used for detection and analysis of gamma spectra. The results are given in the below tables. Here the experimental and calculated values of errors are presented as ratio of the experimental and calculated to true value of activity. The experimental inaccuracies are in the range of 1-4 %.

Table 1.a presents the result for the cases of point sources in homogeneous matrix. Generally, the systematic errors are small and lightly depend on the position of the sources. In case of the source next the edge of drum as in position 4, the maximum error is about 45%.

When distance between the centre of the drum and the detectors is equal to about four times the half of the height of the drum. the maximum variation is less than 10 % as shown in the case of one source in position 5.

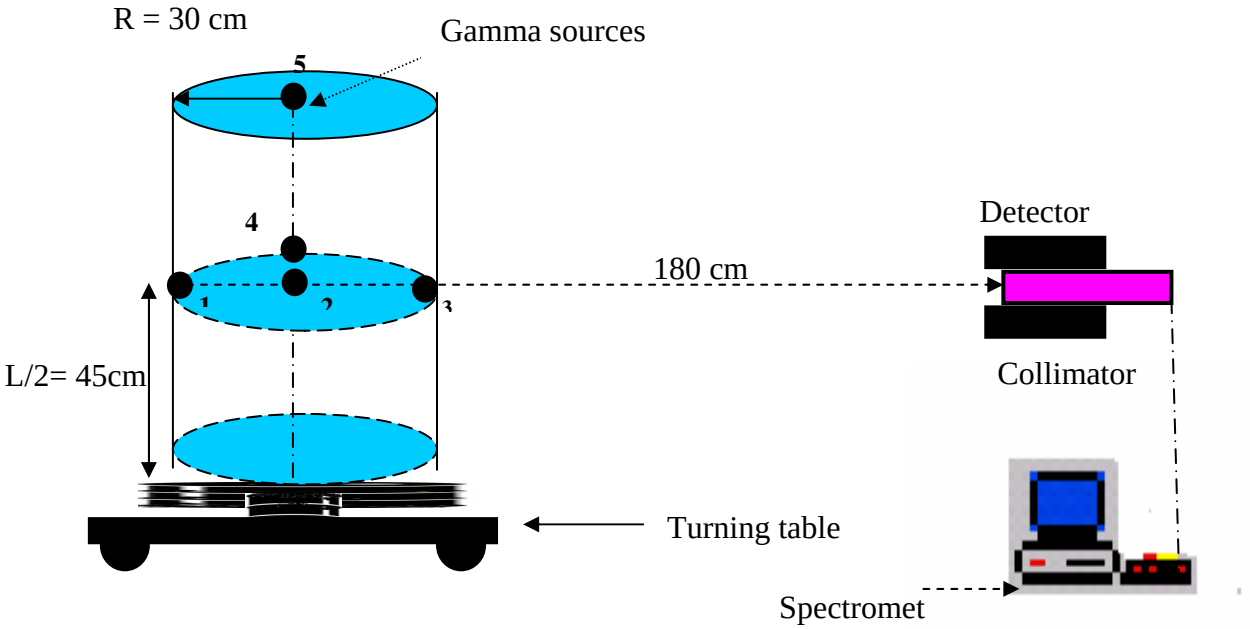

Fig. 2: Waste drum counting geometry. The drum is measured two times. In the second measurement the drum is rotated 180^0.

The errors are caused mainly by the horizontal inhomogeneity of the source in the drum such as case of two sources with the same activity in position 1 and 2, 1 and 3 given Table 1.b. The longer distance between the sources is the more inaccurate the measurement results is. The larges errors happen when two sources with the same activity are in position 1 and 3.

Table 1.a: Evaluation of errors caused by a point source in position 1, 2, 4 and in homogenous matrix.

Case of study		**One source in position 1**		**One source in position 2**		**One source in position 4**	
Gamma Energy (kev)	*Linear attenuation coefficient (cm^{-1})*	*Experimental value of error*	*Calculated value of error*	*Experimental value of error*	*Calculated value of error*	*Experimental value of error*	*Calculated value of error*
661	0.016	0.97	0.99	0.91	0.95	1.25	1.27
661	0.024	0.92	0.95	1.04	0.91	1.37	1.35
661	0.031	0.92	0.91	1.01	0.87	1.43	1.48
1173	0.013	0.99	1.00	0.90	0.96	1.19	1.17
1173	0.014	0.99	1.00	0.88	0.96	1.21	1.19
1173	0.023	0.96	0.95	0.91	0.91	1.34	1.33
1332	0.011	0.99	1.01	0.90	0.97	1.16	1.14
1332	0.019	0.97	0.97	0.91	0.93	1.28	1.27
1332	0.021	0.96	0.96	0.93	0.92	1.31	1.30

Table 1.b: Errors caused by a point sources in position 5 and two sources in homogeneous matrix.

Case of study		**One source in position 5**		**Two sources in position 1 and 2**		**Two sources in position 1 and 3**	
Gamma Energy (kev)	*Linear attenuation coefficient (cm^{-1})*	*Experimental value of error*	*Calculated value of error*	*Experimental value of error*	*Calculated value of error*	*Experimental value of error*	*Calculated value of error*
661	0.016	0.81	0.85	1.11	1.07	1.15	1.21
661	0.024	0.87	0.81	1.16	1.08	1.27	1.30
661	0.031	0.76	0.77	1.28	1.10	1.38	1.41
1173	0.013	0.82	0.87	0.98	1.06	1.16	1.18
1173	0.014	0.81	0.86	1.03	1.06	1.15	1.19

1173	0.023	0.78	0.81	1.05	1.07	1.31	1.29
1332	0.011	0.80	0.88	1.04	1.06	1.14	1.17
1332	0.019	0.90	0.83	1.02	1.07	1.17	1.24
1332	0.021	0.88	0.82	1.04	1.07	1.30	1.26

As theoretical prediction, the experimental results also show that the affect of the non-uniform matrix on the systematic errors are small. They are about 3-12 % for almost cases. The maximum error (~ 30 %) happens when two sources are in the matrix having large differential level of the linear attenuation coefficients (μ= 0.07 and μ*=0.034 cm^{-1}).

Numerous experiments with the the point sources in the different matrix were carried out. In these experiments many small pieces matrix with attenuation coefficients in the range of 0.011-0.034 cm^{-1} and sources were randomly arranged. The results give the small values of systematic errors that do not exceed 45%.

The method was used to measure the radioactive isotopes and activity of some real radwaste of Dalat Research Reactor. The result of the radwaste drum No S-156 is given in Table 2 as an example.

Table 2: The radioactive isotopes and activity of the radwaste drum No S-156

Code of the drum	**Gamma Energy (Kev)**	**Isotope**	**μ(cm^{-1})**	**Factor G**	**Activity**	**Max. Error (%)**
S-156	428	Sb-152	0.033	6.082×10^{-6}	0.038	37.689
	794	Cs-134	0.032	1.369×10^{-5}	0.095	35.305
	1115	Zn-56	0.029	7.103×10^{-6}	0.418	27.354
	1332	Co-60	0.026	1.312×10^{-5}	7.417	19.552
	1408	Eu-152	0.025	2.830×10^{-6}	0.070	16.502
Total Activity (MBq)	**8.038**					

IV. CONCLUSION

As far as systematic errors are concerned, the maximum error (~ 40%) of this method is slightly larger than that (~30%) of SGS techniques. However its measurement apparatus is very simple, perform of measurement is faster, and it can be used for most of the situations encountered in practice. For practical application when having only one detector the drum can be measured two times in two directions opposite each other at the same distances from the detector.

Although the assumption of homogeneous matrix in this method is not satisfied in practice, the above investigations show that it can be used for the case of inhomogeneous matrix having low and medium density (μ = 0.03 cm^{-1}).

The above calculated and experimental results confirm the performance of the technique using two identical detectors for assay of radioactive waste in practice. Base on this investigation a measuring system for assay the radwaste drums will be set up and the systematic errors can be estimated.

Acknowledgement

The authors express the gratitude to all staff of Department of Nuclear Physics and Electronics, Dalat Nuclear Research Institute, for their valuable help. This work was supported by Ministry of Science and Technology through the Research Contract No. BO/06/02-01.

REFERENCES

[1]. Bjork C. W . Proc. 3rd Int. Conf. on Facility Operation Safeguards Interface, Nov. 29-Dec. 4, 1987, San-Diego, California, p. 129.

[2]. Sprinkle J. K and Hsue S. T. Proc. 3rd Int. Conf. on Facility Operation Safeguards Interface, Nov. 29-Dec. 4, 1987, San-Diego, California, p.188.

[3]. R. J. Estep, Trans. Am. Nucl. Soc., Vol. 62, (1990) 178.

[4]. Tran Quoc Dung , Ann. Nucl. Energy, Vol. 24, No. 1, (1997) 33-47.

[5]. B. M. Gillespie, IAEA Symp. on International. Safeguards, 8-14 May, Vienna 1994.

[6]. T. H. Prettyman, L. A. Foster, and R. J. Estep, LA-UR-96-2620 (1996).

[7]. Tran Ha Anh , Tran Quoc Dung, Ann. Nucl. Energy, Vol. 24, 2001, p. 265-273.

[8]. Tran Ha Anh, Nguyen Duc Thanh, Tran Quoc Dung, Ann. Nucl. Energy, Vol. 32, Iss.13, 2005, p. 1516-1523.

[9]. A. Cesana, M Terrani and G. Sandrelli, Appl. Radiat. Isot, Vol. 44, No. 3, p.517,1993.

[10]. Tran Quoc Dung. Journal of Science and Technology, Vol. 44. No.1, 2006.

[11]. Tran Quoc Dung, Ann. Nucl. Energy, Vol.24, No.8, 1997.

[12]. Augustson R. H and Reilly T. D (1974). *Los Alamos Scientific Laboratory*, LA-5651-M.

DEVELOP THE SPECTROMETER SYSTEMS TO MEASURE GAMMA CASCADE, NUCLEAR DATA AND OTHER APPLICATIONS ON THE NEUTRON BEAM

Vuong Huu Tan, Pham Dinh Khang, Nguyen Xuan Hai, Pham Ngoc Son, Tran Tuan Anh Ho Huu Thang, Nguyen Canh Hai, Pham Ngoc Tuan and Nguyen Thi Thuy Nham

Vietnam Atomic Energy Commission (VAEC), Vietnam.

ABSTRACT: This report mentions the results of the development of spectrometer systems used to measure prompt gamma and gamma cascade, the manufacture of neutron filter, the gamma two steps cascade research, the nuclear data measurement, and the other application researches at Dalat Nuclear Reactor (DNR).

I. OBJECTIVES

The aim of this project is to support equipments for fundamental study on the horizontal neutron channel at DNR, such as making filter neutron beams with energies of 24 keV, 59 keV and 133 keV, improving (n,2γ) spectrometer to (n,3γ), installing neutron spectrometer uses recoil proton counter, and training manpower who are working in field of neutron physics and postgraduate students.

II. CONTENTS

The contents of this project are as follows:

- To improve qualities of thermal neutron beam, and to reduce gamma background for spectrometer systems at third channel and fourth channel of DNR by shield and coincidence techniques;

- To use neutron filter techniques to make new monoenergy neutron beam with 24 keV, 59 keV and 133 keV of energy, and to install a neutron spectrometer with recoil proton counter;

- To complement TAC and to change from (n,2γ) spectrometer to (n,3γ) spectrometer, to use the above equipments to measure average radiator capture cross section, to analyze some elements such as H, B, C, N, Na, Cl, K, Ca, Cr, Mn, Fe of geological samples and to analyze Hydrogen index for oil industry;

- To measure gamma cascade data that are emit from non sphere nucleus after capture thermal neutron, to research exited intermediate level of nucleus, to analyze and to evaluate the parameters of level densities.

- To help to train qualified students with modern techniques of nuclear experiment physics.

III. METHODS

In order to increase the ratio cadmium of neutron beam and to design neutron filter for monoenergy neutron beam with 24 keV, 59 keV and 133 keV, the simulation techniques and experiment techniques were used.

For calculation of average radiative cross section, the neutron and gamma measurement techniques were used.

The event-event measurement method and the modern statistic method were used to make intermediate excited level schema of ^{172}Yb and ^{153}Sm nucleus. The level density parameters of those nucleuses were evaluated by using the summation of amplitude of coincident pulses (SACP) method.

IV. RESULTS

- The cadmium ratio of neutron beam was increased from 112 to 149 at horizontal channel N_0.4 and from 70 to 900 at horizontal channel N_0. 3.

- The gamma background of spectrometer for prompt gamma neutron activation analysis (PGNAA) was reduced significantly. For example the 2223 keV peak of Hydrogen was reduced from 0,8 cps to 0,5 cps. That result was applied to analyze Hydrogen index for oil industry.

- The characteristic parameters of monoenergetic filtered neutron beams are neutron spectra, relative intensity, energy resolution, dimension of filters, and suitable composition of materials. These parameters have been calculated to create the new filtered neutron beams with monoenergies of 1.9 keV, 24.3 keV, 53.9 keV, 58.80 keV, 133 keV and 148.3 keV, at the horizontal channel No.4 of the Dalat research reactor. In which, the two available filtered neutron beams of 55 keV and 144 keV were recalculated with resulting that the beam energies should be 54 keV and 148.3 keV, respectively. The results of calculated parameters in the present work are useful for the development of new filtered neutron beams in the near future at the Dalat research reactor.

- The calculated parameters for new filters have been applied for development of three new filtered neutron beams with energies: 24 keV, 59 keV and 133 keV at the horizontal channel No. 4 of DNR. For experimental measurement of the neutron energy spectra, a proton recoil spectrometer has been installed with counter model is LND-281.

- The SACP spectrometer was completed with TAC module and an interface which uses FPGA technique were completed. These improved ability of SACP spectrometer for research (n,3γ) reactions; the timing resolution is about 14 nano seconds.

- To help data processing of (n,3γ) reaction with timing combining, the some computer codes were written.

- The level density parameters of ^{172}Yb and ^{153}Sm according to Fermi shift back model were calculated, and evaluated with experiment data.

- With this project, three master students were successful, and two others students are doing thesis; five national conference reports and two international conference reports were presented.

Table 1: Calculated results for new filtered neutron beams at Dalat reactor

En keV	ΔEn keV	Φ x10^5 n/cm^2/s	Purity (%)	Filter materials	Size of filter composision
1.8	1.5	24.0	95.79	^{10}B + Sc + Ti	0.2g/cm^2+200g/cm^2+1cm
24[a]	**1.8**	**2.6**	**96.72**	**^{10}B + Fe + Al + S**	**0.2g/cm^2+20cm+30cm+35g/cm^2**
54[b]	1.5	1.7	78.05	^{10}B + Si + S	0.2g/cm^2+98cm+35g/cm^2
59[a]	**2.7**	**1.1**	**92.28**	**^{10}B + Ni +V +Al+S**	**0.2g/cm^2+10cm+15cm+5cm+100 g/cm^2**
133[a]	**3.0**	**0.5**	**92.89**	**^{10}B + Cr + Ni+Si**	**0.2g/cm^2+50g/cm2 +10cm+60cm**
148[b]	14.8	7.2	95.78	^{10}B + Si + Ti	0.2g/cm^2+98cm+2cm

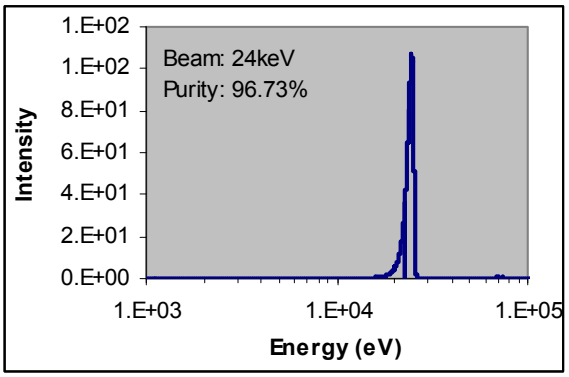

Fig. 1: Calculated energy spectrum for 24 keV filtered neutron.

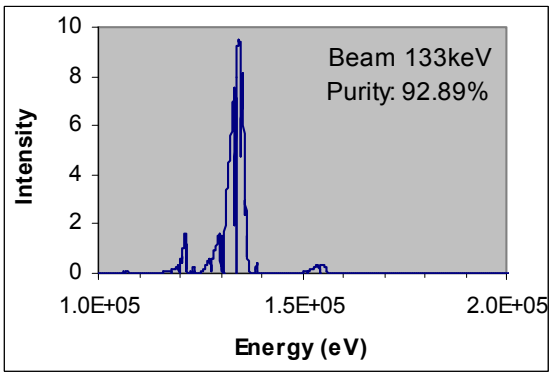

Fig. 2: Calculated energy spectrum for 133 keV filtered neutron beam.

Fig. 3: The new proton recoil spectrometer installed at the Dalat Nuclear Research Institute

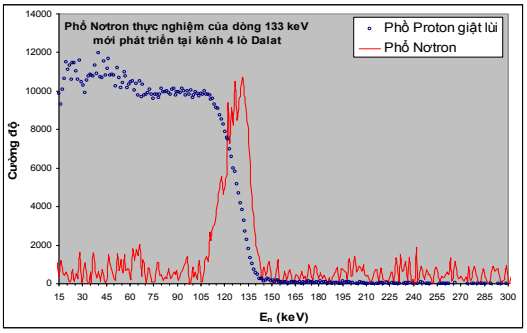

Fig. 4: Pulse high proton recoil spectrum of 133 keV filtered neutron beam, developed presently in this project.

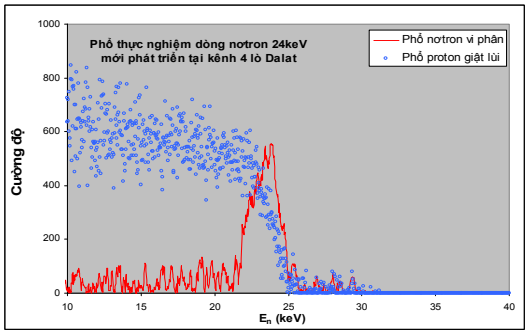

Fig. 5: Pulse high proton recoil spectrum of 24 keV filtered neutron beam, developed presently in this project.

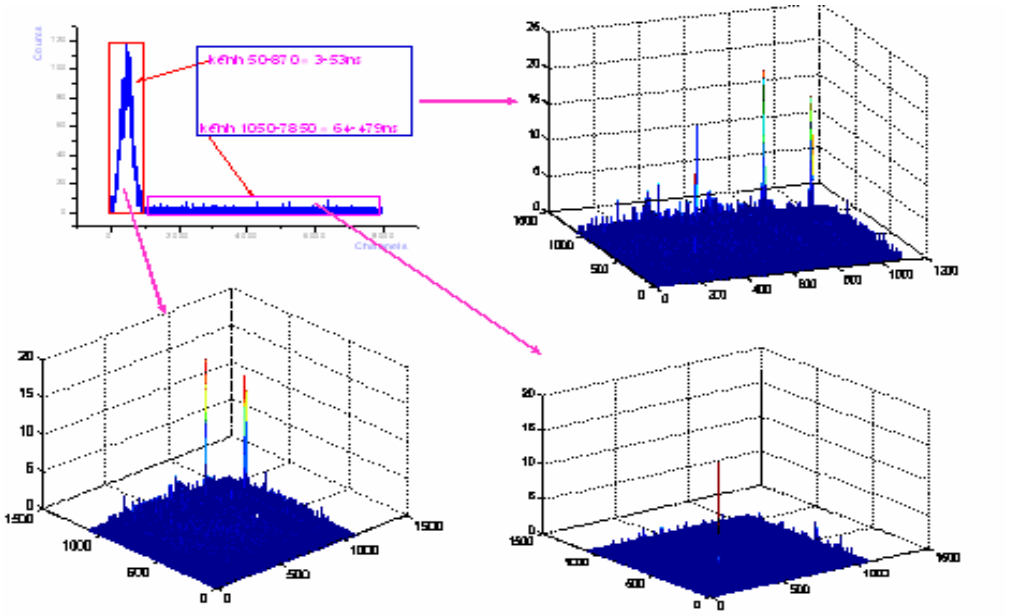

Fig. 6: The spectroscopic information of SACP spectrometer with TAC.

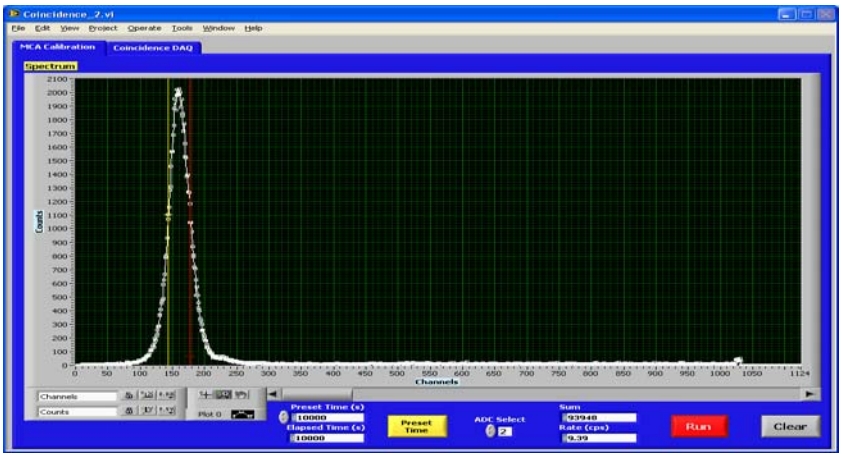

Fig. 7: The TAC spectra of ^{60}Co, measured presently in this project.

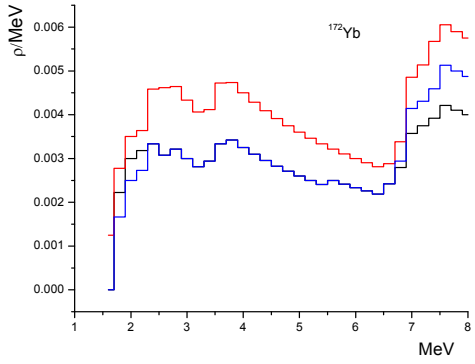

Fig. 8: The experimental excited level densities of ^{172}Yb with primary transitions of gamma, measured recently in this project.

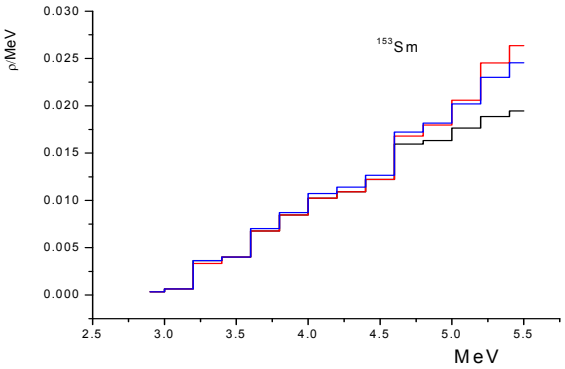

Fig. 9: The experimental excited level densities of ^{153}Sm with primary transitions of gamma, calculated recently in this project.

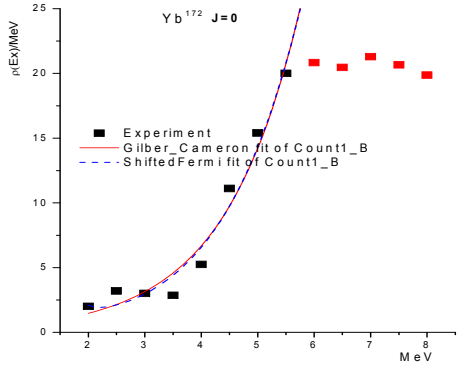

Fig. 10: The experiment and theory calculation of level densities of ^{172}Yb, the dash line is calculated according to constant of temperature model and line is calculated according to Fermi shift back model.

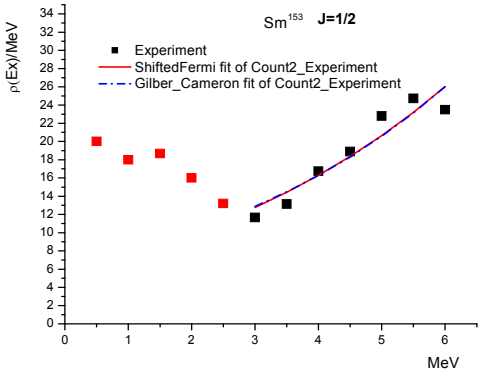

Fig. 11: The experiment and theory calculation of level densities of ^{153}Sm, the dash line is calculated according to constant of temperature model and line is calculated according to Fermi shift back model.

V. CONCLUSIONS

The project is implementing timely. It is useful to the fundamental research and application research on the neutron beam at the DNR.

The experimental ability of participants in this project are much more improved. They can do and carry out the new complex experiment.

The project creates good conditions for graduate students.

The authors would like to thank to Ministry of Science, Vietnam Atomic Energy Commission and Nuclear Research Institute for kind supports.

REFERENCES

[1]. Vương Hữu Tấn và cộng sự, Báo cáo tổng kết đề tài khoa học công nghệ cấp Bộ năm 2005-2006, Đà Lạt tháng 12/2006.

[2]. Vương Hữu Tấn, Phạm Đình Khang, Nguyễn Xuân Hải, Nghiên cứu phổ bức

xạ gamma nối tầng của ^{153}Sm và ^{172}Yb trong phản ứng bắt nơtron nhiệt, Hội nghị Khoa học và Công nghệ Hạt nhân toàn quốc lần thứ 7, Đà Nẵng, 30-31/8/ 2007.

[3]. V. H. Tan, T. T. Anh, N. C. Hai, P. N. Son and T. Fukahori, "*Measurement of Neutron Capture Cross Section of ^{139}La, ^{152}Sm and ^{191,193}Ir at 55keV and 144keV",* SND2006-V.02-1, Proc. of 2006 Symposium on Nuclear Data, Jan. 25-26, 2007, RICOTTI, Tokai, Ibaraki, Japan, ISBN978-4-89047-138-6, [CD], (2007).

[4]. V. H. Tan, T. T. Anh, N. C. Hai, P. N. Son, *Measurement of Neutron Capture Cross Section of ^{191,193}Ir at 55 keV and 144 keV*, Nuclear Science and Technology, Vol. 5, No. 1, pp. 13-20, VAEC, ISSN 1810-5408, (June 2007).

[5]. V. H. Tan, P. N. Son, T. T. Anh, N. C. Hai, T. Tu Anh, M. X. Trung, *Nghiên cứu xác định các tham số hiệu chính trong phép đo tiết diện bắt bức xạ nơtron,* Hội nghị Khoa học và Công nghệ Hạt nhân toàn quốc lần thứ 7, Đà Nẵng, 30-31/8/2007.

[6]. V. H. Tan, P. N. Son, T. T. Anh, N. C. Hai, "*Tính toán các thông số đặc trưng phục vụ phát triển các dòng nơtron phin lọc mới tại lò phản ứng Đà Lạt"*. Hội nghị Khoa học và Công nghệ Hạt nhân toàn quốc lần thứ 7, Đà Nẵng, 30-31/8/2007.

[7]. Hồ Hữu Thắng, Nguyễn Thị Thuý Nhâm, Nguyễn Kiên Cường, Nguyễn Xuân Hải, Ứng dụng mcnp4c2 xác định cấu hình che chắn tối ưu cho hệ phổ kế cộng biên độ các xung trùng phùng, Hội nghị Khoa học và Công nghệ Hạt nhân toàn quốc lần thứ 7, Đà Nẵng, 30-31/8/2007.

[8]. Nguyễn Thị Thuý Nhâm, Nguyễn Xuân Hải, Hồ Hữu Thắng, Phạm Ngọc Sơn, một số vấn đề về mật độ mức hạt nhân thực nghiệm của ^{36}Cl thu được từ hệ phổ kế SACP tại NRI, Hội nghị Khoa học và Công nghệ Hạt nhân toàn quốc lần thứ 7, Đà Nẵng, 30-31/8/2007.

[9]. V. A. Khitrov, A. M. Sukhovoj, Pham Dinh Khang, Vuong Huu Tan, Nguyen Xuan Hai, On the correctness of various approaches in the extraction of the nucleus parameters on example of analysis of the two-step gamma-cascades in ^{163}Dy compound nucleus, Proceedings of the XIV International Seminar on Interaction of Neutrons with Nuclei, May 24-27 2006, Dubna, JINR E3-2007-23, pp. 257-265.

[10]. V. A. Khitrov, A. M. Sukhovoj, Pham Dinh Khang, Vuong Huu Tan, Nguyen Xuan Hai, Possibilities to verify the level density and radiative strength functions, extracted from the two-step gamma-cascade intensities, Proceedings of the XIV International Seminar on Interaction of Neutrons with Nuclei, May 24-27 2006, Dubna, JINR E3-2007-23, pp. 266-283.

STUDY OF BEAM DYNAMICS IN CYCLOTRON

Nguyen Tien Dung, Trinh Dinh Truong, Nguyen Manh Hung
Pham Dinh Khang and Others

Institute for Nuclear Science and Technology, VAEC, Vietnam.

ABSTRACT: PET cyclotron, joint project between Hospital-108, VAEC, Physics institute, Universities,.. has been implementing in 108 hospital. Study of beam dynamics in cyclotron and operation of IBA 30 is carrying out in order to operate, maintain the operation of IBA in the near future.

This project concentrates in two parts: Theory of beam dynamics in cyclotron and detailed techniques applied in IBA 30 cyclotron. The first part presents the progress of cyclotron from first O.E Lawrence cyclotron 1929 up to now. The importance idea of Thomas on the AVF cyclotron had been constructed at Berkeley in 1950. After that, separated sector cyclotron with magnet edge focusing effect has been applying widely in the word. Two kinds of this cyclotron, radial and spiral separated sector cyclotron, are implementing so much in many countries. The basic theory calculations for beam line of cyclotron are presented. The second part presents the main structure and operation of IBA30 cyclotron. The magnet of IBA, RF electrical field, accelerated gap, ion source,… are presented deeply. Theory of calculation for beam stability, flutter, field index,.. are also presented more details.

Content

1. Theory of beam dynamics in cyclotron

a. Classical cyclotron: Charged particles that move perpendicularly to a uniform magnetic field, will move on a circular orbit continuously. An appropriate oscillating electrical field put on the particle trajectories (diametral gap separating the dees) provides the acceleration for particles. The equation of motion: $mv^2/r = qvB$. From this equation we get angel velosity $\omega = qB/m$ and period of particles motion $T=2\pi m/qB$.

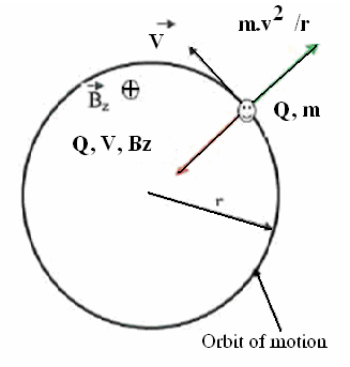

Fig. 1: Closed orbit of cyclotron

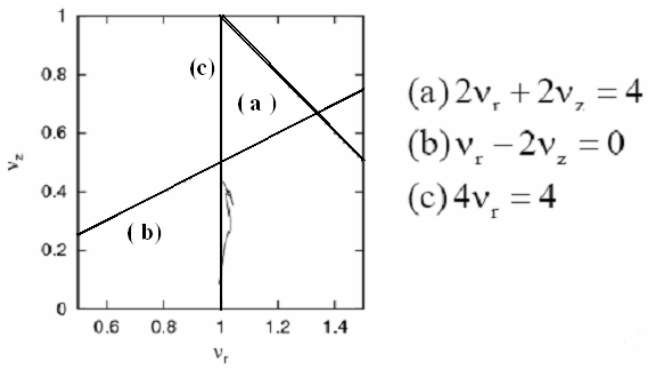

Fig. 2: Betatron motion of KIRAM cyclotron

Beside the basic motion of cyclotron, betatron motion is also studying. This motion is in both direction: radial and vertical motion.

Equation of vertical motion: $$\frac{d^2z}{d\theta^2} - \mu' z = 0.$$

And Radial motion equation: $$\frac{d^2x}{d\theta^2} + (1+\mu')x = 0$$

Condition for stability of these motion in both direction: **$-1 < \mu' < 0$**

b. Relativistic cyclotron: There are some limitation of classical cyclotron: isochronism condition and vertical focusing. Thomas had the idea to solve this limitation:

- Isochronism condition: Increase mean magnetic field with radius

- Vertical focusing: separated azimuthal sectors provide an azimuthally varying field providing addition vertical focusing force

The magnetic field of cyclotron has the shape in Pic.3

The magnet field could be written as : $$B(\theta) = \bar{B}(1 + f\cos N\theta).$$

In theory, Thomas proves that, isochronism condition and vertical focusing are solved. The idea was checked for the first time in 1950 at Berkeley by E.M. McMillan.

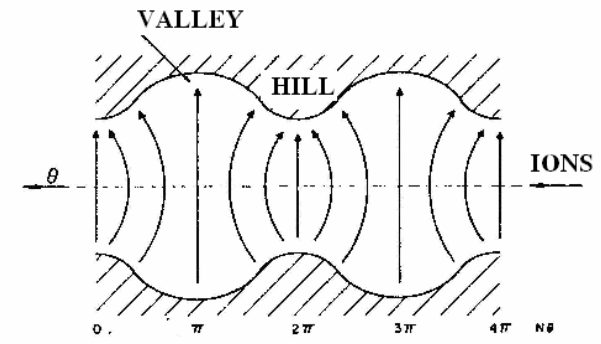

Fig. 3: Shape of magnet field of Thomas cyclotron

c. Radial and Spiral separated sector cyclotron

The present time, separated sector cyclotron was made largely based on the applying of edge focusing effect. The vertical focusing force depends on the angel between trajectory of particle and edge magnet. Two kinds are paid attention is Radial and Spiral separated sector cyclotron.

2. Structure and operation of IBA 30

The presentation focuses on the main parameters of IBA and technique related to the beam dynamics of this cyclotron: Magnet and RF generator.

a. Main parameters of IBA 30

- Acceleration of 30 MeV protons (H-)

+ Fixed field, fixed frequency

+ Variable dual proton beams (18 -30 MeV)

- Simultaneous dual target bombardment

- Four external beam lines

- Dual particle acceleration (Proton and Deuteron (9 -15MeV)

- Minimal running cost

+ Patented deep valley technology

- Integrated PLC (Programmable Logic Controller)

- High flux versions

+ 500 μA

+ External "multicusp" ion source

+ Extraction efficiency of 99.9 % at strippers

b. Magnet of IBA30: Magnet is created from 4 separated sectors. In order to make isochronism magnet (mean value of magnet increase with radius), flaps are installed in the valley region. There are some parameters of IBA magnet:

- Number of sectors: 4

- Sector angel: 54 -58 degree

- Magnet in Hill region: 1,7 Tesla

- Magnet in Valley region: 0,12 Tesla

- Diameter: 3,5 m, hight: 4 m, weigh: 70 tones, total power: 140 kW

Coil of magnet is supplied by power of 7,2 kW with voltage of 85 V. Magnet coil is coolled by water

c. Dee acceleration

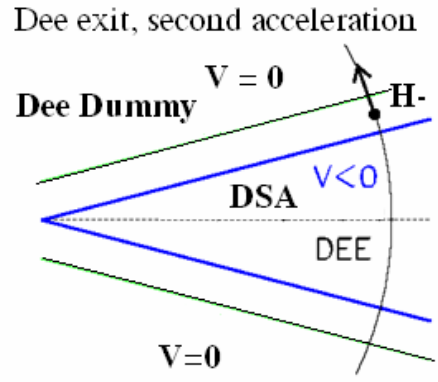

Fig. 4: Angel of dee.

Particles are accelerated when across the electrical gap.

The dee angel is 30 degree. Particle pulled in the dee entrance (Vdee > 0) and push in the dee exit (Vdee < 0).

Number of dee: 2

Dee voltage is 50 kV.

Frequency range: 65,5 MHz, frequency tuning by capacitor

Hamonic number mode: 4

3. Conclusion: The beam dynamics in cyclotron is complicated process. For the first year 2007, accelerator group concentrates on the theory of cyclotron, some detailed technique of IBA30. The other techniques of cyclotron are carrying out in the next years such as vacuum, ion source, RF resonance in accelerated gap,..

REFERENCE

[1]. Goto, Beam dynamic in cyclotrons.

[2]. F.I.M. FARLEY Progress in nuclear techniques and instrumentation, Volume 1, 1963.

[3]. E.J.Burge, The transport of charged particle beam.

[4]. http://en.wikipedia.org/wiki/Maxwell's_equations.

[5]. http://hyperphysics.phy-astr.gsu.edu/hbase/electric/vandeg.html.

[6]. Reference of IBA 30.

[7]. Reference of KIRAMS 13.

STANDARDIZATION OF IRRADIATION VALUES AT THE RADIATION CALIBRATION LABORATORY

Pham Van Dung, Hoang Van Nguyen, Phan Van Toan, Phan Dinh Sinh
Tran Thi Tuyet and Do Thi Phuong

Nuclear Research Institute, VAEC, Vietnam.

ABSTRACT: The objective of the theme is to determine dose rates around radiation facilities and sources in the NRI's Radiation Calibration Laboratory. By improving equipment, calibrating a main dosemeter and carrying out experiments, the theme team received the following results:

1. The controller of a X-rays generator PYA-200 was improved. It permits to increase accuracy of radiation dose calibration up to 2-4 times.
2. The FAMER DOSEMETER 2570/1B with the ionization chamber NE 2575 C of the NRI's Radiation Calibration Laboratory was calibrated at SSDL (Hanoi).
3. Dose rates at 4 positions around a high activity Co-60 source were determined.
4. Dose rates at 3 positions around a low activity Co-60 source were determined.
5. Dose rates at 3 positions around a low activity Cs-137 source were determined.
6. Dose rate at 1 position of a X-rays beam (Eaverage = 48 keV) was determined.
7. Dose rate at 1 position of a X-rays beam (Eaverage = 65 keV) was determined.

CONTENTS

Tasks

Calibrating a Dose Meter of the NRI's Radiation Calibration Laboratory Establishing at the SSDL (Hanoi) and then using it to determine dose rate values at some positions around gamma and X-rays radiation irradiating facilities.

Research contents

- Calibrating the FAMER DOSEMETER 2570/1B with an ionization chamber NE 2575 C at the SSDL (Hanoi).

- Determining Dose Rates at 3 irradiating positions around a low activity Co-60 source (No.8).

- Determining Dose Rates at 4 irradiating positions around a high activity Co-60 source (No.7).

- Determining Dose Rates at 3 irradiating positions around a Cs-137 source (No.25).

- Determining a Dose Rate at one irradiating position in a X-rays beam (Eaverage = 48 keV).

- Determining a Dose Rate at one irradiating position in a X-rays beam (Eaverage = 65 keV).

Methods and techniques

- *Methods*: Using experimental methods.
- *Techniques*: Thermoluminescence and radiation calibration techniques.

Results

1. Calibrating the FAMER DOSEMETER 2570/1B

The FAMER DOSEMETER 2570/1B with an ionization chamber NE 2575 C was calibrated at the SSDL (Hanoi) on a Cs-137 source, a X-rays beam ISO N60 and a X-rays beam ISO N80.

2. Standardization of Irradiation Values of a Co-60 source (No.7)

Gamma dose rates at 04 irradiation positions around the Co-60 (No.7) were determined. Experimental Results were presented on Table 1.

Table 1: Dose Rates (P) in air at some irradiating positions around the Co-60 source (No.7) (20^{th}, Novem. 2007).

Position	P [mGy/h]
6	16.410 ± 0.023
12	8.564 ± 0.014
22	3.596 ± 0.006
24	3.122 ± 0.005

3. Standardization of Irradiation Values of a Co-60 source (No.8)

Gamma dose rates at 03 irradiation positions around the Co-60 (No.8) were determined. Experimental Results were presented on Table 2.

Table 2: Dose Rates (P) in air at some irradiating positions around the Co-60 source (No.8) (25^{th}, Novem. 2007)

Position	P [mGy/h]
0.5 m from the source	0.0449 ± 0.0018
0.8 m from the source	0.0176 ± 0.0002
1.0 m from the source	0.0112 ± 0.0006

4. Standardization of Irradiation Values of a Cs-137 source (No.25)

Gamma dose rates at 03 irradiation positions around the Cs-137 source (No.25) were determined. Experimental Results were presented on Table 3.

Table 3: Dose Rates (P) in air at some irradiating positions around the Cs-137 source (No.25) (15^{th}, Novem. 2007)

Position	P [mGy/h]
0.5 m from the source	0.0144 ± 0.0008

1.0 m from the source	0.00344 ± 0.00023
1.5 m from the source	0.00157 ± 0.00015

5. Standardization of Irradiation Values of a X-rays beam (Eaverage = 48 keV)

Dose rate at one irradiating position in a X-rays beam (Eaverage = 48 keV) was determined. Experimental Results were presented on Table 4.

Table 4: Dose Rates (P) in air at one irradiating position in a X-rays beam (Eaverage = 48 keV)

Experiment	P [mGy/h]	P_{TB} [mGy/h]
1	0.478	0.463 ± 0.016
2	0.465	
3	0.446	

6. *Standardization of Irradiation Values of a X-rays* beam (Eaverage = 65 keV)

Dose rate at one irradiating position in a X-rays beam (Eaverage = 65 keV) was determined. Experimental Results were presented on Table 5.

Table 5: Dose Rates (P) in air at one irradiating position in a X-rays beam (Eaverage = 65 keV)

Experiment	P [mGy/h]	P_{TB} [mGy/h]
1	0.615	0.617 ± 0.002
2	0.618	
3	0.619	

Conclusion

The theme fulfilled all proposed contents and aims.

REFERENCES

[1]. Pháp lệnh An toàn và Kiểm soát bức xạ và văn bản hướng dẫn thi hành, Nhà xuất bản Chính trị Quốc gia, Hà Nội, 1998.

[2]. IAEA (2000), Calibration of radiation protection monitoring Instruments, SRS No.16.

[3]. ISO 4037-1 (1996), Radiation characteristics and production methods.

[4]. ISO 4037-3 (1999), Calibration of area and personal dosemeters and the measurement of their response as a function of energy and angle of incidence.

[5]. ICRU Report 51 (1993), Quantities and Units in Radiation Protection Dosimetry.

[6]. Hoàng Văn Nguyện và các tác giả (1999), *Một số nghiên cứu trong lĩnh vực định liều lượng bức xạ ion hóa,* Đề tài KH cấp Bộ.

DESIGN AND CONSTRUCTION OF THE 8K MULTI-CHANNEL GAMMA SPECTROMETER MODULE (AMPLIFIER+ADC+MCD)

Truong Van Dat, Hoang Thi Ngoc Bich, Pham Ngoc Tuan
Dang Lanh, Tuong Thi Thu Huong and Vu Xuan Cach

Nuclear Research Institute, VAEC**,** Vietnam.

ABSTRACT: A multichannel pulse-height analyzer system (MCA) consists of an spectroscopy Amplifier, ADC with 8192 channel performance, a histogramming memory, and a visual display of the histogram implemented on a Personal Computer (PC). The purpose of the analog-to-digital converter (ADC) is to measure the maximum amplitude of an analog pulse, and convert that value into a digital number. This digital output is a proportional representation of the analog amplitude at the ADC input. The digital ADC outputs are stored in a histogram memory, where each bin represents a pulse height interval and the number of events in each bin represents the number of events in that interval. The combination of ADC, histogramming memory and display functions are the minimum to constitute a multichannel analyzer or MCA based on PC. It is designed and fabricated on a single NIM module.

The communication between MCA module and PC implements via USB bus. In our application, performance of the USB standard version 1.1 is good enough for purposes.

The application program was designed in LabWIEW 8.0 software. This application is the main display and acquisition software for the MCA module. It is compatible with Windows 98SE/XP. The libraries USB driver, with their supporting files, are in the FTD2XX driver DLL Package and D2XX function 7.0 for LabWIEW supporting. These libraries are used to write custom code to control the MCA module.

I. INTRODUCTION

MCA 8K General description

A modern multichannel pulse-height analyzer system (MCA) consists of a spectroscope Amplifier, an ADC, a histogramming memory and visual display of the histogram recorded in the memory implemented almost universally on a Personal Computer (PC).

I.1. Spectroscopy Amplifier

The amplifier is one of the most important components in a pulse processing system for applications in counting, timing, or pulse-amplitude (energy) spectroscopy. Normally, it is the amplifier that provides the pulse-shaping controls needed to optimize the performance of the analog electronics.

For pulse-height or energy spectroscopy, the linear, pulse-shaping amplifier performs several key functions. Its primary purpose is to magnify the amplitude of the preamplifier output pulse from the millivolt range into the 0.1 to 10 V range. This facilitates accurate pulse amplitude measurements with analog-to-digital converters, and single-channel pulse-height analyzers. In addition, the amplifier shapes the pulses to optimize the energy resolution, and to minimize the risk of overlap between successive pulses. Most amplifiers also incorporate a baseline restorer to ensure that the baseline between pulses is held rigidly at ground potential in spite of changes in counting rate or temperature.

I.2. The ADC and MCA Circuits

The purpose of the analog-to-digital converter (ADC) is to measure the maximum amplitude of an analog pulse, and convert that value into a digital number. This digital output is a proportional representation of the analog amplitude at the ADC input.

For sequential, randomly spaced pulses, the digital ADC outputs are stored in a histogram memory, where each bin represents a pulse height interval and the number of events in each bin represents the number of events in that interval. In a conventional radiation spectroscopy system, the input to the MCA is the output from a pulse-counting radiation detector preamplifier, after suitable processing by a filter amplifier ("spectroscopy amplifier") to optimize the signal-to-noise ratio, the output of such detector is linear proportional to the energy of the incident particle or photon, and thus the histogram represents the energy spectrum of the source.

The combination of main Amplifier, ADC, histogramming memory and display functions are the minimum to constitute a multichannel analyzer or MCA based on PC. It is designed and fabricated on a single add-on card (full 2M wide NIM standard module).

As introduction, the general construction of MCA plug-in card is the combination of ADC, histogramming memory with several auxiliary blocks for pulse-height analys is and storage function, USB Interfacing circuit.

Successive Approximation Analog-to-Digital Converter

The main ADC device named AD7899BR1 was used in circuits.

Lower and Upper Level Digital Discriminators

The Lower Level Discriminator (LLD) and the Upper Level Discriminator (ULD) controls set the limit for the input signals to be accepted by the ADC for conversion. If an input pulse falls within the selected window (higher than the LLD setting but lower than the ULD setting) the input will be converted. If the input does not fall within the window, the input will not be converted. The window check is made at the conclusion of the linear gate time.

These discriminators stages are built based on two comparators and DAC circuits. Adjust cutting levels can do by programing in order to give out two DC voltage levels of LLD and ULD. According to LLD and ULD levels, two comparators will discriminate the input pulse to output the logic signal for controlling the pulse stretcher.

Pulse stretcher (sample and hold).

Analog-to-digital converters, especially to the successive approximation ADCs, used in nuclear spectroscopy need a certain time interval to convert the measured voltage into its binary equivalent. Therefore the peak value of pulses from spectroscopic amplifiers must be kept until the conversion is completed. This is the purpose of the PULSE STRETCHER.

The requirements on the pulse stretcher are several. It must:

1. Detect and hold the peak of a pulse

2. Tell the ADC that the peak has arrived

3. Disconnect itself from the source of pulse

4. Receive a signal from the ADC indicating that the conversion is done

5. Discharge the peak holding capacitor

6. Reconnect itself to the pulse source to repeat the process.

The most important logic signals from and to ADC are:

- DRDY: Data Ready, to start the acquisition cycle on memory
- DACC: Data Accepted, end of data transfer to memory
- SC: Start conversion of ADC
- LIVE TIME: Output pulse to indicate that ADC is not busy.

Multichannel Data Acquisition

A design for an interfacing unit to connect an external ADC to a computer is described. An add-on card for a PC computer was constructed, with the circuits required to control the data flow and storage.

A half remain part of MCA plug-in card is for multichannel data acquisition interfacing with PC computer via USB Port. It consists of several functional logical elements as follows:

- Depth latch for ADC, Address latch for Micro-controller, Histogram memory, Adder and rewrite to memory, Data readout latch from Histogram memory, Logic control unit, Live and real time counter.

- The pulse height after analyzed by ADC is presented in a 14-bit binary code. This code is used as an address of a channel in memory. The content of channel according to the address defined by ADC is incremented each time the DATA READY apears. As shown in the timming diagram, all the timing logical cycle of acquisition part is divided into two small phases with 50% for each. One is for ADC acquisition and the other is for accessing from computer. An extra important work is to record the real and live time information of pulse height analysis. It is done by two real and live time counter based on counter and micro-controller.

Interface

Most PC peripheral devices and interface cards are controlled through the input/output (I/O) ports. In our design, the USB controller chip named FT245RL is used for all I/O functions with PC via USB bus with full transmite speed rate, following USB standard specification version 1.1.

Firmware

Firmware has been written in extended C language for 805X micro-contoller family to perform transmiting/receiving data between device and PC. This firmware is edited and compiled by Keil C51 C compiler software then program into program momory of micro-controller.

Software application

Main software applicaion has been written in LabVIEW 8.0 to perform some main functions for multi-channel analyzer system as follow:

- Interfacing between device and PC
- Control the device
- Readout histogram memory and send to PC
- Displaying and processing pulse-height analyzer spectrum.

II. PURPOSES OF THE PROJECT

Research on design and construction of MCA 8 K Add-on Module interfaced with PC via USB bus. This module consists of spectroscope amplifier, ADC, MCA and USB interface and uses for multi-channel analyzer of radiation pulses. The transmission of data/command for controling the device and reading out the data histogram performs through USB bus. The full speed rate for transmiting data/command of USB V1.1 standard is use in our design. The application firmware need developing to control the USB bus, to get data from device or to send control command to device, etc,... The main application program should be developed in LabVIEW environment for controling the device, getting data histogram, displaying, viewing and preprocessing the multi-channel spectrum.

III. RESEARCH ACTIVITIES

Design and construction the multi-channel analyzer which has some main modules and application software as follow:

- Spectroscope Amplifier
- Fast analog to digital converter circuit with capacity of 8192 codes perfomance
- MCA and data histogram circuit
- Main controller circuit consists of AT89C52 micro-controller, Timer/counter, I/O port and USB controller
- Write the firmware for AT89C52 micro-controller and FT245 USB controller
- Write the main MCA application program in LabVIEW for running on PC.

IV. METHOD USED FOR RESEARCH

- Design and contruction some suitable electronic circuit with have the mentioned-above specification.
- Reseach on the field of application standard USB bus, version 1.1 and FT245 USB controller.
- Study on for writing and developing the application program in LabVIEW.
- The firmware was developed in the C language and the application software is writen in LabVIEW 8.0 for running in win 9X or winXP.

V. RESULTS

The MCA 8K module has the main following hardware specifications:

- Amplifier INPUT Polarity : positive or negative, $Z_{in} \approx 1k\Omega$

- Amp. COARSE Gain : 5; 10; 20; 100; 200
- AMP. Fine Gain : 0.5 1.5
- Shaping Time : 0.5μs; 1μ s; 2μs; 4μs; 6μs; 10μs
- Amp. OUTPUT : Unipolar positive, semi-gausse 0 ÷ 10V
- ADC Successive-approximation type with sliding scale linearization
- RESOLUTION : 8192 channels
- DEAD TIME PER EVENT 5μs, including memory transfer
- INTEGRAL NONLINEARITY ≤ ± 0.025% over the top 98% of the dynamic range
- DIFFERENTIAL NONLINEARITY < ±1% over the top 98% of the dynamic range
- DATA memory capacity: 2^{24} counts per channel (16.7 millions counts)
- PRESETS: Real Time/Live Time Multiples of 1 s
- ADC LLD AND ULD Adjustable from 0 to 100% of full scale via hardware and software control
- POWER REQUIRED +6V/800mA, ± 24V/250mA
- DIMENSIONS NIM Standard module 2M wide.

CONCLUSIONS

Based on the technical standard and specifications specified in the contract, we carried out to design and construct the NIM electronic module named MCA 8K. After checking and testing, the results shown that this system operates well and meet almost specifications above-mentioned.

REFERENCESR

[1]. LabWIEW user manual: LabWIEW concepts, Aprill 2003 Edition.

[2]. LabWIEW user manual: Getting Started with LabWIEW, Aprill 2003 Edition.

[3]. LabWIEW user manual: Building and Editing VIs, Aprill 2003 Edition.

[4]. Microcontroler Data Book, AT89 series Flash MCUs, December 1997.

[5]. Selected Topics in Nuclear Electronics, IAEA-TECDOC-363, Vienna 1986.

[6]. Troubleshooting in Nuclear instruments, IAEA-TECDOC-426, Vienna 1987.

[7]. Universal Serial Bus Specification, Revision 1.1,September 1998, PDF Document.

[8]. D2XX_Function 7.0 for USB driver, supported for LabWIEW function call in LabWIEW, www.ftdichip.com

[9]. FTD245 Datasheet, PDF Document, www.ftdichip.com

[10]. D2XXPG32.pdf manual guide for using and programming FTD245 USB controller, www.ftdichip.com

[11]. Model 2026 Spectroscopy Amplifier, Canberra.

DESIGN AND CONSTRUCT AN INTERFACE CARD FOR SPECTROSCOPY OF AMPLITUDE OF COINCIDENT PULSES

Nguyen Xuan Hai, Pham Ngoc Tuan, Pham Dinh Khang, Vu Xuan Cach, Ho Huu Thang Tran Tuan Anh, Hoang Thi Ngoc Bich, Nguyen Canh Hai, Nguyen Thi Thuy Nham Tuong Thi Thu Huong, Pham Ngoc Son and Pham Duy Tung

Nuclear Research Institute, VAEC, Vietnam.

ABSTRACT: In 2005, the spectroscopy basing on the summation of amplitude of coincidence pulses had been setup completely on the third horizontal channel of neutron beam at Dalat Research Reactor (DRR). In 2006, it was planted to improve the specifications. It was increased from two channels to three channels for data acquisition. To solve this problem, the project which designs and constructs an interface card with three channels for control of data acquisition of spectroscopy of summation of amplitude of coincidence pulses (SACP) has been done. And some new techniques have been used in designing and manufacturing.

I. The objects

The task of project is to design and construct an interface card for multi-parameters analyses system (MPA); it is used for SACP spectroscopy to improve its qualities such as:

1. Determine isomer ratios and specific characteristics.

2. Perform prompt gamma neutron activation analysis (PGNAA) with dual channel simultaneously.

3. Perform gamma cascade research on intermediate energy regions below neutron binding energy with high qualities.

II. The contents

1. Design and construct the interface card for SACP spectroscopy which uses AN2131QC chip. It is connected with computer by universal serial bus (USB).

2. Write firmware to control the interface base on C++ language.

3. Write the application program to operate the data acquisition by LabVIEW language.

III. The methods

The instrument has been based on the SACP method, the principal operation is described in the Fig. 1.

In the coincidence mode:

In order to synchronize signals, ADCs are necessary to operate in a non-overlap mode, which disables the internal buffer. In this mode the ADCs cannot accept a second input for conversion until the first conversion has been accepted by the MPA. In this configuration the INHIBIT signal is now considered an INVALID signal, flagging an invalid input but not inhibiting storage. The MPA would use this INVALID indication as an input to record these types of events.

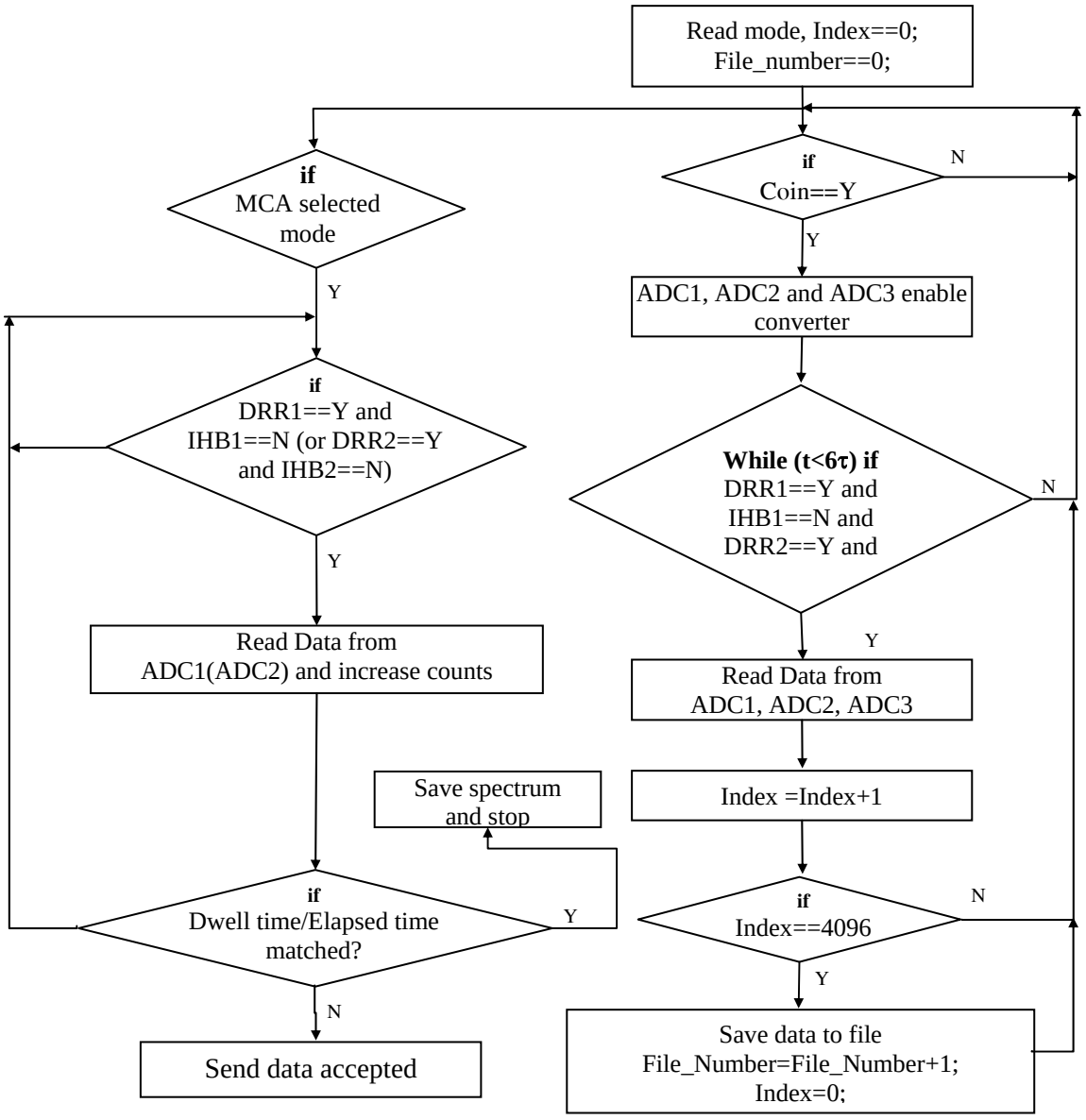

Fig. 1: The algorithm of act of interface card.

The interface will read data from all ADCs when the following conditions are satisfied:

- The coincident signal and the ADC's data ready signals are present.
- The ADC's inhibit signal are absent.

When the above conditions are satisfied, the data from all of ADCs are read by MPA, the coincident event index is increased by adding one, after that the accepted signal is sent to all of ADCs to permit of ADC's conversion. When the index of events number reaches 4096, the data are stored on file with three columns and 4096 rows, the file number is increased by adding one, and index is set by zero, then the new one will repeat this process.

In the MCA mode:

With this mode, when the interface is received the data ready from ADC, the ADC will be serviced, if INHIBIT signal is invalid; the pulse-height information from ADC needs to be stored in an array that gives the cumulative number of code observed in spectrum. This is done simply by adding a one to content of code of corresponding array to the pulse height measured. In others case, data will not be stored.

IV. The results

The MPA was designed and the first prototype was appeared in Nuclear Physics and Electronics Department-Nuclear Research Institute. The good testing results and good spectrogram results showed success of our works. The MPA was passed to the gamma two step cascades (TSC) research to setup in spectroscopy of SACP.

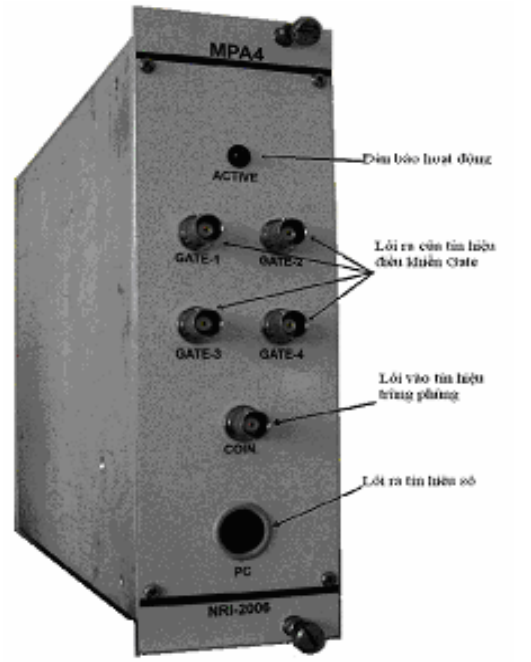

Fig. 2: The interface card.

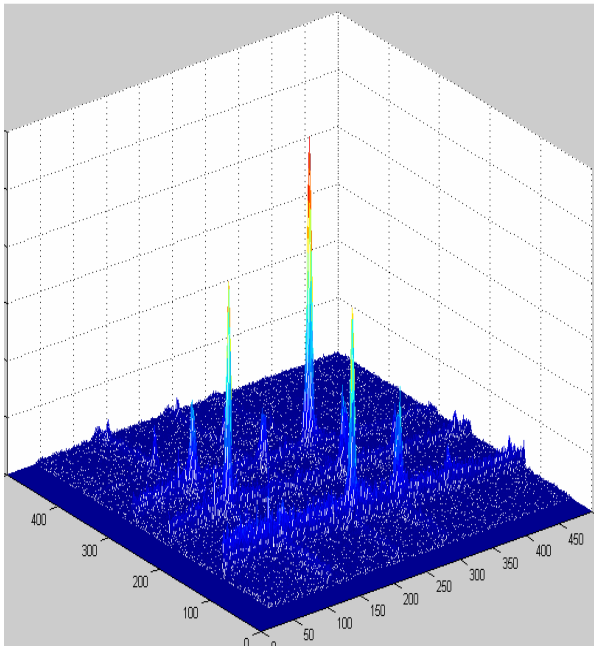

Fig. 3: The gamma spectrum of $^{149}Sm(n,\gamma)^{150}Sm$ reaction with thermal neutron.

The MPA is standard double width NIM module, the required power is +12V-800mA, inputs accept TTL positive pulses with BNC connector (01 BNC connector for coincident input and 04 BNCs connector for output to control gates of ADCs), and 01 socket is to connect with computer by USB. The front panel there is an active LED, it indicates operation status; at the rear there are three cables for data are 34 pins type, and two BNC connectors for pileup rejecter.

V. Conclusions

In fact, on the performance of the project, the participants have many opportunities to approach to gamma cascade research on the reactor. The participants studied themselves and improved knowledge to master a new measurement technique that belongs to nuclear data; it could be applied to multi-detector used in other fields and coincident measurement.

With the help of new instrument, the SACP spectroscopy has been became easy to use efficiently on studying physics on the neutron beam of reactor. The interface card has been developed the SACP spectroscopy with the ability to such as: Determine isomer ratios and specific characteristics, to perform PGNAA with dual channel simultaneously.

The authors would like to thank the Vietnam Atomic Energy Commission, the Nuclear Research Institute for kind supports to this project research.

REFERENCES

[1] Lab View user manual.pdf, document in pdf file.

[2] Microcontroller Data Book, AT89 series Flash MCUs, December 1997.

[3] Universal Serial Bus Specification, Revision 1.1, September 1998, document in pdf file.

[4] AN2131QC.PDF datasheet, document in pdf file.

[5] EZUSB52_ENG.PDF user manual guide document for using USB functions and USB software driver.

[6] User's manual Model 8713 ADC, Canberra.

[7] Pham Dinh Khang, Vuong Huu Tan, Nguyen Xuan Hai, Nguyen Duc Tuan, A.M. Sukhovoj and V.A. Khitrov, A Facility for the (n,2γ) Reaction Investigation at the Dalat Reactor, ISINN-14, May 25-28, 2006, Dubna.

DESIGN AND CONSTRUCTION OF THE ETHANOL-CHLOROBENZENE DOSIMETRY SYSTEM USING OSCILLOMETRIC METHOD

Nguyen Duc Hoa [(1)], Tran Khac An [(1)]
Huynh Dong Phuong [(2)], Bui Phi Khanh [(2)], Chau Le Ha [(2)], et al.

[(1)] Research and Development Center for Radiation Technology, VAEC, Vietnam.

[(2)] Center for Nuclear Techniques, VAEC, Vietnam.

ABSTRACT: The main objective of the project is to carry out the studies aiming at design and construction of a prototype Ethanol-Chlorobenezene (ECB) dosimetry system.

The research group has successfully designed and constructed the sample holder for the ECB ampoule- the most important part of the system, the measuring and processing circuits of the system based on the AT89C55WD microcontroller. The calibration and measurement are easily performed by using the interactive menu on the LCD display and keypads. With 8Kbytes of NVRAM and real time clock, the equipment is capable of storing about 100 calibration data and 500 measurement data during a rather long period without main power. The measurement range of the system is (0 - 50) kGy with the accuracy of ±3% and electronic drift of 0.05 kGy/^{o}C.

At present, the prototype dosimetry system, DOSIMETER D-001 has been used at Research and Development Center for Radiation Technology (VINAGAMMA) to measure absorbed doses in irradiated products for routine quality control.

1. Introduction

VINAGAMMA is a pioneer in the application of radiation technology with industrial scale for sterilization of medical products and pasteurization of foodstuffs. The dosimeter types of ECB are used at VINAGAMMA and other irradiation centers in Vietnam for quality assurance, quality control and irradiation service management. These type dosimeter were supplied in accompany with purchase contracts of irradiators for almost Cobalt-60 irradiation centers in Vietnam. Due to some weak points in the design, the accuracy and stability of these dosimetry systems sometimes give unreliable measurement results.

As the above mentioned reasons, the research project has been set up and implemented to design and construct a prototype ECB dosimetry system with higher quality and more reliability for improving QA-QC work at VINAGAMMA and other irradiation centers as well. After one year of the project implementation, the research group has successfully designed and constructed a prototype of the ECB dosimetry system. The report presents briefly the carried out work within scope of the project and its main results.

2. Project activities

a. Selection of dosimeter type

At present, there are many types of dosimeter for absorbed dose such as: Perspex, Themoluminescent, Ethanol-Chrolobenzene (ECB), Ferrous sulphate/Cupric sulphat, Ceric sulphat, Ceric sulphat/Cerous sulphat, ferrous sulphat, etc. A selection of

a type of dosimeter depends on the required accuracy and the purposes of dose measurement for each irradiation center. Among the above mentioned types of absorbed dose dosimeter the ECB dosimeter which was recommended by ISO and ASTM has been widely applied in many irradiation centers in the world for irradiation quality assurance.

ECB dosimeters (often ampoule shape) are put inside irradiation box filled with products and measured after irradiation. The basic principle of ECB method is based on a formation of HCl (Hydrochloric Acid) in ECB solution under the effects of ionizing radiation (gamma rays, electron beams, etc.). It was found that in the absorbed dose range from 0.1 kGy to 100 kGy, the created concentration of HCl in the ECB solution is linearly proportional to the value of dose absorbed by the solution. Therefore, the absorbed dose can be determined by measuring the concentration of HCl. The measurement of HCl concentration can be done by several methods such as *color titration*, *spectrophotometry*, *oscillometry*. However, for routine measurement, the oscillometry method of measurement is much more preferred. In this measurement method, the concentration of HCl is measured via conductivity of the solution inside ampoule ECB at high AC frequencies (45 MHz).

The results of studies in [6] and [7] have shown that the *oscillometry* method can be well applied for the dose range from 1 kGy to 300 kGy. The biggest advantage of this method is a non-destructive analysis method. These studies also indicated that ECB dosimeters are weakly effected by irradiation temperature. The temperature coefficient was about 0.05%/ ^{o}C at the temperature range of (-30 - +60) ^{o}C in the dose range of (1 - 30) kGy. The irradiated ampoule can be kept for long time in the light tight conditions and can be re-read if needed. The ECB also can be used to measure absorbed dose in irradiation field at low temperature because of low freezing temperature (-80^{o}C) of ECB solution.

b. Design and construction

The principle diagram of DOSIMETER D-001 is presented in figure 1.

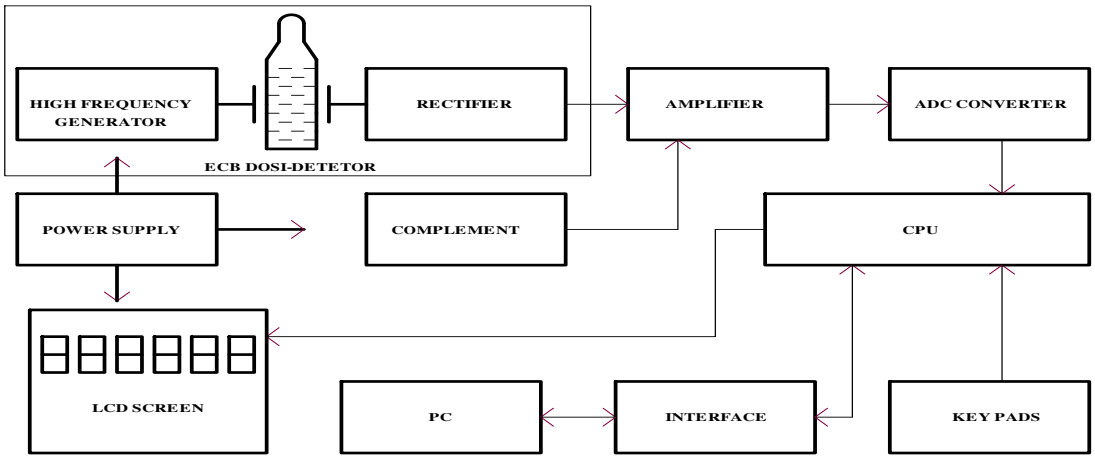

Fig. 1: Block diagram of the ECB Dosimeter D-001

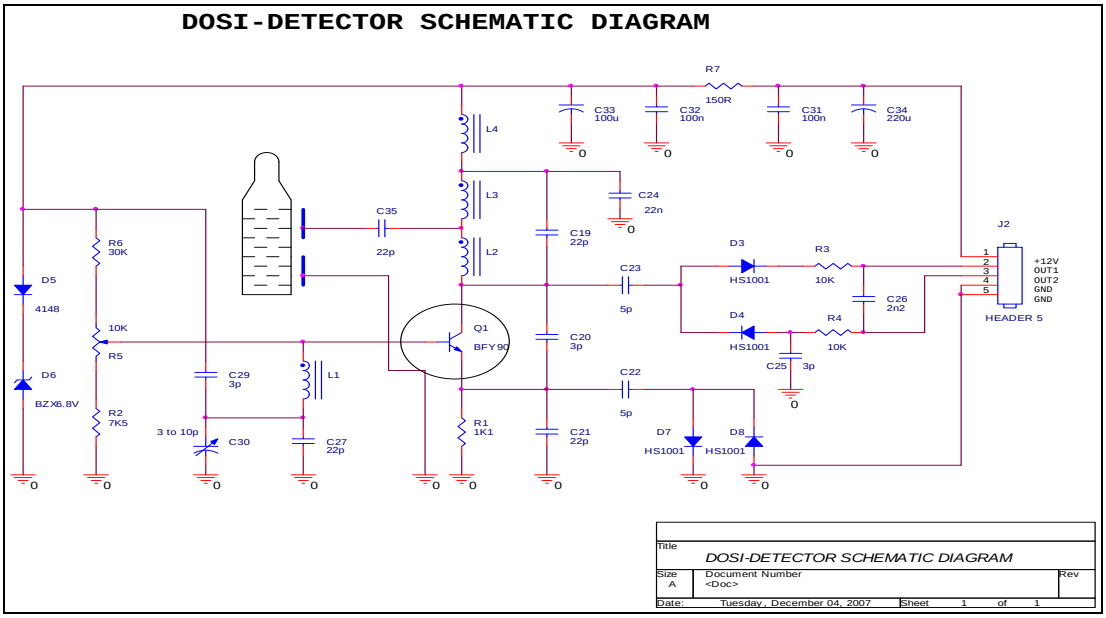

Fig. 2: Circuit diagram of detector

The sample holder (ECB Dosi-Detector) used as the sensing circuit for the instrument has been designed and constructed based on the above mentioned principle.

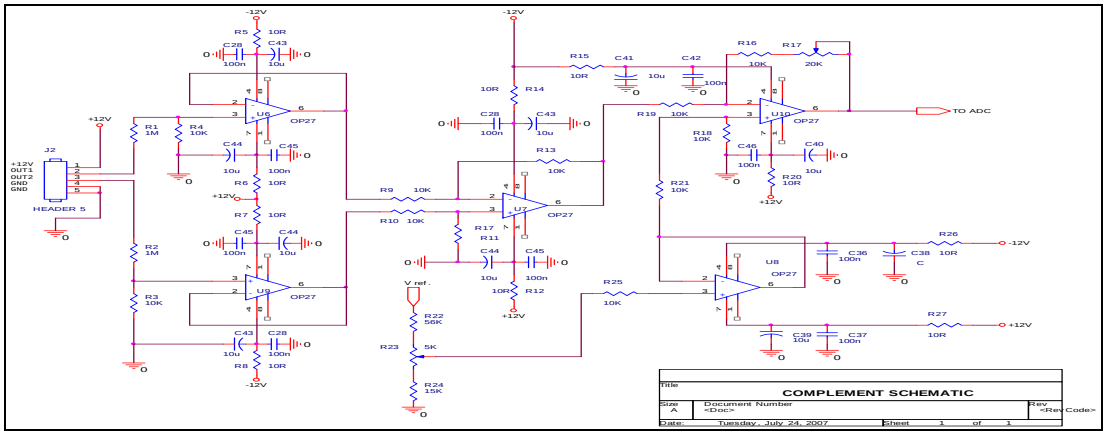

Fig. 3: Circuit diagram of Amplifier

The AC high frequency of 45 MHz generated by a sine wave generator is applied to two sides of the ECB ampoule in the sample holder. The signal from the ampoule is rectified and led to the amplifier circuit. The circuit diagram of the sample holder is given in figure 2. The signal from the amplifier is adjusted by the complement circuit before entering the input of an Analogue-Digital Converter (ADC). The circuit diagram of the amplifier is shown in the figure 3. The amplitude of the input signal for the ADC is proportional to the dose absorbed by the ECB dosimeter.

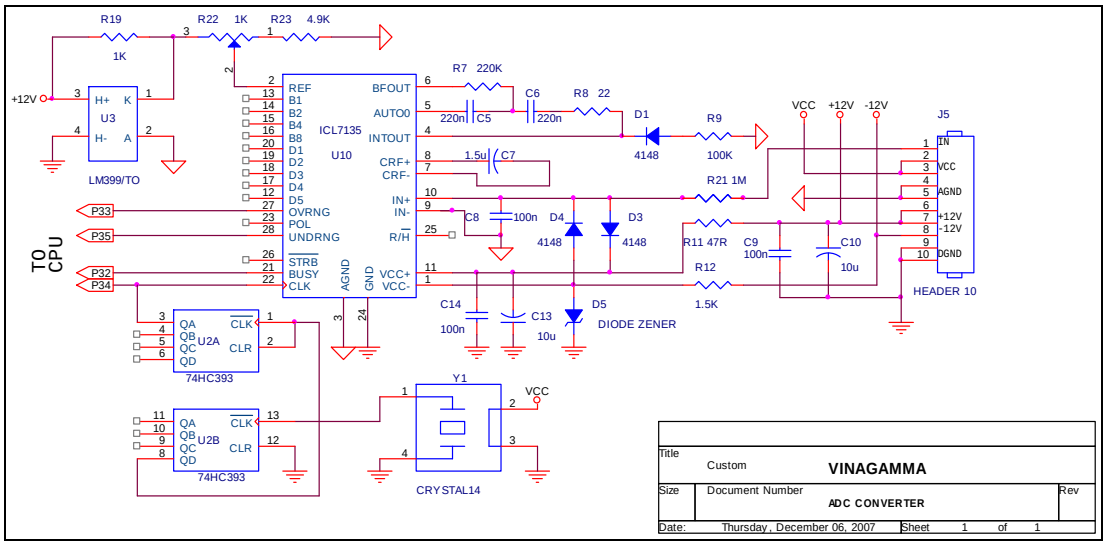

Fig. 4: Application circuit of ADC7135

The ADC circuit is built upon the industrial dual slope ADC, ICL7135. In this ADC BUSY signal is utilized due to its width proportional to the amplitude of the input signal. It makes the interfacing between ADC and the microcontroller very simple. The application schema of ADC converter is shown in figure 4.

The Central Processing Unit (CPU) of the instrument has the following circuits: the micro controller circuit, the Non Volatile RAM and Real Time Clock circuit (NVRAM-RTC) and peripheral circuits to interface with Keypads, ADC, LCD display and RS-232 transceiver. The schema of the CPU is shown in figure 5.

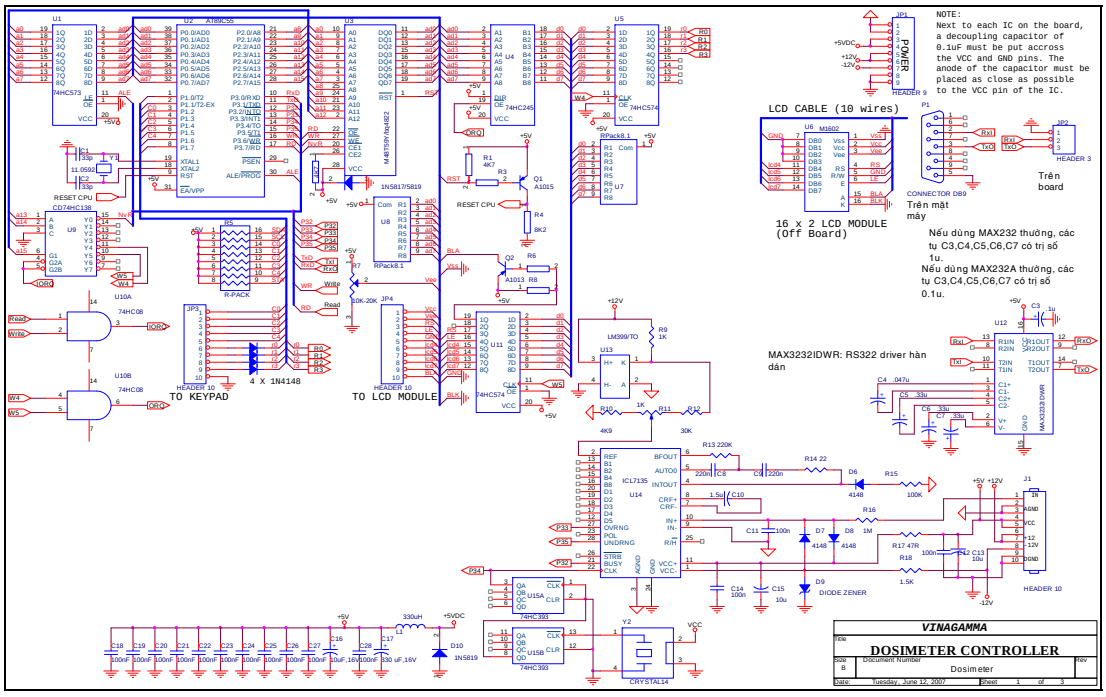

Fig. 5: Circuit diagram of CPU

The LCD display is used to interface the system with users. It can display 20 alpha-numeric characters in 4 lines. The LCD is connected to the mC via a 4-bit parallel data bus.

The system software has been written in C-language and built by using menu - driven method.

The measurement data can be transferred to PC by using built-in RS232 interface. The small program in Visual Basic has been written for data transfer.

c. Main specifications of ECB DOSIMETER D-001

d. ower supply: 220VAC ±10%, 0.1A

- Dose range: (1 - 50) kGy
- Accuracy: ± 3%
- Electronic drift: 0.05 kGy/^{o}C
- Calibration data: (2-100) points
- Data storage capacity: 500 records

Fig. 6: ECB DOSIMETER D-001

3. Results and discussions

Based on a powerful microcontroller and a control software written in C language the system can work as an independent dose meter with basic functionalities

of calibration and absorbed dose measurement. The use of integrated NVRAM and RTC allows short term storage of calibration data (maximum 100 points) and actual measurement data (maximum 500 records) with related information such as sample identifications, time and date of measurements, ADC counts and actual absorbed doses. The measurement data can be transferred to PC by using serial communication. The data is kept on PC hard disk in Excel format files. With the interactive and simple menu system on the LCD and the built-in keypad it is very easy to use the instrument to perform its functions. However, there are several problems which need to be solved to further improve the quality of the next reproduction instrument:

- Reduce as much as possible the electronic drift of detector.

- The sample hoder should be improved to get more stability of ampule holding.

- At present, the calibration of the system has been simply done by using linear interpolation between two adjacent calibration points. The calibration should be applied by using least-square method if the two above mentioned problems could be improved.

4. Conclusions

Although there are several points needed to be improved, the prototype dosimetry system ECB DOSIMETER D-001 has met the technical specifications which were set for the project. At present, the system has been used at VINAGAMMA for the quality assurance and management of the irradiation service. The prototype system is much lower cost than imported systems having the same main specifications.

REFERENCES

[1]. Dvornik, I: The Ethanol-Chlorobenzene Dosimeter. *Manual on Radiation Dosimetry*, N.W. Holm and R.J. Berry eds., Marcel Deker, Inc., New York, NY, 1970 345-349.

[2]. ISO/ASTM (2002) 51538. Practice for use of the ethanol-chlorobenzene dosimetry system. Standards on dosimetry for radiation processing- Second Edition 2004 ASTM stock number: RADPR2004.

[3]. Absorbed dosimetry system using ECB solution dosimeter at VINAGAMMA-Made in Hungary.

[4]. Vu Quoc Trong, Huynh Dong Phuong, Nguyen Duc Hoa, et al.. Design and construction of portable real-time irradiation measurement system- PRMS-01", VAEC Project report, 1999.

[5]. IAEA-TECDOC-1386, Edition January 2004.

[6]. A.Kovács, M. Baranyai, L. Wojnárovits: Characterization of fluorometric, calorimetric, oscilometric and radiomic dye film dosimeter under processing conditions at electron accelerators, [Dosimetry for radiation processing, IAEA-TECDOC-1156, IAEA, Vienna, June 2000, pp 71-79].

[7]. http://www.iki.kfki.hu/radsec/emds.htm.

IMPROVEMENT OF QUALITY OF RADIATION INDICATOR USED FOR FOOD IRRADIATION IN DOSE RANGE OF 3-10 kGy

Hoang Hoa Mai , Pham Duy Duong and Nguyen Dinh Duong

Institute for Nuclear Science and Technology, VAEC, Vietnam.

ABSTRACT: A sensitive indicators based on the polyvinyl butyral dyed with leuco-malachite green and metyl orange were made for use as devices for discriminating and monitoring radiation treatment in food irradiation. The sensitivity and stability of the indicator have been improved by using several additives such as CCl_4 in combination with di(nonylphenyl) isophthalate [dinonyl phthalate $–C_6H_4(COOC_9H_{19})_2$]

The dosimeters change their color from orange to greenish when irradiated with gamma rays or electrrons to dose just about 2 kGy. The greennish continue to develop to deep-green upon the increase of dose to 7 kGy. This makes the indicators useful for the dose range of food irradiation application, especially in treatment of fronzen meat and sea products for elimination of micro-organism. The quality of indicators are also improved by adjusting of factors and procedures during preparation of film and dosimeters. The indicators were produced in a stick-on label type showing attractive characteristics in use. The orange color before irradiation keep well stable for as long as 20 months under normal conditions in laboratory. The green after irradiation was maintained upto 12 months in pratical conditions of products. The indicator can be produced in big amount to supply to the irradiation facilities in Vietnam instead of imported devices.

Keywords: Indicators; irradiation; gamma rays; electron; stability; food irradiation; polyvinyl butyral; leuco-malichite green, metyl orange; dose rang.

1. Introduction

Stick-on label or dose indicator may be used as dose monitoring devices in the control of food irradiation. The dose indicator help to discriminate between irradiated and un-irradiated products as well as they may serve as evidence of irradiated food during post irradiation storage and commerce. There are some kinds of dose indicators have been developed and commercially available for use in radiation sterilization of medical supplies (Mclaughlin et al.1978; Ueno, 1988; Abdel Fahta, 1996; Hoang Hoa Mai et.al.1997). These indicators work well and prove their usefulness in high dose range of radiation sterilization of medical supplies with visible color change in the range of 20 -30 kGy. Meanwhile, there is very few systems have been developed and used for food irradiation range, especially the stick-on lable type for use in low dose range of several kGy (Sattar et al.1995, Razem, 1997; Ehlermann,1997). This work aims to improved the new kind dose indicators as the stik-on lables for use in dose rage of food irradiation in dose range of 3-10 kGy. The indicator is produced based on the polyvinyl butyral dyed with leuco-malachite green and metyl orange.

2. Experiment

2.1 Chemicals and preparation of samples

Poly(vinyl butyral - co-vinyl alcohol co-vinyl acetate) with molecular weight M = 90000 – 120000, 2- methoxy ethanol [$CH_3OCH_2CH_2OH$], 2-ethoxy ethanol [$C_2H_5OCH_2CH_2OH$], N,N – dimethyl formamide [$HCON(CH_3)_2$], ethanol [C_2H_5OH], chloral hydrate [$CCl_3CH(OH)_2$], 2,2,2-trichloro ethanol [CCl_3CH_2OH], leuco-malachite

green $[C_6H_5CH[C_6H_4N(CH_3)_2]_2$ and methyl orange were purchased from the Sigma-Aldrich Corporation and used without any further purification.

The stock gel polymer solution of PVB was prepared by dissolving in a mixture solvents incuding 2-ethoxy ethanol and 2-methoxy ethanol in a ratio of 50:50. The additives such as N,N-dimethyl formamide and 1-butanol were added in the system to control the viscosity of solution as well as the vaporation rate of solvents during drying later.

The mixture solution owns yellow color of orange methyl. The self adhesive paper was selected as base sheet for coating and preparation of stick-on label dose indicators. The dose indicators were made by cutting the coated sheet in to round pieces of 9mm in diameter.

2.2. Irradiation and analysis

Irradiation of samples was carried out using gamma ^{60}Co source having radioactivity of 6.3 TBq. The absorbed dose rate at irradiation position was measured to be 0.72 kGy/h using reference standard Fricke dosimeter. The radiation induced color change of the indicators is mostly identified visually, however, the grade or tone of color could be estimated by a spectrophotometor or densitometer.

3. Results and discussion

Fig.1 shows the samples of indicators made of PVB film coated on the adhesive paper, irradiated at different dose from 0 – 7 kGy. It is seen that, the color change from yellow to green occurs early at dose 2 kGy. This means that the sensitivity of indicators has been improved by adding a small amount of CCl_4.

0 kGy 2 kGy 3 kGy 5 kGy 7 kGy 10 kGy

Fig. 1: Indicator changes color at different dose levels of gamma rays

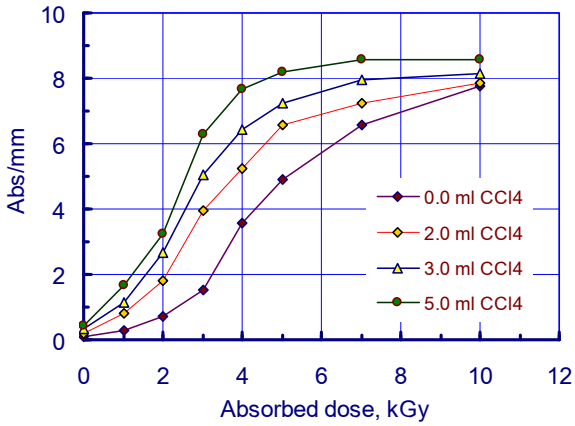

Fig. 2: The dependence of optical absorbance of indicator film upon the dose in the effect of sensitizer.

Fig 2 shows the effect of sensitizer on the sensitivity of indicator to gamma rays. The sample with higher concentration of CCl_4 added has higher absorbance at the same dose level and becomes saturated earlier than the sample with smaller sensitizer added.

Fig 3 shows the effect of sensitive additive on the stability of indicator. The figure indicates that if the amount of CCl_4 exceed 5 ml and without stabilizer added it may cause the samples severely unstable. The color of samples may change into green under normal conditions in a short time after manufactured.

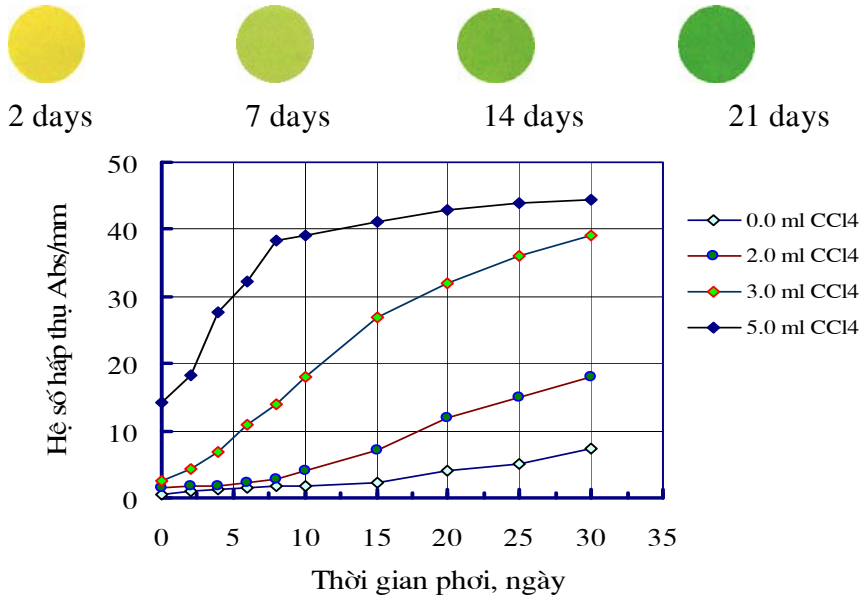

Fig. 3: The effect of sensitizer (CCl_4) on the stability of indicators

The unstability of samples may be improved by using several stabilizers naamely the antioxidant and UV-cut additives. The authors found that in combibnation with di(nonylphenyl) isophthalate [dinonyl phthalate $–C_6H_4(COOC9H_{19})_2$] the stability of samples before irradiation has been much improved. Fig 4 shows the color change of the indicators kept in different conditions of light. It is clear that, the samples kept in the dark the yellow color does change for 9 months.

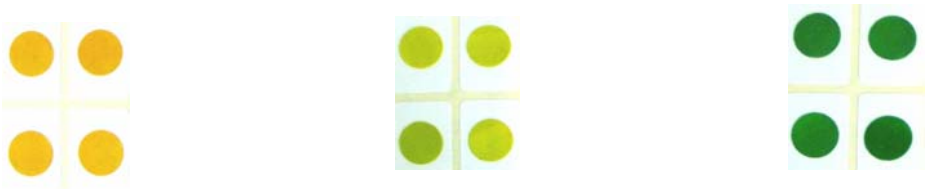

a) 9 months in dark b) 1 month under neon light c) 3 weeks under day light

Fig. 4: The appearance of new indicators kept in the different light conditions

The samples kept in the conditions of laboratory with neon-electric lights the yellow color changes to just slight green after three weeks. This indicates that the stability of dosimeters have been improved in comparison with the previous one.

IV. CONCLUSION

The indicator based on the polyvinyl butyral dyed with leuco-malachite green and metyl orange were was produced with enhanced sensitivity and stability. The indicator has been improved by adding a small amount of additives such as CCl_4 in combination with di(nonylphenyl) isophthalate [dinonyl phthalate–$C_6H_4(COOC9H_{19})_2$].

The indicators change their color from orange to greenish when irradiated with gamma rays or electrons to dose just start at 2 kGy and continue to develop to deep-green upon the increase of dose to 7 kGy. This makes the indicators useful for the dose range of food irradiation application, especially in treatment food products and medicinal herb products for elimination of micro-organism in dose range 3-5 kGy.

The orange color before irradiation keep well stable for as long as 20 months under dark shield conditions in laboratory. The green after irradiation was maintained more than 12 months in pratical conditions of products. The indicator can be produced in big amount to supply to the irradiation facilities in Vietnam instead of imported devices.

REFERENCE

[1]. Abdel-Fattah, A.A., El-Kelany, M. and Abdel Rehim, A., 1996. Development of a radiation sensitive indicator. *Int. J. Radiat. Phys. Chem.* **48**, pp. 497503.

[2]. Buenfil-burgos, A.E., Uribe, R.M., De La Piedad, A., McLaughlin, W.L. and Miller A, ., 1983. Thin plastic radiochromic dye film as ionizing radiation dosimeters. *Radiat. Phys. Chem.* **22**, pp. 325332.

[3]. Chu, R.D.H., Van Dyk, G., O'Hara, K.P.J., Bucland, B.W. and Dinelle, F., 1990. GafChromic dosimetry media. *Radiat. Phys. Chem.* **35**, pp. 767–773.

[4]. Hoang Hoa Mai, (1997), Development of dose sensitive indicators for industrial radiation processing. Journal of Chemistry, National Center for Natural Science and Technology Vietnam, Vol. 35, No.4 pp 78-82.

[5]. Mai, H.H., Duong, N.D. and Kojima, T., 2004. Dyed Polyvinylchloride films for use as high-dose routine dosimeters for radiation processing. *Radiat. Phys. Chem.* **69** 5, pp. 439444.

[6]. ISO/ASTM E 1539 - 93. Standard Guide for Use of Radiation Sensitive Indicators. American Society for Testing and Materials, West Conshohocken, PA, USA.

THYROID UPTAKE MEASUREMENT SYSTEM

Nguyen Duc Tuan, Nguyen Thi Bao My and Nguyen Van Sy

Institute for Nuclear Science and Technology, VAEC, Vietnam.

ABSTRACT: The NED-UP.M7 (Fig.1.) is a complete thyroid uptake and analysis system specifically designed for nuclear medicine. Capable of performing a full range of studies this system provides fast, accurate results for Uptake Studies. The heart of the NED-UP.M7 is a microprocessor-controlled 2048 channel Compact Multi-Channel Analyzer, coupled to a 2" x 2" NaI(Tl) detector with a USB personal computer interface. The system offers simple, straight-forward operation using pre-programmed isotopes, and menudriven prompts to guide the user step by step through each procedure. The pre-programmed radionuclides include I-123, I-125, I-131, Tc-99m and Cs-137. The user-defined radionuclides also allow for isotope identification while the printer provides hard copy printouts for patient and department record keeping. The included software program running on PC (Windows XP-based) is a user friendly program with menudriven and graphic interface for easy controlling the system and managing measurement results of patient on Excel standard form.

Fig. 1:

1. Introduction

In vivo measurement techniques are the most direct and widely used approach for assessing the burden of iodine radioisotopes within the body. The *in vivo* measurement of these radioisotopes within the body is performed with various radiation detectors and associated electronic devices that are collectively known as *in vivo* thyroid monitors or whole body counters, depending on the body site of interest. These radiation detectors commonly utilize sodium iodide (NaI), hyperpure germanium, and organic liquid scintillation detectors to measure the gamma rays and x-rays emitted from ^{125}I and ^{131}I. Applying this technique, the purpose of the project is to design and construct a PC-based compact multichannel analyzer system using NaI scintillation detector for performing, interpreting and reporting the results of thyroid uptake measurements.

2. Results

The hardware configuration of the thyroid uptake measurement system is described on figure 2 block diagram, consisting of three main parts which have specifications as follows.

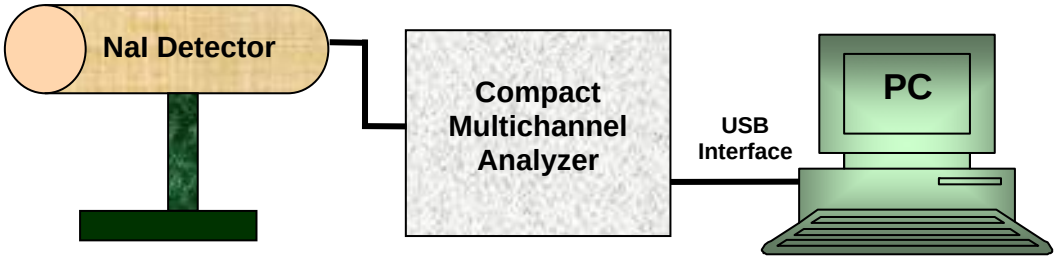

Fig. 2: System Block Diagram

- ***Computer:*** PC for Windows® XP with P4, 3 GHz processor, 512 megabyte RAM, 40g HD, 48x CD-RW.

- ***Probe Detector:*** 2" x 2" Nal (T1) integral line scintillation detector with tube base.

- ***Compact Multi-Channel Analyzer (Fig. 3):***

Resolution: 2048 channels

Spectral Resolution: FWHM 8% (Cs-137)

Maximum Count Rate: 100,000 cps

Connectors: Signal (BNC); high voltage (MHV)

Power Supply: 220V AC

Detector High Voltage Adjustment: H.V. adjustable, uses 10uCi Cs-137 as the calibration source.

Windows Application Programs: Thyroid Uptake, CD-ROM package

Pre-programmed Radionuclides: I-123, I-131, Tc-99m, Cs-137.

Uptake Stand:

Dimensions: 42" l x 31" w x 62" h (106.7 x 78.7 x 157.5 cm)

Collimated Shield: Flat field collimator meeting IAEA specifications

Lead Shielding Collimator: 1" thick (2.5 cm)

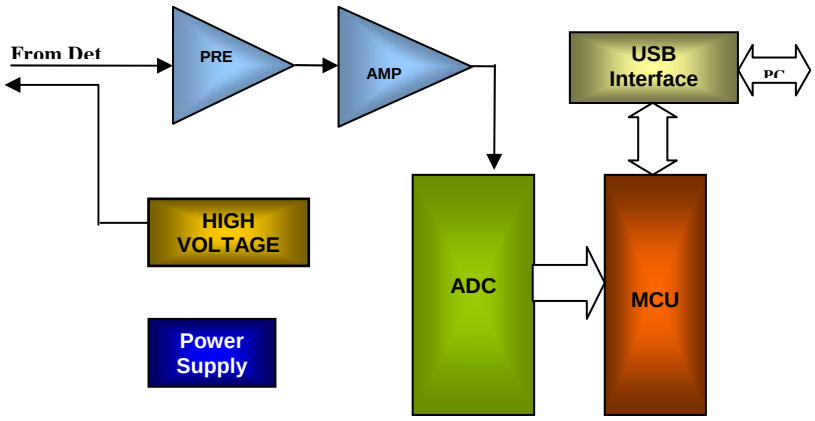

Fig. 3: Block Diagram of Compact Multichannel Analyzer

The software program provides fast, dedicated modules which cover all necessary procedures for QA-QC and uptake measurement as functions of **Energy Calibration** (use of Cs-137 reference source)**, Chi-Square Test, Uptake Measurement** and **Excel Output Standard Form** of results as described on figures 4, 5, 6, 7, 8.

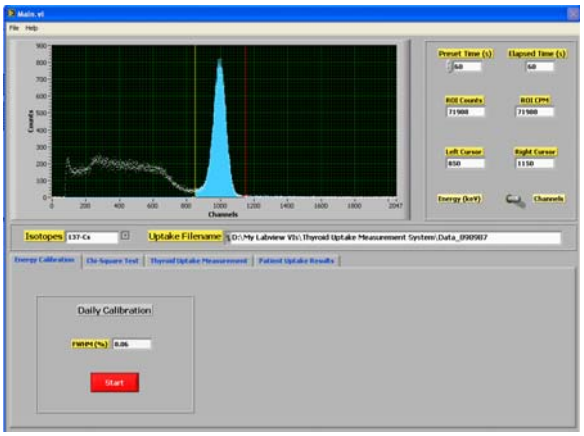

Fig. 4: Calibration function

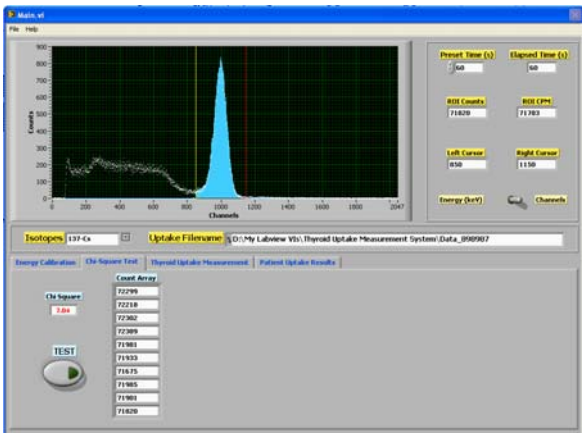

Fig. 5: Chi-Square Test Function

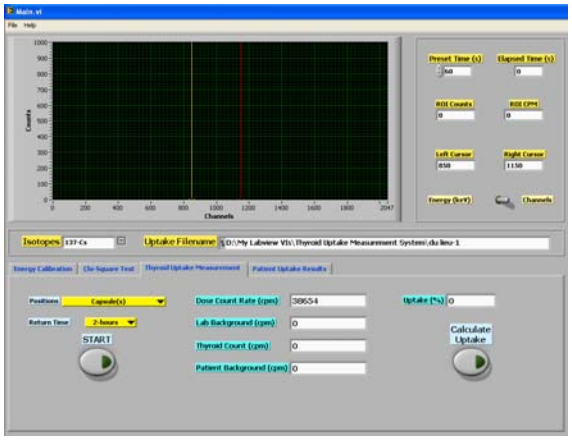

Fig. 6: Thyroid Uptake Measurement Function

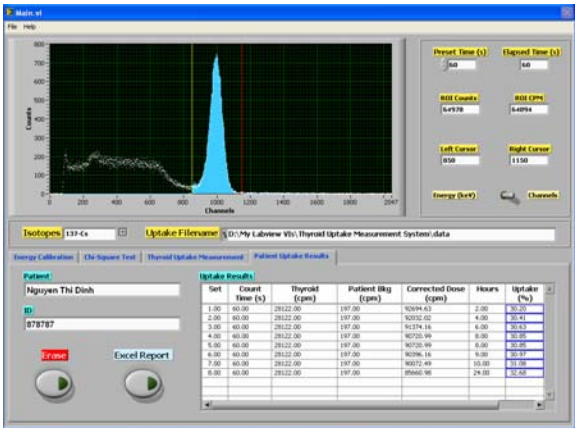

Fig. 7: Patient Uptake Results Function

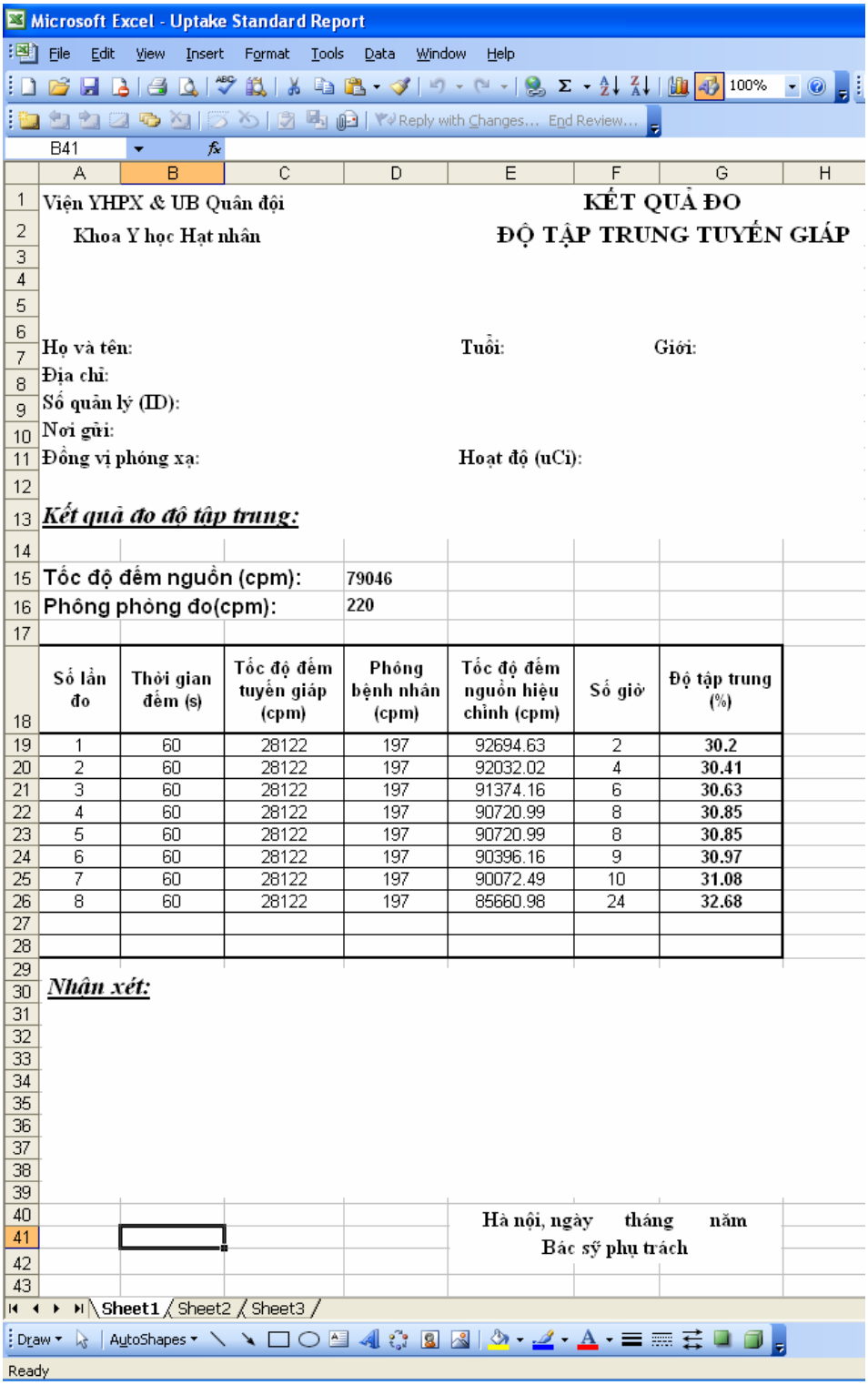

Fig. 8: Excel Standard Output Form for Patient Results

In addition, the prepared procedures with detailed protocols for regular quality control cover the function of its counting circuits, energy calibration, energy resolution, sensitivity, counting precision, linearity of energy response, background count rate, linearity of activity response and preset analyzer facilities, listed on the table below.

Test No.	Test	Reference	Acceptance	Frequency in routine testing		
				Daily	*Weekly*	*Half-yearly*
1	Channel-energy calibration	**x**	**x**	**x**		
2	Energy resolution (%FWHM)	**x**	**x**			**x**
3	Sensitivity	**x**	**x**		**x**	
4	Counting precision (Chi-Square)	**x**	**x**		**x**	
5	Linearity of energy response	**x**	**x**			**x**
6	Intergral background count rate	**x**	**x**		**x**	
7	Linearity of activity response	**x**	**x**			**x**

Test Schedule for Uptake Measurement System

3. Conclusion

All the hardware system and included software are designed and manufactured completely on the framework of the project. The thyroid uptake measurement system has been put into operation successfully as test experiment for 4 months at Military Institute of Medical Radiology and Oncology in Hanoi. The system has been used for uptake measurement in diagnostics and therapy on thousands of patients. In addition, beside the detector imported from foreign manufacturers, all the remained parts of electronics of the system and software are made and developed by ourselves as domestic products with low cost. These are extremely significant and possible in widely supplying for national nuclear medical applications.

REFERENCE

[1]. Handbook of Nuclear Medical Instruments-B.R.Bairi, Balvinder Singh, N.C.Rathod, P.V.Narurkar.

[2]. Instrumentation in Nuclear Medicine - Gerald J. Hine, Academy Press.

[3]. Radiation Detection and Measurement - Glenn F. Knoll.

[4]. Nuclear Electronics - P. W. Nicholson.

[5]. Quality Control of Nuclear Medicine Instruments - IAEA - TECDOC - 602 (1991).

[6]. Practical Nuclear Medicine - P.F. Sharp, H.G. Gemmell, F.W. Smith.

1.4 - Industrial Applications

ESTABLISHMENT OF TRACER TECHNOLOGIES IN GAS PHASE

Nguyen Huu Quang, Bui Quang Tri, Huynh Thai Kim Ngan, Dang Nguyen The Duy
Tran Tri Hai, Pham Hoang Ha, To Ba Cuong, Bui Trong Duy and Phan Thanh Khoa

Nuclear Research Institute, VAEC, Vietnam.

ABSTRACT: In industry it is very common problem of investigation of multiphase of gas, liquid and solid in which possibly exist complicated status between phases.

In the previous Projects, the Centre for Applications of Nuclear Technique in Industry has carried out the research on the phases of liquid, solids such as water, acid sulphuric, sand, microball carrier... To meet the increasingly requirement of gas industry it is necessary to estabish the base for gas tracing technologies which are not available yet in Vietnam.

However, because the scope of the gas tracing technologies is rather large and specific from case to case, this Project is mainly aimed at research of procedures of preparation of very common tracers such as Ar-41, CH_3Br-82 and Au-198 labeled water and organics along with tracer injection and tracer data acquisition, which are the base for starting gas tracing development. As results, the protocols, procedures of iradiation, preparation of tracer compounds, tracer injection and acquisition were built. A field experiment was also carried out to practice. Through the implementation of the Project the Tracer Lab of CANTI has been enhanced in competency.

PROJECT ELEMENT TASKS

- Summary of status and requirement of use of tracer in gas industry of the Country and the main applications of tracer to problem solving;

- Study of specifications of common tracers such as Ar-41, CH_3Br-82 and Au-198 labeled water and organics;

- Research on procedures of tracer preparation for Ar-41, Methyl Bromide and Au-198 labeled water and organics; tracer injection and data acquisition.

- Carry out a field test.

RESULTS

1. Summary of status and requirement of use of tracer in gas industry of the Country and the main applications of tracer to problem solving.

The gas industry of the Country is in development but still rather poor at present. In the last decade it were chemical industries at small scale and production of gas products such as chloride, amoniac, acid sulphuric, nitrogen, argon, hydrogen, dioxide carbon... Most of them was built before and just after 1975 with behind the time technologies.

Recently along with development of petroleum and natural gas exploitation industries the industry of gas proccesing and gas utilization are being founded. They are gas power plants, fertilizers, bulding materials and chemicals.

The common properties of gas industry is concerned with pressure, temperature, leakage and toxicity therefore high requirement of safety. In addition of optimization of production lines the gas industry also needs tracers and relevant radiation tests for ensurring safety and leakage. With the emerging and unique advantages of radioactive tracer in high penetration of radiation that allows carrying out investigation online with out shutdown the system the radioactive tracer becomes and promises a very efficient investigation tool beside the gas industry.

The main applications of tracers in gas industry include flow rate measurement, leak test, phase distribution, residence time distribution...

2. Preparation of Ar-41, Methyl Bromide-82 and Au-198 labeled water and organics

2.1 Preparation of Ar-41

Ar is known as the inert gas with isotope Ar-41 emmitting gamma is very common tracer due to not absorption, chemical reaction with material and fluids. The disadvantage of Ar-41 is short half life, 1.83h, that is just suitable to the fields near to the reactor and convenient transport.

Ar-41 is produced by neutron activation of Ar-40 which is of 99,6% in abundance, in the nuclear reacor. Argon gas is filled in the quartz ampoule to charge into the reactor. The filling system for gas is shown in figure 1, where the vaccum pump and low temperature of liquid nitrogen is used for emptying ampoule and calibration cylindre and trapping Ar gas into ampoule.

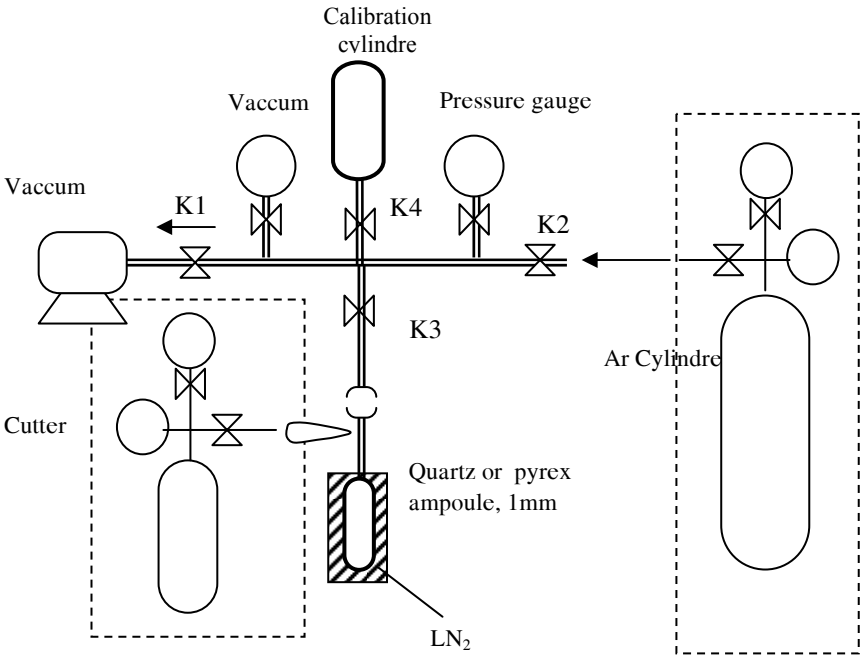

Fig. 1: Scheme for filling Ar

Ar ampoule is then tested in boilling water for 15 minutes before putting in the reactor for irradiation. The neutron activation equation for estimation of irradiation time, weight of Ar gas is introduced as following:

$$A = k.\sigma.(m/A_T).\eta.6{,}023.10^{23}) [1-\exp(-\lambda t_i)] [\exp(-\lambda t_d)] \quad (1)$$

where:

A – activity, Bq

σ- thermal neutron cross section, barn

k – dimension conversion factor

Φ – thermal neutron flux, n/cm^2.s

N_T – target nuclides

$N_T = (m/A_T).\eta.6{,}023.10^{23}$,

where η isotope abundance; A_T atomic mass, g; m sample weight, g.

λ - decay constant, s^{-1}

t_i – irradiation time, s

t_d – decaying time, s

Ar-41 was produced with the parameters shown in the table 1.

Table 1: Paraeters of irradiation Ar in Đà Lạt reactor

Reaction	Cross section (barn)	T ½	Weight of sample	Irradiation time, min	Activity (mCi)
$^{40}Ar(n,\gamma)^{41}Ar$	0.66	1.83 h	6 ml ~ 0.0144g	5	0.032

Radioactive gas is then transferred in the calibration cylindre for calibration of activity using detector BGO 3'x3", MCA Digidart and simulation by MCNP code.

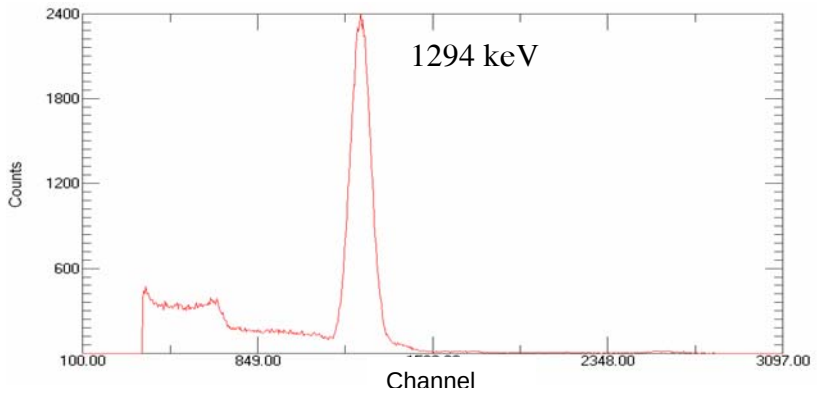

Fig. 2: Gamma spectrum of Ar-41; detector BGO 3'x3", MCA Digidart

2.2 Preparation of Methyl Bromide-82

Methyl Bromide is prepared from KBr activated in the reactor to $K^{82}Br$ with H_2SO_4 as catalyst at 70^{0}C:

$$(CH_3)_2SO_4 + 2KBr \longrightarrow K_2SO_4 + 2\ CH_3Br \uparrow$$

Methyl Bromide-82 is liquidified at -30^{0}C and stored in transport A container (Figure 3).

Table 2: The parameters of Br-82 irradiation

Reaction	Cross section (barn)	T ½	Weight of sample	Irradiation time, min	Activity (mCi)	Calibrated activity	Remark
$^{81}Br(n,\gamma)^{82}Br$	2.69	35.3 h	1.3 g x 2 Channel 7-1	5	5.25 x 2	5.25 x 2	2 ampoule

The procedures of preparation of MB are as below:

- KBr-82 with carrier KBr at ratio 1:15 w/w is diluted in 40ml DW, stirred thoroughly - solution A.

- Put solution A in the round flask 100ml, added 25ml of $(CH_3)_2SO_4$) 100%.

- Allow reaction for 15min in 70^{o}C with catalyst of 6ml H_2SO_4. The products are CH_3Br and K_2SO_4.

- The Ludlum 220 is used to monitor the completion of the reaction.

The efficiency of methyl bromide-82 converted from KBr-82 is 79.8%. Figure 4 shows the gamma spectrum of Br-82.

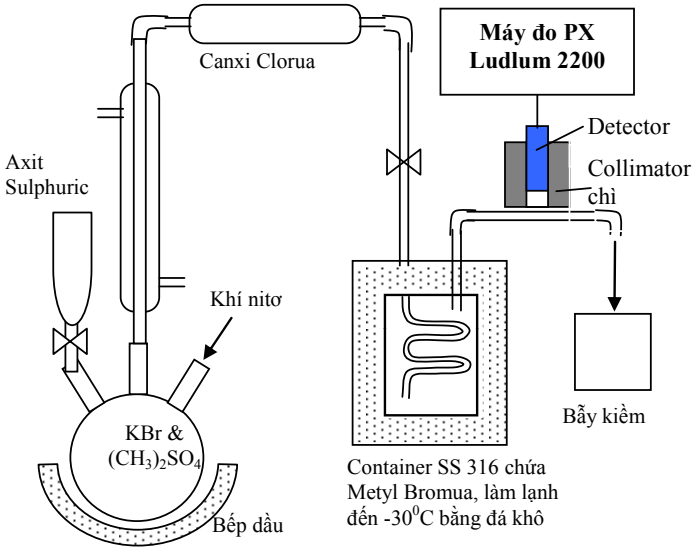

Fig. 3: Scheme of preparation of Methyl Bromide

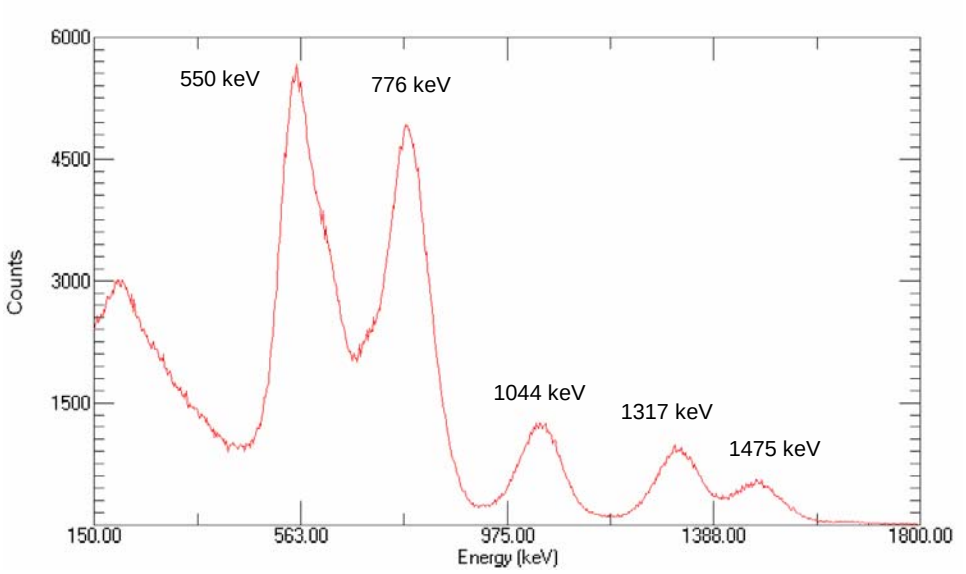

Fig. 4: Gamma spectrum of Br-82 - detector BGO 3'x3", MCA Digidart

2.3 Labeling Au-198 on water and organics

The labeled gold in liquids is the colloidal form with nano size particle of gold. This particles is of high dispersity in the liquid phase that makes them a good physical tracer.

Commonly. nano particle gold is created by reduction of $H(AuCl_4)$ into Au^0. However the stabilizer is needed to control the particle size and avoid the precipitation. In water phase citrate can be used for stabilization. For organics such as condensate, toluene, nano particle gold is formed by the existing hydrocarbons which the detailed mechanism is still unclear or transferred from water phase by the transformer such TOAB (tetraoctylammonium bromide).

In this study, water labeled gold was tried to prepare with citrate and $NaBH_4$, but the good result was with citrate, while transfer method for organics was not succeded but the direct method was acceptable.

The procuderes for labeling water are below:

- Preparation of gold solution by aquaregia at concentration of 1mM in 10ml

- Boilling 200ml citrate 1%, add gold solution. The color changes from dark blue to dark red and lastly red.

- Transfering the obtained solution to the stainless steel cylindre, allowing precipitating for 12h, then extract the upper part for use.

- Calibration of activity of obtained solution.

The sample was sent to test on TEM to determin the particle size. The nanoparticle size was 11±3,8nm.

The procuderes for labeling condenstae are below:

- Preparation of 100ml of condensate which was filtered by centifuger, heated to 70^0C then is added gold solution. The color changes to very yellow after 10min. Transfering the obtained solution to the stainless steel cylindígh" NPT of 500mm high, allowing precipitating for 12h, then scanning radiation vertical profile to extract the plateau part for use.

- Calibration of activity of obtained solution.

The efficiency of both methods is appoximately 80%.

3. Procedures of tracer injection and data acquisition

The tracer injection devices for gas and liquid tracing were designed and manufactured with testing pressure up to 5,000psi according to ASTM standard. In the gas injector the tracer ampoule is laid in the Tee in the container and is broken by the stick and hammer. The compessed air or nitrogen then is used to push tracer into the pipe line (figure 5).

The liquid injector is designed with two cylindre, 1 for tracer containing and another for carrier of working organics (condensate, gasoline...). The compressed air or nitrogen is used to push tracer into the pipe line (figure 6).

The tracer data is acquired by Tracer Data Acquisition System (TDAS) provided by Project RAS/8091 (figure 7). The system includes 10 channels of detection incorporated in datalogger. The minimum reading time is 1ms which is enough to catch the tracer signals at high speed. The system is computer communication with 200m of cable for each channel that allow to conduct a test in an area of 100,000m2 of plant.

The obtained data is the radiation count rate timely recorded in seperated channel. It is recommended to do calibartion of high voltage, energy calibration brfore implementation of experiment.

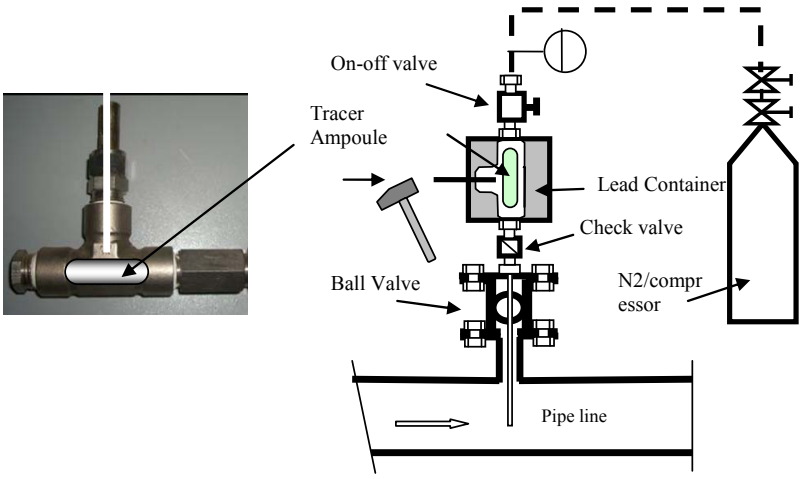

Fig. 5: Scheme of gas tracer injection.

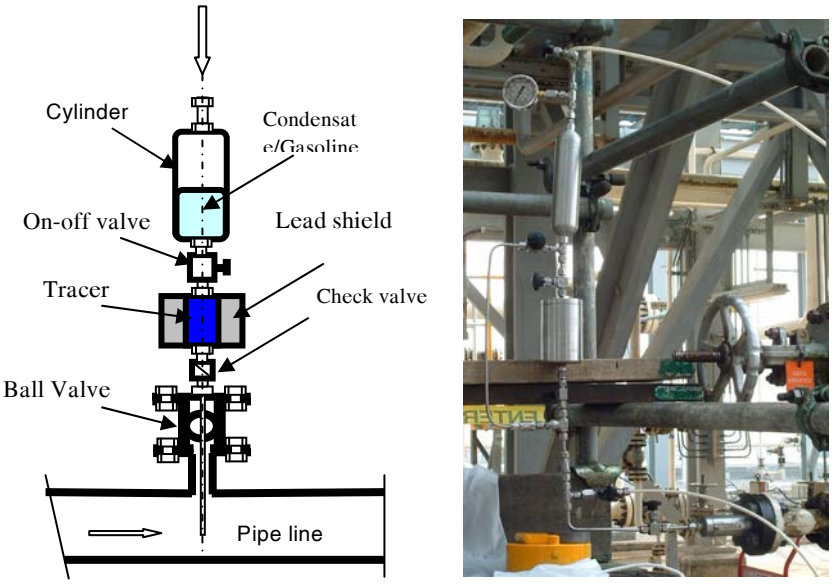

Fig. 6: Scheme of liquid tracer injector

Fig. 7: The Tracer Data Acquisition System 10 channels TDAS (left)-
detector installed in pipe line (right)

4. Field test

The tracers were applied to determine the flow rate at gas processing plant. The problem was to estimate the fraction of condensate in two brances A and B at power of 30m3/h. The scheme of experiment is shown in figure 8.

Detector D1 for monitoring input tracer pulse;

Detector D7, D8 for determination of flow in A;

Detector D9, D10 for determination of flow in B.

10mCi of Au-198 labeled in condensate was injected as pulse. The detection was conducted by TDAS, detector NaI 2"x2". The tracer response curves and data processing by K-RTD software are shown in figure 9. The flow rate is calculated by equation:

$$Q = v.S$$

Hence v velocity of tracer pulse;

S pipe cross section.

The results of flow rate measurement are shown in table 3. Branch A 19,5m^3/h, branch B 10m^3/h. Total flow is 29,5 m^3/h (at power of 30m^3/h.).

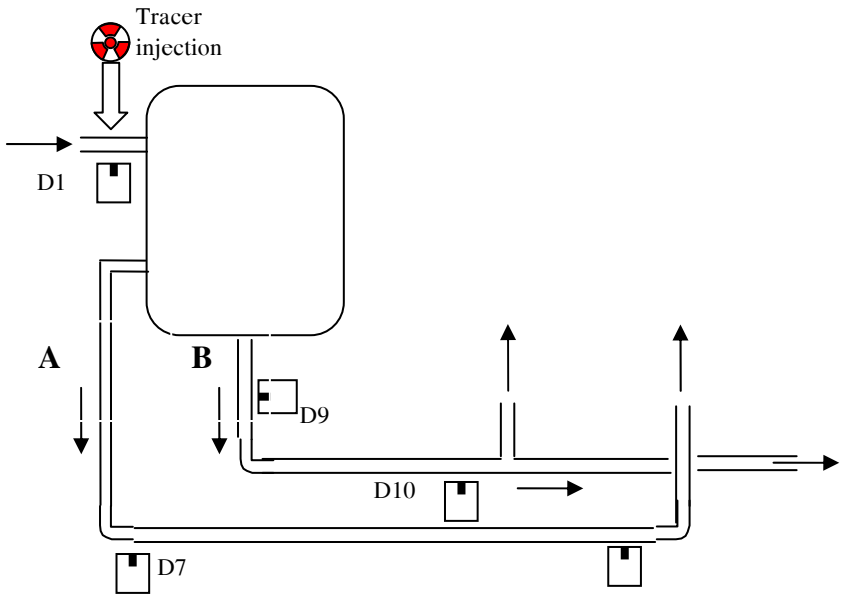

Fig. 8: Scheme of flow rate measurement in the boilled condensate lines.

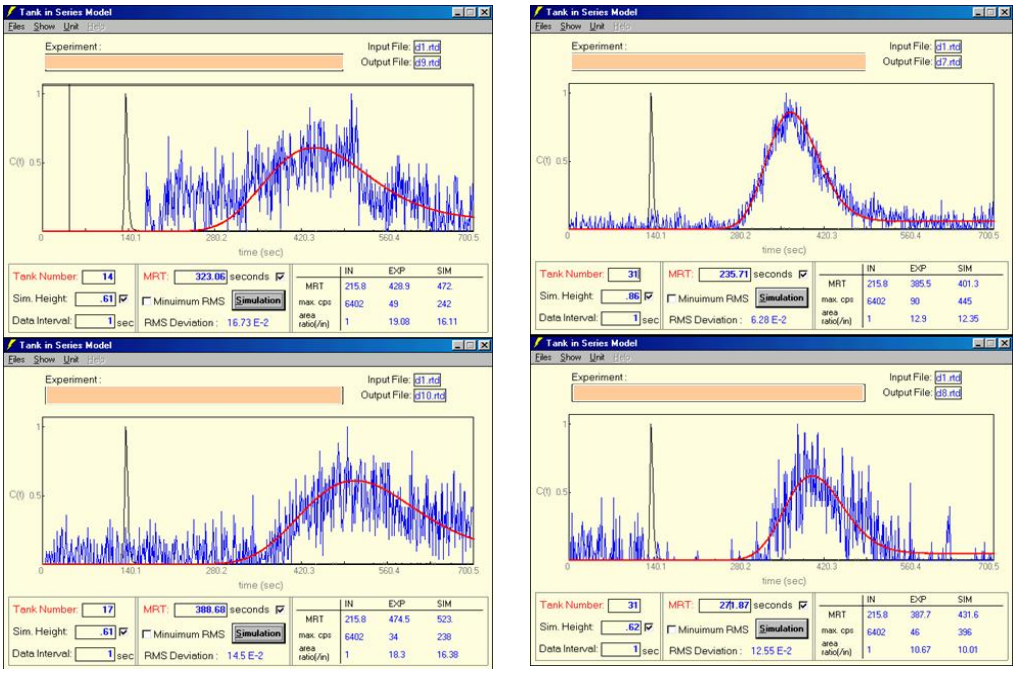

Fig. 9: Tracer response curves at D9, D10 (right) and D7, D8 (left).

Table 3: The results of determined flow rate in A and B branches.

Calculation of MRT					
	d7	***d8***	***d9***	***d10***	***Total flow rate***
MRT, s	236	272	323	389	
Δt (s)		36,2		65,6	
Δt (h)		0,010		0,018	
V (m3)		0,19		0,19	
Q (m3/h)	Branch A 19,2		Branch B 10,2		29,3

5. Conclusions

In industry it is very common problem of investigation of multiphase of gas, liquid and solid in which possibly exist complicated status between phases.

In the previous Projects, the Centre for Applications of Nuclear Technique in Industry has carried out the research on the phases of liquid, solids such as water, acid sulphuric, sand, microball carrier... To meet the increasingly requirement of gas industry it is necessary to estabish the base for gas tracing technologies which are not available yet in Vietnam.

However, because the scope of the gas tracing technologies is rather large and specific from case to case, this Project is mainly aimed at research of procedures of preparation of very common tracers such as Ar-41, CH_3Br-82 and Au-198 labeled water and organics along with tracer injection and tracer data acquisition, which are the base

for starting gas tracing development. As results, the protocols, procedures of iradiation, preparation of tracer compounds, tracer injection and acquisition were built. A field experiment was also carried out to practice. Through the implementation of the Project the Tracer Lab of CANTI has been enhanced in competency.

The results obtained from this study are preliminary in development of multiphase tracing technology. It is the need to improve in professinal and industrial quality to meet the production requirement actually.

REFERENCES

[1]. Đề tài cấp Bộ 1999-2000, Ứng dụng một số kỹ thuật đánh dấu đồng vị phóng xạ nghiên cứu nước bơm ép phục vụ tăng cường thu hồi dầu lần hai trên mỏ Bạch Hổ, Nguyễn Hữu Quang, Viện NCHN, Đà Lạt.

[2]. Đề tài cấp Bộ 2001-2002 BO/01-01-01, Thiết lập công nghệ đánh dấu đồng vị phóng xạ khảo sát dầu dư bão hoà trên mỏ Bạch Hổ, Nguyễn Hữu Quang, Viện NCHN, Đà lạt.

[3]. Đề tài cấp Bộ 2003-2004 BO/03-01-01, Thiết lập công nghệ xác định dầu dư bão hoà bằng kỹ thuật đánh dấu đơn giếng trên tầng cát kết mỏ Bạch Hổ, Nguyễn Hữu Quang, Viện NCHN, Đà Lạt.

[4]. Đề tài cấp cơ sở 2003 Xây dựng công nghệ đánh dấu kết hợp soi gamma khảo sát tháp đệm, Bùi Quang Trí, Viện NCHN, Đà Lạt.

[5]. Contract Radioisotope Investigation of Condensate Stabilizer in Nam Con Son Pipeline Terminal, Dinh Co, Ba Ria-Vung Tau, 2005.

[6]. Đề tài Nghiên cứu sự di chuyển của cát đáy tại luồng tàu cảng Hải Phòng Chương trình KC-09A, 1993-1994.

[7]. Radioisotope Techniques in Industry, IAEA TECDOC No. 316, Vienna 1995.

[8]. Đề tài cấp cơ sở 2005 MS CS/05-01-02, "Xác định tốc độ ăn mòn đường ống dẫn khí bằng kỹ thuật TLA", Đặng Nguyễn Thế Duy.

[9]. Contract No. CANTI-IND-05-2005 Report of Investigation of condensate stabiliser and reboiler in Nam Con Son terminal by using radioisotope techniques, Nguyen Huu Quang, Dalat, 2006.

[10]. Berlin MA, VG. Gortrencov, HP Volkov, Công nghệ chế biến khí thiên nhiên và khí dầu mỏ, ĐH BK Tp. HCM, Tài liệu giảng dạy.

[11]. V. R. Reddy, "Gold Nanoparticles: Synthesis and Applications" 2006, 1791, and references therein

[12]. B.L. Campbell, W.R. Ellis, Australian AEC, Sutherland, NSW, Australia The Development of Oil-Soluble Gold-198 Compounds for Industrial Radiotracing, International Journal of Applied Radiation and Isotopes, 1965, Vol. 16, pp.257-259.

[13]. D.K. Donhoffer, K.E. Duftschmid, "Labelling of Oil by Colloidal Au-198 for Tracer Studies, International Journal of Applied Radiation and Isotopes, 1967, Vol. 18, pp.541-542.

[14]. IAEA Technical Report Series No. 423, Radiotracer Applications in Industry A Guide Book, IAEA, Vienna, 2004.

[15]. IAEA Training Course Series Radiotracer Methodology and Technology as Applied to Industry and Environment Material for Education and on-job training of radiotracer practioners, IAEA, Vienna, May 2006.

BUILDING OF TRAINING PROGRAM OF NON-DESTRUCTIVE TESTING FOR CONCRETE STRUCTURES

(Part 1: Radiographic testing; Ultrasonic pulse velocity measurement; Nuclear moisture-density gauge)

Nguyen Le Son, Phan Chanh Vu, Pham The Hung and Vu Huy Thuc

Center for Nuclear Techniques, VAEC, Vietnam.

ABSTRACT: Non-destructive testing methods (NDT) have been identified as a strong candidate for remote sensing of concrete structures over recent years. This has accelerated the powerful development of the NDT techniques in Vietnam.

Hence, there is an urgent need to promote the awareness of NDT methods which could give an improved estimate of the condition concrete. As a result, the topic: "Building of training program of non-destructive testing for concrete structures" is a necessary duty, in aiming to build a unified training program, possibly satisfying the requirements on training as well as researching.

Under the framework of the basic VAEC project (CS/07/02-03), a training program for the first 03 NDT methods: 1. Radiographic testing; 2. Ultrasonic pulse velocity measurement; 3. Nuclear moisture- density gauge was prepared. The main products of this project include:

1. Set out 03 training notes for 03 methods.
2. Set out the practical exercises to train for 03 methods.
3. Editing a set of examination questions in aiming to familiarize with various questions in 03 trained methods.
4. Fabricating practical test specimens to demonstrate for 03 techniques.

INTRODUCTION

Non-destructive testing methods (NDT) were identified as a strong candidate for remote sensing of concrete structures over recent years. In Viet Nam due to the door-opening policy and integration with the regional countries, the quality of the structure or component produced have felt as a key factor in long term economic and engineering success of that process. This has accelerated the powerful development of the NDT techniques in Vietnam.

Hence, there is an urgent need to promote the awareness of NDT methods which could give an improved estimate of the condition concrete. Center for nuclear techniques, Hochiminh City (CNT) has been active in the promotion of nondestructive testing (NDT) technology for many years. As a result, the topic: "*Building of training program of non-destructive testing for concrete structures*" is a necessary duty, in aiming to build a unified training program, possibly satisfying the requirements on training as well as researching.

Under the framework of the basic VAEC project (CS/07/02-03), a training program for the first 03 NDT methods: 1. Radiographic testing; 2. Ultrasonic pulse velocity measurement; 3. Nuclear moisture – density gauge was prepared. The main products of this project include:

1. Set out 03 training notes for 03 methods.

2. Set out the practical exercises to train for 03 methods.

3. Editing a set of examination questions in aiming to familiarize with various questions in 03 trained methods.

4. Fabricating practical test specimens to demonstrate for 03 techniques.

CONTENT OF THE PROJECT

Included the following parts:

1. Editing the document set of 03 NDT methods for concrete structures: 1. Radiographic testing; 2. Ultrasonic pulse velocity measurement; 3. nuclear moisture – density gauge.

2. Set out the practical exercises to conduct in 03 methods: 1. Radiographic testing; 2. Ultrasonic pulse velocity measurement; 3. Nuclear moisture – density gauge.

3. Editing a set of examination questions, approximately over 700 questions on various issues of 03 techniques, in aiming to familiarize with various questions in 03 trained methods.

4. Fabricating practical test specimens to demonstrate for 03 techniques.

MAIN PRODUCTS OF PROJECT

1. Editing the document set of 03 NDT methods for concrete structures: 1. Radiographic testing; 2. Ultrasonic pulse velocity measurement; 3. Nuclear moisture – density gauge based on:

a) "Guidebook on non-destructive testing of concrete structures", Training course series No.17, IAEA, 2002.

b) IAEA-TECDOC-628: "Training guidelines in Non-Destructive Testing Techniques", Vienna 2002.

c) ISO 9712-2005 (E): "Non-destructive testing Qualification and Certification of Personnel".

d) Viet Nam standards TCVN 5868-1965: Volume 1.

And training program complying with training system is discripbed below.

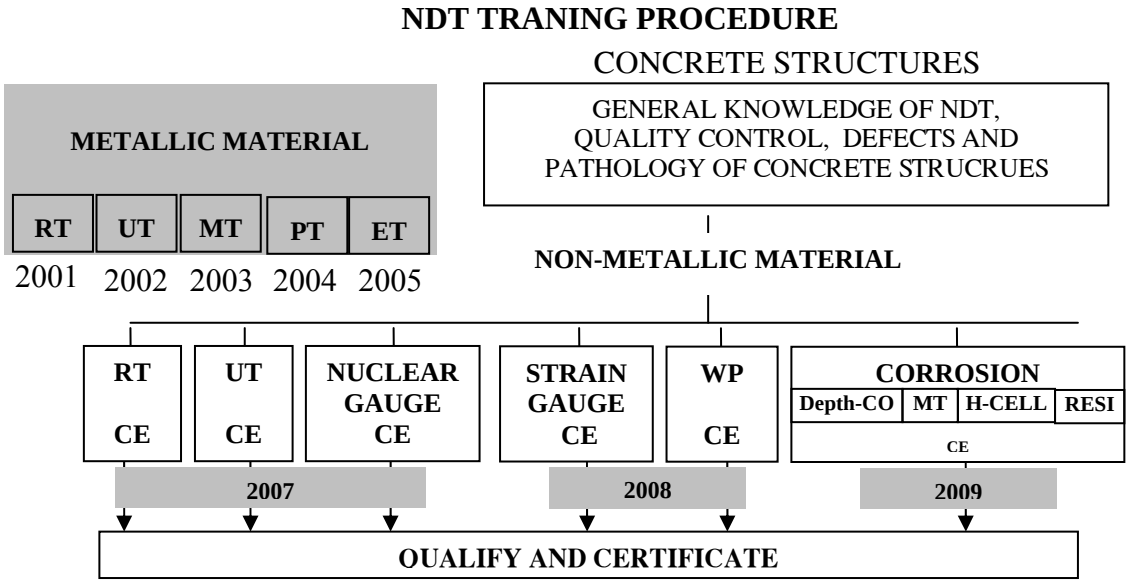

Remarks

RT-CE: Radiographic testing for concrete structures; UT-CE: Ultrasonic testing for concrete structures

Nuclear Gauge-CE: Nuclear moisture-density gauge

Strain Gauge-CE: Strain gauge measurement for concrete structures

WP-CE: Windsor probe test for concrete structures.

Corrosion-CE: Combined methods for corrosion situation of concrete structures (Depth-CO: Depth carbonation measurement; MT: Cover meter; H-CELL: half cell potential measurement; RESI: Resistivity measurement)

***1.1. The training note of nuclear moisture-density gauge for civil engineering*:** this document set included 8 chapters: 1. General knowledge of NDT, quality control, defects and pathology of concrete structures; 2. Terminology, physical principles; 3. Testing techniques and their limitations; 4. Equipment and accessories; 5. Calibration of the testing system; 6. Specific applications; 7. Codes, standards, specifications and procedures; 8. Personal safety and radiation protection. Minimum training hours include both practical and theory courses is 40 hours.

***1.2. The training note of radiographic testing for reinforced concrete*:** this document set included 6 chapters: 1. General knowledge of NDT, quality control, defects and pathology of concrete structures; 2. Terminology, physical principles; 3. Equipment- radiation sources, film recording and darkroom works; 4. Work parameters and conditions; 5. Selection of techniques according to standards and specific applications; 6. Personal safety and radiation protection. Minimum training hours include both practical and theory courses is 40 hours.

***1.3. The training note of ultrasonic pulse velocity measurement for concrete*:** included 6 chapters: 1. General knowledge of NDT, quality control, defects and pathology of concrete structures; 2. Terminology, physical principles; 3. Testing techniques and their limitations; 4. Equipment and accessories; 5. Specific applications; 6. Codes, standards, specifications and procedures. Minimum training hours include both practical and theory courses is 40 hours.

2. Set out the practical exercises to conduct in 03 methods:

2.1. There are 08 practical exercises for Nuclear moisture – density gauge: 1. to familiarize and to operate equipments, to get standard count; 2. to take the stability test; 3. to calibrate equipment for density measurement; 4. to calibrate equipment for moisture measurement. 5. to recheck equipment after calibration; 6. to study the useful depth of technique; 7. to practice on test specimens; 8. to practice of radiation safety.

2.2. There are 05 practical exercises for Radiographic testing technique: 1. to familiarize and to operate equipments; 2. Darkroom; 3. to practice of radiation safety; 4. to examine the rebar in concrete; 5. to determine the sizes of rebar; 6. to detect the defects in concrete.

2.3. There are 05 practical exercises for Ultrasonic testing technique: 1. to familiarize and to operate equipments; 2. to study the effects of the steel bars in concrete

on the ultrasonic pulse velocity; 3. to evaluate the in homogeneity of concrete; 4. to determine the depth of cracks in concrete; 5. to estimate the concrete strength.

3. Editing a set of examination questions: approximately over 800 questions on various issues of 03 techniques, in aiming to familiarize with various questions in 03 trained methods.

4. Fabricating practical test specimens to demonstrate for 03 techniques: 04 test specimens for radiographic testing techniques; 03 test specimens for ultrasonic testing technique: to study effects of steel bars; a set of 10 test specimens for ultrasonic testing technique: to estimate the concrete strength.

CONCLUSION

The issue of this first document set is duly and timely, satisfying the needs of researching, learning of the 03 enhanced NDT methods for concrete structures, and also contributing its parts in training, teaching NDT systematically, textually and methodically in Vietnam now and later. This issue also establishes a fundamental for similar document sets that will be edited in the future, through that accelerating development of NDT techniques in Vietnam reaching a common level in the region.

REFERENCE

[1]. "Guidebook on non-destructive testing of concrete structures, Training course series No.17, IAEA, 2002.

[2]. John H.Bungey: "The testing of concrete in structures, Surrey University Press distributed in the USA by Chapman and Hall New York. 1982.

[3]. Nguyễn Lê Sơn và cộng sự: Báo cáo kết quả nghiên cứu đề tài KHCN cấp Bộ Nghiên cứu xây dựng một số quy trình công nghệ sử dụng kết hợp các phương pháp kiểm tra không phá hủy NDT kiểm định hiện trạng các công trình xây dựng, giao thông - 1996-1998.

[4]. Nguyễn Lê Sơn: "Kiểm tra không phá hủy và Ứng dụng trong xây dựng giao thông Hội thảo quốc gia lần I do Hội NDT Việt Nam và Viện Khoa học Công nghệ giao thông tổ chức tại Hà Nội, 25/10/2000.

[5]. Nguyễn Lê Sơn: "Kiểm tra không phá hủy công cụ hiệu quả chẩn đoán chất lượng các công trình xây dựng Hội thảo quốc gia lần 2 về NDT do Hội NDT Việt Nam và Viện Khoa học Công nghệ Xây dựng tổ chức tại Hà Nội, 20/11/2001.

[6]. IAEA-TECDOC-1025**:** "Assessment and management of ageing of major nuclear power plant components important to safety: Concrete containment buildings 1998.

[7]. VIC ROADS: Manual for assessment, maintenance and rehabilitation of concrete bridges, November 1990. Roads Corporation Australia.

[8]. BS 1881: Part 201: 1986: "Testing concrete: part 201. Guide to the use of non-destructive methods of test for hardened concrete. British Standards Institution.

1.5 - Ecology, Environment and Geology

STUDY OF ISOTOPIC TECHNICAL APPLICATION TO ESTIMATE ORIGIN OF NITROGEN COMPOSISION OF GROUNDWATER IN HANOI AREA

Trinh Van Giap, Dinh Bich Lieu, Dang Anh Minh, Vo Thi Anh, Bui Dac Dung, Nguyen Thi Hong Thinh, Nguyen Manh Hung, Nguyen Van Hoan and Nguyen Van Hai

Institute for Nuclear Science and Technology, VAEC, Vietnam.

ABSTRACT: Groundwater in Hanoi area as well as some other areas in Bacbo Delta is being contaminated by heavy metals and nitrogen compounds, especially arsenic and ammonium..The origin of nitrogen compounds in groundwater in Hanoi area is estimated in order to exploit and manage sustainable groundwater served for production and live .

The results of the project are following:

1. Establish the procedure to analyze the isotope ratio $^{15}N/^{14}N$ in NH_4^+ and NO_3^- of water samples using diffusion method and isotope ratio mass spectrometer.

2. Area of highest contaminant concentration is located in the southern of the city.

3. Groundwater in Hanoi area has origin of mixture of meteoric water and surface water evaporated.

4. The results of total nitrogen, concentration of NH_4^+ and NO_3^- and isotope composition of ^{15}N in two aquifer columns show that soil layers of aquifer consist of organic matter produced from wastes of crop plants with high concentration of nitrogen, and in the mineralization, the organic matter is disintegrated into ammonium.

5. The data of isotope composition N-15 in groundwater samples show that portion of NH_4^+ in groundwater is produced from organic matter of aquifer is higher than that from inorganic fertinizer used in agriculture activities. The model of isotope mass balance is applied to calculate the contribution of NH_4^+ origined from from organic matter and inorganic fertinizer at 39 positions of grounwater sampling and portion of NH_4^+ in groundwater is produced from organic matter of aquifer is from 23% to 97%.

Total 40 groundwater samples were collected in the study to analyze ammonium and composition of $^{15}N(NH_4^+)$.The results show that high concentration of ammonium is located in the southern part of Hanoi area, where groundwater level is decreasing, it is showed in the figure 1. The compositon of $^{15}N(NH_4^+)$ is in the range of 1.33‰ to 7.7‰. It mean that origin of NH_4^+ in grounwater is the mixture of fertilizer and NH_4^+ of organic matter.

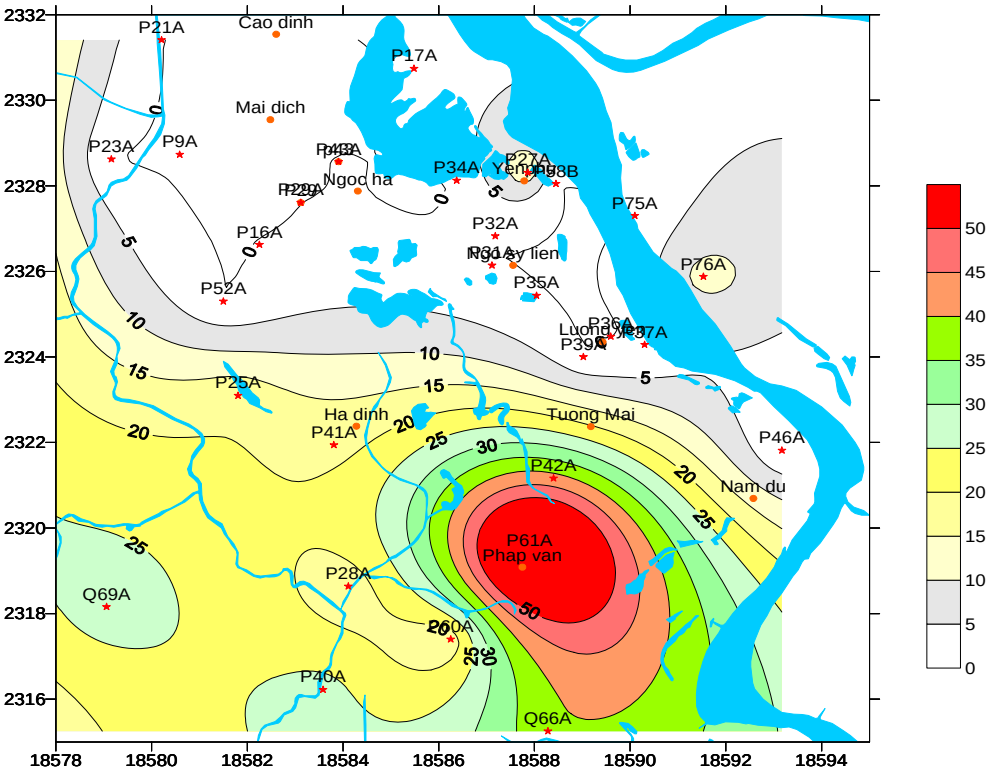

Fig. 1: Distribition of NH_4^+ cocentration of Qp in Hanoi area.

The stable isotope compositions ^{18}O, ^{2}H of groundwater samples in Hanoi area were also analyzed to estimate the resourses of groundwater. The results show that groundwater in Hanoi area has meteoric resource and has relation to evaporated surface water in some positions. The relation of delta ^{18}O and delta ^{2}H is presented in figure 2.

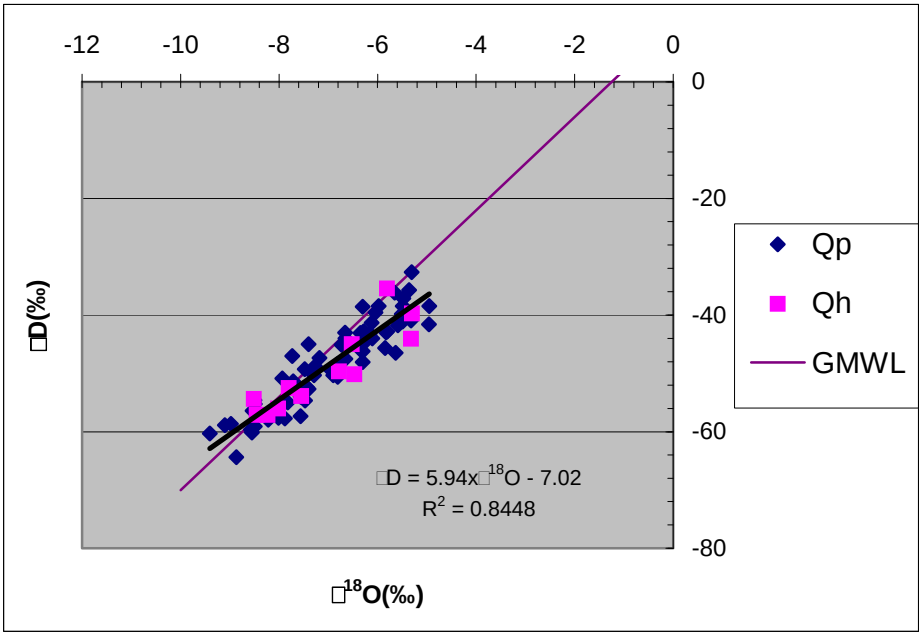

Fig. 2: Relation of delta ^{2}H and delta ^{18}O of groundwater

In two aquifer columns, stable isotope ^{15}N is more enriched in the deeper layers and has origin of organic matter; in the surface layer, isotope ^{15}N composition has origin of fertilizer used in agriculture activities. And composition of isotope ^{15}N of organic matter in aquifer is more enriched than that in groundware, this is mean that ammonium in groundwater is origin from organic matter in aquifer and due to the isotope fractionation of the dissolution process of ammonium from aquifer to groundwater . In order to calculate portion of ammonium in groundwater from organic matter, isotope mass balance model was applied. It is presented as following:

$$\delta^{15}N_{NN} = p.\ \delta^{15}N_{VC} + (1-p).\delta^{15}N_{HC} \qquad (1)$$

with: p – portion of fertilizer.

$\delta^{15}N_{NN}$ - Composition of ^{15}N in groundwater.

$\delta^{15}N_{VC}$ - Composition ^{15}N in fertilizer. It is 0 (‰).

$\delta^{15}N_{HC}$ - Composition ^{15}N of organic matter in aquifer. The value of 5.68 ‰ of groundwater at position P40 was chosen to calculate. The calculated data shows that the organic matter in aquifer contribute ammonium from 23% to 97% in groundwater in Hanoi area.

In conclusion, The first results of the project show that allmost of amonium in grounwater in Hanoi area has origin of organic matter of aquifer and in some positions of this area where the groundwater level is decreasing the organic matter in the surface water may be carried to grounwater. In order to distinguish origin of amonium from different organic matter sourses, it is necessary to continue more detail research, as well as expand the research area. The detail works are collection some aquifer columns in the area with decreasing water level and the surrounding area for analyzing chemical, isotope composition, and the ammonium origin of various organic matter sources in positions will be estimated by the chemical and isotope data. And. Isotope fractionation phenomena of ^{15}N of evolution processes of chemical NH_4^+ from organic matter in aquifer to groundwater must be researched more details.

REFERENCES

[1]. Mook W.G.(2001), "Environmental Isotopes in the Hydrological Cycle", *IHP-V/Technical Documents in Hydrology*, Vol.I-VI.

[2]. IAEA, Vienna (1998), Application of Isotope Techniques to Investigate Groundwater Pollution. IAEA-TECDOC-1046.

[3]. F. BUZEK, Nitrate Pollution of a Karstic Groundwater System. IAEA-SM-349/31.

[4]. W. DURKA, Atmospheric Nitrate in Near Surface Groundwater of Forest Ecosystems. IAEA-SM336/133P.

[5]. C. KENDALL, Use of the $\delta^{18}O$ and $\delta^{14}N$ of Nitrate to Determine Sources of Nitrate in Early Spring Runoff in Forested Catchments. IAEA-SM-336/29.

[6]. M. GOPPEL, Tracing The Source of NO_3 by Means of ^{15}N-^{18}O Isotopic Fingerprints. IAEA-SM-349/14P.

[7]. BIJAY-SINGH,Fertilizer-N Use Efficiency and Nitrate Pollution of

Groundwater in Developing Countries. Journal of Contamination Hydrology, 20(1995) 167-184.

[8]. Trafford J.M., Lawrence A.R., Macdonald D.M., Nguyen Van Dan, Dang Ngoc Tran and Nguyen Thu Ha (1996), "The Effectôif Urbanizationoi on The Groundwater Quality Beneath The City of Hanoi, Vietnam", *Technical Report WC/96/22 Overseas Geology Series*. Keyworth, Nottingham, British Geological Survey.

[9]. Hoàng Đắc Lực và các cộng sự (2003), *Nghiên cứu sủa dụng kỹ thuật đồng vị để đánh giá nguồn gốc nước ngầm khu vực Hà nội*. Báo cáo két quả đề tài cấp Bộ năm 2000-2001, Bộ Khoa học cà Công Nghệ.

[10]. Trịnh Văn Giáp và các cộng sự (2006), *"Nghiên cứu sử dụng kỹ thuật đồng vị đánh giá mối liên hệ giữa nước ngầm và nước bề mặt khu vực Hà Nội"*. Báo báo kết quả đề tài cấp Bộ năm 2004-2005, Bộ Khoa học và Công Nghệ.

[11]. Bùi Học, Nguyễn Thượng Hùng, Vũ Ngọc Kỷ (1981), "Những nghiên cứu đầu tiên về các chất đồng vị trong nước ở Việt Nam", Tuyển tập các công trình khoa học Trường Đại học Mỏ và Địa chất 1978-1981.

[12]. Bùi Học (1992), *Địa chất thuỷ văn đồng vị lãnh thổ Việt Nam*. Luận án Tiến sỹ, Trường Đại học Tổng hợp, Viện Hàn lâm Mỏ Freiberg, Cộng Hòa Liên bang Đức.

[13]. Bùi Kim Tuyến (1994), *Phương pháp đồng vị nghiên cứu tuổi và nguồn gốc nước dưới đất trầm tích đệ tứ đồng bằng bắc bộ*. Luận án tiến sỹ khoa học địa chất, Trường Đại học Mỏ-Địa chất.

[14]. Trịnh Văn Giáp và các cộng sự (2004), *Thiết lập quy trình xác định hàm lượng các đồng vị của ôxy và hyđrô trong nước nhằm tiến tới nghiên cứu nước ngầm khu vực Hà Nội*. Báo báo kết quả đề tài cấp Bộ năm 2003-2003, Bộ Khoa học và Công Nghệ.

[15]. Trịnh Văn Giáp (2006), *Nghiên cứu kỹ thuật đồng vị và ứng dụng để xác định tuổi nước ngầm khu vực Hà Nội*. Luận án tiến sỹ vật lý, Viện Năng lượng nguyên tử Việt Nam.

PAPERS PUBLISHED IN RELATION TO THE PROJECT

1. Trinh Van Giap, Hoang Dac Luc, Dang Duc Nhan, "Use of environmental isotopes of hydrogen and oxygen to determine Red River water and groundwater mixing in Hanoi area of Vietnam". International Symposium on Advances in Isotope Hydrology and its role in Sustainable Water Resources Management, (IHS–2007) Vienna International Centre (VIC), Austria, 21 - 25 May 2007.
2. Trịnh Văn Giáp, Đặng Anh Minh, Võ Tường Hạnh, Võ Thị Anh, Đinh Bích Liễu, *"Sử dụng kỹ thuật đồng vị xác định nguồn gốc nước ngầm đang khai thác khu vực Hà Nội",* Báo cáo tại Hội nghị Khoa học và Công nghệ hạt nhân toàn quốc lần thứ 7, Đà Nẵng, tháng 8/2007.

BIODEGRADATION OF ORGAN CHLORINE PESTICIDES IN CONTAMINATED SOIL COLLECTED FROM YEN TAP CAM KHE, PHU THO

Nguyen Thuy Binh, Nguyen Van Toan, Pham Thi Thai and Dinh Thi Thu Hang

Institute for Nuclear Science and Technology, VAEC, Vietnam.

ABSTRACT: Biodegradation of POPs contaminant in soil collected from Phu Tho and Nghe An had carried out. The process comprises treating soil, which contains anaerobic and aerobic microbes capable of transforming lindan and DDT into harmless material and being under anaerobic and aerobic steps. Significant biodegradation of POPs contaminants occurred in there tests. But some of toxic organic compounds remained.

1. Introduction

Numerous methods were selected for degradading pesticides in contaminated soil. Chemical and biological methods are more interested. However, bioremedation seems to be an attractive method to solve the problem. Some reports have mentioned that bacteria have an ability to degrade such compounds. It demonstrated that biodegradation of chlorinated organic compounds proceed by metabolic pathways. Metabolities were formed, microoganisms use it as sole source of carbon and energy.

The bacterial and fungal strains, which have an ability to decompose some lindan and DDT in soil, are used for investigation of pesticides bioremediation in soil collected from PhuTho.

2. Material and methods:

Sample of soil for experiments was collected in various places of hillock Muon Chom, Yen Tap, Cam Khe, Phu Tho. Soils characters, such as pH, humid and texture, are defined before treatment. The concentration of organochlorine pesticides in contaminated soil was extracted for 8 h in a soxhlet appature with n-hexane and extract was cleaned up on activated copper. With florisil columm three fractions were eluted for separation of organochlorinated compounds and analyzed by gas-chromatograph GC-ECD (Varian 3800).

Pseudomonas sp. and Aspergillus sp were chosen for degrading organochlorine pesticides in contaminated soil. They have a high tolerance to lindan and DDT toxic effect and can use it as co-metabolites for cells growing. Microorganisms are enriched with 90% dry rich soil, 1% rice bran, 0, 3% glucose. The cells growth in contaminated soil was estimated by two methods. First method is counting colony on agar plats, another ones is estimated by Mac Craby test.

3. Result and discussion

Soil sample, which collected from hillock Muon Chom, Yen Tap, Cam Khe, Phu Tho, is sandy-loam (table 1).

Table 1: Texture of soil sample

Sample	Particle size (%)			Texture
	2-2.10^{-2}mm	2.10^{-2}-2.10^{-3}mm	2.10^{-3}-2.10^{-4}mm	
YT1	68.90	13.22	17.88	Sandy-loam
YT2	71.82	10.48	17.70	Sandy-loam
YT3	48.40	19.77	31.83	Sandy-clay-loam

YT1: Sample soil in Do tien Tins garden.

YT2: Sample soil in floor former pesticides store.

YT3: Sample soil in dust-hole.

Soil pH is about 6, 5-7, 5; soil humid is about 12, 4%-18, 4%. Organic matter in the soil is about 1, 65%-4, 01%.

The results in the table 2 decorated that concentration of organochlorine pesticides contaminated in sample soil is low, but various organochlorinated compounds are detected in contaminated soil as Heptachlor, α-HCH, β-HCH, lindane, Cis-nanochlo, Tran-chlordane, o,p-DDD, o,p-DDT+tran, p,p-DDT, α-endosul, Diedrin (table 2).

Table 2: Organochlorine pesticides in contaminated soil

Soil sample TTS(mg/kg)	YT1	YT2	YT3
Heptachlor	no detect	no detect	0,0022
α- HCH	0,00025	0,00030	0,0010
β- HCH	no detect	no detect	0,0664
Lindan	no detect	0,0025	0,0026
Cis-nanochlor	0,0014	0,0015	0,0065
Tran-chlorda	0,0024	no detect	no detect
o,p-DDD	0,0548	no detect	no detected
o,p-DDT+tran	no detect	0,0063	0,0004
p,p-DDT	no detect	0,0014	0,0083
α- endosul	0,0028	no detect	0,0025
Diedrin	no detect	no detect	0,0016

Because of bacterial and fungal strain have a high tolerance to lindan and DDT toxic effect and can use it as co-metabolites for cells growing, we have carried out another experiment with contaminated soil, which collected from Yen Thanh, Nghe An (concentration of DDT in soil about 6,12 mg/kg).

The results of cells density show that bacteria and fungi grow well in contaminated soil. The cells growth achieved microbial density 10^{14}CFU/g (in soil sample from Nghe an) and 10^{7}CFU/g (in soil sample from Phu Tho).

The analyzed result show that all most of oganochlorine pesticides in soil sample decreased after three mouths. (table3 and table 4)

Table 3: Concentration of DDT, DDD, DDE in soil sample from Nghe an

	Before treat (ppm)	**Experiment 1(ppm)**	**Experiment 2(ppm)**
DDT	6,12	1,073	1,983
DDD	16,33	13,75	14,072
DDE	7,354	4,292	5,133

Table 4: Concentration of arganochlorine pesticides after three mouth

Soilsample TTS(mg/kg)	**YT1**	**YT2**	**YT3**
Heptachlor	no detect	no detect	no detect
α- HCH	no detect	no detect	0,0010
β- HCH	no detect	no detect	0,0064
Lindane	no detect	0,0019	0,0021
Cis-nanochlor	no detect	no detect	no detect
Tran-chlorda	no detect	no detect	no detect
O,p-DDD	0,0066	no detect	no detect
O,p-DDT+tran	no detect	0,0046	0,0003
p,p-DDT	no detect	no detect	no detect
α- endosul	0,0008306	no detect	0,00019
Diedrin	no detect	no detect	no detect

4. Conclusion

It demonstrated that Microorganisms, which are enriched with 90% dry rich soil, 1% rice bran, 0, 3% glucose, have very good growth in sample soil. They can use organochlorine pesticides in containing in soil as co metabolites for cells growth. Concentration of organochlorinated compound such as DDT in sample soil from Nghe An is remaining about 30% after three mouths. However, it must mention investigations in biotechnology. It would be applied the method to clean up contaminated soil in another contaminated area.

REFERENCE

[1]. A. Bachman, P. Walet,P. Wunen, de Bruin, J.L. Hutjens.
Biodegradation of Alpha- and Beta- Hexanchlorocyclohexan in soil Slurry and

Different Red of Conditions. Department of microbiology, Agricultural University, 6703 CT Wageningen, The Northland; Applied and Environmental Microbiology, Jan. 1988, p.143-149.

[2]. AOAC methods, 1984, 6.214-6.219.

[3]. Bindu Sreedharan; Neera Singh ang Nambratil Sethunathan (google.com). Degradation of soil-sorbet isomer of hexanchlorocyclohexane in soil under flooded condition.

[4]. Bhyuan, S., Sreedharan, B., Adhaya, T. K., and Sethunathan, N., Enhanced biodegradation of n-hexachlorocyclohexane (n-HCH) (commercial) acclimatized flooded soil: Factors affecting its development and persistence, Peptic. Sci., 38, 1993, 49-55.

[5]. Dang Duc Nhan, Carvalho, F. P., Nguyen Manh Am, Nguyen Quoc Tuan, Nguyen Thi Hai Yen, Villeneuve, J-P., and Cattini, C., Chlorinated pesticides and PCBs in sediments and mollusks from freshwater canals in the Hanoi region, Environmental Pollution, 112, 2001, 311-320.

[6]. Dang Duc Nhan, Nguyen Manh Am, Nguyen Chu Hoi, Luu Van Dieu, Carvalho, F.P., Villeneuve, J-P., and Cattini, C., Organochlorine pesticide and PCBs in the Red River Delta, North Vietnam, Marine Pollution Bulletin, 36,1998, 742-749.

[7]. Drego, J., Murthy, N. B. K., and Raghu, K., [14C]-n-hexachlorocyclohexane in a flood soil with green maturing. J. Agri. Food. Chem., 38, 1990, 266-268.

[8]. Ferreira, J., and Raghu, K., Decontamination of HCH isomers in soil by green manure application, Environ. Technol. Lett., 2,1981,357-364.

[9]. http//www.inchem.org/documemts/ehc/ehc124.htm

[10]. MacRae, I. C., Raghu, K., and Bautista, E. M., Anaerobic degradation of the insecticide lindane by Closstridium sp., Nature, 221, 1969, 859-860.

[11]. MacRae, I. C., Raghu, K., and Castro, T. F., Persistence and biodegradation of four common isomers of benzene hexachloride in submerged soils. J. Agri. Food Chem., 15, 1967, 911-914.

[12]. Raghu, K., and MacRae, I. C., Biodegradation of the isomer of BHC in submerged soils. Science, 154, 1966, 263-264.

[13]. Ramesh, A., Tanabe, S., and Tatsukawa, R., Seasonal variation of organochlorine insecticide residues in air from porta Nono, Soth India, Environmental Pollution, 62, 1989, 213-222.

[14]. Siddaramappa, R., and Sethunathan, N., persistence of gamma-BHC and beta-BHC in Indian rice soils under flooded conditions, Pestic. Sci., 6, 1975, 395-403.

[15]. Siddhartha K Sahu, Kamala kumari patnak, Manikonda sharmila and N. sethunathan. Degradation of Alpha- and Beta- Hexanchlorocyclohexan by a Soil Bacterium under Aerobic Condition. Applied and Environnmental microbiology, Nov. 1990, p3620-3622.

[16]. Tanabe, S., Ramesh, A., Sakashita, D., Iwata, H., Mohan, D., Subramaniam, A. N., and Tatsukawa, R., Fate of HCH in tropical paddy field: Application test in South India. Int. J. Environ. Anal. Chem., 45, 1992, 45-53.

[17]. Thao, V. D., Kawano, M., Matsuda, M., Wakimono, T., Tatkusawa, R., Cau, H. D., and Quynh, H. T., Chlorinated-hydrocarbon insectiside and polychlorinated biphenyl residues in soils from southern provinces of Vietnam. Int. J. Environ. Anal. Chem., 50, 1993, 147-159.

[18]. Thao, V. D., Kawano, M., and Tatkusawa, R., Persistent organochlorine residues in soil s from tropical and subtropical Asian countries, Environmental Pollution, 81, 51993, 61-71.

[19]. The pesticide manual: A World Compendium, 8th Ed., And Editor: Worthing, C. R., and and British Crop Protection Council. London, UK, 1987.

[20]. Usarat Pakdeeesusuk, Mahmut pulat and George M. Huddleston III. Environmental Fate Evaluation of DDT, chlordane and lindane; EE&845 Environmental Engineering Chemistry III; Environmental Organic Chemistry; spring 1998.

[21]. Yoshida, T., Castro, T. F., degradation of gamma-BHC in rice soils, Soil Sci. Am. Proc., 34, 1970, 440-442.

STUDYING ON THE CONTAMINATIVE DETERMINATION OF EXISTING FORMS OF As^{3+}, As^{5+}, Sb^{3+} AND Sb^{5+} IN GROUND WATER AT LAMDONG PROVINCE

Nguyen Giang, Nguyen Thanh Tam, Truong Phuong Mai
Ho Tran The Huu and Nguyen Van Minh

Nuclear Research Institute, VAEC, Vietnam.

ABSTRACT: The project describes hydride generation atomic absorption spectrometry techniques for determination of arsenic (III), total arsenic, antimony (III) and total antimony concentration in water sample by investigating type and concentration of acide and sodium tetrahydroborate concentration.

The optimal conditions for determination of arsenic (III) were: 2% (m/v) citric acide and 2%(m/v) sodium tetrahydroborate. The same paramaters for determinaion of arsenic (V) were: 4N of HCl and 2%(m/v) of sodium tetrahydroborate in 10% (m/v) of KI.

The optimal conditions for determination of antomony (III) were: 2% (m/v) citric acide and 2%(m/v) sodium tetrahydroborate. The same paramaters for determination of antimony (V) were: 6 N of HCl and 2%(m/v) sodium tetrahydroborate in 10% (m/v) of KI.

Interference from ions on the analysis for arsenic (III), total arsenic, antimony (III) and total antimony were also investigated.

The sensitivity of this method was estimated to be 0.001ppm, 0.002ppm, 0.002ppm and 0.003ppm for As^{3+}, $As^{3+,5+}$, Sb^{3+} and $Sb^{3+,5+}$ respectively.

INTRODUCTION

In analytical chemistry, Atomic absorption Spectrophotometry method is a technique for determining the concentration of a particular metal element in a sample. Atomic absorption spectroscopy can be used to analyze the concentration of over 62 different metals in a solution and provides accurate quantitative analyses for metals in water, sediments, soils or rocks.

The atomic absorption spectrophotometry include: Flame - Atomic Absorption Spectrophotometry technique (F-AAS), hydride generator - Atomic Absorption Spectrophotometry technique (HG-AAS) graphic funace Atomic Absorption Spectrophotometry technique (GF-AAS), and Cold Vapor Atomic Absorption Spectrophotometry technique in which HG-AAS has been used extensively for determination of volatile element. It is base on hydride generation systems.

Arsenic and Antimony were formed hydridres (AsH_3, SbH_3) in acidic solution with $NaBH_4$ for example the reaction of As^{3+} with $NaBH_4$ forms arsine AsH_3 and can be presented as follows:

$$3BH_4^- + 2H^+ + 4H_3AsO_3 \rightarrow 3H_3BO_3 + 4AsH_3 + 3\ H_2O$$
$$4BH_4^- + 4H^+ + 4H_3AsO_4 \rightarrow 4H_3BO_3 + 4AsH_3 + 4\ H_2O$$
$$3BH_4^- + 2H^+ + 4H_3SbO_3 \rightarrow 3H_3BO_3 + 4SbH_3 + 3\ H_2O$$
$$4BH_4^- + 4H^+ + 4H_3SbO_4 \rightarrow 4H_3BO_3 + 4SbH_3 + 4\ H_2O$$

Hydride generation involves several steps: the hydride is generated by chemical reation, it is swept out of the solution into the atomizer by a carrier gas and they are determined by F-AAS and measured at 193.7nm and 231.2nm for As and Sb, respectively.

I. MATERIALS

I.1. Equipment

- An Atomic Absorption Spectrophotometer system (Chemito –AA230).

- Balance, micropipette, glassware, glass beakers. etc.

I.2. Reagents

- All chemicals used were of analytical grade. Deionized water was obtained by processing distilled water in an ion exchange unit.

- Hydrochloric acid (density 1.12 g/cc), citric acid: Acids must be analyzed to determine levels of impurities.

- Single-element solutions standards (1000 μg ml^{-1}) of As^{3+}, Sb^{3+} were obtained from Merck (Germany).

- Single-element solutions standards (1000 μg ml^{-1}) of As^{5+}, Sb^{5+} were prepared from $SbCl_5$ and $NaAsO_3$ (Germany)**.**

- Intermediate antimony and arsenic solution**:** Pipet 1 mL stock antimony and arsenic solution into a 100-mL volumetric flask and bring to volume with reagent water containing 1.0 mL concentrated HCl/liter (1 mL = 10 μg each of Sb and As).

- Standard antimony and arsenic solution**:** Pipet 10 mL intermediate antimony and arsenic solution into a 100-mL volumetric flask and bring to volume with reagent water containing 1.0 mL concentrated HCl/liter (1 mL = 1 μg each of Sb and As).

- 10% Potassium iodide (KI): A 10% KI solution (10 g reagent-grade KI.

- Dissolved and brought to volume in 100 mL reagent water) must be prepared for reduction of antimony and arsenic to their +3 valence states.

- Sodium borohydride (NaBH4).

- All equipments used for sampling and storing were washed with soap and water, treated with dilute nitric acid and then thoroughly rinsed with deionized water.

II. METHOD

II.1. HG-AAS method for determination of As^{3+}

25ml of water sample was filtered through with size 0.45μm membrane filter in order to remove suspending materials.

- A solution containing 2 percent (w/v) of citric acid was prepared.

- A solution containing 2 percent (w/v) of $NaBH_4$ was prepared.

- Prepare working standards from the standard solution of As^{3+}. Transfer 0, 0.1, 0.2, 0.5, 1.0, and 2.0 mL of standard to 100-mL volumetric flasks and bring to volume with diluent. These concentrations will be 0, 1, 2, 5, 10, and 20μg As^{3+}/liter.

- The HGAAS analysis was performed immediately.

II.2. HG-AAS method for determination of total arsenic

- 25ml of water sample was filtered through with size 0.45μm membrane filter in order to remove suspending materials.

- A solution containing 4N of hydrochloric acid was prepared.

- A solution containing 2 percent (w/v) of $NaBH_4$ in 10 percent (w/v) of KI was prepared.

- Prepare working standards from the standard solution of total arsenic. Transfer 0, 0.1, 0.2, 0.5, 1.0, and 2.0 mL of standard to 100-mL volumetric flasks and bring to volume with deionized water. These concentrations will be 0, 1, 2, 5, 10, and 20μg As (T) /liter.

- The HGAAS analysis was performed a minimum of 30 minutes after sample preparation.

Preconcentration of Sb^{3+} and Sb^{5+}

500ml filtered samples, adjusting to approximately pH=3 then 0.05g of TiO_2 was added. After the solution was stirred for 15 minutes, the titanium dioxide was filtered out, washed twice with 5ml of 0.001N of HCl, Sb^{3+} and Sb^{5+} were eluted by 10ml of 5N of HCl.

II.3. HG-AAS method for determining of Sb^{3+}

- A solution containing 2percent (w/v) of citric acid was prepared.

- A solution containing 2 percent (w/v) of $NaBH_4$ was prepared.

- Prepare working standards from the standard solution of Sb^{3+}. Transfer 0, 0.1, 0.2, 0.5, 1.0, and 2.0 mL of standard to 100-mL volumetric flasks and bring to volume with deionized water.. These concentrations will be 0, 1, 2, 5, 10, and 20μg Sb^{3+} /liter.

- The HGAAS analysis was performed immediately.

II.4. HG-AAS method for determining total antimony

- A solution containing 6 N of hydrochloric acid was prepared.

- A solution containing 2 percent (w/v) of $NaBH_4$ in 10 percent (w/v) of KI was prepared.

- Prepare working standards from the standard solution of total antimony . Transfer 0, 0.1, 0.2, 0.5, 1.0, and 2.0 mL of standard to 100-mL volumetric flasks and bring to volume with deionized water.. These concentrations will be 0, 1, 2, 5, 10, and 20μg Sb(T) /liter.

- The HGAAS analysis was performed a minimum of 30 minutes after sample preparation.

III. RESULTS AND DISCUSSION

Analytical quality control.

From analytical results of trace elements in multi – elements standard were determined by HG-AAS. The present results show that the implemented methods were reliable and have good accuracy and precision. Our results were usually within the quality control plan acceptance range 15 % of the certified value.

Table 1a: Comparison of the present results with certified values in multi-element standard.

As^{3+}(ppb)		**As^{5+}(ppb)**	
Certified values	*This work*	*Certified values*	*This work*
4	3.8 ± 0.4	4	4.2 ± 0.5
6	6.2 ± 0.6	6	6.3 ± 0.9
10	10.5± 0.9	10	9.6± 0.8

Table 1b: Comparison of the present results with certified values in multi-element standard.

Sb^{3+}		**Sb^{5+}**	
Certified values	*This work*	*Certified values*	*This work*
6	5.8 ± 0.6	6	6.3 ± 4.2
8	7.8 ± 0.7	8	7.5 ± 0.9
10	11.4± 0.14	10	9.7± 0.8

Table 2: Concentration of As^{3+}, As^{5+}, Sb^{3+} and Sb^{5+} in groundwater at Di Linh.

Site	**As (µg/L)**			**Sb(µg/L)**		
	As^{3+}	As^{5+}	As^{3+}/As^{5+}	Sb^{3+}	Sb^{5+}	Sb^{3+}/Sb^{5+}
DL-1	1.31±0.15	0.73±0.08	1.79	0.77±0.08	0.22±0.03	3.50
DL-2	1.15±0.12	1.94±0.14	0.59	0.61±0.07	0.36±0.03	1.69
DL-3	0.92±0.11	1.33±0.11	0.69	0.72±0.07	0.51±0.05	1.41
DL-4	1.52±0.18	1.16±0.12	1.31	0.45±0.05	0.62±0.07	0.73
DL-5	1.27±0.13	0.67±0.07	1.90	0.81±0.07	0.17±0.02	4.76

Table 3: Concentration of As^{3+}, As^{5+}, Sb^{3+} and Sb^{5+} in groundwater at BaoLam.

Site	**As (µg/L)**			**Sb(µg/L)**		
	As^{3+}	As^{5+}	As^{3+}/As^{5+}	Sb^{3+}	Sb^{5+}	Sb^{3+}/Sb^{5+}
BLA-1	0.84±0.09	1.11±0.13	0.76	0.33±0.04	0.11±0.01	3.00
BLA-2	1.17±0.09	1.00±0.12	1.17	0.41±0.05	0.14±0.02	2.93
BLA-3	2.75±0.22	3.67±0.28	0.75	0.52±0.05	0.17±0.02	3.06
BLA-4	1.60±0.11	0.93±0.10	1.72	0.37±0.04	0.21±0.03	1.76
BLA-5	1.35±0.14	1.80±0.15	0.75	0.28±0.03	0.13±0.02	2.15

Table 4: Concentration of As^{3+}, As^{5+}, Sb^{3+} and Sb^{5+} in groundwater at Baoloc.

Site	As (µg/L)			Sb(µg/L)		
	As^{3+}	As^{5+}	As^{3+}/As^{5+}	Sb^{3+}	Sb^{5+}	Sb^{3+}/Sb^{5+}
BL-1	2.65±0.21	2.53±0.26	1.05	0.62±0.07	0.22±0.02	2.82
BL-2	1.31±0.14	1.47±0.12	0.88	0.91±0.09	0.10±0.02	9.10
BL-3	2.82±0.29	1.93±0.24	1.45	0.83±0.09	0.17±0.02	4.88
BL-4	1.23±0.15	1.61±0.18	0.75	0.94±0.11	0.27±0.03	3.48
BL-5	1.11±0.10	1.73±0.11	0.64	0.66±0.08	0.13±0.02	5.08

Table 5: Concentration of As^{3+}, As^{5+}, Sb^{3+} and Sb^{5+} in groundwater at Date.

Site	As ((µg/L)			Sb(µg/L)		
	As^{3+}	As^{5+}	As^{3+}/As^{5+}	Sb^{3+}	Sb^{5+}	Sb^{3+}/Sb^{5+}
DT-1	41.1±5.2	23.4±2.1	1.76	1.12±0.11	0.54±0.06	2.07
DT-2	17.7±2.4	18.5±2.0	0.96	0.78±0.09	0.52±0.06	1.50
DT-3	21.5±2.3	8.30±1.0	2.59	1.07±0.09	0.38±0.05	2.82
DT-4	3.12±0.41	4.40±0.51	0.71	0.55±0.06	0.27±0.03	2.04
DT-5	0.81±0.09	0.45±0.05	1.80	0.76±0.08	0.14±0.02	5.43

IV. CONCLUSION

Establish procedures for determination of As^{3+}, As^{5+}, Sb^{3+} và Sb^{5+} in groundwater by hydride generator - Atomic Absortion Spectrometry.

Determination of As^{3+}, As^{5+}, Sb^{3+} và Sb^{5+} in groundwater at Dilinh, Baolam, Baoloc and Date districts.

The concentration of As^{3+}, As^{5+}, Sb^{3+} và Sb^{5+} are presented in tables 2,3, 4 and 5. They are shown that concentration of As^{3+}, As^{5+}, Sb^{3+} và Sb^{5+} in groundwater which collected from Dilinh, Baolam and Baoloc district are lower respective permissible limits according to Vietnam standard. However, concentration of $As^{3+}$and As^{5+} in groundwater at Date are higher than recommended values by WHO and respective permissible limits according to Vietnam standard.

REFERENCES

[1]. Tong Ngoc Thanh Arsenic pollution in groundwater in Red river Delta, Geological survey of Vietnam, annual report 2003.

[2]. Arsenic contamination of groundwater, Uton Muchtar Rafei, Regional Director, WHO suoth - East Asoa Rigon, Volune II 1997-2000.

[3]. Arsenic in drinking water World Health Organization (WHO), N210 may 2001.

[4]. R. Blaine McCleskey, D Kirk Nordstrom, James W Ball. Metal interference and their Removal Prior to Determination of As (T) and As (III) in acidic mine water

by HG-AAS Boulder, Colorado 2003.

[5]. Wash. A. The application of atomic absorption spectra to chemical analysis. Spectrochim. Acta, 7, (1955), p.p 108-117.

[6]. WASH A. The development of the atomic absorption spectrophotometer. Spectrochim. Acta, part B54., (1999), p.p 43-52.

[7]. Vietnamese standards - Water quality and coastal water quality Vol-1, Hanoi 1995 pp. 52-53.

[8]. Erico Marlon de Moraes, Eliane Pereira dos Santos. J anal. At. Spectrum 2002. p.p 819-523.

COMBINED USE OF Cs-137 AND Be-7 TO ASSESS THE EFFECTIVENESS OF SOIL CONSERVATION FOR VETIVER GRASS STRIPS IN COFFEE CROP LANDS IN THE CENTRAL HIGHLANDS

Phan Son Hai, Nguyen Dao, Tran Van Hoa, Tran Dinh Khoa
Nguyen Thi Mui and Trinh Cong Tu

Nuclear Research Institute, VAEC, Vietnam.

ABSTRACT: The combined use of ^{137}Cs and ^{7}Be for assessment of medium- and short-term soil erosion rates for sloping lands with and without soil conservation technologies in the Central Highlands of Vietnam has been carried out. Studies were performed at five 128 m^2 runoff plots and two 0.5 ha coffee plots with the slope gradient of about 25%. Experiments carried out at runoff plots showed that: (i) In the case of low erosion rates (less than 30 t ha^{-1} y^{-1}), soil erosion rates estimated by ^{7}Be technique using the Profile-Distribution Model were consistent with net soil erosion rates obtained by runoff plots when particle size correction factor P is taken into account; (ii) In the case of high erosion rates (greater than 30 t ha^{-1} y^{-1}), the conversion model overestimated soil erosion rates when P was not allowed for, and underestimated erosion rate when P factor was taken into account.

Studies carried out at two 0.5 ha coffee plots showed that: (i) For the plot without soil conservation, soil erosion occurred for all sampling points with medium-term erosion rates ranging between 1.2 t ha^{-1} y^{-1} and 35 t ha^{-1} y^{-1} (the average erosion rate was 22.7 ± 1.2 t ha^{-1} y^{-1}). The short term soil erosion rate estimated by ^{7}Be technique was 32.7 ± 6.1 t ha^{-1} y^{-1} for this plot; (ii) For the plot with the last seven year presence of Vetiver strips, about 93% of the area suffered from medium term erosion with erosion rates varying from 3 t ha^{-1} y^{-1} to 33 t ha^{-1} y^{-1} (the mean is 22,2 t ha^{-1} y^{-1}), and medium term deposition occurred for only 7% of the area with the deposition rates ranging between 1,3 and 1.4 t ha^{-1} y^{-1}, resulting in the net erosion rate of 20.4 ± 0.6 t ha^{-1} y^{-1}. The short term soil erosion rate at this plot estimated by ^{7}Be technique was 2.3 t ha^{-1} y^{-1}. By using Vetiver strips as a soil conservation technology, soil erosion was almost controlled and the net erosion rate was reduced from 32.7 t ha^{-1} y^{-1} to 2.3 t ha^{-1} y^{-1}.

I. INTRODUCTION

The Central Highlands of Vietnam (11° - 16°N, 107° - 108°E) is a region located at elevations between 150 m - 1500 m asl., that occupy an area of 57,370 km^2, about 17.6% of the Vietnam's land. This region has become more vulnerable to erosion under heavy monsoon rainfalls due to deforestation. Some studies carried out in the period of 1992 - 1997 (Luong Duc Loan, Ho Cong Truc, Nguyen Tu Hai, 1998) using 300 m^2 runoff plots reported that soil erosion rates ranged between 5 t ha^{-1} y^{-1} and 105 t ha^{-1} y^{-1} depending on vegetation cover and soil conservation practices.

During the last three decades, fallout radionuclides in particular ^{137}Cs have successfully been used in studies of soil erosion and redistribution (Ritchie, 1974; Longmore, 1983; McHenry, 1985; Loughran, 1990; Sutherland, 1992). In recent years besides ^{137}Cs, radionuclide ^{7}Be has also been used for studying short term soil erosion (Wallbrink P.J., 1996; Walling, 1999; Zapata, 2003). In this study, ^{137}Cs and ^{7}Be were

applied for assessment of soil redistribution patterns and rates of soil loss on sloping land cultivated with coffee in the Central Highlands.

II. RESULTS AND DISCUSSION

2.1. Validation of Conversion Models

Conversion Models were tested using 5 runoff plots at Dalat which have the same area of 127.5 m^2 (17 m x 7.5 m) and the slope of about 25%. When soil samples were taken in the plots for estimation of erosion rates using ^{7}Be, eroding soils in the sediment traps were also collected. By this way we can compare the net soil loss obtained by runoff plot with the estimate of ^{7}Be technique, and the validity of conversion models can be examined. Results showed that:

- In the case of low erosion rates (less than 30 t ha^{-1} y^{-1}), soil erosion rates estimated by ^{7}Be technique using the Profile-Distribution Model were consistent with net soil erosion rates obtained by runoff plots when particle size correction factor P is taken into account.

- In the case of high erosion rates (greater than 30 t ha^{-1} y^{-1}), the conversion model overestimated soil erosion rates when P was not allowed for, and underestimated erosion rate when P factor was taken into account.

- Shallow penetration of ^{7}Be in soil and high soil erosion rate account for the big difference between the net soil loss and the result given by the Profile-Distribution Model. This conversion model will give results not close to real values when it is applied for estimation of soil erosion at high sloping areas in the Central Highlands.

2.2. Assessment of the effectiveness of soil conservation for Vetiver grass strips

2.2.1. Study area

The study was carried out in the 1.5 ha coffee plantation field ($11^{0}35N$; $108^{0}03E$) located at the elevation of 980 m with the mean annual rainfall of 2590 mm, where six year old coffee trees stood 1.2 - 1.5 m apart. In this field two plots each of 0.5 ha (84m x 60m) were laid down. One plot was used for testing soil conservation practices, in which seven 0.4m wide Vetiver strips created in the year 2000 to reduce surface flow rates and to retain eroding soil. According to soil classification of FAO-UNESCO these plots were built on Xanthic Ferralsols. The mean slope gradient of the plots is about 25%.

2.2.2. Results

2.2.2.1. ^{137}Cs and ^{7}Be depth distribution at reference sites

a) Depth distribution of ^{137}Cs

The depth distribution of ^{137}Cs at the reference sites was shown in Figure 2.1. The mean reference inventories of ^{137}Cs was 430 ± 26 $Bq.m^{-2}$. By using the Regression Model (P.D. Hien et al., 2002) described the relationship between the ^{137}Cs inventory at virgin sites I (Bq m^{-2}) and latitude L (degree) and annual rainfall AR (m),

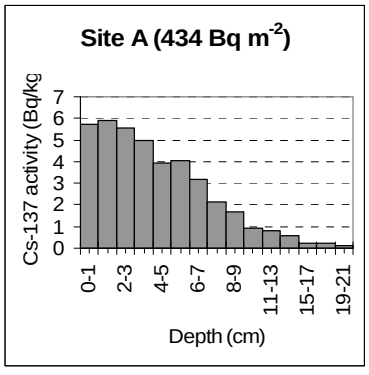

Fig 2.1: *The depth distribution of ^{137}Cs in undisturbed soils at virgin site*

^{137}Cs inventories ranged between 348 and 533 Bq m^{-2} (the mean value: 431 Bq m^{-2}). The predicted values are consistent with experimental values in the range of uncertainties.

b) Depth distributions of ^{7}Be

The depth distribution of ^{7}Be at reference site was shown in Figure 2.2. The ^{7}Be activity exhibits an exponential decline with depth for both reference sites with high correlation coefficients. This evidence suggests that the Profile-Distribution Model is appropriate for assessment of soil erosion rates at the study sites. The relaxation mass depth h_0 estimated from the distribution was 8.5kg.m^{-2}. The mean reference inventory of ^{7}Be obtained from bulk soil samples at reference site was 450 Bq.m^{-2} at the time of sampling.

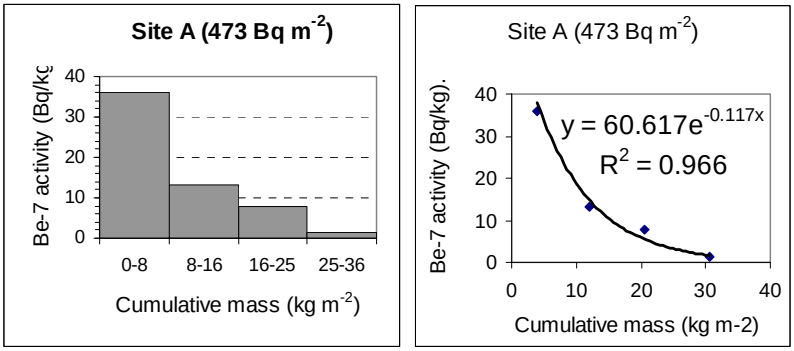

***Fig. 2.2**: The depth distribution of ^{7}Be in undisturbed soil at reference site*

2.2.2.2. Estimation of erosion rates and soil redistribution

a) Medium term soil erosion rates assessed by ^{137}Cs

Soil erosion rates within the coffee field were assessed by ^{137}Cs inventories using the Empirical Model and the Proportional Model. Two Models gave data on soil erosion/ deposition rate with a difference of 10% - 20%. The mean soil erosion rate for the plot with soil conservation and without soil conservation was 20.4 ± 0.6 t ha^{-1} y^{-1} and 22.7 ± 1.2 t ha^{-1} y^{-1}, respectively.

In taking uncertainties into account the difference between soil erosion rate for the plot with Vetiver strips and for the other without Vetiver strips is 0.5 t ha^{-1} y^{-1}. This difference did not reflect accurately the ability of Vetiver strips in retaining eroding soil and the net erosion rate in the plot applied soil conservation practices for the last five years. In this situation ^{137}Cs technique revealed limitations in assessing soil redistribution rates for the short duration of erosion as mentioned by Zapata (2003).

The pattern of soil redistribution:

The pattern of soil redistribution rates within two plots was showed on Figure 2.3. Although the net erosion rates for two plots are not much different from each other as mentioned above, the difference of soil redistribution patterns within two areas is obvious. Therefore, though the use of ^{137}Cs for quantitative assessment of the effectiveness of Vetiver strips in retaining eroding soil is unable, the qualitative assessment is quite possible in this case. The pattern of medium-term soil redistribution reflects areas where local erosion and concentrated flow occurred. For the plot without Vetiver strips, soil erosion occurred for all sampling points with medium-term soil loss ranging between 5 kg m^{-2} and 160 kg m^{-2}. For the plot with Vetiver strips, about 93% of the area suffered from erosion with the soil loss varying from 5 kg m^{-2} to 150 kg m^{-2}, and deposition occurred for only 7% of the area with the deposition rates ranging between 6 kg m^{-2} and 8 kg m^{-2}.

b) Short term soil erosion rates assessed by ^{7}Be

Soil erosion rates:

Radionuclide ^{7}Be was applied for estimating soil loss of the coffee field for the duration of a seven month rainy season . Short-term erosion rates estimated by Conversion Models for the plot without Vetiver strips and the other with Vetiver strips were 32.7 ± 6.1 t ha^{-1} y^{-1} and 2.3 ± 0.9 t ha^{-1} y^{-1} respectively. With the presence of Vetiver strips soil erosion was almost controlled and the net erosion rate was reduced from 32.7 t ha^{-1} y^{-1} to 2.3 t ha^{-1} y^{-1}.

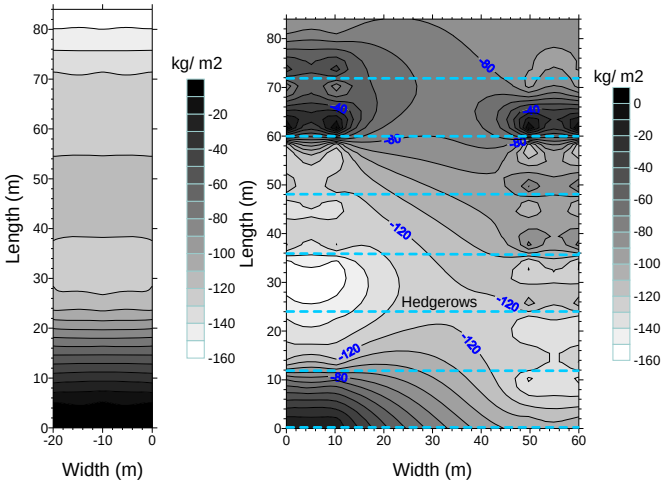

***Fig. 2.3**: The pattern of soil erosion rates obtained from ^{137}Cs data - without hedgerow (left) and with Vetiver hedgerows (right).*

The pattern of soil redistribution:

The patterns of short-term soil redistribution within two plots were showed on Figure 2.4. For the plot without soil conservation, soil erosion occurred for all sampling points with erosion rates ranging between 18 t ha^{-1} y^{-1} and 56 t ha^{-1} y^{-1} (the mean value is 33 t ha^{-1} y^{-1}). For the plot with soil conservation practices, sediment deposition occurred for most of sampling points up slope of Vetiver strips with the deposition rates varying from 1,2 t ha^{-1} y^{-1} to 100 t ha^{-1} y^{-1} (the mean value is 22,4 t ha^{-1} y^{-1}), whereas soil erosion occurred for most of sampling points down slope of Vetiver strips with the erosion rates varying from 0,4 t ha^{-1} y^{-1} to 33 t ha^{-1} y^{-1} (the mean value is 8,0 t ha^{-1} y^{-1}). The sediment delivery ratio is 34.3% for the plot with Vetiver strips. In comparison with the medium-term soil redistribution pattern obtained by ^{137}Cs data, the short-term soil redistribution pattern obtained by ^{7}Be for the plot with soil conservation practices suggested that the concentrated flow erosion has been declined owing to the presence of Vetiver strips for the last five years.

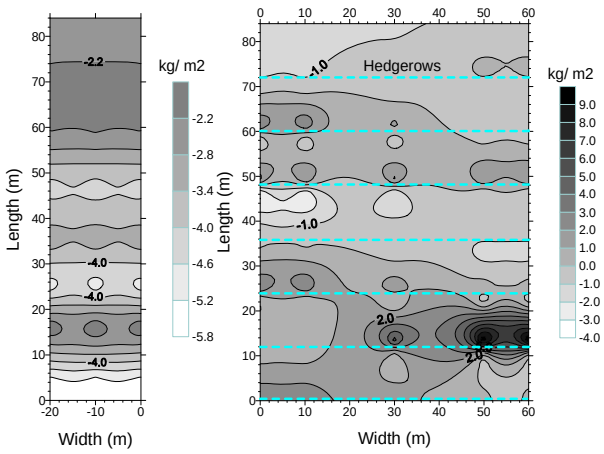

***Fig. 2.4**: The pattern of soil erosion rates obtained from ^{7}Be data - without hedgerow (left) and with Vetiver hedgerows (right).*

III. CONCLUSION

Radionuclide ^{7}Be technique can be utilized for assessment of short term soil erosion rates and the effectiveness of soil conservation technologies in the Central Highlands of Vietnam. Owing to the dry season lasting five month with a very low

rainfall, the ^{7}Be inventory remaining in soil is very low at the end of the dry season. Consequently, the application of ^{7}Be for assessment of soil erosion/ deposition rates in the Central Highlands has the advantage.

When P was not allowed for, the conversion model (1) overestimated soil erosion rates. When P factor was taken into account, the conversion model gave the results consistent with net soil loss in the range of uncertainty in the case of low erosion rates (less than 30 t ha^{-1} y^{-1}) and underestimated soil erosion rate in the case of high erosion rates (greater than 30 t ha^{-1} y^{-1}). Shallow penetration of ^{7}Be in soil and high soil erosion rate account for the big difference between the net soil loss and the result given by the Profile-Distribution Model. This conversion model will give results not close to real values when it is applied for estimation of soil erosion at high sloping areas in the Central Highlands.

By using Vetiver strips as a soil conservation technology, soil erosion was almost controlled and the net erosion rate was reduced 14 times compared with the control, from 32.7 t ha^{-1} y^{-1} to 2.3 t ha^{-1} y^{-1}.

REFERENCES

[1]. Hien, P.D. et al., 2002. Derivation of Cs-137 deposition density from measurements of Cs-137 inventories in undisturbed soils. *Journal of Environmental Radioactivity, 62 295 - 303.*

[2]. Loughran, R.J., B.L. Campbell, G.L. Elliott, D.J. Shelly, 1990. Determination of Rate of Sheet Erosion on Grazing Land Using Cs-137. J. *Applied Geography, 10, pp. 125-133.*

[3]. McHenry, J.R., G.D. Bubenzer, 1985. Field Erosion Estimated from Cs-137 Activity Measurements. *TRANSACTIONS of the ASAE, pp. 480-483.*

[4]. Phan Sơn Hải, 2003. Xác định mối tương quan giữa tốc độ mất Cs-137 và xói mòn đất bề mặt. *Báo cáo tổng kết đề tài cấp Bộ 2001-2002, Viện Năng lượng Nguyên tử Việt Nam, 2003.*

[5]. Phan Son Hai, Nguyen Thanh Binh, Nguyen Dao, 2003. Spatial variability of 137Cs inventory at reference sites and influence of sampling strategy on the uncertainty in estimation of soil erosion rates. *Proceedings of the fifth National Conference on Nuclear Physics and Techniques, Ho Chi Minh City, 27–28 April, 2003, pp. 234–237.*

[6]. Ritchie, J.C., J.R. McHenry, A.C. Gill, 1974. Fallout Cs-137 in the Soils and Sediments of Three Small Watersheds. *Ecology, Vol. 55, No. 4, pp. 887-890.*

[7]. Sutherland, R.A., 1992. Cs-137 Estimates of Erosion in Agricultural Areas. *Hydrological Processes, Vol. 6, pp. 215-225.*

[8]. Wallbrink P.J., A.S. Murray, 1996. Distribution and Variability of Be-7 in Soils under Different Surface Cover Conditions and its Potential for Describing Redistribution Processes. *Water Resources Research, Vol. 32, No. 2, pp. 467-476.*

[9]. Walling, D.E., Q. He, W. Blake, 1999. Use of ^{7}Be and ^{137}Cs measurements to document short- and medium-term rates of water-induced soil erosion on agricultural land. *Water Resources Research, Vol. 35, No. 12, pp. 3865-3874.*

PAPERS PUBLISHED IN RELATION TO THE PROJECT

1. Phan Sơn Hải, Nguyễn Thanh Bình, Trần Văn Hòa, Trần Đình Khoa, Nguyễn Đào, Nguyễn Thị Mùi, Trình Công Tư (2007). Đánh giá tốc độ xói mòn và hiệu quả các giải pháp bảo vệ đất bằng phương pháp đồng vị phóng xạ và ô thí nghiệm. *Tạp chí Khoa học đất, No. 27, pp. 154-159.*
2. PHAN S. HAI, T. D. KHOA, N. DAO, N. T. MUI, T. V. HOA, T. C. TU. Application of Cs-137 and Be-7 to assess the effectiveness of soil conservation technologies in the Central Highlands of Vietnam. *Journal of Nuclear Science and Technology (Đã gửi đến Ban biên tập và sẽ đăng trong số tới của năm 2008).*

DETERMINATION OF 22 ELEMENTS IN MARINE ENVIRONMENTAL SAMPLES IN SPECIAL AREAS AT THE SOUTH OF VIETNAM

Nguyen Ngoc Tuan, Nguyen Giang, Nguyen Thanh Tam and Truong Phuong Mai

Nuclear Research Institute, VAEC, Vietnam.

ABSTRACT: In 2007 year, we continued to determine the contents of 22 elements in marine environmental samples such as marine sediment, seawater and marine creature.

The methods for the determination of elements in these objects are Neutron Activation Analysis and Atomic Absorption Spectrophotometer.

The obtained analytical results are a database to monitor marine environmental pollution and to evaluate the impact of exploitation of rare earth- radioactive ores near by the sea coast; exploitation of crude oil in offshore and technology activities at the south of Vietnam in the future.

The analytical results of toxic and trace element's contents are also to attend the Forum for Nuclear Cooperation of Asia (FNCA) in which Vietnam is one of member's nine counties.

The analytical results have been presented in the FNCA 2007 workshop on utilization of the research reactor from 28 Seprember-02 October in Serpong, Indonesia.

I. INTRODUCTION

Since 1999, the Ministry of Science and Technology and Vietnam Atomic Energy Commission have approved some projects as "studying and applying main nuclear analytical techniques for assessment of the present situation of marine environmental radioactivity in Vietnam". The objectives of these projects are to establish procedures for collection, preparation and preservation of marine environmental samples and standard procedures for the determination of radio nuclides in the samples collected at the selected sites of Vietnam's sea areas. However, many elements such as: Cu, Pb, As, Cu, Hg, Sb, Se, Zn etc… have not been considered.

The aim of our work is to develop and apply NAA techniques to analyze concentration of minor and trace elements in marine environmental samples collected in Nha Trang, Phan Thiet and Ganh Rai bays. The results were compared with the recommended values by World Health Organization (WHO) and maximum permissible limits according to standard of Vietnam -TCVN.

II. MATERIAL AND METHODS

II.1. Equipments

- The Dalat Research Reactor of 500kW swimming pool type is available for neutron irradiation at a flux of 5.10^{12}n.cm^{-2}s^{-1}(in pneumatic transfer system) and of 1.10^{12} n.cm^{-2}s^{-1} (in rotary specimen rack). Gamma spectrometry system connected detector of HPGe. The resolution of detector is of 1.9 keV at 1173 keV and 1332.5 keV of ^{60}Co.

- Atomic Absorption Spectrophotometer-AA6800 Shimadzu, Japan.

II.2. Sampling and sample preparation

Co-ordinates of sampling sites are following:

- Nha Trang bay: 12^{O}.14'.59" North Latitude; 109^{O}.11'.97" East Longitude; 7,2 meters Depth.
- Phan Thiet bay: 10^{O}.55'.25" North Latitude; 108^{O}17'39" East Longitude; 6,5 meters Depth.
- Ganh Rai bay: 10^{O}.25'19" North Latitude; 106^{O}58'27" East Longitude; 5,6 meters Depth.

All marine environmental samples (sediment, biota and seawater) were collected from the coast of Nha Trang, Phan Thiet and Ganh Rai bay in May 2007. Before sampling all the equipment was cleaned according to standard cleaning procedures.

Seawater samples collected at the locations about 0.5km from the coats and were filtered through 0.45μm membrane filters; acidified with nitric acid to pH = 2.

Sediment samples were collected in polyethylene containers. Sample is surface layer of sediment (0-20cm), in the same sampling site of the seawater samples. The collected samples were stored in ice-filled cooler boxer until return to the laboratory. After that the samples were dried at 40^{0}C until the weight reached a constant value; they were grounded in blender and kept in the clean polyethylene bottles for elemental analysis.

Biota samples were purchased from fishermen who were seine fishing at Nha Trang Phan Thiet and Ganh Rai bays and stored in ice-filled cooler boxer until return to the laboratory. They were cut into small pieces by a stainless steel knife and washed under tap water to remove blood and other fluid materials; then with deionizered water for several times. After that the samples were dried by lyophilization. After drying the samples have been grounded in blender and kept in the clean polyethylene bottles for elemental analysis.

II.3. Preparation of standard materials

Standard Reference Material Pine Needle 1575 obtained from the National Institute of Standards and Technology (NIST) and lake sediment (SL-1) obtained from the International Atomic Energy Agency (IAEA) were used for quality control of analytical procedures. Standard solutions As, Cu, Hg, Se, Sb, Zn, etect... were prepared from single-elemental and multielemental standards (1000μg ml^{-1} Merck - Germany). Ultra-pure nitric acid, hydrofluoric acid, perchloric acid and hydro peroxide were purchased from Merck - Germany and freshly purified water.

III. METHODS FOR ANALYSES

III.1. The analytical procedure for minor and trace elements by INAA

About 150-200mg samples, in triplicate, and the multielemental standards along with the suitable control material were separately sealed in PE bags; then samples and standards were placed in polyethylene and aluminum containers for short and long irradiations, respectively.

Table 1: The experimental condition for NAA

Irradiation time	Cooling time	Counting time	Group of nuclides
2-5 min	2-5min	100-200sec	^{28}Al, ^{52}V, ^{66}Cu, ^{51}Ti, ^{37}S, ^{49}Ca, ^{27}Mg, ^{80}Br, ^{38}Cl, ^{128}I, ^{56}Mn, ^{24}Na, ^{116m}In, ^{165}Dy, Si(^{29}Al).
15-20min	30-40h	1200sec	^{42}K, ^{64}Cu, ^{69m}Zn, ^{82}Br, ^{76}As, ^{72}Ga, ^{122}Sb, ^{140}La, ^{115}Cd, ^{153}Sm, ^{187}W, ^{198}Au, ^{99}Mo, ^{24}Na, U(^{239}Np)
6-10 hours	2-3 days	1800sec	^{42}K, ^{64}Cu, ^{69m}Zn, ^{82}Br, ^{76}As, ^{72}Ga, ^{122}Sb, ^{140}La, ^{115}Cd, ^{153}Sm, ^{187}W, ^{198}Au, ^{99}Mo, ^{24}Na, U(^{239}Np).
10-20	3 weeks	3600sec	^{46}Sc, ^{51}Cr, ^{59}Fe, ^{60}Co, Ni(^{58}Co), ^{65}Zn, ^{75}Se, ^{110m}Ag, ^{113}Sn, ^{124}Sb, ^{134}Cs, ^{131}Ba, ^{177m}Lu, ^{141}Ce, ^{152}Eu, ^{203}Hg, Th(^{233}Pa), ^{147}Nd, ^{181}Hf, ^{86}Rb, ^{182}Ta, ^{175}Yb.

Radiochemical Activation Analysis is used in the cases, the concentration of some elements such as Hg, Cd, Ni, Se, As, U, etc. in the samples are very low or matrix of the samples are complicated. We have to separate and concentrate the elements in the samples before or after irradiation.

Atomic Absorption Spectrophotometer Method-AAS is used to determine Pb and other elements to compare with analytical results of NAA.

IV. RESULTS AND DISCUSSION

Analytical quality control

The concentrations of minor and trace elements in standard reference materials such as Pine Needles 1575 and SL-1 were determined by INAA, RNAA and AAS. The obtained results show that the implemented methods were reliable and have good accuracy and precision.

The concentrations of 22 elements in the sediment, seaweed and biota samples at NhaTrang, Phan Thiet and Ganh Rai bay are shown in tables 3, 4, 5, 6, 7, 8, 9, 10, 11 and 12.

+ The obtained analytical results showed that the concentrations of some elements in marine sediment samples in three areas are very various:

Aluminum:

- Nha Trang: 1.67 - 4.11%; average: 2.67%
- Phan Thiet: 1.25 - 1.52%; average: 1.31%
- Ganh Rai: 3.23 - 5.12%; average: 3.68%
- Hai Phong habour: 4.42 - 6.15%; average: 5.37%
- Malaysia: 3.84 - 9.49%; average: 760%

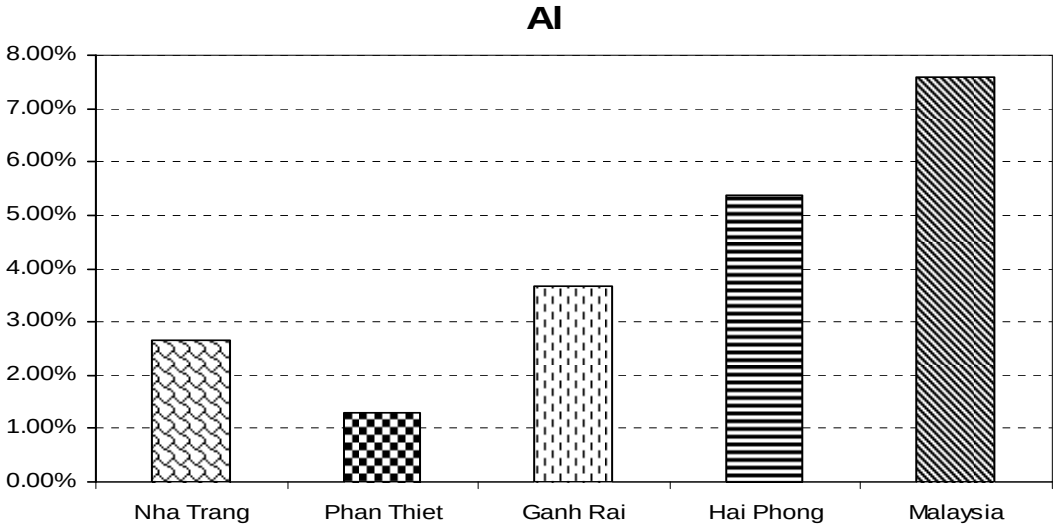

Fig. 1: The concentration of Al in marine sediments samples in three areas

Iron:

- Nha Trang: 0.20 - 0.59%; average: 0.41%
- Phan Thiet: 0.64 - 0.77%; average: 0.69%
- Ganh Rai: 0.16 - 0.34%; average: 0.27%
- Hai Phong habour: 3.98 - 5.50%; average: 4.55%
- Malaysia: 1.84 - 4.43%; average: 2.63%

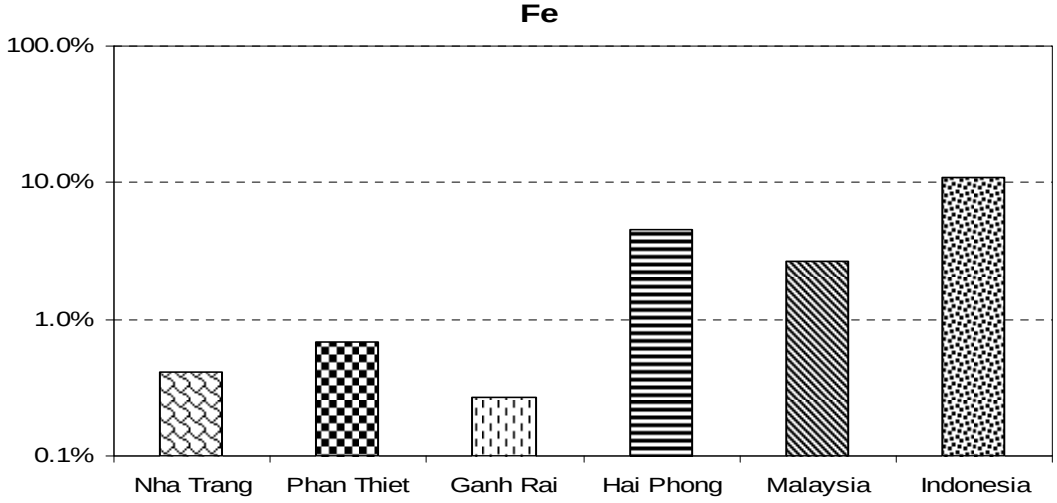

Fig. 2: The concentration of Fe in marine sediments samples in three areas

Calcium:

- Nha Trang: 2.6 - 3.8%; average: 3.16%
- Phan Thiet: 0.71 - 1.02%; average: 0.86%

- Ganh Rai: 0.27 - 0.63%; average: 0.46%
- Hai Phong habour: 0.41 - 0.58%; average: 0.48%
- Malaysia: 0.87 - 15.13%; average: 2.23%

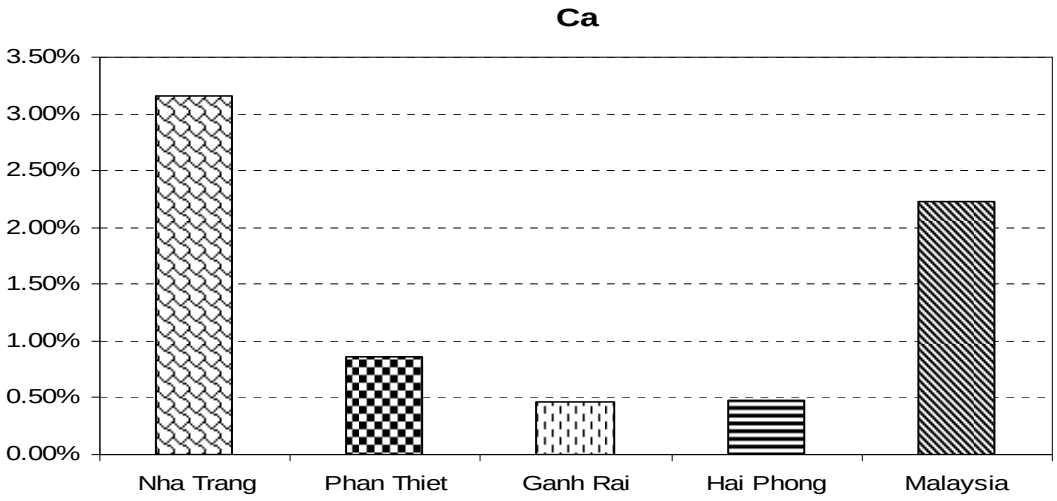

Fig. 3: The concentration of Ca in marine sediments samples in three areas

Potassium:

- Nha Trang: 0.97 - 1.43%; average: 1.32%
- Phan Thiet: 1.8 - 2.4%; average: 2.0%
- Ganh Rai: 0.91 - 1.74%; average: 1.32%
- Hai Phong habour: 2.13 - 2.64%; average: 2.34%
- Malaysia: 0.87 - 1.93; average: 1.55%

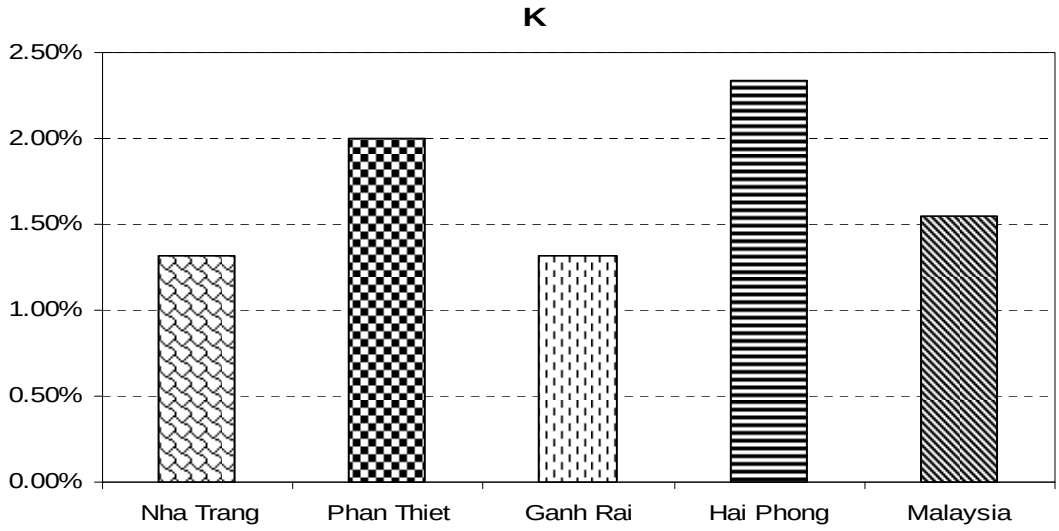

Fig. 4: The concentration of K in marine sediments samples in three areas

The concentrtion of Ca in Nha Trang bay is much higher than that in Phan Thiet and Ganh Rai bays. It can be explained that there are many small mountains around the Nha Trang bay; calcium in the moutains can be dissolved in seawater and settled down into sediment.

The contents of Fe in three areas are very low, much lower than that in Hai Phong habuor and in Malaysia and Indinesia.

The concentration of V and Al in sediment samples at Nha Trang and Phan Thiet bays is less than those of the samples at Ganh Rai bay. The sea area is affected directly by the biggest oil exploiting industrial zones in Vietnam. V is present in crude oil and Al is an element of materials utilized in oil exploiting industry.

The concentrations of trace elements (As, Cd, Cu, Hg, Pb, Sb and Zn) in coastal water samples were lower than the permissible limits according to Vietnam standards and recommended values by World Health Organization (WHO).

It was observed that seaweed and shellfish contain high amount As, Cd, Hg, Pb and Sb in comparison with other foodstuffs; it is explained the biota living in the bottle level accumulated the heavy metals much higher than that in the middle level and surface layer. Specially the concentration of Cd in shellfish samples in Nha Trang bay is higher than that in Phan Thiet and Ganh Rai bays.

The highest concentration of Zn were found in shellfish and seaweed respectively (Zn = 53.0mg/kg.dry; Zn = 43.5mg/kg.dry).

V. CONCLUSION

The analytical procedures for determination of minor and trace elements in sediments, seawater and biota samples has been established. More than 1300 data on the minor and trace elements in marine environmental samples collected from 3 coastal locations in the south of Vietnam were received.

The concentration of minor and trace elements in marine environmental samples are shown that cadmium, zinc and arsenic contents in seaweeds and shellfish are higher than other foodstuffs; calcium contents in seawater and sediment samples at Nha Trang are higher than at Phan Thiet and Ganh Rai bays.

The concentration of trace elements (As, Cd, Cu, Hg, Pb, Sb, Se, Zn, etec…) in seawater and biota samples which collected from the above mentioned locations are lower respective permissible limits in according to Vietnam standards and recommended values by the WHO.

The received analytical data will provide a database for investigation program on minor and trace elements concentration in the marine environmental samples in the future.

REFERENCES

[1]. Nguyen Giang, Nguyen Ngoc Tuan Simultaneous determination of As and Cu in vegetable samples by RNAA. J Chem. Vol. 8. No 3. (2003) p.p. 62- 66.

[2]. Ministry of Health - The standards of safe values for foodstuffs - Hanoi 1998 pp. 38-39.

[3]. Vietnamese standards - Water quality and coastal water quality Vol-1, Hanoi 1995 pp. 52-53.

[4]. Lam Minh Triet, Diep Ngoc Suong Analytical methods for determination of trace elements in water and waste water (2000).

[5]. Y.Sakai, T.Tomura, K Ohshita, S. Koshimuzu. *J. Radio anal. Nucl. Chem.* Vol. 230 No. 1-2 (1998) p.p.261-263.

[6]. Y.Sakai, T.Tomura, K Ohshita, S. Koshimuzu. *J. Radio anal. Nucl. Chem.* Vol. 216 No. 2 (1997) p.p.203-212.

[7]. H.S. Dang, V.R. Pullat, K.c.Pillai *J. Radioanal. Nucl. Chem.* Vol. 162, No. 1 (1992) p.p.163-169.

[8]. Ho Manh Dung. The final report of the project: "Determination of toxic and trace elements in human hair and in sediment sample by Analytical Neutron Activation Analysis Techniques based on K-zero method.

[9]. P.D. Hien, P.S. Hai, N.H.Quang, P.N.Chuong, N.M.Xuan. Elemental composition of sediments in the Hai phong harbour area as determined by Nuclear Analytical Techniques Applications of Isotopes and Radiation in Conservation of the Environment. Proceeding of a symposium, Karlsruhe, 9-13 March 1992, p 606-607.

[10]. Wee Boon Siong and Abdul Khalik Hj. Wood. Detremination of Trace and Toxic elements in Marine Sediments collected from the Strait of Malaca, Malaysia. Proceeding of the FNCA 2006 Workshop on Utilization of Research Reactors August 28-September 1, 2006; Manila, Philippines; p19-25.

[11]. Sutisna, Saryati, Saeful Yusuf, Theresia Rina, Rina Suryani. Monitoring environmental pollution by Ko-INAA for Environmental Protection in Indonesia. Proceeding of the FNCA 2006 Workshop on Utilization of Research Reactors August 28-September 1, 2006; Manila, Philippines; P 09-18.

PAPERS PUBLISHED IN RELATION TO THE PROJECT

1. Nguyễn Giằng, Nguyễn Ngọc Tuấn, Nguyễn Thanh Tâm. Xác định As, Cu, và Mn trong nước biển bằng phương pháp kích hoạt nơtron có xử lý hoá. Tạp chí phân tích Hóa, Lý và Sinh học; Tập 12, số 1/2007; trang 55-58.
2. Nguyễn Ngọc Tuấn, Nguyễn Giằng, Nguyễn Thanh Tâm. Xác định 25 nguyên tố Cu, Ca, Mg, Br, I, Mn, As, Sb, La, Cd, Sm, Mo, U, Sc, Fe, Co, Ni, Zn, Se, Cs, Ce, Eu, Hg, Th, Sr trong các mẫu sinh vật và trầm tích biển bằng phương pháp phân tích kích hoạt nơtron và quang phổ hấp thụ nguyên tử.

   Phần 1. Xác định đồng thời Ca, Mg, Cu, Br, I, Mn và As trong mẫu rong và mẫu trầm tích biển bằng phương pháp kích hoạt nơtron. Tạp chí phân tích Hóa, Lý và Sinh học; Tập 12, số 1/2007; trang 72-77.
3. Nguyễn Ngọc Tuấn, Nguyễn Giằng. Xác định 25 nguyên tố Cu, Ca, Mg, Br, I, Mn, As, Sb, La, Cd, Sm, Mo, U, Sc, Fe, Co, Ni, Zn, Se, Cs, Ce, Eu, Hg, Th, Sr trong các mẫu sinh vật và trầm tích biển bằng phương pháp phân tích kích hoạt nơtron và quang phổ hấp thụ nguyên tử.

   Phần 2. Xác định đồng thời Cu, Ca, Mg, Br, I, Mn, As, Sb, La, Cd, Mo, U, Sc, Fe, Co, Ni, Zn, Se, Cs, Ce, Eu, Hg, Th, Sr trong mẫu rong mơ bằng phương pháp kích hoạt nơtron. Tạp chí phân tích Hóa, Lý và Sinh học; Tập 12, số 2/2007; trang 31-36.

4. Nguyễn Ngọc Tuấn, Nguyễn Giằng, Nguyễn Thanh Tâm. Xác định 25 nguyên tố Cu, Ca, Mg, Br, I, Mn, As, Sb, La, Cd, Sm, Mo, U, Sc, Fe, Co, Ni, Zn, Se, Cs, Ce, Eu, Hg, Th, Sr trong các mẫu sinh vật và trầm tích biển bằng phương pháp phân tích kích hoạt nơtron và quang phổ hấp thụ nguyên tử.

Phần 3. Xác định đồng thời Cu, Ca, Mg, Br, I, Mn, As, Sb, La, Cd, Sm, Mo, U, Sc, Fe, Co, Ni, Zn, Se, Cs, Ce, Eu, Hg, Th, Sr troing mẫu sinh vật biển (sò và cá sòng) bằng phương pháp kích hoạt nơtron. Tạp chí phân tích Hóa, Lý và Sinh học; Tập 12, số 3/2007; trang 20-24.

5. Nguyen Giang, Nguyen Ngoc Tuan, Nguyen Van Minh, Nguyen Thanh Tam, Truong Phuong Mai, Ho Tran The Huu. Determination of minor and trace elements in marine environmental samples at South coast of Vietnam.

Proceeding of FNCA 2006 Workshop on the Utilization of Research Reactors; August 28-September 1, 2006, Manila, Philipines, P 43-54.

6. Nguyen Giang, Nguyen Mong Sinh, Nguyen Ngoc Tuan. Instrument of Neutron activation Analysis for Environmental Administration. Proceeding of FNCA 2006 Workshop on the Utilization of Research Reactors; August 28-September 1, 2006, Manila, Philipines, P 80-91.

7. Nguyen Ngoc Tuan. Determination of 25 elements in marine sediment, seawater and biota samples by Neutron Activation Analysis Method. Reported in FNCA 2007 Workshop on the Utilization of Research Reactors; September 28-October 02, 2007, Serpong, Indonesia.

1.6 - Biology, Agriculture and Medicine

STUDY ON THE PROCEDURES FOR DETERMINING OF PESTICIDE RESIDUES IN GREEN VEGETABLES

Le Tat Mua, Nguyen Tien Đat, Nguyen Van Minh, Nguyen Ngoc Tuan, Le Thi Ngoc Trinh
Ta Thi Tuyet Nhung, Truong Van Tai, Tran Thanh Nha and Nguyen Thi Hong Tham

Nuclear Research Institute, VAEC, Vietnam.

ABSTRACT: Researchs presented in this work are divided into two main parts. One part embraces the residue analytical methods. The other part comprises applying of these residue analytical methods for analysis of plant material.

Part I: Residue analytical methods (Analytical procedures)

Residue analytical methods presented in this work are the single method and the multiresidue methods. There are nine methods:

Determination of Endosulphan in plant material by GC/ECD.

Determination of Methamidofos in plant material by GC/FTD.

Determination of Deltamethrin, Cyhalothrin, Cyfluthrin in plant material by GC/ECD.

Determination of Maneb in plant material by HPLC/UV.

Determination of Zineb in plant material by F-AAS.

Determination of Organo-Asenic and Mercury in plant material by RNAA.

The limits of detection and determiation (LOD, LOQ), Recovery, Efficiency, the Calibration curve are validated.

Part II: Applying of Residue Analytical Methods for analysis of endosulphan, methamidofos, maneb, zineb, cyhalothrin, deltamethrin, cyfluthrin, metallo-organic compounds in Spinach, Cabbage, Pimento, Japanese Bean, Japanese Pumpkin, Tomato, Potato, Sweet Potato.

The results, and conclution are present in this work.

Part I:

RESIDUE ANALYTICAL METHODS

A/ Determination of endosulphan, methamidofos, cyhalothrin, deltamethrin, cyfluthrin in plant material by GC/ECD/ FTD

1. INSTRODUCTION

ORGANOCHLORINE, ORGANOPHOSPHORUS PESTICIDES

ENDOSUPHAN, METHAMIDOPHOS

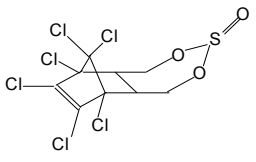

ENDOSULPHAN

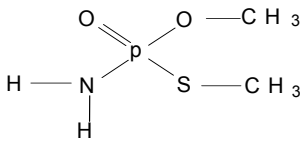

M E T H A M ID O F O S

PYRETHROIDS

DELTAMETHRIN , CYFLUTHRIN và LAMDACYHALOTHRIN

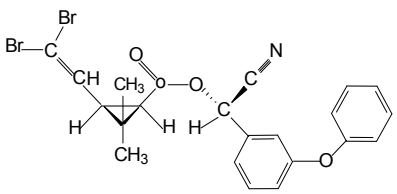

DELTAMETHRIN

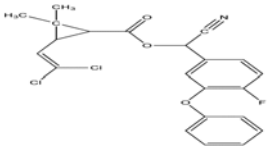

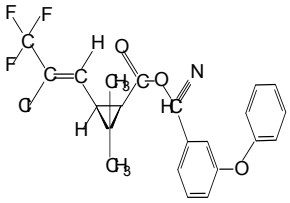

2. OUTLINE OF METHOD

The samples is extracted with a solvent of a type depending up the nature of the analytical material. The residue is taken up in aceton, then Ethyl acetate, cleaned up on a column, or SPE column, and determined by GC/ECD or FTD.

3. APPARATUS

Gas Chromatograph GC-17A, GC-2010 equipped with ECD, FTD; Buchner procelain funnel; Rotary vacuum avaporator, Chromatographic tube, Liquid liquid extractor, Separatory funnel 500mL

4. REAGENTS

All chemicals used were of analytical grade. Deionized water was obtained by processing distilled water in an ion exchange unit.

Acetone, Ethyl Acetate (chemical pure) distilled in rotary evaporator at 40^0C

Diclhoromethane, p.a. (Merck No. 6050).

n-Hexan, Toluene for residue analysis.

Eluting mixtures.

Pesticide standard solutions: Endosulphan, Methamidofos, deltamethrin, Cyhalothrin, Cyfluthrin.

Sodium chloride solution, saturated; sodium sulphate, active carbon, silicagel 0.063-0.200mm, SPE ODS C18.

Nitrogen

Sample collection and sample preparation

More than 300 samples of vegetables such as: Spinach, Cabbage Pimento, Japanese Bean, Japanese Pumpkin, Tomato, Potato, Sweet Potato were collected from the vegestable farms of Dalat City, Duc Trong and Don Duong District during 2 years 2006-2007.

5. PROCEDURE

5.1. Extraction

5.1.1 Samples with a high content of water (vegetables).

Weigh a 50g portion of sample (G) into the beaker, add 200ml acetone and homogenize for 30 s. Filter the homogenate with suction through a fast flow rate filter

paper in a Buchner funnel. Rinse filter cake with acetone. Transfer the combined filtrates to a round bottomed flask rotary evaporate to an aqueous residue and proceed as described in.

5.1.2. Potato, sweet potato

Grind 50g potatos (sweet potatoes) (G) in the blendor, add 10 g Celite and 150mL aceton water miture and homogenate for 5 min. Filter the homogenate with suction through a fast flow rate filter paper in a Buchner funnel.

5.2. Clean up

5.2.1 Liquid-liquid partition

Transfer the aqueous residue derived from 5.1.1 to a separatory funnel saturate with sodiumchloride (14g NaCl for 50ml solution) with shaking and then extract three times with 150 ml portions of dichloromethane in the separatory funnel for 5 min. If a stubborn emulsion forms that can not be broken also by centrifugation. It is recommended to extract it with dichloromethane for 1 h in a liquid- liquid extraction for extraction with heavy solvents.

Dry the combined organic phases on 50 g sodium sulfate and filter throught a fluted lilter paper into a round bottomed flask. Wash the sodium sulfate and the flute filter paper portionwise with 50 ml dichoromethane. Rotary-evaporate the combined filtrates almost to dryness. Then continue as described in 5.22. for apples, column-chromatography cleanup can be emitted.

5.2.2. Column chromatography

Fill a chromatography tube with approx. 50 ml diethyl ether. Tamp a plug of cottonwool to the bottom of the tube, slowly add 15 g silicagel and let the supernatant liquid drain to the surface of the silicagel. Cover the silicagel with 5 g sodium sulfate. Dissolve the residue derived from 5.2.1 or 5.1.3 in 5 ml diethyl ether and elute part of the co-extractives with 100 ml diethyl ether. Then re-wash with 100mL eluting mixture 1. Elute the compound with 100 ml eluting mixture 2 at a flow rate of 10 to 12 ml/min. To avoid obtaining false the results, the mixture ratio must be strickly observed. It is also essensial to check elution of the compounds form the column with the silicagel anh eluting mixture used.

Rotary-evaporate the eluate containing the compounds almost to dryness. Remove the residual solvent by swirling the flask in the hand.

5.3 Gas-chromarography determination

Dissolve the residue derived from 5.22 or 5.1.3 or 5.2.1. in acetone and make up to a given volume (V_{end}) which should not be less than 2 ml. Inject an aliquol of this solution (V_1) in to the gas-chromatograph.

Operating condition

Gas chromatograph	GC-17A; GC-2010
Column	Capillary column MDN-12, L30m, ID 0.32mm, Film Silica 0.25µm, Capillary column SPB^{TM}-608, L30m, ID 0.25mm, Film Silica 0.25µm

Column temperature	80^0C
Injecter port temperature	230^0C
Detector	300^0C
Gas flow rates	Nitrogen carrier 30 ml/min
	Air 200ml/min
	Hydrogen 2ml/min
Injection volume	1-2µL
Retention times for	
- Methamidophos	6.3 min
- Endosuphan	10.3 and 13.6 min
- Deltamethrin	32.3 add 34.1 min
- Cyhalothrin	15.1 min
- Cyfluthrin	20.15; 20.51 and 20.88 min

6. EVALUATION

6.1. Method

Quantitation is performed by measuring the peak heights of sample solutions and comparing them with those of standard solutions. Equal volumes of sample solutions and standard solutions should be injected.

6.2. Recoveries, Limit of Detection and Limit of Determination

Recoveries from untreated control sample fortified at levels of 0.005 -1.0 mg/kg usually ranged from 70-100% , averaging 87% for endosulphan, 90% for methamidophos, 85% for deltamethrin, 84% for Cyhalothrin and 87% for cyfluthrin. The limit of detection was 0.003 mg/kg for endosulphan, 0.010 for methamidophos, 0.008 for deltamethrin, 0.007 for Cyhalothrin and 0.010 for cyfluthrin.

6.3. Calibration of residues

The residue R, expressed in mg/kg for endosulphan, methamidophos, deltamethrin, Cyhalothrin or cyfluthrin, is calculated from the following equation:

$$R = \frac{W_A . V_{Ex} . V_{End}}{V_{RI} . V_i . G} (mg / kg)$$

Where:

G: Sample weight (in g)

V_{end}: Terminal volume sample solution from 5.3 (in ml)

V_i: Portion of volume V_{end} injected into gas chromatograph

W_{St}: Amount of compound injected with standard solution

H_A: Peak height obtained from V_i

$H_{St:}$ Peak height obtained from W_{St}

B/ Determination of maneb, zibed in plant material by HPLC/UV and F-AAS

1. INSTRODUCTION

Dithiocarbamate- **MANB and ZINEB**

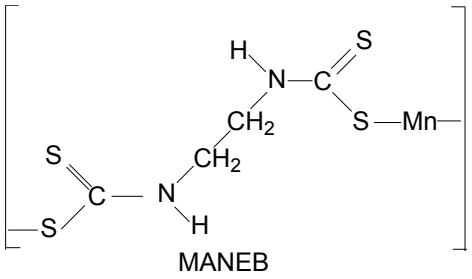

MANEB

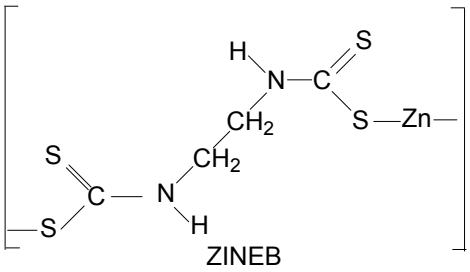

ZINEB

2. OUTLINE OF METHOD

3. APPARATUS

- HPLC/UV: Perkin Elmer 200 IC equipped with Spectra-Phyics UV 150; GC-MS HP-6890, VARIAN UV-Vis CARY 50 ; Buchner procelain funnel; Rotary-vacuum evaporator, Chromatographic tube, Liquid liquid extractor, Separatory funnel 500ml.

- F-AAS: Perkin Elmer 3300; HCL Zn: Perkin Elmer.

4. REAGENTS

All chemicals used were of analytical grade. Deionized water was obtained by processing distilled water in an ion exchange unit.

Dimethylsulfoxid (DMSO) (PA, Belgium) for AAS.

Chloroform 99 %

Acetonitril (PA,HPLC).

Metanol (PA,HPLC).

Maneb standard (PA, HPLC).

EDTA 0.25M/NaOH solution.

Benzyltrietyl Amonium Cloride 0.41M Solution.

CH_3I 0.1M /$CHCl_3$:Hexan (3:1 v/v) solution.

Nabam solution.

Sample collection and sample preparation

More than 300 samples of vegetables such as: Spinach, Cabbage Pimento, Japanese Bean, Japanese Pumpkin, Tomato, Potato, Sweet Potato were collected from the vegestable farms of Dalat City, Duc Trong and Don Duong District during 2 years 2006-2007.

5. PROCEDURE

5.1. Analytical proedure of Maneb in plant material

ANALYTICAL PROCEDURE OF MANEB IN PLANT MATERIAL BY HPLC/UV

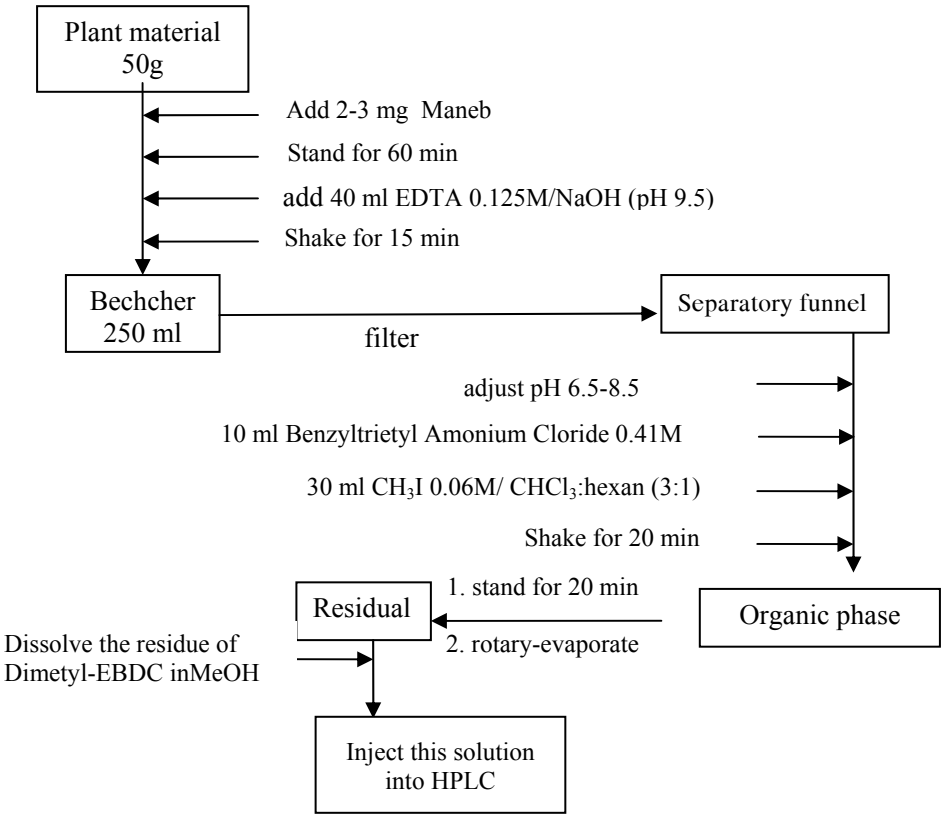

5.1.1. HPLC method

HPLC condition

Gas chromatograph	Perkin Elmer 200 IC, Spectra-Phyics UV 150
Column	Gemini C18 (250mm, 4.00 mm id., 5 µm particle size). Capillary column MDN-12, L30m, ID 0.32mm, Film Silica 0.25µm, Capillary column SPB^{TM}-608, L30m, ID 0.25mm, Film Silica 0.25µm
Mobile phase	0.8 mL/min
Flow rate	0.8 mL/min
UV detector	272 nm
Injection size	10µL
Retention times for ethylenebiditiocarbamate	39 min

5.2. Analytical proedure of Zineb in plant material

ANALYTICAL PROCEDURE OF ZINEB IN PLANT MATERIAL BY F-AAS

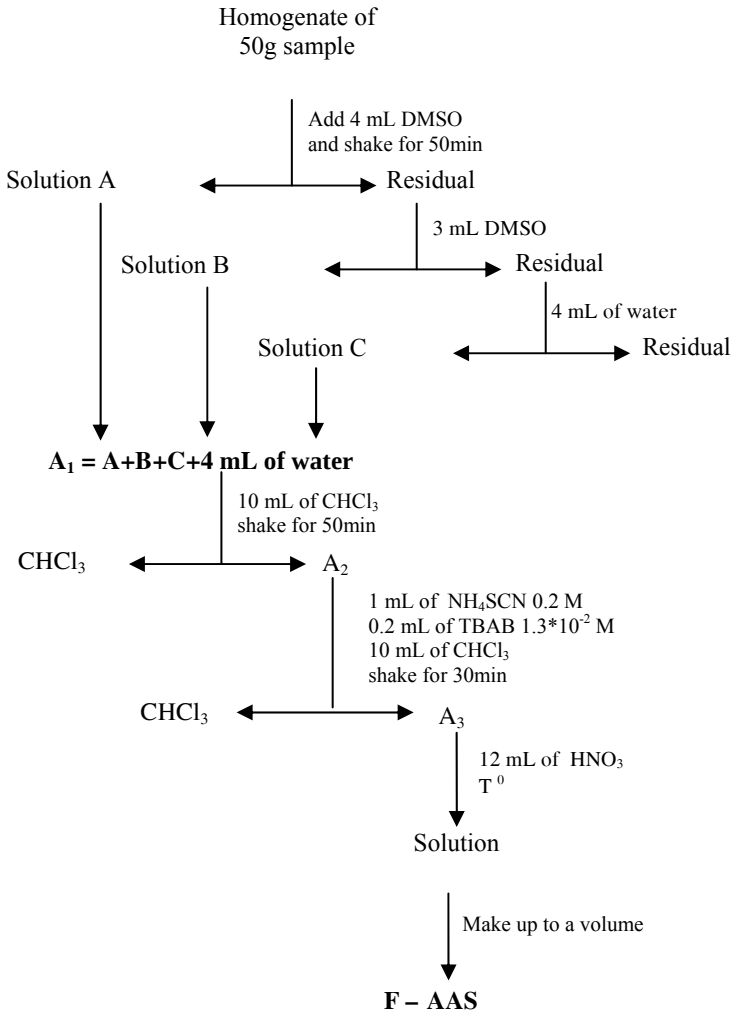

5.2.1. Parameter

- Current lamp: 18 mA.
- Wave lenght: 213.7 nm.
- Energy lamp: 41.
- Slit: 0.7 nm.

6. EVALUATION

6.1. Method

Quantitation is performed by measuring the peak heights of sample solutions and comparing them with those of standard solutions. Equal volumes of sample solutions and standard solutions should be injected.

6.2. Recoveries, Limit of Detection and Limit of Determination

6.2.1. Maneb in plant material, using HPLC/UV method

Recoveries from untreated control sample fortified at levels of 0.005 -1.0 mg/kg usually ranged from 65-80% , averaging 75% for Methyl EthyleneBiDitioCarbamate.

The limit of detection was LOD($mg.L^{-1}$) = 0.066 for

The limit of determination was LOQ($mg.L^{-1}$) = 0.22

6.2.1. Zineb in plant material, using F-AAS method

Recoveries from untreated control sample fortified at levels of 0.005 -1.0 mg/kg usually ranged from 72-79% , averaging 75%

The limit of detection was LOD(mg/kg) = 0.011

The limit of determination was LOQ($mg.L^{-1}$) = 0.038

6.3. Calibration of residues

The residue R, expressed in mg/kg for endosulphan, methamidophos, deltamethrin, Cyhalothrin or cyfluthrin, is calculated from the following equation:

$$R = \frac{W_A.V_{Ex}.V_{End}}{V_{RI}.V_i.G}(mg/kg)$$

Where:

G: Sample weight (in g)

V_{end}: Terminal volume sample solution from 5.3 (in ml)

V_i: Portion of volume V_{end} injected into gas chromatograph

W_{St}: Amount of compound injected with standard solution

H_A: Peak height obtained from V_i

$H_{St:}$ Peak height obtained from W_{St}

REFERENCES

[1]. Manual of Pesticide Residue Analysis. Volume I, II. DFG Deutsche Fforchungs Gemeinschaft, 1997.

[2]. AOAC Official Method 985.22. Organochlorine and Organophosphorous Pesticide Residues. Gas chromatographic Method. 1996.

[3]. H.A. MOYE, Opportunities for pesticide residue analytical method development: the potential for aqueous extraction of pesticide residues from fruits and vegestables. Conference proceeding series, Eight International Congress of pesticide chemistry, American Chemistry Sosiety, Washington DC, 193-203,1995.

Part II:

DETERMINATION OF PESTICIDE RESIDUES* IN GREEN VEGETABLES COLLECTED FROM DUCTRONG, DONDUONG AND DALAT BY USING GC/ECD/FTD, HPLC/UV AND F-AAS

Sampling: Green vegtables such as Spinach, Cabbage, Pimento, Japanese Bean, Japanese Pumpkin, Tomato, Potato, Sweet Potato were collected from the vegestable farms of Dalat City, Duc Trong and Don Duong District during 2 years 2006-2007.

Pesticide residues analysis: Endosuphan, Methamidofos, Maneb, Zineb, Delthamethrin, Cyfluthrin, Cyhalothrin.

Method: GC/ECD/FTD, HPLC/UV AND F-AAS

Residue analytical data

Table 1: Pesticide residue in green vegetables in Don Duong province. 2006-2007

Pesticide residues in (mg/kg,fresh±15-20%)

SAMPLES	CODE NUMBER	ENDO-SULPHAN	METHA-MIDOFOS	MANEB	ZINEB	CYHA-LOTHRIN	CYFLU-THRIN	DELTA-METHRIN
Sweet potato	07101SP	ND	ND	ND	ND	ND	ND	ND
	07102SP	ND	ND	ND	ND	ND	ND	0.02±0.003
	07103SP	ND	ND	ND	ND	ND	ND	ND
	07104SP	ND	ND	ND	ND	ND	ND	ND
Potato	07101PO	ND	ND	ND	ND	ND	ND	ND
	07102PO	ND	ND	1.0±0.15	ND	ND	ND	0.03±0.005
	07103PO	0.02±0.003	ND	ND	0.2±0.03	ND	ND	ND
	07104PO	ND	ND	0.6±0.09	ND	ND	ND	0.06±0.009
Japanese Pumpkin	07101PK	ND	ND	ND	0.2±0.03	0.01±0.002	ND	0.07±0.01
	07102PK	ND	0.01±0.002	1.0±0.15	ND	ND	0.01±0.002	0.1±0.015
Japanese bean	07101SB	ND	ND	1.0±0.15	0.5±0.075	ND	ND	ND
	07102SB	ND	0.02±0.003	1.3±0.2	ND	0.02±0.003	ND	0.5±0.08
	07103SB	0.05±0.008	0.01±0.002	0.72±0.10	ND	ND	ND	ND
	07104SB	0.1±0.015	0.1±0.015	1.0±0.15	0.62±0.09	0.05±0.008	ND	ND
Spinach	07101SN	ND	ND	ND	ND	ND	ND	ND
	07102SN	ND	ND	ND	ND	ND	0.02±0.003	ND
	07103SN	ND	ND	ND	ND	0.01±0.002	ND	0.02±0.003
	07104SN	ND	ND	ND	ND	ND	ND	ND
Water Cress	07101SW	ND	ND	ND	ND	ND	ND	ND
	07102SW	ND	ND	ND	ND	ND	ND	0.01±0.002
	07103SW	ND	0.02±0.003	ND	ND	ND	ND	ND
Cabbage	07101CB	ND	ND	ND	ND	ND	ND	ND
	07102CB	0.01±0.002	0.01±0.002	0.1±0.015	0.1±0.015	ND	ND	0.07±0.01
	07103CB	ND	ND	0.2±0.03	ND	0.02±0.003	ND	ND
Chingensai	07101CC	ND	ND	ND	ND	ND	ND	ND
	07102CC	ND	ND	ND	ND	ND	0.02±0.003	ND
	07103CC	ND	0.01±0.002	0.05±0.008	0.1±0.015	0.01±0.002	ND	ND
Tomato	07101TO	0.1±0.015	ND	ND	ND	ND	ND	ND
	07102TO	ND	0.02±0.003	0.3±0.045	ND	0.01±0.002	ND	0.04±0.006
	07103TO	0.2±0.03	ND	ND	0.6±0.09	0.01	0.01±0.002	0.07±0.011
Pimento	07101PP	ND	ND	ND	1.0±0.15	ND	ND	ND
	07102PP	ND	0.01±0.002	ND	ND	ND	ND	ND
	07103PP	0.1±0.015	ND	1.3±0.195	ND	ND	0.02±0.003	0.1±0.015
	07104PP	ND	0.02±0.003	ND	ND	0.02±0.003	ND	ND

Table 2: Pesticide residue in green vegetables in Duc Trong province. 2006-2007

Pesticide residues in (mg/kg,fresh ± 15-20%)

SAMPLES	CODE NUMBER	ENDO-SULPHAN	METHA-MIDOFOS	MANEB	ZINEB	CYHA-LOTHRIN	CYFLU-THRIN	DELTA-METHRIN
Sweet potato	06031SP	0.02±0.003	ND	ND	ND	ND	ND	ND
	06032SP	ND	ND	ND	ND	0.02±0.003	ND	ND
	06033SP	ND	ND	ND	ND	ND	0.01±0.002	ND
	06034SP	ND	ND	ND	ND	ND	ND	ND

Potato	06031PO	ND	ND	0.63±0.09	0.95±0.13	0.01±0.002	0.02±0.003	0.10±0.015
	06032PO	ND	ND	ND	ND	0.02±0.003	ND	ND
	06033PO	0.01±0.002	ND	1.20±0.18	ND	0.02±0.003	0.01±0.002	0.05±0.008
	06034PO	ND	ND	0.87±0.13	1.07±0.16	ND	0.01±0.002	ND
Japanese Pumpkin	06031PK	ND	ND	ND	ND	0.08±0.012	0.02±0.003	0.1±0.015
	06032PK	ND	ND	ND	ND	ND	ND	0.2±0.03
	06033PK	0.10±0.015	ND	0.7±0.1	0.2±0.03	0.05±0.008	ND	ND
	06034PK	ND	ND	ND	0.4±0.06	0.1±0.015	ND	ND
Japanese bean	06031SB	ND	ND	0.7±0.11	0.5±0.075	0.01±0.001	0.01±0.001	0.05±0.008
	06032SB	0.10±0.015	ND	1.6±0.24	ND	0.02±0.003	0.02±0.0031	0.1±0.015
	06033SB	0.06±0.009	ND	0.5±0.075	0.7±0.10	0.01±0.001	0.01±0.001	0.03±0.005
	06034SB	ND	ND	1.0±0.15	ND	ND	0.03±0.001	0.01±0.002
Spinach	06031SN	ND	ND	ND	ND	0.02±0.003	ND	0.02±0.003
	06032SN	ND	ND	ND	ND	ND	ND	ND
	06033SN	0.01±0.002	ND	0.03±0.005	ND	0.01±0.002	ND	0.01±0.002
	06034SN	ND	ND	ND	ND	0.01±0.002	ND	ND
Water Cress	06031SW	0.02±0.003	ND	ND	ND	ND	ND	0.03±0.005
	06032SW	ND	ND	0.05±0.008	0.04±0.006	ND	ND	ND
	06033SW	ND	ND	ND	ND	ND	ND	0.1±0.02
Cabbage	06031CB	ND	ND	ND	ND	0.01±0.002	ND	0.10±0.02
	06032CB	ND	ND	ND	ND	ND	0.01±0.002	ND
	06033CB	0.11±0.015	ND	0.5±0.075	0.5±0.075	ND	ND	0.05±0.008
Chingensai	06031CC	ND	ND	ND	ND	0.01±0.002	ND	0.05±0.008
	06032CC	ND	ND	ND	ND	ND	ND	ND
	06033CC	0.02±0.003	ND	ND	ND	0.01±0.002	ND	ND
Tomato	06031TO	0.02±0.003	ND	1.07±0.165	0.9±0.135	0.02±0.003	ND	0.05±0.01
	06032TO	ND	ND	2.00±0.3	1.00±0.15	ND	ND	0.05±0.01
	06033TO	0.06±0.009	ND	ND	ND	0.04±0.006	ND	0.07±0.006
Pimento	06031PP	0.14±0.02	ND	ND	ND	ND	ND	ND
	06032PP	ND	ND	ND	0.5±0.075	ND	ND	ND
	06033PP	ND	ND	0.4±0.06	ND	0.02±0.003	0.02±0.003	0.08±0.012
	06034PP	ND	ND	1.30±0.19	ND	ND	ND	0.06±0.009

Table 3: Pesticide residue in green vegetables in Dalat city. 2006-2007

Pesticide residues in (mg/kg,fresh±15-20%)

SAMPLES	CODE NUMBER	ENDO-SULPHAN	METHA-MIDOFOS	MANEB	ZINEB	CYHA-LOTHRIN	CYFLU-THRIN	DELTA-METHRIN
Sweet potato	07101SP	ND	ND	ND	ND	ND	ND	ND
	07102SP	ND	ND	ND	ND	ND	ND	ND
	07103SP	ND	ND	ND	ND	ND	ND	ND
	07104SP	ND	ND	ND	ND	ND	ND	ND
Potato	07101PO	ND	ND	0.7±0.10	ND	ND	ND	ND
	07102PO	ND	ND	ND	0.12±0.015	ND	ND	ND
	07103PO	ND	ND	0.45±0.06	ND	ND	ND	ND
	07104PO	ND	ND	ND	0.45±0.06	ND	ND	0.04±0.006
Japanese Pumpkin	07101PK	ND	ND	ND	ND	ND	ND	0.1±0.0150.
	07102PK	0.01±0.002	ND	0.43±0.06	ND	ND	0.02±0.003	07±0.011
Japanese bean	07101SB	ND	ND	ND	0.4±0.06	0.02±0.003	ND	0.2
	07102SB	ND	ND	2.3±0.3	ND	ND	ND	0.03±0.005
	07103SB	0.02±0.003	ND	ND	ND	ND	0.02±0.003	ND
	07104SB	ND	ND	1.0±0.15	ND	ND	ND	0.1
Spinach	07101SN	ND	ND	ND	ND	0.04±0.006	ND	ND
	07102SN	ND	ND	ND	ND	ND	ND	0.01±0.002
	07103SN	ND	ND	ND	ND	ND	ND	ND
	07104SN	0.01±0.002	ND	ND	ND	ND	ND	ND
Water Cress	07101SW	ND	ND	0.03±0.005	ND	0.02±0.003	ND	0.01±0.002
	07102SW	0.01±0.002	ND	ND	ND	ND	ND	ND

Cabbage	07101CB 07102CB	ND ND	ND ND	ND ND	ND 0.45±0.06	ND ND	ND ND	ND 0.03±0.005
Chingensai	07101CC 07102CC 07103CC	ND ND ND	ND ND ND	ND ND ND	ND ND ND	ND 0.02±0.003 ND	0.02±0.003 ND 0.02±0.003	ND ND ND
Tomato	07101TO 07102TO 07103TO	ND ND 0.02±0.003	ND ND ND	0.52±0.075 ND 1.23±0.18	ND ND ND	ND ND ND	ND ND ND	ND 0.06±0.009 ND
Pimento	07101PP 07102PP 07103PP 07104PP	ND 0.01±0.002 ND ND	ND ND ND ND	0.06±0.009 0.23±0.03 ND 0.4±0.06	0.5±0.07 ND ND 0.15±0.02	0.02±0.003 ND ND ND	ND 0.02±0.003 ND ND	ND 0.05±0.008 ND 0.08±0.012

Pesticide residues: Endosuphan, Methamidofos, Maneb, Zineb, Delthamethrin, Cyfluthrin, Cyhalothrin in Spinach, Cabbage, Pimento, Japanese Bean, Japanese Pumpkin, Tomato, Potato, Sweet Potato.

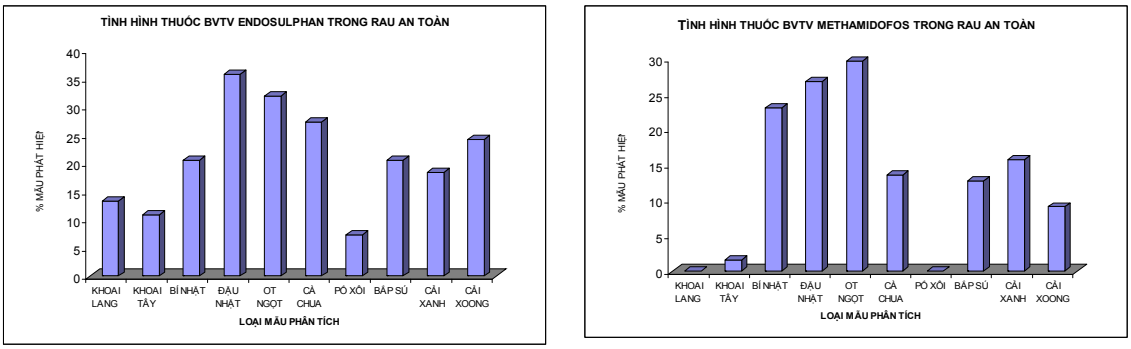

Fig. 1: Endosulphan and Methamidofos in green vegetables

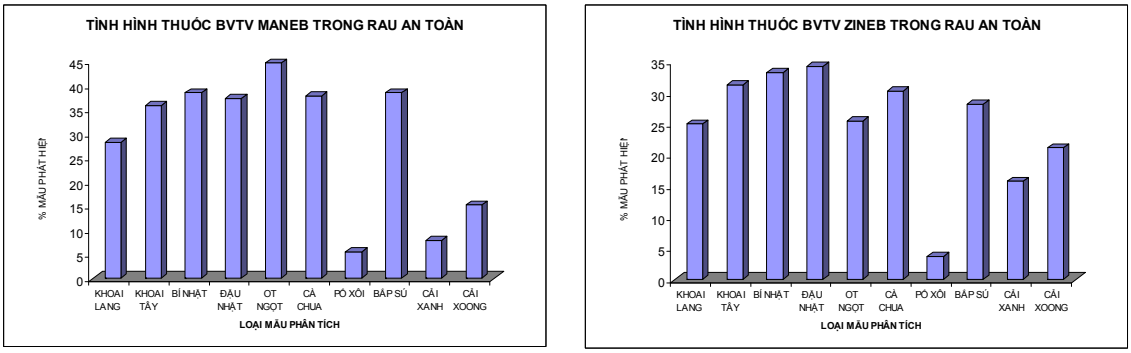

Fig. 2: Maneb and Zineb green vegetables

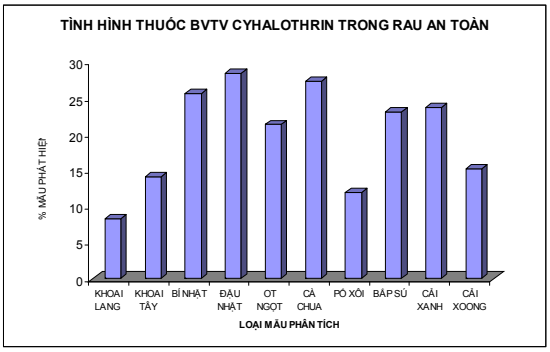

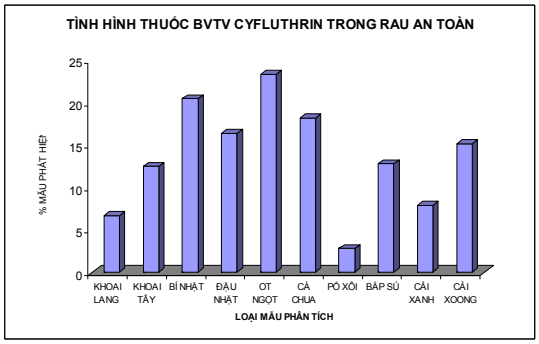

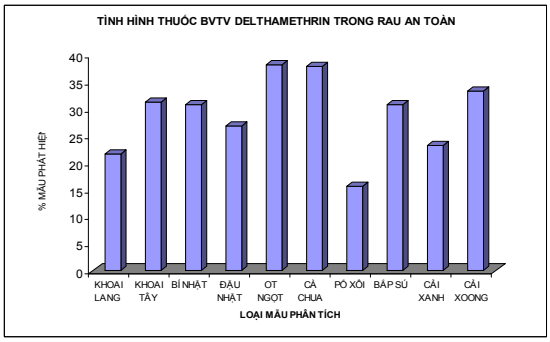

Fig. 3: Deltamethrin, Cyhalothrin and Cyfluthrin in green vegatables

CONCLUSIONS

Gas chromatography using an Electron Capture Detector or Flame Thermal Detector has become a valuable method for determination of the organochlorine pesticides-Endosuphan, organophosphorus pesticides-Methamidofos and pyrethroid groups as Deltamethrin, Cyhalothrin, and Cyfluthrin in green vegetable samples. Limit of detection and limit of quantitation are determinated in range of 5-10ng and 0.01-0.05ppm. Recovery is in range 80-98%. Precision and accuracy can be kept within 10-15%.

HPLC/UV and F-AAS method are applied for analysis of Maneb and Zineb fungicide.

The pesticide residues as Endosuphan, Methamidofos, Maneb, Zineb, Delthamethrin, Cyfluthrin, Cyhalothrin in Spinach, Cabbage, Pimento, Japanese Bean, Japanese Pumpkin, Tomato, Potato, Sweet Potato presented in the tables 1, 2, 3 showed that the residues in vegetabes are in range of limit (< MRL_s). Pesticide residue concentrations in potatos, sweet potatos are in level of permissible limit (28%), in the level of a maximum residude limit (2-6%). Pesticide residue concentrations in Spinach, Cabbage, Pimento, Tomato are in level of permissible limit (17-20%), in the level of a maximum residude limit (>15%), in Japanese Bean, Japanese Pumpkin, Pimento, Tomato are in level of permissible limit (20-35%), in the level of a maximum residude limit (>18%). Methamidofos and Endosulphan are still used in regions of Duc Trong and Don Duong, and not found in Dalat.

The results of extensive residue trials on a number of vegetable and argricultural crops are available. The analytical data confirm pesticide residues in relatively low persistence.

Gas-chromatographic methods making use of flame thermionic detectors are avilable for the determination of methamidofos in various crops. They are combined with apropriate extraction and clean-up procedures and are likely to be suitable for regulatory purposes.

REFERENCES

[1]. Maneb/Zineb(organicmethod # 107)www.osha.gov/dts/sltc/methods/organic/org

[2]. Manual of Pesticide Residue Analysis. Volume I, II. DFG Deutsche Fforchungs Gemeinschaft, 1997.

[3]. AOAC Official Method 985.22. Organochlorine and Organophosphorous Pesticide Residues. Gas chromatographic Method. 1996.

[4]. H.A. MOYE, Opportunities for pesticide residue analytical method development: the potential for aqueous extraction of pesticide residues from fruits and vegestables. Conference proceeding series, Eight International Congress of pesticide chemistry, American Chemistry Sosiety, Washington DC, 193-203,1995.

[5]. Methamidofos (pesticide residue in food: 1976 evaluatins), page 3-29

[6]. Evaluations of some pesticide residues in food The monograph, Joint Meeting of the FAO Working Party of Experts and the WHO Expert Committee on Pesticide Residues, Rome, December 4 -11, 1967.

[7]. Cassella, R.J.; Salim, V.A.; Garrigues, S. ; Santelli, R.E.; Guardia, M., Flow injection/ Atomic absorption spectrometric determination of zineb in commercial formualations of pesticide based on slurry sampling, *Analytical Sciences* 2002, 18, 1253 1256.

[8]. Canadian Food Inspection Agency, SPR-002-V2.4, Determination of EBDC in fruits and vegetables, 2003, 11, 7.

[9]. Mehta, S.K.; Makik, A.K.; Singh, B.; Rao, A.L.J., Development of new adsorbent chitin for column preconcentration and spectrophotometric trace determination of ziram and zineb in synthetic, commercial samples and food stuffs, *Talanta* 2005, 67, 725 - 729.

PAPERS PUBLISHED IN RELATION TO THE PROJECT

1. Lê Tất Mua và cộng sự. Xác định lamdacyhalothrin trong rau quả an toàn bằng phương pháp GC/ECD. Tạp chí Hoá Sinh, T9, 2008.

STUDY ON THE APPLICATION OF NUTRIENT IMMOBILIZED HYDROGEL AS A SUBSTRATE FOR HYDROPONICS CULTURE

Vo Thi Thu Ha [(1)]***, Le Quang Luan*** [(1)]***, Nguyen Thi Nu*** [(1)]***, Nguyen Thi Vang*** [(1)]
Phan Dinh Thai Son [(1)]***, Nguyen Quang Khanh*** [(2)]

[(1)] Center for Nuclear Technique, VAEC, Vietnam.

[(2)] LangBiang Farm Ltd., Dalat City, Vietnam.

I. INTRODUCTION

The agricultural products of Vietnam have some difficulties for exporting, because of some shortcomings in production still remain. Hydroponics technique has been studied in many countries on over the world. This technique also has been widely used for producing clean agro-products and some advantages such as induction of high yield and high quality products in a small area and without dependence of the soil; saving of materials and labour; and high profit. In addition, using hydroponics techniques for production of ago-products will give many significant benefits for the heath of both producer and user, high economical effect, protection of environment. Even so, the substrates used for hydroponics techniques are mainly natural substrates such as rice husk, sand, coir, etc; or synthetic materials such as vermiculite, synthetic foam, etc, these materials are very difficult for degradation [1-4]. On the order hand, the study and preparation of hydrogels by radiation techniques have been carried out in many countries. Vietnam is an active country for research and application of these materials [5-11]. These hydrogels were mainly applied in medicine, pharmaceutical industry, etc, and a small number of them were used in agriculture field. Since the research and application of hydrogels for hydroponics is very few, the aim this study is preparation of a nutrient hydrogel from CMC by irradiation for hydroponics culture.

II. EXPERIMENT

1. Material: The polymers used in this study are carboxylmethylcellulose (CMC) and polyacrylamide (PAM). The tested vegetables are Chinese mustard (*Brassica juncea* Var rugosa) and Lettuce TN 591 (*Lactuca Sativa*).

2. Preparation of hydrogels by radiation technique: the nutrients were dissolved in water before adding CMC and/or PAM. The mixture was kept overnight for swelling before irradiation by γ-rays from a ^{60}Co source.

3. Characterization of hydrogels:

Gel fraction: The gel fraction was determined by the following equation:

Gel fraction *(%) = 100 x M_2/M_1*

Where as: M_1 is the initial weight of sample before irradiation; M_1 is the weight of gelling part.

Swelling: The gel fraction was determined by the following equation: ***Swelling = $(M_{gel} - M_1) / M_1$***

Where as: M_{gel} is the weight of swollen gel; M_1 is dried weight of gel.

4. Determination of the growth and development of plants grown on hydrogels:

Germination and seedling test: Put 30g swollen hydrogel in a plastic pot, then place the seed on the surface of the gel. The germination rate was recorded after 4 days and the growth of seedling was determined after 2 weeks.

Hydroponics cultural test: The 2 weeks old seedling plants were grew in a plastic pot containing 50g swollen hydrogel then applied in hydroponics system for culture.

5. The collapse of hydrogels:

To determine the collapse of hydrogel, 50g swollen gel was put into a pot and then applied in a hydroponics system, then the remaining gel was determined every week.

III. RESULTS AND DISCUSSIONS

1. Preparation and characterization of hydrogel: After selecting the suitable nutrient component, it was mixed with polymers and then irradiated by Gamma Co-60. The prepared samples were used for characterization and evaluation the effect on plant growth. On the first experiment, the results showed that both CMC and PAM without nutrient could be formed gel by irradiation. But for the sample of CMC supplementation with nutrients, the formation hydrogel was quite low (less than 10%), event with high doses, while the mixture of PAM and nutrients could be formed gel easily by irradiation. Therefore, we select the mixture of CMC and PAM for preparing nutrient immobilized hydrogels.

1.1. Gel fraction of CMC and PAM by gamma irradiation: The results from several previous studies showed that CMC hydrogels prepared at high irradiated doses (70-100kGy) had a high strong but low swelling. While the hydrogels prepared from PAM at lower irradiated doses showed a high strong and swelling. Based on the above information, we prepared hydrogel from CMC and PAM in order to induce a suitable material for plants.

The results from Fig. 1 showed that the gel fraction obtained from PAM was higher compared to that of CMC or the CMC combined with PAM at the concentration of 20%. In particularly, the gel fraction obtained from PAM solutions of 20% with the irradiation doses from 10 - 30kGy were from 74.3 to 96.2%, respectively. While, the gel fraction of sample with only CMC (20%) was very low (from 34.1 – 67.2% with the irradiated doses at 10 -30kGy, respectively). For the sample with CMC (20%) and PAM (20%), the gel fraction were formed from 58.2 – 91.4% at the dose from 1 - 30kGy, respectively, and it was higher than that of sample with 20% CMC and 10% PAM (49.2 - 76.2%) at the same range of irradiated dose.

In addition to, the results from Fig. 1 also showed that compared to the sample of 20% PAM and without nutrients, the gel content formed from the sample contained PAM 20% supplementation with nutrients irradiated at the does of 10 - 30kGy was lower from 14.5 to 23.5%, respectively than that of the sample with only PAM. The same results were also obtained with the sample consist of PAM and CMC with and without addition of nutrient. In case of the sample contained CMC 20%, PAM 20% and nutrient, the supplementation of 1% alginate increased the gel fraction in 10%.

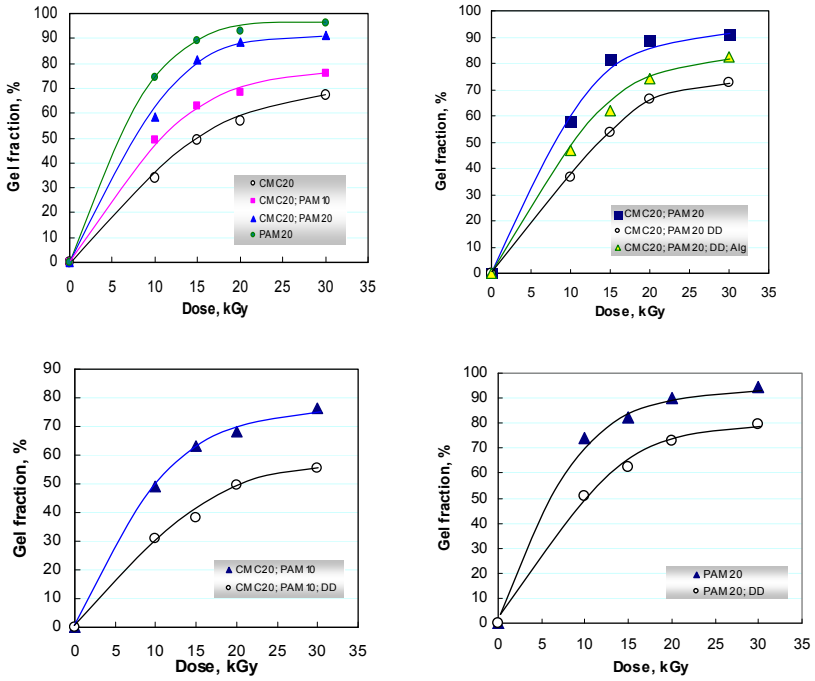

Fig. 1: The effect of irradiation dose on gel fraction of CMC, PAM and CMC combined with PAM

1.2. The swelling of hydrogel prepared from CMC and PAM by gamma irradiation: The results in Fig. 2 showed that the swelling of hydrogel prepared from 20% CMC, 20% PAM and 20% CMC combined with 20% PAM with and without supplementation of nutrients as follow:

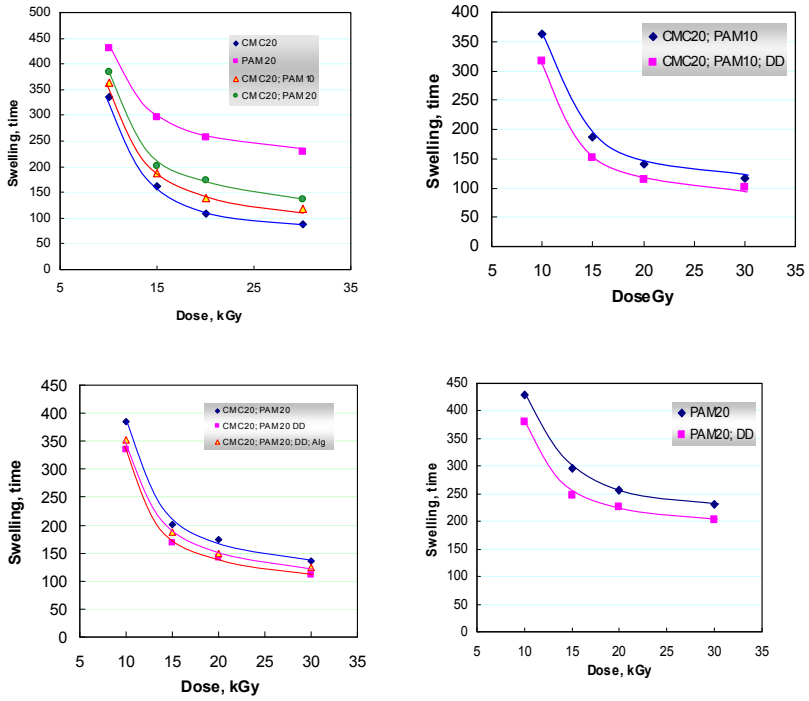

Fig. 2: The swelling of hydrogel

The swelling of all hydrogels was decreased with the increase of the irradiation dose. The reason may due to the increase of gel fraction with the increase of the irradiation dose. The swelling degree was dramatically reduced at dose range from 10 - 15kGy and then it was gradually reduced in the range of 20 - 30kGy. In particularly, the swelling of the hydrogel prepared from mixture of 20% PAM and nutrients irradiated at 15kGy was reduced 133 -134 compared to that of the same hydrogel but irradiated at 10kGy. In addition, the swelling of hydrogel prepared from PAM and CMC was higher than that of hydrogel prepared only from CMC. It was easy to see that the higher PAM content in irradiation mixture, the higher swelling of the hygrogel. On the other hand, the addition of nutrients in the mixture reduced the swelling of the hydrogel more than 20 times compared to that of the non-addition one, while the supplementation of alginate enhanced the swelling of the hydrogel about 17.4.

2. The growth and development of vegetables on hydrogel: The germination ratio after 4 days germination and growth of seedling after 14 days were investigated at first in this experiment. The results in Fig. 3 showed that the germination ratio of seeds on all hydrogels was higher than that of on coconut fine and unirradiated sample. The beds A9 (20%CMC + 20% PAM + nutrients + alginate) and A10 (20%CMC + 20% PAM + Nutrients + chitosan) showed good results compared to the other ones and the sample supplementation with alginate displayed the best results among tested samples. The results in Fig. 4 also showed the samples A7 (20%CMC + 20% PAM + nutrients), A9 and A10 good affected on the increase of shoot height, root length and fresh biomass of 14 days seedlings, especially a higher effect was obtained with samples irradiated from 10 - 15kGy. In addition the samples supplemented with alginate and chitosan also showed a positive effect on the growth of seedling and the effect of alginate supplemented sample was the highest.

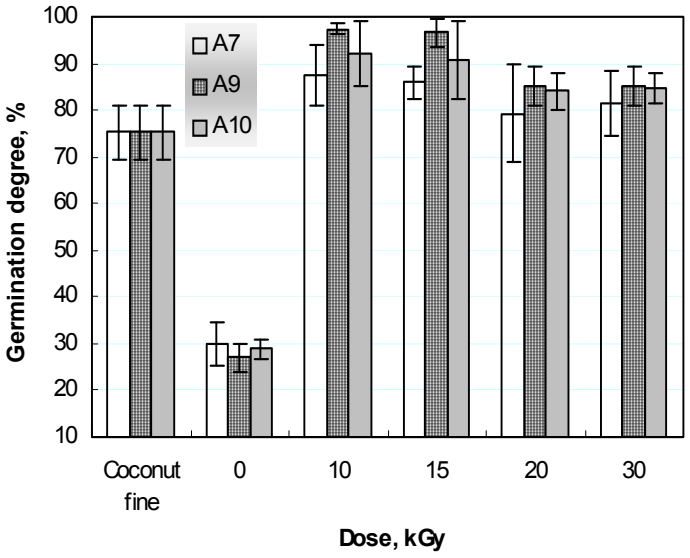

Fig. 3: *The germination of Chinese mustard on hydrogel after 4 days*

Thus, the A9 samples prepared at the doses of 10 and 15kGy showed an optimum effect on the germination ratio and growth of 14 days seedling, and it was selected to apply for hydroponics cultivation. Since the sample irradiated at 10kGy had a very high swelling, but a low gel fraction resulted to a low strong gel, and this was very easy to be broken and not easy for application as a substrate in hydroponics culture.

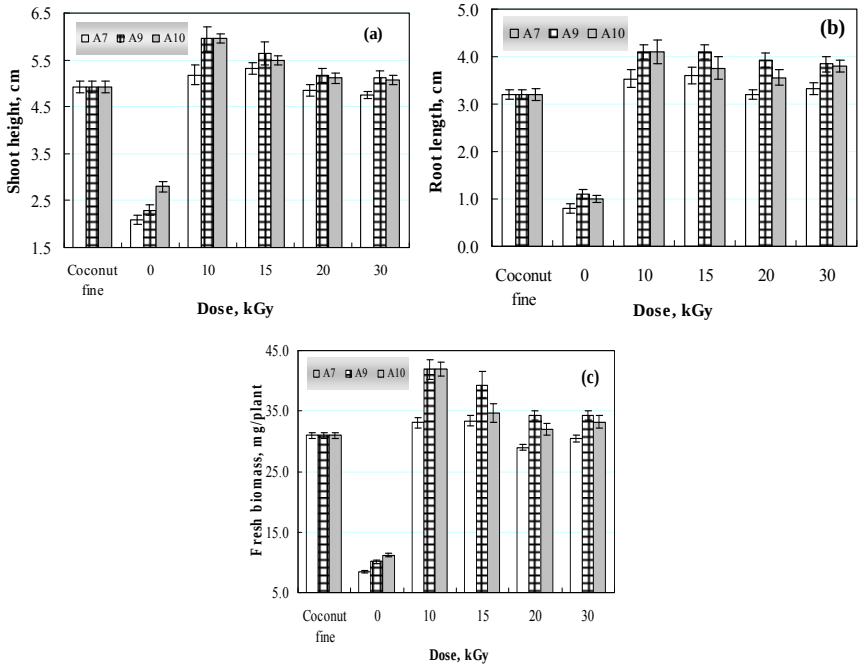

Fig. 4: The growth of seedling after germination 14 days on hydrogel;
(a): Shoot height; (b): Root length; (c): Fresh biomass

3. The growth and development of vegetables on hydrogel in hydroponics cultivation: In this experiment, the A7, A9 and A10 hydrogels were applied as substrates for growing of lettuce and Chinese mustard in hydroponics.

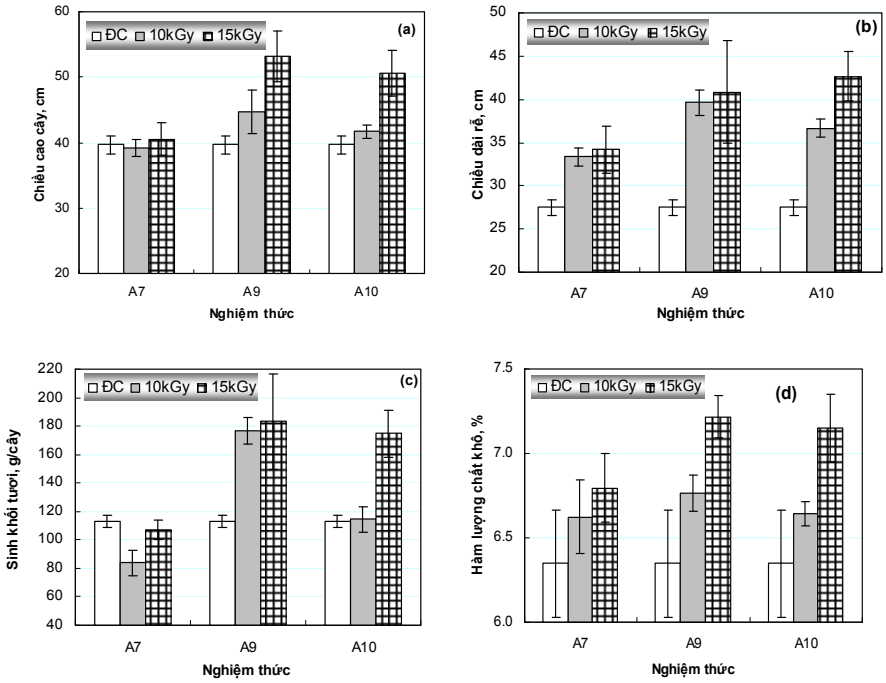

Fig. 5: Growth of Chinese mustard in hydroponics system using hydrogels,
(a): Shoot height; (b): Root length; (c): Fresh biomass; (d): Dried matter content

The results in Fig. 5 & 6 showed that the growth parameters such as shoot height, root length and fresh biomass of lettuce and Chinese mustard grown on hydrogels were much better than that of the mentioned vegetables planted on coconut fine. The interesting point in this experiment is the growth of plants grown on hydrogel irradiated at 15kGy was better than that of vegetable grown on hydrogel irradiated at 10kGy. In addition to, the dried matter content of both lettuce and Chinese mustard planted on hydrogel irradiated at 15kGy was also higher than that of vegetable grown on hydrogel irradiated 10kGy and on coconut fine.

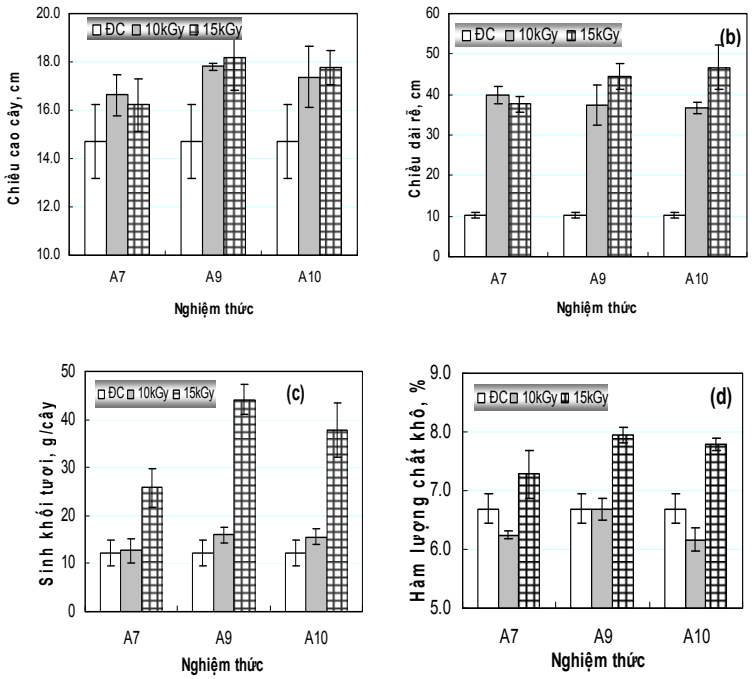

Fig. 6: Growth of lettuce in hydroponics culture using hydrogel
(a): Shoot height; (b): Root length; (c): Fresh biomass; (d): Dried matter content

The results from Fig. 7 also showed that the vegetables planted on hydrogel grew better than that of vegetables planted on coconut fine. In particularly, compared to the plants growth on coconut fine, the root length, shoot height and fresh biomass lettuce grown on hydrogel were increased 130%, 22% and 290%, respectively, while the root length, shoot height and fresh biomass Chinese mustard were increased 88%, 108% and 83%, respectively.

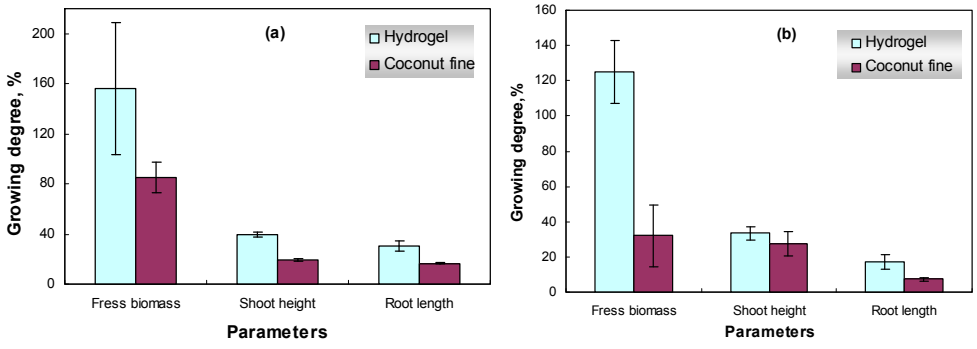

Fig. 7: The growth of Chinese mustard and lettuce; (a): Chinese mustard and (b): lettuce

4. The collapse of hydrogel: The results from Fig. 8 showed that the collapse of hydrogels prepared from the component of 20% CMC, 20% PAM and nutrients supplemented with alginate and without alginate irradiated at 15kGy was almost the same during 5 weeks applying in hydroponics culture. The gel was collapsed about 84% in first 3 weeks, then in the next 2 weeks, the collapse rate was lower and finally, the gel was completely collapsed after 5 weeks application in hydroponics.

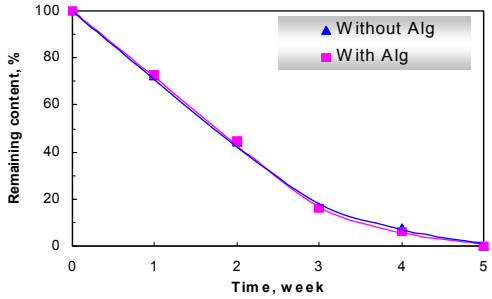

Fig. 8: *The collapse of hydrogel in hydroponics cultivation*

IV. CONCLUSIONS

1. The hydrogel with different swelling prepared from CMC combined with PAM, nutrient and alginate by gamma-Co-60 irradiation.

2. The hydrogel prepared by irradiation of the component with 20% CMC, 20% PAM, 1% alginate and nutrients at 15kGy was suitable for the growth and development of plants. In particularly, the hydrogel showed a positive effect on germination ratio of seeds, the growth of 14 days seedling and the growth of lettuce and Chinese mustard in hydroponics cultivation.

3. The hydrogel was completely collapsed after 5 weeks use in a hydroponics culture.

4. The hydrogel showed a promising for application in hydroponics culture, a new technique for production of high yield and high quality vegetables.

REFERENCES

[1]. Department of Agriculture, Ministry of Agriculture, Hydroponics, USA, 2000.

[2]. John Mason, Commercial hydroponics, Kangaro Press, Australia, 2005.

[3]. Peter Code, Hydroponics as an agricultural production system, Hassall & Associates Pty Ltd., 2001.

[4]. Howard M. Resh, Hydroponics food production: *A definitive guidebook of soilless food-growing method*, Woodbridge Press Publishing Company, USA, 2002.

[5]. Tran Thi Thuy, et al., *Proceeding of The 6th National Conference on Nuclear Science and Technology*, Dalat, 2005.

[6]. Y. Fumio Yoshii, et al., *Nuclear Instruments and Methods in physics Research B: Beam Interation with Materials and Atoms*, VI, p. 208 – 302, 2003.

[7]. Nguyen Quoc Hien, et al., *J. Chemistry (in Vietnamese)*, 34, tr.19 – 22, 1999.

[8]. A. K. Bajpai, et al., *Carbohydrate Polymers*, 53, p. 271 – 279, 2003.

[9]. Pham Thi Le Ha, et al., *Proceeding of The 6th National Conference on Nuclear Science and Technology*, p. 213 – 219, Dalat, 2005.

[10]. R. A. Wach, et al., *Radiat. Phys. And Chem.*, 54, 253-270, 2003.

[11]. R. A. Wach, et al., *Macromol. Mater. Eng.*, 287, 285-295, 2002.

STUDY ON PROCEDURE FOR DETERMINATION OF Cr, As, Se, Cd, Hg, Pb IN SOME KINDS OF HERB PRODUCTS SUCH AS: KIND OF FUNGUS, PHILAMIN... BY ICP-MS"

Pham Ngoc Khai, Do Van Thuan, Nguyen Thi Kim Dung and Nguyen Hong Minh

Institute for Technology of Radioactive and Rare Elements, VAEC, Vietnam.

ABSTRACT: The determination of Cr, As, Se, Cd, Hg, Pb in herb products such as: kind of fungus, philamin, etc by ICP-MS has been studied. The effects of the parameters of ICP-MS instrument, concentration of nitric acid and high concentration of some elements on the determination of Cr, As, Se, Cd, Hg, Pb by ICP-MS has been concerned. The study and choice the suitable internal standard for the accurate determination of Hg has been sold. The suitable parameters of the microwave, composition and content of the acid mixture for the complete decomposition of the sample have been studied. The recommended procedure has been applied to the determination of Cr, As, Se, Cd, Hg, Pb in the standard samples and real samples. The error of the results is acceptable.

Key words: Herb products, heavy metal, ICP-MS, digression, Microwave.

Introduction

The determination of heavy metals in herb products is interested in many countries over the world such as: China, India, Turkey, Poland, Germany, Australia, etc. All medical products for human and animal must meet regulatory guidelines for quality, safety and efficacy. For example, the European Union (EU) recently established a Traditional Herbal Medicinal Products Directive. As a result, manufacturers who export herbal medicines to the EU must ensure that product quality complies with requirements of the European Pharmacopoeia. In Vietnam this is problem being not much interested in, there are only some basic studies.

This work focused on finding technical parameters for procedure of the simultaneous determination of trace level of heavy metals in herb products by ICP-MS such as: the parameters of ICP-MS instrument, nitric acid concentration, time and microwave parameters for complete digression of sample, the use of internal standard for accurate determination of mercury. The results of the studies are the base to choose the suitable parameters for accurate determination of the elements above.

Result and discussion

An analytical procedure for determination of Cr, As, Se, Cd, Hg, Pb in some kinds of herb products has been established. In this report the following isotopes have been chosen for the measurement of the elements:

Elements	Isotopes	Elements	Isotopes
Cr	53	Cd	111
As	75	Hg	202
Se	82	Pb	208

This procedure is based on the result of the following studies:

1. Study to find the suitable parameters of the ICP-MS instrument for simultaneous determination of the elements in the real samples. The results are following:

Element	**Concentration** (ppb)	**RF Power**				
		1300W	1350W	1490W	**1550W**	1600W
Cr	4.0	9,669.60	9,391.61	8,687.75	**8,084.01**	7,660.40
As	0.35	1,403.47	1,467.92	1,532.38	**1,550.16**	1,611.30
Se	0.4	630.0403	667.8226	642.2621	**571.1463**	602.2588
Cd	0.4	1,211.22	1,310.13	1,524.61	**1,684.63**	1,666.85
Hg	0.35	1,402.36	1,741.32	2,498.16	**2,844.92**	**3,100.56**
Pb	20	304,482.80	357,521.40	466,023.10	**539,785**	566,751
		Sample depth				
		4.50mm	**5.00 mm**	**5.50 mm**	6.00mm	6.50mm
Cr	4.0	9,791.91	**10,212.33**	**10,184.49**	9,024.66	8,413.13
As	0.35	1,796.87	**1,799.10**	**1,731.30**	1,575.72	1,483.48
Se	0.4	860.0642	**776.725**	**754.4989**	686.7131	544.477
Cd	0.4	1,730.20	**1,772.43**	**1,837.99**	1,696.86	1,466.82
Hg	0.35	2,394.81	**2,500.39**	**2,612.63**	2,393.69	2,100.29
Pb	20	486,467.70	**526,974.00**	**542,696.90**	523,211	450,424.30
		Carrier gas				
		1.10l/ph	1.15 l/ph	**1.20 l/ph**	**1.22** l/ph	1.25 l/ph
Cr	4.0	3,001.61	5,491.41	**7,992.83**	**9,436.09**	10,517.00
As	0.35	1,324.57	1,401.25	**1,539.04**	**1,567.97**	1,599.06
Se	0.4	261.1251	465.5826	**621.1489**	**673.3764**	697.8251
Cd	0.4	1,027.86	1,416.80	**1,616.84**	**1,790.20**	1,653.51
Hg	0.35	1,497.94	2,409.25	**2,334.78**	**2,246.99**	2,033.61
Pb	20	290,568.20	473,614.50	**529,559.50**	**530,956.90**	457,075
		Prepump				
		0.02v/s	**0.05** v/s	**0.10** v/s	0.15 v/s	0.20 v/s
Cr	4.0	2,056.92	**5,459.19**	**9,436.09**	11,595.73	12,950.41
As	0.35	605.5958	**1,131.22**	**1,567.97**	1,785.82	1,873.55
Se	0.4	265.5692	**470.0272**	**673.3764**	771.1654	801.171
Cd	0.4	645.6024	**1,199.00**	**1,790.20**	1,793.54	1,759.09
Hg	0.35	1,870.23	**2,214.76**	**2,246.99**	2,106.95	1,873.57
Pb	20	219,537.60	**449,797.60**	**530,956.90**	534,944	477,966.00

The suitable parameters of the ICP-MS instrument for simultaneous determination of these elements in the real samples are following:

- RF Power: 1550W.
- Sample depth: 5,0-5,5 mm.
- Carrier gas: 1,15-1,22 l/ ph.
- Prepump: 0.05-0.1 v/s.

The influence of the concentration of nitric acid on the ICP-MS signals of Cr, As, Se, Cd, Hg, Pb

Element	Concentration (ppb)	Acid Concentration (%)						
		0.36	1.82	2	2.18	3.64	7.28	10.92
Cr	4.0	9126.977	8030.644	8009.481	8335.293	8197.411	6427.423	8308.608
As	0.35	2467.633	1949.12	1967.175	1980.238	1869.106	1449.033	1601.275
Se	0.40	524.4758	504.4763	438.9147	477.8076	401.1339	306.6829	323.3504
Cd	0.40	1567.94	1227.89	1244.554	1293.457	1106.76	803.3917	877.8457
Hg	0.35	1746.87	1480.159	1113.442	1164.556	1178.997	777.839	770.0664
Pb	20	411021.6	341242.4	342757.8	349646.5	317561.5	239616.1	288683

2. Study to use Tl, Bi, Pt, Au as an internal standard for accurate determination of mercury. The Results are following:

Acid concentration (%)	2	0.364	1.82	2.184	3.64	7.28	10.92
No internal Standard	0.353	0.911	0.644	0.412	0.519	0.105	0.065
Internal standard is Tl	0.418	0.731	0.621	0.669	0.651	0.110	0.073
Internal standard is Bi	0.291	2.651	0.328	0.512	0.507	0.043	0.019
Internal standard is Pt	0.35	0.348	0.342	0.382	0.347	0.224	0.206
Internal standard is Au	0.352	0.345	0.290	0.368	0.386	0.315	0.294

RF Power (W)	1300	1350	1490	1550	**1600**
No internal Standard	0.029	0.085	0.229	0.313	**0.350**
Internal standard is Tl	0.240	0.247	0.309	0.316	0.312
Internal standard is Bi	0.218	0.232	0.346	0.292	0.291
Internal standard is Pt	0.362	0.356	0.305	0.322	0.311
Internal standard is Au	0.346	0.314	0.355	0.307	0.305

Carrier gas (l/min)	1.1	1.15	1.2	1.22	1.25	1.3
No internal Standard	0.023	0.228	0.203	0.157	0.144	<0.000
Internal standard is Tl	0.268	0.295	0.196	0.141	0.194	0.115
Internal standard is Bi	0.239	0.263	0.171	0.117	0.166	0.084
Internal standard is Pt	0.246	0.303	0.305	0.362	0.326	0.33
Internal standard is Au	0.339	0.353	0.336	0.351	0.301	0.283

Sample depth (mm)	4.50	5.00	6.00	6.50	7.00
No internal Standard	0.197	0.245	0.207	0.133	0.135
Internal standard is Tl	0.228	0.243	0.204	0.196	0.235
Internal standard is Bi	0.183	0.207	0.175	0.174	0.209
Internal standard is Pt	*0.313*	0.292	0.322	0.308	0.304
Internal standard is Au	*0.317*	0.337	0.319	0.294	0.312

Pripump (r/s)	0.02	0.05	0.1	0.15	0.2
No internal Standard	0.139	0.145	0.229	0.158	0.109
Internal standard is Tl	0.808	0.212	0.309	0.131	**0.127**
Internal standard is Bi	0.730	0.183	0.346	0.117	**0.114**
Internal standard is Pt	0.679	0.323	0.305	0.295	**0.253**
Internal standard is Au	0.900	0.385	0.355	0.320	**0.317**

3. Study to find the optimum parameters of the microwave for the complete digression of the sample. The Results are following:

Element	**Concentration ($x10^{-3}$ mg/l)**			
	2min.-2min.-2min.	3min.-2min.-2 min.	3min.-3min.-3 min.	3min.-4min.-4 min.
Cr	61.21	69.8	71.77	71.50
As	19.16	23.6	24.11	24.24
Se	0.638	0.809	0.817	0.820
Cd	1.736	2.148	2.217	2.207
Hg	0.4733	0.691	0.836	0.828
Pb	60.5	71.12	76.26	76.50

The Results of the sample digression by different mix solutions are following:

Element	Concentration ($x10^{-3}$ mg/l)		
	5ml HNO_3 + 2ml H_2O_2	3ml HNO_3 + 2ml H_2O_2	2ml HNO_3 + 2ml H_2O_2
Cr	70.34	71.77	69.47
As	25.27	24.11	21.39
Se	0.815	0.817	0.823
Cd	2.248	2.217	2.103
Hg	0.752	0.836	0.799
Pb	73.7	76.26	82.96

Element	Concentratiopn ($x10^{-3}$ mg/l)		
	1,5ml HNO_3 + 2ml H_2O_2	2ml HNO_3 + 1ml H_2O_2	2ml HNO_3 + 2ml H_2O_2 + 0,25ml HF
Cr	49.77	56.8	101.77
As	14.92	18.62	29.11
Se	0.623	0.691	0.917
Cd	1.816	1.795	2.917
Hg	0.644	0.621	1.536
Pb	58.07	61.12	76.26

4. Analysis the Standard Reference, descriptive statistics, evaluation error.

Analyze the standard reference 6 times, descriptive statistics the data, we have the results as in the following table:

Element	found content (µg/g)	Certified content (µg/g)	Relative Error (%)	Absolute Error (µg/g)
Cr	1.219±0.082	1.30	6.75	-0.0810
As	0.102 ± 0.011	0.1	10.64	0.0020
Se	0.119 ± 0.020	0.12	16.50	-0.0010
Cd	0.118 ± 0.021	0.12	17.28	-0.0020
Hg	0.0125 ± 0.0014	0.013	11.50	-0.0005
Pb	0.684 ± 0.018		2.62	

The recommended procedure has been applied to the determination of Cr, As, Se, Cd, Hg, Pb in some real samples.

Conclusion

The proposed matters are well fulfilled by this project. They are following:

- The suitable parameters of ICP-MS instrument for simultaneous determination of Cr, As, Se, Cd, Hg and Pb in herb products by ICP-MS have been studied and chosen.

- The optimum parameters of microwave and suitable content of mix acids for complete digression of the sample have been studied and chosen.

- The effects of nitric concentration and high content of some metals in real samples on the determination of Cr, As, Se, Cd, Hg and Pb in herb products by ICP-MS have been studied.

- The study on using some different metals as internal standard for accurate determination of mercury by ICP-MS has been carried out.

- Analysis the Standard Reference, descriptive statistics and evaluation the errors have been carried out. The calculations of relative Errors are from 3 to 20 percent.

- The recommended procedure has been applied for the determination of Cr, As, Se, Cd, Hg and Pb in some real Vietnamese herb products by ICP-MS.

STUDY ON APPLICATION OF MOLECULAR TECHNIQUES (RAPD-PCR AND RAMP-PCR) TO DETECT MUTATION IN RICE BREEDING

Hoang Thi My Linh, Phan D. T. Son, N. T.Vang
Nguyen T. T. Hien and Le Xuan Tham

Center for Nuclear Techniques, VAEC, Vietnam.

ABSTRACT: Project: "Study on application of molecular techniques (RAPD-PCR and RAMP-PCR) to detect mutation in rice breeding was carried out in 2007 with the purpose of consideration for using the two simple and inexpensive molecular techniques to estimate changes in DNA of rice mutant after gamma irradiation.

Three rice cultivars: Basmati370, Tam Thom (TT1), IR64 and three gamma irradiated mutants BDS, TDS and VND 95-20 respectively, were used. Suitable DNA extraction procedure was obtained. PCR optimization was conducted on three important factors including: amount of $MgCl_2$, DNA concentration and annealing temperature. 2.5mM of $MgCl_2$ for RAPD-PCR and 3.75mM for RAMP-PCR were found the best. 40 ng DNA provided a good amplification for RAMP-PCR; this figure was 50ng for RAPD-PCR. Annealing temperatures were determined at 36^0C for RAPD primer and at 553^0C for Microsatellite primer.

Final results showed that, both RAPD-PCR and RAMP-PCR could detect changes in DNA of rice mutants after gamma irradiation compared to their parents. Percentage of DNA changes determined by RAPD-PCR and RAMP-PCR on Basmati370 and its mutant BDS were 11.49% and 21.2% respectively; These on TT1 and TDS were 8.98% and 15.4%; and on IR64 and VND 95-20 were 3.45% and 4.95%.

1. INTRODUCTION

Spontaneous and induced mutations are the ultimate source of all existing genetic variation in plants, and are commonly used in plant breeding. However the occurrence of spontaneous mutations in nature is relatively rare and difficult to identify because they are mainly recessive, or are deleterious and quickly eliminated [1]. Therefore, increasing the rate of mutation (ie induced mutations) can provide additional sources of variant genotypes important in plant breeding.

The objectives of this study were to consider whether or not the two simple and inexpensive molecular techniques RAPD-PCR (Random Amplified Polymorphic DNA-Polymerase Chain Reaction) and RAMP-PCR (Random Amplified Microsatellite Polymorphism-Polymerase Chain Reaction) can be used to estimate changes in DNA of rice mutant after gamma irradiation in rice breeding.

RAPD-PCR amplifies random genomic DNA sequences using single, short arbitrary primers, and these can be effectively used as genetic markers. The RAPD technique therefore surveys (scans) numerous loci in the genome, which makes this method particularly attractive for analysis of genetic distance and similarity between closely related species [3,4]. A new method to compensate for some weakness in RAPD-PCR has been developed by using microsatellite primers, called RAMP (random amplified microsatellite polymorphisms)-PCR [5]. The method utilizes the ubiquitous and highly polymorphic nature of microsatellites. RAMP-PCR has been reported to

potentially detect and map co-dominant polymorphisms in DNA without cloning and sequencing [6].

2. MATERIALS AND METHODS

2.1. Plant material

Tissue culture leaves of varieties Tam Thom (TT1) and its mutants TDS, Basmati 370 - its mutants BDS, and IR 64 - its mutants VND 95-20 (induced by gamma irradiation) were used.

2.2. Extraction of genomic DNA

Genomic DNA from leaf of rice mutants, varieties Tam Thom (TT1) TDS, Basmati 370 BDS IR 64 and VND 95-20 were extracted using CTAB method [7,8].

2.3. PCR optimization

To obtain reproducible results from a PCR reaction, it was necessary to determine the optimum reaction conditions for each primer. In this project, different amounts of genomic DNA (10, 20, 25, 30, 40 and 50 ng) and three different concentrations of Mg^{2+} (2.5 mM, 3.75 mM and 4.0 mM were tested, along with the three different PCR program temperature profiles described below.

2.4. RAPD and RAMP amplification

RAPD-PCR was carried out on DNA samples using 50 RAPD primers from UBC set 1 (University of British Columbia) in an Eppendorf Master Cycler Gradient. Each reaction was performed in a final volume of 25µl containing 2.5 l of 10 X *Taq* Polymerase Reaction Buffer [67 mmol/L Tris-HCl - pH 8.8, 16.6 mmol/L $[NH_4]_2SO_4$, 0.45% (w/v) Triton X-100, 0.2 mg/ml gelatin] (Biotech), 0.6 mM betaine, 200 M of each of dATP, dTTP, dCTP, dGTP (mix dNTP- Biotech), varying amounts of genomic DNA (10, 25, 40, 50, and 70 ng), $MgCl_2$ (2.5 mM, 3.0 mM and 4.0 mM), and *Taq* DNA polymerase (1.0 and 1.5 units) (Biotech), with 12 nmol/mL of each primer. Three annealing temperatures 40^0C; 35^0C and 32^0C were tested with following profile: Denaturation at 94°C for 5 minutes, followed by 40 cycles of denaturation at 94°C for 1 minute, annealing at (40^0C or 36^0C and 32^0C) for 1 minute and extension at 72^0C for 2 minutes, with a final round of extension at 72^0C for 2 minutes.

2.5. RAMP-PCR

Each PCR reaction was performed in a final volume of 25µl containing 2.0 l of 10 X *Taq* Polymerase Reaction Buffer including $MgCl_2$; 1.0 µl of mix 10mM dNTPs; 20ng DNA; 1.25 Unit *Taq* DNA polymerase; 0.8µl of 10nmol/µl of each forward and reverse primers and varying amounts of sterile distilled water to make the final volume up to 25µl. Reactions were carried out in a PCR cycler (Eppendorf Master Cycler Gradient). Three annealing temperatures 52^0C ±3 ^{0}C, 55^0C ±3 ^{0}C and 57^0C ±3 ^{0}C were tested with following profile: Denaturation at 94°C for 5 minutes, followed by 35 cycles of denaturation at 94°C for 1 minute, annealing at (52^0C ±3 ^{0}C or 55^0C ±3 ^{0}C or 57^0C ±3 ^{0}C) for 1 minute and extension at 72^0C for 2 minutes, with a final round of extension at 72^0C for 5 minutes.

PCR products were separated on 1,5% agarose gel containing 25% of fine agarose and 75% of routine agarose.

2.6. Data analysis

Data was analysed with PopGen and Phylip Tree software.

3. RESULTS AND DISSCUSION

3.1 PCR optimization

The optimum amount of $MgCl_2$ required in each PCR reaction varied according to the particular primer combinations. Optimum concentration of MgCl2 was determined based on the brightness, sharp and the consistency of bands [9]. In this experiment, 2.5mM of $MgCl_2$ was found suitable and produced strong and consistent banding patterns for the RAPD primers and 3.75mM of $MgCl_2$ was the best for RAMP-PCR. At a concentration of $MgCl_2$ lower than these amounts (about 1.5 mM for RAPD and 2.5 mM for RAMP) bands were faint and difficult to record. Higher concentrations of $MgCl_2$ (approximately 4.0 mM) showed no further improvement on the pattern and strength of the bands obtained, or on their reproducibility.

Of the six genomic DNA concentrations tested (10 ng, 20 ng, 25 ng, 30 ng, 40 ng and 50 ng,), 50 ng of genomic DNA produced the strongest and most consistent bands in RAPD and 40 ng genomic DNA was found the best for RAMP-PCR.

The most suitable thermal profile for RAPD-PCR in this study was: denaturation at 94^0C for 5 minutes, followed by 40 cycles of denaturation at 94^0C for 1 minute, annealing at 36^0C for 1 minute and extension at 72^0C for 2 minutes, with a final round of extension at 72^0C for 5 minutes. Two other thermal profiles, with different annealing temperatures, were tested. At a higher annealing temperature (i.e. 40^0C), low molecular weight bands were absent from the profile, while at a lower annealing temperature (i.e. 32^0C), the bands were faint and inconsistent. Optimum thermal profile for RAMP-PCR in this study was: denaturation at 94^0C for 5 minutes, followed by 35 cycles of denaturation at 94^0C for 1 minute, annealing at 55^0C ± 3 ^{0}C for 1 minute and extension at 72^0C for 2 minutes, with a final round of extension at 72^0C for 5 minutes.

RAPD-PCR products of IR64 - VND95-20 and Basmati 370 BDS with 2.5 mM $MgCl_2$, 50 ng genomic DNA, annealing temperature at 36^0C and primer UBC9 separated on 1.5% agarose gel, is shown in figure 1a. Figure 1b shows RAMP-PCR products of IR64 - VND95-20 and Basmati 370 BDS with 3.75 mM $MgCl_2$, 40 ng genomic DNA, annealing temperature at 55^0C 3^0C and primers RM238, RM243, RM256, RM259, RM265, RM272.

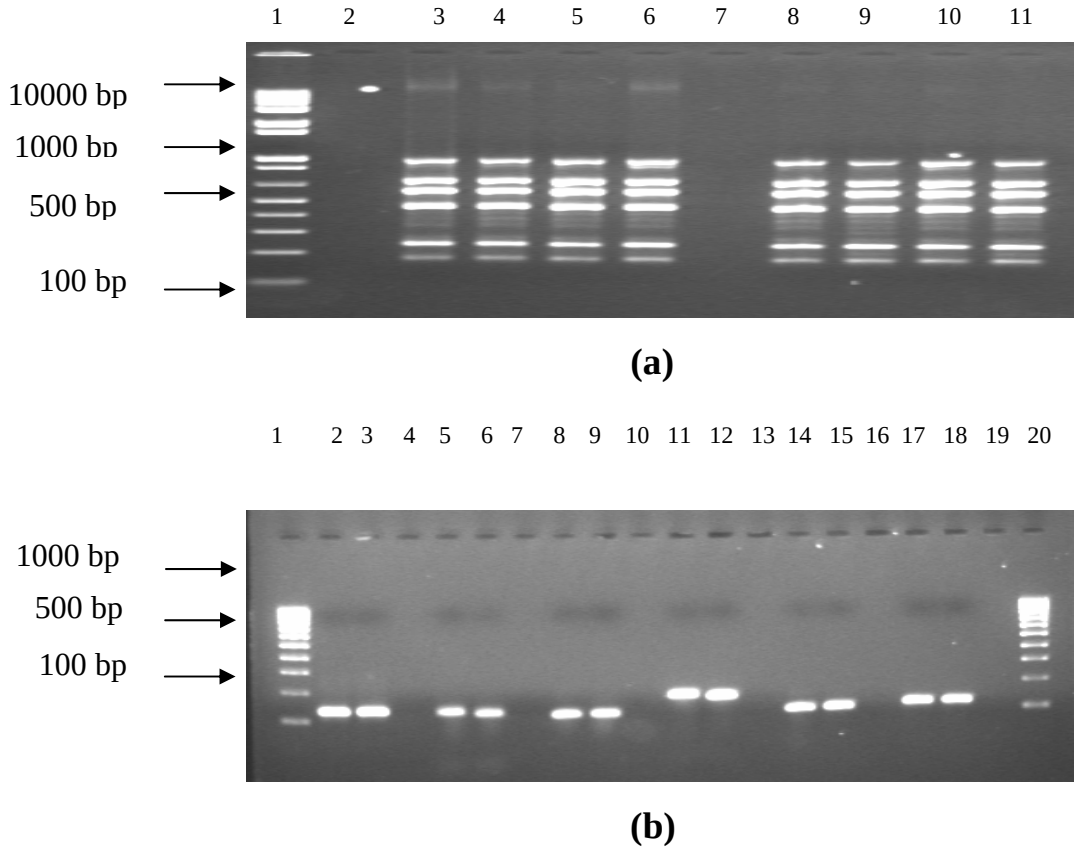

Fig. 1: PCR performance with optimized amounts of $MgCl_2$, genomic DNA and temperature profile in IR64 - VND95-20 and Basmati 370 – BDS. Gel (a): PCR with RAPD primer UBC9. Lane 1 contained a DNA ladder (10Kb plus, Biofly); lanes 3-6 contained PCR products of IR64 and VND95-20; Lane 7 contained the products of a negative control (all components of the PCR reaction except genomic DNA). Lanes 8-11 contained PCR products of Basmati 370 and BDS; Gel (b): PCR with Microsatellite primers. Lanes 1, 20 contained a DNA ladder (1Kb plus, Promega); lanes 2,3,5,6,8,9,11,12,14,15,17 and 18 contained PCR products of TT1 and TDS with RM238, RM243, RM256, RM259, RM265, and RM272 respectively; Lane 19 contained the products of a negative control (all components of the PCR reaction except genomic DNA).

3.2. RAPD-PCR

The total number and number of polymorphic bands generated by RAPD primers in Basmati 370 BDS; Tam Thom (TT1) –TDS; and IR 64 - VND 95-20 is given in table 1.

Table 1: DNA Polymorphism between Basmati 370 BDS; Tam Thom (TT1) – TDS; and IR 64 - VND 95-20 as detected by RAPD-PCR using 50 RAPD primers. Results are for duplicate PCR and only consistent bands were recorded.

RAPD-PCR	Basmati 370 BDS	Tam Thom (TT1) –TDS	IR 64 - VND 95-20
Total bands scored	174	178	174
Number of polymorphic bands	20	16	6
% Polymorphism	11.49	8.98	3.45

Of the 50 RAPD primers tested, 27 primers could produce shape, bright and consistent bands in all cultivars and mutants examined. Amongst these, 13 primers generated different bands in Basmati 370 and BDS, these figures were 8 primers in Tam Thom (TT1) –TDS and 5 primers for IR 64 - VND 95-20. Percentage of polymorphism between parent and its mutant varies from 3.45% in IR 64 - VND 95-20 to 8.98% in Tam Thom (TT1)–TDS and 11.49% in Basmati 370 and BDS. An example of polymorphic bands between parents and mutants detected by UBC11 is shown in figure 2.

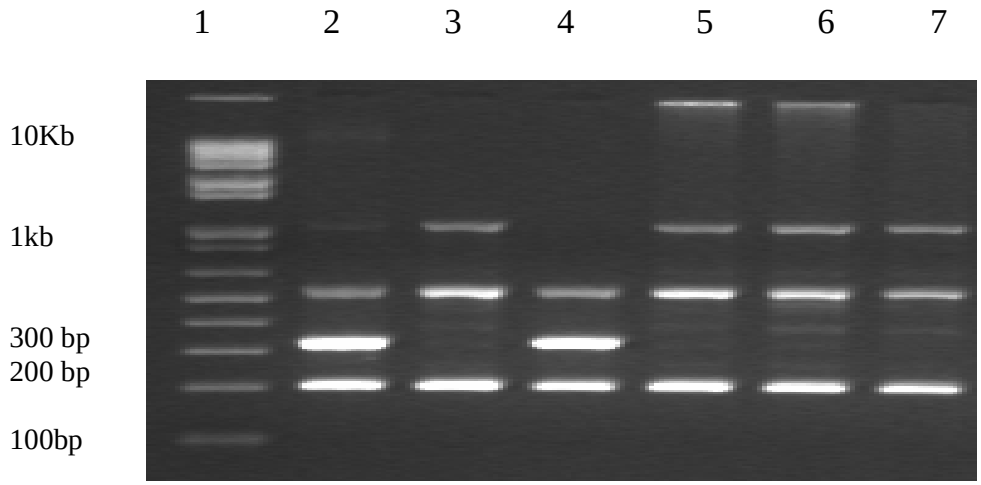

Fig. 2: Polymorphic bands between Basmati370 - BDS and TT1 TDS detected by RAPD primer UBC11. Lane 1 DNA ladder (10Kb, Biofly); lane 2-3 contained PCR of Basmati370 and BDS; lanes 4-5 contained PCR of TT1 and TDS; lanes 6-7 contained PCR of IR64-VND 95-20.

The dendrogram of similarity index (Figure 3) resulting from analysis of the presence and absence of bands generated by 27 RAPD primers in 6 cultivars and mutants not only shows significant differences in the relationship between each parent and mutant but also separates 6 cultivars and mutants into groups. There are two main groups in Figure 3. The first was Basmati 370 and TT1, the second was the rest. This result agrees with the fact that Basmati 370 and TT1 are quite close to each others in terms of aroma, height, life cycle, photoperiod sensitive,… As the same trend, IR 64, VND 95-20, TDS, BDS were grouped together. They are quite similar in the duration of growth, height, high yield,…Our results support the suggestion of Williams *et.al,* 1990

[4]; Chen and DeFillipis, 1996 [10] and Linh, 2002 [11] that RAPD primers are good in distinguish between individuals within species.

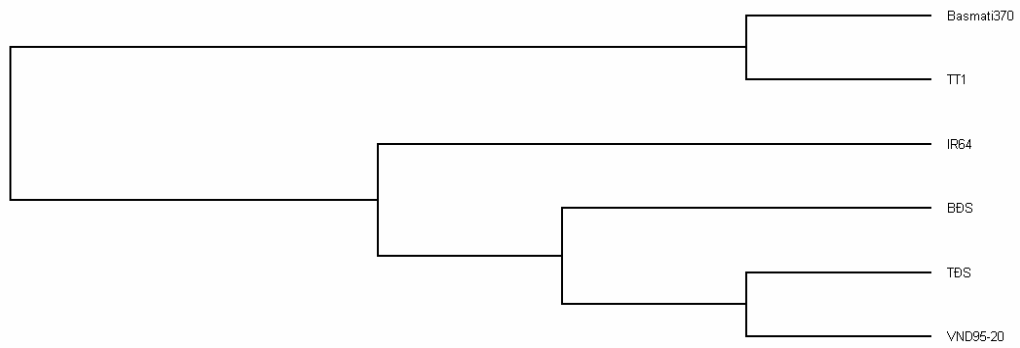

Fig. 3: Genetic relationship (i.e. similarity index) between Basmati 370, BDS, TT1, TDS, IR64 and VND 95-20 determined by RAPD-PCR. Analysis was based on the presence and absence of bands produced by 27 well-working RAPD primers using the Population Genetic program. Results are for triplicate PCR, and only consistent bands were recorded.

3.3. RAMP-PCR

The total number and number of polymorphic bands generated by Microsatellite primers in Basmati 370 BDS; Tam Thom (TT1) –TDS; and IR 64 - VND 95-20 is given in table 2.

Table 2: DNA Polymorphism between Basmati 370 BDS; Tam Thom (TT1) – TDS; and IR 64 - VND 95-20 as detected by RAMP-PCR using 60 Microsatellite primers. Results are for triplicate PCR and only consistent bands were recorded.

RAMP-PCR	Basmati 370 BDS	Tam Thom (TT1) –TDS	IR 64 - VND 95-20
Total bands scored	101	103	99
Number of polymorphic bands	21	15	5
% Polymorphism	21.2	15.4	4.95

Of the 60 Microsatellite primers tested, 50 primers could produce shape, bright and consistent bands in all cultivars and mutants examined. Amongst these, 11 primers generated different bands in Basmati 370 and BDS, these figures were 8 primers in Tam Thom (TT1) –TDS and 3 primers for IR 64 - VND 95-20. Percentage of polymorphism between parent and its mutant varies from 4.95% in IR 64 - VND 95-20 to 15.4% in Tam Thom (TT1) –TDS and 21.2% in Basmati 370 and BDS.

3.4. RAPD versus RAMP

Though there was a difference in percentage of DNA polymorphism between parents and mutants examined by RAPD and RAMP, both could detect changes in DNA between cultivars and mutants tested. Percentage of DNA Polymorphism detected by Microsatellite markers is higher than that of RAPD markers. The differences might be

resulted from the natural Dominant and Co-dominant characteristics of RAPD and Microsatellite markers. The two techniques supplement each other and can be used to detect changes in DNA of rice mutants after gamma irradiation.

4. CONCLUTIONS

The success or failure of a PCR reaction depends upon the optimization of conditions for the PCR. Different primers in PCR have different optimal conditions. Optimum amounts of $MgCl_2$ in this study were 2.5mM for RAPD-PCR and 3.75mM for RAMP-PCR. Suitable concentrations of genomic DNA for RAPD and RAMP were 50ng and 40ng respectively. Annealing temperatures were determined at 36^0C for RAPD primer and at 553^0C for Microsatellite primer.

The most suitable thermal profile for RAPD-PCR in this study was: denaturation at 94^0C for 5 minutes, followed by 40 cycles of denaturation at 94^0C for 1 minute, annealing at 36^0C for 1 minute and extension at 72^0C for 2 minutes, with a final round of extension at 72^0C for 5 minutes.

The most suitable thermal profile for RAMP-PCR in this study was Denaturation at 94°C for 5 minutes, followed by 35 cycles of denaturation at 94°C for 1 minute, annealing at 55^0C 3 ^{0}C for 1 minute and extension at 72^0C for 2 minutes, with a final round of extension at 72^0C for 5 minutes.

Percentage of DNA polymorphism between Basmati370 and BDS, TT1 and TDS, IR64 and VND 95 -20 determined by RAPD were 11.49%; 8.98% and 3.45% respectively. Those determined by RAMP were 21,2%; 15,4% and 4,95%.

Both RAPD and RAMP can detect changes in DNA of parents and mutants. The two techniques should be used to assist rice breeding.

ACKNOWLEDGMENTS

We thank VAEC for supporting this research.

REFERENCES

[1]. H. Wada, T. Koshiba, T. Matsui, M. Sato, Involment of peroxidase in differential sensitivity to γ-radiation in seedlings of two *Nicotiana* species, Plant Sci. 132 (1998) 109-119.

[2]. X.T. Le, T.M.L. Hoang, T.D. Le, V.T. Nguyen, H.T. Hoang, T.V. Nguyen, V.V. Nguyen, N.N. Nguyen, V.K. Tong, Improvement of aromatic rice cultivars by gamma irradiation-induced mutation techniques: preliminary results at M3 in some traditional varieties. Proceedings of the fourth national conference on nuclear physics and techniques. Hanoi, 2001.

[3]. H.A. Persson, B.A. Gustavsson, The extent of clonality and genetic diversity in lingonberry (*Vaccinium vitis-ideae* L.) revealed by RAPDs and leaf-shape analysis, Mol. Ecol. 10 (2001) 1385-1397.

[4]. Williams, J.G.K., Kubelik, A.R., Liuck, K.J., Rafalski, J.A. and Tingey, S.V. (1990). DNA polymorphism amplified by arbitrary primers are useful as genetic marker. *Nucleic Acids Research*, **18**, pp. 6531-6535.

[5]. K.S. Wu, R. Jones, L. Danneberger, P.A. Scolnik, Detection of microsatellite polymorphisms without cloning, Nucleic Acids Res. 22 (1994) 3257-3258.

[6]. O. Panaud, X. Chen, S.R. McCouch, Development of microsatellite markers and characterization of simple sequence length polymorphism (SSLP) in rice (*Oryza sativa* L.), Mol. Gen. Genet., 252 (1996) 597-607.

[7]. E. Magel, S. Hauch, L.F. De Filippis, Random amplification of polymorphic DNA and reverse transcription polymerase chain reaction of RNA in studies of sapwood and heartwood, in: N. Chaffey (Ed.), Wood Formation in Trees, Harwood Academic, Malaysia, 2000, pp. 317-335.

[8]. L. De Filippis, E. Hoffmann, R. Hampp, Identification of somatic hybrids of tobacco generated by electrofusion and culture of protoplasts using RAPD-PCR, Plant Sci. 121 (1996) 39-46.

[9]. Park, Y.H. and Kohel, R.J. (1994). Effect of concentration of $MgCl_2$ on random amplified DNA polymorphism. *Bio Techniques*, **16**, pp. 652- 653.

[10]. Chen, D.M. and De Filippis, L.F. (1996). Application of genomic DNA and RAPD-PCR in genetic analysis and fingerprinting of various species of woody trees. *Australian Forestry*. **59:** 46-55.

[11]. Hoang Thi My Linh (2002). Salt Tolerance and Changes in DNA of rice Mutants induced by Gamma Irradiation. *Master Thesis*, University of Technology, Sydney.

1.7 - Radiation Protection and Radioactive Waste Management

STUDY ON TECHNOLOGY FOR RADIOACTIVE WASTE TREATMENT AND MANAGEMENT FROM URANIUM PRODUCTION

Vu Hung Trieu, Vu Thanh Quang, Nguyen Duc Thanh, Trinh Giang Huong, Tran Van Hoa, Hoang Minh Chau, Ngo Van Tuyen, Nguyen Hoang Lan and Vuong Huu Anh

Institute for Technology of Radioactive and Rare Elements, VAEC, Vietnam.

ABSTRACT: There is some solid and liquid radioactive waste created during producing Uranium that needs being treated and managed to keep our environment safe. This radioactive waste contains Uranium (U238), Thorium (Th232), Radium (Ra226) and some heavy metals and mainly is low radioactive waste. Our project has researched and built up appropriate technology for treating and managing the radioactive waste.

After researching and experimenting, we have built up four technology processes as follows:

- Technology for separating Radium from liquid waste.
- Technology for treating and managing solid waste containing Ra.
- Technology for separating Thorium from liquid waste after recovering radium.
- Technology for stabilizing solid waste from Uranium production.

Key words: Radioactive Waste.

Introduction

Radioactive waste generated from treating radioactive ore and other radioactive actions is dangerous for people's health and our environment. Environmental protection from radioactive waste is one of the problems concerned in Vietnam and in over the world. Vietnam government has issued the law for managing radioactive waste.

Nowadays, Institute for Technology of Radioactive and Rare Elements (ITRRE) is researching the Uranium ore process by heap leaching method. During processing ore for recovering Uranium, there is some radioactive waste created that needs to be treated and managed to keep the environment safe. ITRRE has established a safe area for managing, treating radioactive waste and storing it temporarily. The project "Study on technology for radioactive waste treatment and management from uranium production" is carried out in order to protect surrounding of the waste's storage conforming to the Vietnamese safety standard as well as to international safety standard.

Results and discussions

1. Characters of radioactive waste created from processing Uranium ore by heap leaching method carrying out in ITRRE

Radioactive waste mainly consists of:

- Solid waste:

+ Uranium tailing after heap leaching for recovering Uranium.

+ Waste tailing containing Ra after precipitating liquid waste.

- Liquid waste: effluent created after ion exchange and filter processes for recovering technical uranium.

Compositions of the effluent are shown in the table 1.

Table 1: Compositions of the effluent from leaching uranium ore

Elements	Composition (%)	Radioactive dose (kBq/Kg)
U	0.012	-
Th	4.10^{-3}	-
Fe	9.68	-
Pb	0.42	-
Ra_{-226} and isotopes		96
pH = 2.7		

Note: Radioactive dose of Ra_{-226} and isotopes (96 kBq/kg) is higher than limited dose (compared with standard of Vietnam TCVN 4397-87: limited radioactive dose < 1.7 kBq/kg). So, we have chosen appropriate basic parameters to decrease radioactive dose and increase pH of samples for stabilizing effluent by separating Ra and Th from that effluent.

2. Experimental operation

2.1. Separating Ra_{-226} from effluent after recovering Uranium

2.1.1. Separating Ra by precipitating with barium chloride ($BaCl_2$)

+ Research on the effect of pH value on the purifying treatment:

pH value is a very important factor in processing acidic uranium effluent. So it is necessary to research on the effects of pH on removal of elements from effluent. Take a liter of effluent, adjust its pH to different values by lime milk.

Note: The results show that pH has a great influence on processing acidic uranium effluent. At pH of effluent = 10, radioactive dose can meet the required discharge standard.

+ Research on relationship between consumption of CaO and pH of sludge solution:

The experimental results for 1litter of sample are shown in the table 2

Table 2: Relationship between consumption of CaO and pH

pH	2	3	4	5	6	7	8	10
CaO(g/l)	6.5	9.3	11.0	11.6	12.0	12.4	12.6	13.2
V(l)	10	10	10	10	10	10	10	10

The results show that: At pH = 10, we can add 132g of CaO for 10l of effluent. It is useful for calculating expenses of radioactive treatment during processing Uranium ore in industrial scale.

+ Research on the effect of Barium chloride content on the results of removing radium:

Use a liter of effluent, adjust its pH to 8, and add different amounts of barium chloride into effluent. Stir that solution for 30 minutes, then adjust its pH to 10 and continue stir for 20 minutes. The results are shown in the table 3.

Table 3: The effect of Barium chloride content on the results of removing radium

$BaCl_2$ (mg/l)	10	15	20	30	50
U (mg/l)	0.06	0.04	0.03	0.008	0.004
Ra (Bq/l)	1.8	1.1	0.6	0.5	0.5

Note: The results show that when content of $BaCl_2$ is 30 mg/l, the efficiency of removing Ra is the highest.

+ Research on the effect of stirring time on removing radium:

Add barium salt into effluent, stir solution with different stirring time, measure radium contents in sample. The results are shown in the table 4.

Table 4: The effect of stirring time on removing radium

Stirring time (minutes)	**Ra content (Bq/l)**
5	0.56
10	0.50
15	0.26
20	0.11
30	0.10

It can be seen from the table 4 that co-precipitation of radium with barium sulfate is fast. With stirring time is between 20-30 minutes, separating Ra from effluent can meet the requirement of safety standard.

Note: According to above results, we have proposed a technological process for separating Ra from radioactive effluent after recovering Uranium by ion-exchange method:

- Put 50 liters of radioactive effluent created after recovering technical Uranium into the precipitator, stir the solution with speed 240 rpm.

- Add lime milk solution containing 13.2g CaO/l, adjust pH = 8.

- Add $BaCl_2$ solution 30 mg/l, stir 20 minutes.

- Use lime to adjust pH = 10, add 500 ml of stearic acid, continue stir in 10 minutes for co-precipitation of Ra and $BaSO_4$ completely.

- Deposit in the container about 20 days, and then filter in the centrifugal filter, waste mud is collected for cementing. The solution containing Th, U is treated by ion-exchange method.

3. Research on separation of Th from radioactive effluent by ion-exchange method

a. Use ion- exchange resin KPS-110 cation, column d = 10 cm, H = 50 cm.

b. Determine ion exchange capacity of resin to Th.

The result are shown in the table 5.

Table 5: Ion-exchange capacity of resin to thorium

Number	1	2	3	4	5	6	7	8	9	10
Content Th in resin (mg)	83.5	83.7	83.2	83.3	83.6	83.4	83.5	83.4	83.5	83.5
Content Th in effluent (mg)	66.5	66.3	66.8	66.7	66.4	66.6	66.5	66.6	66.5	66.5

Ion-exchange of resin to Thorium is: 83.5 mg Th/1g resin.

c. Determine parameters ion exchange process with thorium.

+ Research on the effect of pH value on adsorption of thorium:

The results are shown in the table 6:

Table 6: Effect of pH value on adsorption of thorium

Concentration of H_2SO_4(M)	0.01	0.025	0.05	0.1	0.25	0.5
Capacity (%)	85.6	92.5	98.8	80.6	72.4	65.2

The results show that when concentration of sulfuric acid in the solution is 0.05 M, Thorium is completely adsorbed on the ion column.

+ Research on the effect of some ions on adsorption process:

Sodium sulfate solution is added into the adsorption solution. The results are shown in the table 7.

Table 7: Effect of some ions on adsorption process

Concentration of Na_2SO_4 (%)	0.1	0.5	1.5	2.0	2.5	5.0
Adsorption capacity (%)	97.3	98.5	99.2	99.5	98.4	97.6

The results show that: When concentration of Sodium sulfate is 2%, adsorption capacity of Thorium on the ion exchange resin is the highest.

d. Effect of concentration of Thorium on adsorption process.

Experimental results are shown in the **table 8**.

Concentration of Th (mg/l)	5	10	15	20	25	30
Adsorption capacity (%)	82.7	85.3	86.9	87.4	87.8	89.3

e. Effect of time on ion-exchange process

The contact time is a very important in the resin adsorption practice. This is especially true for column operation. Therefore, proper contact time is necessary to achieve high adsorption effectiveness. The result are shown in the table 9.

Table 9: Effect of time on ion-exchange process

Time (h)	0.5	1.0	1.5	2.5	3.0
Content Th in resin(mg)	45.7	72.6	79.5	80.3	80.5
Content Th in solution(mg)	104.3	77.4	70.5	69.7	69.5
Capacity (%)	54.7	86.9	95.2	96.1	96.3

4. Research on stabilization process of solid waste after separating thorium from effluent by ion-exchange method

a. Non-treatment of solid waste.

Solid waste mainly consists of tail from the extraction process is added into column d = 11 cm, H = 1.2m, after that natural water is passed with different velocities. The results are shown in the table 10 and 11.

Table 10: Effect of water velocity on stabilization process (3 liter/h)

Volumn (liter)	**Radioactive dose (kBq/m^3)**
3	40
6	22
9	11
12	7
15	4

Table 11: Effect of water velocity on stabilization process (5 liter/h)

Volumn (liter)	**Radioactive dose (kBq/m^3)**
5	25
10	8.5
15	5.5
20	3.0
25	1.8

b. Solid waste treatment.

+ Research on effect of pH value on solid waste treatment:

Solid waste created from uranium production has pH from 2.5 to 2.7. Adjust its pH to 10 by adding CaO, put it to column. Measure uranium content. The results are shown in the table 12.

Table 12: Effect of pH value on solid waste treatment

Samples	pH value	Content U(mg/l)	Radioactive dose (kBq/m^3)
1	7	2.1	-
2	8	1.3	7.4
3	9	0.6	5.2
4	10	0.12	2.6
5	11	0.1	2.1
6	12	0.1	-

+ Research on effect of water speed on stabilization process:

- Experimental results are shown in the **table 13:**

Volumn (liter)	Radioactive dose (kBq/m^3)
3	3.2
6	1.8
9	-
12	0.8
15	0.2

Note: The results showed that radium and other radioactive nuclides can be removed from solid waste created after heap leaching to obtain Uranium. Its pH is adjusted to 10 by adding CaO. The sample can meet the radioactive safety standard of Vietnam (TCVN 4397-87). So, we have proposed three following ideas:

- After heap leaching to recover Uranium, there are a lots of effluent with low radioactive activity and shouldn't be cemented.

- Effluent must be adjusted pH to 10 by adding CaO (4.5 kg of CaO/ ton of effluent), then heap it or move to certain places.

- It is necessary to build containers for testing and treating radioactive waste around areas containing effluent for environment ptotection.

5. Research on technological process for treating radium solid waste containing Ra

5.1. Research on ratio of solid waste to cement in cementation process

The results are shown in the **table 14:**

Ratio Ra/cement	1/0.1	1/0.2	1/0.3	1/0.4
Surface dose (μSv/h)	0.95	0.9	0.8	0.8
Press intensity (kg/cm^2)	18	27	95	110

The results showed that appropriate ratio of solid waste to cement is 1/0.3.

5.2. Research on ratio of sand to cementation process

In some cases, sand is added into cementation process for increasing press intensity. Experimental results as followings:

Table 15: Ratio of solid waste/cement/sand

Solid waste/ Cement/ Sand	1/0.3/0.1	1/0.3/0.2	1/0.3/0.3
Surface dose (μSv/h)	0.65	0.54	0.48
Press intensity (kg/cm^2)	98	120	135

The results showed that with ratio of solid/cement/sand = 1/0.3/0.2, treating process of radium solid waste takes place completely. When press intensity = 120 kg/cm^2, it is possible to meet the requirement of process of treating radioactive waste by cement method.

5.3. Research on effect of nuclide isotope discard on the environment

Experimental results are shown in the **table 16:**

Number of week	1	2	3	4	5
Radioactive Dose in water (Bq/l)	0.8	0.8	0.8	0.78	0.78

Note: According to above results, we have built technology processes for cementing radioactive waste containing Ra as followings.

+ The first stage:

- Prepare materials: effluent, cement, sand, water.

- Prepare paint, equipments for stirring, protective clothes.

- Container 200liter have alid and a hoop. Paint the container with yellow color, draw radioactive symbols, write radioactive parameters on the outside of the container according to the safe rules.

+ The second stage:

- Treatment process is carried out in the determined areas with labor protection equipments meeting the requirement of radioactive safety standard.

- The ratio of effluent/cement/sand = 1/0.3/0.2, add water for stirring.

- Put all of materials into the container, keep for 24 h, then cover the container with a lid, clip a hoop to the container, test radioactive parameters, move the container to the store to keep temporarily.

Conclusions

After research and experiment, we have proposed a technology flow sheet of radioactive waste treatment and management. These are:

- Technology for separating radium from liquid waste.

- Technology for treating and managing solid waste containing Ra.

- Technology for separating thorium from liquid waste after recovery radium by ion exchange method.

- Technology for stabilizing solid waste from uranium production.

REFERENCES

[1]. IAEA, Classification of radioactive Waste, IAEA No 111-G1., Vienna, 1994.

[2]. IAEA, Treatment and Conditioning of Radioactive Solid Wastes, IAEA-TECDOC -655, Vienna 1992.

[3]. IAEA, The principles of Radioactive Wastes Management, Safety series, No.111-F, IAEA, Vienna 1992.

[4]. IAEA, Management of Radioactive Wastes from the Mining of Ores, Safety series, No.WS-G-1.2, IAEA, Vienna 2002.

[5]. IAEA, Application of Ion Exchange Processes for the Treatment of Radioactive Wastes, Vienna 2002.

[6]. VAEC. Tiêu chuẩn an toàn quốc tế cơ bản. Bảo vệ Bức xạ ion hoá và an toàn đối với nguồn bức xạ. 2000.

STUDY OF EXPOSURE DOSE IN SOME SERIOUS HYPOTHESIS ACCIDENTS OF SVST-Co 60/B IRRADIATOR FOR PLANNING ACCIDENT RESPONSES

Tran Van Hung, Tran Khac An, Cao Van Chung and Nguyen Anh Tuan

Research and Development Center for Radiation Technology, VAEC, Vietnam.

ABSTRACT: In this study two most serious accidents for SVST-Co60/B irradiator at Research and Development Center for Radiation Technology (VINAGAMMA) have been hypothesized namely jams of source racks and a source pencil knocked out on the production maze by tote-box. Radiation dose distributions have been calculated by using MCNP code in order to assess the seriousness of the accidents, to give out some important proposals and recommendations to remedy accidents if occurred.

1. Introduction

The applications of industrial gamma irradiators for radiation processing and sterilization of health cares have been started since the late 1950s in developed countries. There are no reports on accidents in these applications during the period 1950-1975, but since 1989 at least one serious accident has been reported each year. Between 1975 and 1994 five accidents were reported, i.e. Italia (1975), Norway (1982), El Salvador (1989), Israel (1990) and Belarus (1991) [1, 2, 3, 4, 5]. From these accidents important lessons have been drawn for designs, constructions and operations of irradiators. It is important for irradiator owners to well learn these lessons, to be able to anticipate the worst accident and to have necessary measures for presentation of the similar accidents might be happened or for mitigation of accident consequences by the improvements of irradiator designs, constructions and operation procedures.

Based on the overview serious accidents already occurred in the world and the Evaluation of the radiation safety for the SVST-Co60/B, we could anticipate probabilities of serious accidents extremely low, but it would still occur. In this report, we brought out two types of supposed accidents:

- The source racks are jammed, could not return to the storage position
- The source pencil is knocked out on the product maze

The calculations includes:

- Calculations of dose distribution in the irradiation room and for the case of source rack jam at the irradiation position and at the height of 0.5 m over the water surface of the water pool when the irradiation room filled with the product densities of 0.2, 0.4 and 0.6 g/cm^3.

- Dose distributions in the upstairs room and surrounding areas of the irradiator spot while opening the concrete plugs in the case of source rack jam at the irradiation position.

- Dose distributions in the upstairs room while opening the concrete plugs in the case of source rack jam at the height of 0.5 m over the water surface.

- Dose distributions in the irradiation room for a source pencil carried out by a tote box at three positions in the product maze.

These calculations are very important for the making recommendations and response plans to radiological accidents and mitigation of their consequences.

2. Calculation code

MCNP code version 4C has been successfully used in calculations of absorbed dose in the products irradiated in SVST-Co60/B irradiator and also used to calculate the dose distribution for the cases of accidents in our work. All calculated values of dose rate in our work are excluded radiation background.

3. Results and discussion

3.1 The cases of the source racks jammed at the irradiation position and at the height of 0.5 m over the water surface

3.1.1 Dose distribution inside irradiation room

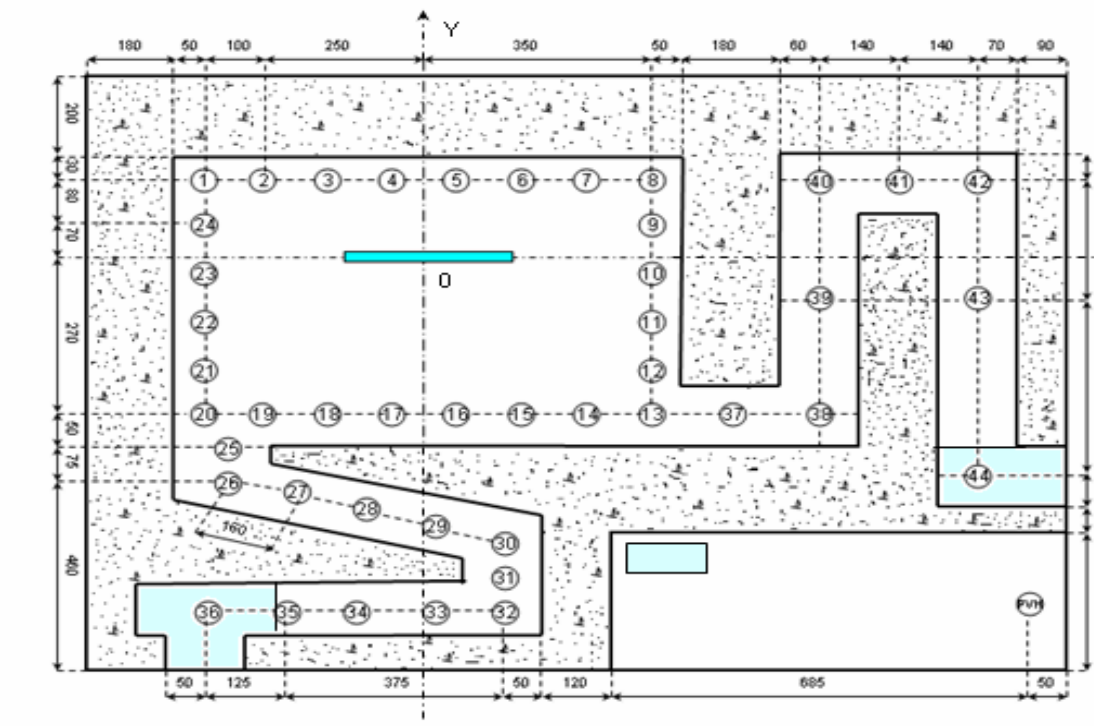

Fig. 1: The calculation points of dose rate at 1 m on the floor

When the accident occurred, three source racks are locked in irradiation position, could not return the storage position. In this accident exposure doses are highest in comparison with other ones among hypothesis accidents. The calculation points for the dose distribution inside the irradiation room with the product densities of 0.2, 0.4 and 0.6 g/cm^3 are presented in fig 1.

All calculation points in this work are at the height of 1 m over the floor. The table 1 shown a typical results of dose rate calculation in the irradiation room in the case of three source racks jammed at the irradiation position and the product density of 0.2 g/cm^3 are shown in table 1.

Table 1: Calculated results of dose distribution in the case source racks jammed at the irradiation position and product density of 0.2 g/cm^3

Position (x, y)	Dose rate (mSv/h)	σ	Position (x, y)	Dose rate (mSv/h)	σ
1 (-345, 150)	8.11E+04	0.01	24 (-345, 10)	1.35E+05	0.01
2 (-245, 150)	1.68E+05	0.01	25 (-335, -320)	7.85E+04	0.01
3 (-145, 150)	4.42E+05	0.01	26 (-335, -432)	1.24E+04	0.01
4 (-45, 150)	9.15E+05	0.01	27 (-236, -453)	2.61E+03	0.01
5 (55, 150)	8.76E+05	0.01	28 (-136, -474)	9.07E+02	0.02
6 (155, 50)	4.05E+05	0.01	29 (-37, -495)	4.32E+02	0.02
7 (255, 150)	1.52E+05	0.01	30 (163, -591)	1.54E+02	0.03
8 (355, 150)	7.71E+04	0.01	31 (163, -646)	1.43E+02	0.02
9 (355, 10)	1.27E+05	0.01	32 (163, -700)	1.80E+01	0.03
10 (355, -60)	9.33E+04	0.01	33 (60, -700)	4.32E+00	0.06
11 (355, -130	7.74E+04	0.01	34 (-43, -700)	2.35E+00	0.16
12 (355, -200)	7.01E+04	0.01	35 (-145, -700)	4.70E-01	0.07
13 (355, -270)	7.61E+04	0.01	36 (-248, -700)	2.31E-01	0.06
14 (255, -270)	1.33E+05	0.01	37 (455, -225)	3.70E+04	0.01
15 (155, -270)	2.21E+05	0.01	38 (650, -255)	5.73E+03	0.01
16 (55, -270)	3.03E+05	0.01	39 (650, -118)	8.08E+02	0.01
17 (-45, -270)	3.08E+05	0.01	40 (650, 64)	1.46E+02	0.01
18 (-145, -270)	2.30E+05	0.01	41 (706, 110)	1.09E+02	0.01
19 (-245, -270)	1.40E+05	0.01	42 (847, 110)	3.62E+00	0.03
20 (-345, -270)	7.97E+04	0.01	43 (930, -88)	2.17E-01	0.17
21 (-345, -200)	7.54E+04	0.01	44 (930, -336)	2.93E-02	0.15
22 (-345, -130)	8.05E+04	0.01	**CR** (930-700)	1.60E-12	0.16
23 (-345, -60)	9.86E+04	0.01	CR: Control room		

In both cases of source rack jam it found that dose rates inside the irradiation room, the personnel and the product mazes are very high in comparison with the occupational dose limits. In this case, the occupational workers can not come into the irradiation room.

3.1.2 Dose rate distribution in the upstairs room

The drawings of concrete plugs in positions, two plugs removed, three plugs removed and the calculation diagram in the upstairs room are presented in Fig. 2, Fig.3 and Fig. 4 respectively.

3.1.3

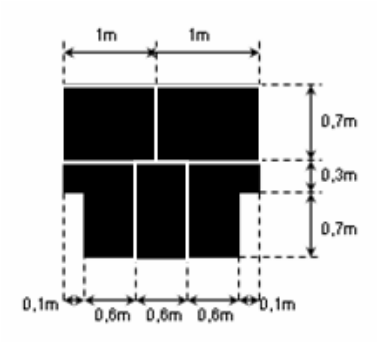

Fig. 2: Concrete plugs

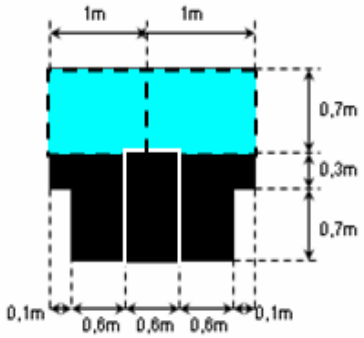

Fig. 3: Two top plugs were removed

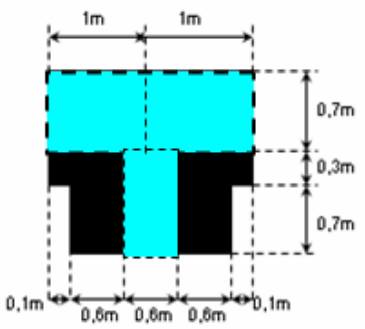

Fig. 4: Two top and one underneath plugs were removed

The dose rates in the upstairs room in the case of Fig. 3 and Fig. 4 when source racks jammed at the irradiation position are shown in Table 2 and Table 3.

Table 2: Calculation results of dose rate distribution in the upstairs room in the case of the source racks jammed at the irradiation position and Fig. 3

Position (x, y)	Dose rate (mSv/h)	σ	Position (x, y)	Dose rate (mSv/h)	σ
1 (-500, -450)	7.13E-03	0.14	9 (0, -45)	8.93E-02	0.05
2 (0, -450)	2.34E-02	0.12	10 (0, 5)	2.08E-02	0.07
3 (500, -450)	6.64E-03	0.13	11 (0, -145)	1.10E-01	0.04
4 (-500, 0)	1.11E-02	0.20	12 (0, -195)	5.66E-02	0.06
5 (500, 0)	9.51E-03	0.14	13 (0, -95)	1.55E-01	0.04
6 (-500, 300)	6.17E-03	0.17	14 (50, -95)	1.52E-01	0.04
7 (0, 300)	1.12E-02	0.13	15 (100, -95)	1.09E-01	0.05
8 (500, 300)	6.22E-03	0.17	16 (150, -95)	2.64E-02	0.07

Table 3: Calculation results of dose rate distribution in the upstairs room in the case of the source racks jammed at the irradiation position and Fig. 4

Position (x, y)	Dose rate (mSv/h)	σ	Position (x, y)	Dose rate (mSv/h)	σ
1 (-500, -450,670)	1.88E+01	0.02	11 (0, -145, 670)	5.65E+04	0.01
2 (0, -450, 570)	6.54E+01	0.01	12 (0, -195, 670)	1.13E+03	0.02
3 (500, -450, 670)	1.86E+01	0.02	13 (0 , -95, 670)	6.74E+02	0.02
4 (-500, 0, 670)	2.34E+01	0.02	14 (50, -95, 670)	4.71E+02	0.02
5 (500, 0, 670)	2.34E+01	0.02	15 (100, -95, 670)	2.42E+03	0.02
6 (-500, 300,670)	1.58E+01	0.02	16 (150, -95, 670)	4.58E+02	0.02
7 (0, 300, 670)	3.53E+01	0.02	17 (-210, 458, 670)	1.68E+01	0.01
8 (500,300,670)	1.62E+01	0.02	18 (150,458 527.5)	3.88E-01	0.03

The data in the Table2 and Table 3 indicated that in the case of Fig. 3 the occupational people can normally work, but in the case of Fig. 4, it must be careful if people have to work due to very high dose rates.

3.1.4 Dose distribution in public area in the case of Fig. 4

It is a sky shine problem, exposure doses in public area around the irradiator are due to the reflected gamma rays from the air after escaping from the irradiation room.

The calculations have proven that dose rates in the X axis, in the positive direction of Y axis and in the negative direction of Y axis at the distance more than 100 m are negligible; in the negative direction of Y at the distance less than 100 m the closer to the sources the higher dose rates. However, in the case of overcoming the accident it required to cover the blank hole (without plugs) by an iron plate with the thickness of 40 cm and the hole of 20 cm in diameter at the center for manipulation. If this measure was taken it do not need to evacuate the resident people around the irradiator. Table 4 and Table 5 present the calculated dose rates on Y axis in Fig. 4 without and with the iron plate.

Table 4: Dose distribution in public area on Y axis (negative direction) in Fig. 4 without the iron plate

Distance (m)	Dose rate(mSv/h)	σ	Distance(m)	Dose rate (mSv/h)	σ
50	3.51E-01	0.01	400	1.53E-03	0.03
100	1.13E-01	0.01	450	8.04E-04	0.02
150	4.67E-02	0.01	500	4.71E-04	0.07
200	2.20E-02	0.01	600	1.40E-04	0.04
250	1.05E-02	0.01	700	4.19E-05	0.04
300	5.44E-03	0.01	800	1.38E-05	0.07
350	3.01E-03	0.05	900	3.89E-06	0.06

Table 5: Dose distribution in public area on Y axis (negative direction) in Fig. 4 with the iron plate

Distance (m)	Dose rate(mSv/h)	σ	Distance (m)	Dose rate (mSv/h)	σ
100	2.38E-04	0.01	450	1.72E-06	0.04
150	9.85E-05	0.02	500	8.60E-07	0.03
200	4.41E-05	0.02	600	3.03E-07	0.12
250	2.14E-05	0.02	700	8.03E-08	0.06
300	1.06E-05	0.02	800	2.47E-08	0.07
350	5.71E-06	0.02	900	8.76E-09	0.14

3.2 Dose distributions for three cases of source pencil carried out by a tote box in the product maze

It hypothesized that a source pencil was carried out from the source racks to points 2, 3 and 4 as illustrated in the Figure 6. Calculated dose rates in the case of a source pencil at point No. 4 are given in the Table 6.

Table 6: Calculated values of dose rate in the case of a source pencil at point No.2

Distance (m)	Dose rate (mSv/h)	σ	Distance (m)	Dose rate (mSv/h)	σ
1 (865,-385)	3.98E+03	0.01	22 (1240,-785)	3.04E-01	0.03
3 (790,110)	4.35E+02	0.01	23 (1240,-685)	6.10E-01	0.01
4 (650,-250)	1.59E+00	0.02	24 (1240,-585)	1.96E+00	0.01
5 (355, -270)	3.27E-02	0.05	25 (1244,-458)	6.79E+00	0.01
6 (5,-270)	3.59E-03	0.08	26 (1240, -258)	1.93E+01	0.01
12 (1240,-385)	3.49E+01	0.01	27 (1240,-158)	3.50E+01	0.01
13 (1440,-385)	1.01E+01	0.01	28 (1240,-85)	1.97E+01	0.01
14 (1640,-385)	4.52E+00	0.01	29 (1240,15)	2.52E+00	0.01
15 (1840, -365)	2.49E+00	0.01	30 (1240,115)	5.35E-01	0.01
PVH (-930,-700)	1.90E+00	0.01			

The calculated results shown that if a source pencil laid at points No. 3 and No. 4 dose rates in the irradiation room and in the product maze are very high but normal outside them; dose rates in the irradiation room are normal but very high in the product maze and outside its door in the case of point No. 2 and the center staff must be evacuated.

3.3 Recommendations and directions to remedy these accidents

Based on the calculated data the recommendations and directions for response to the concrete accidents have been made. The important points should be considered by the irradiator manager are:

In any accidents of facility SVST-Co-60/B, we do not need to evacuate the resident people around the irradiator. However, if the source pencil is knocked out outside the irradiation room, the dose rate is very high. In this case, the staffs in office area have to evacuate.

REFERENCE

[1]. International Atomic Energy Agency, The Radiological Accident in San Salvador, IAEA, Vienna (1990).

[2]. International Atomic Energy Agency, The Radiological Accident in Sore, IAEA, Vienna (1993).

[3]. International Atomic Energy Agency, The Radiological Accident at the Irradiation Facility in Nevis, IAEA, Vienna (1996).

[4]. International Atomic Energy Agency, The Radiation Safety of Gamma and Electron Irradiation Facilities, Safety Series No. 107, IAEA, Vienna (1992).

[5]. ROLLO, C., SUSANNA, A., “The radiological Accidents at the Stimos plant, Italia”, paper presented at the IAEA Technical Committee Meeting on Radiological Accidents in Industrial Irradiation Facilities and their Implications for Regulatory Authorities Designers Manufacturers, Vienna, August 1991.

1.8 - Radiation Technology

STUDY ON THE SYNTHESIS OF COLLOIDAL SILVER NANOPARTICLES BY γ-IRRADIATION FOR USING AS AN ANTIMICROBIAL SUBSTANCE

Dang Van Phu [1], Bui Duy Du [2], Nguyen Trieu [1], Vo Thi Kim Lang [1]
Doan Thi The [1] and Nguyen Quoc Hien [1]

[1] Research and Development Center for Radiation technology, VAEC, Vietnam.

[2] Institute of Applied Material Science, Vietnam National Institute for Science and Technology

ABSTRACT: Colloidal silver nanoparticles of different sizes less than 20 nm were synthesized by γ Co-60 irradiation of Ag^+ in solution containing polyvinyl alcohol (PVA), polyvinyl pyrrolidone (PVP) as stabilizer. The saturated conversion dose (D) of Ag^+ to Ag^0 and particle size (d) depended on Ag^+ concentration from 1 to 50 mM were found out to be as: D (kGy) = - $0.0041[Ag^+]^2$ + $0.8674[Ag^+]$ + 3.2262, d (nm) = $0.0029[Ag^+]^2$ + $0.0529[Ag^+]$ + 0.9259 for PVA 2 g/100ml and D (kGy) = -$0.0151[Ag^+]^2$ + $1.5258[Ag^+]$ + 9.2441, d (nm) = -$0.0016[Ag^+]^2$ + $0.3757[Ag^+]$ + 6.2886 for PVP 2 g/100ml. Colloidal silver nanoparticles showed the maximal absorption peak at λ_{max}~ 400-420 nm. The size and size distribution of silver nanoparticles were characterized by transmission electron microscopy (TEM). The silver nanoparticle size of approximate 10nm showed highly antimicrobial effect against *E.coli* and *S.aureus*.

1. Introduction

In recent years, nanoscience and nanotechnology have attracted considerable interest. Metal nanoparticles with the size of 0.1 to 100nm show unique properties [1]. Silver nanoparticles for instance shows higher antibacterial effect of 20,000 to 60,000 time compared to Ag^+ ions [2]. At present many kind of products containing silver nanoparticles have been already commercialized [3]. A number of synthetic methods have been reported for preparation of silver nanoparticles, such as chemical, photochemical, electrochemical, sonochemical, radiolytic reduction [4, 5]. Compared to other methods, the radiation method provides several advantages such as i) process is carried out at room temperature ii) reducing agents are uniformly distributed in the solution iii) silver nanoparticles can be obtained in highly pure and stable state [5-7]. The mechanism of the radiation method was based on the highly active species occurred due to radiolysed process of water [6].

$$H_2O \xrightarrow{\wedge\wedge\wedge} e^-_{aq}, H^\bullet, OH^\bullet, H_3O^+,.. \quad (1)$$

The solvated electrons and $H^\cdot$ atoms are powerful reducing agents so that they easily reduce Ag^+ ions to the zero-valent state (Ag^0).

$$Ag^+ + e^-_{aq}\ (H^\bullet) \rightarrow Ag^o + \frac{Ag^+}{e^-_{aq}\ (H^\bullet)} \rightarrow Ag^+_2 + ... \rightarrow Ag^+_{n+1} \rightarrow Ag^0_{n+1} \quad (2)$$

$OH^\cdot$ radical formed during irradiation is strongly oxidative agent which must be converted into reducing agent by reacting with alcohol [8]:

$$RCH_2OH\ (R_2CHOH) + OH^\cdot \rightarrow R^\cdot CHOH\ (R_2{}^\cdot COH) + H_2O \quad (3)$$

$$R^\cdot CHOH\ (R_2{}^\cdot COH) + Ag^+_{n+1} \rightarrow Ag^o_{n+1} + RCHO\ (R_2CO) + H^+ \quad (4)$$

Silver atoms which aggregate to silver clusters and these clusters agglomerate with other nearby to form larger particles [6, 8]. To prevent agglomeration of silver clusters, polymers such as PVA, PVP were used as stabilizer [4,9].

In Vietnam the product of colloidal silver nanoparticles has been approved by the Ministry of Health for medical and household utilization as antibactericidal substance [10]. In this work, study to preparation of colloidal silver nanoparticles by γ Co-60 irradiation and to use as antimicrobial substance in medicine and in environment.

2. EXPERIMENTAL

2.1. Chemicals: Silver nitrate was obtained from Shanghai Chemical Co., Absolute ethanol was a product of Vietnam. Polyvinyl alcohol (PVA) with molecular weight $M_w = 8\times10^4$Da was purchased from Kuraray, Japan. Polyvinyl pyrrolidone: PVP K90 ($M_w = 10^6$Da) and PVP K30 ($M_w = 5\times10^4$Da) were obtained from BASF, Germany. Pure water for chromatography was used throughout in this study. Two bacterial strains namely *E.coli* ATCC and *S.aureus* ATCC were supplied by University of Medicine and Pharmacy, Ho Chi Minh City.

2.2. Methods

2.2.1. Preparation of colloidal silver nanoparticles by γ-ray irradiation: The solutions containing PVA, PVP, ethanol and Ag^+ with different concentration from 1 to 50 mM in glass tubes, which were deaerated by bubbling with nitrogen. The γ-ray irradiation was carried out on a Co-60 source with dose rate of 1.5 kGy/h, at VINAGAMMA center, HCM City and gamma cell with dose rate of 0.7kGy/h.

2.2.2. Characterization: Absorption spectra of silver nanoparticles solution which was diluted by water to 0.1mM calculated as Ag^+ concentration were taken on an Uv-vis spectrophotometer model UV-2401PC, Shimadzu, Japan. The size of the silver nanoparticles was measured using a transmission electron microscope (TEM) model JEM 1010, JEOL, Japan operated at an accelerating voltage of 80kV. The size and size distribution of silver nanoparticles were statistically processed using Photoshop CS2, Version 9.0.

2.2.3. Investigation of antibacterial effect: Colloidal silver nanoparticles were diluted to: 0 (Ref.), 5, 10, 20 and 50 ppm in liquid medium containing of 10^6CFU/ml of *E.coli* and *S.aureus*. After contact time of 30 min. determined the survival number of bacteria in samples. It was calculated as follows:

Antibacterial effect (%) = $100\text{-}N_t\times100/N_0$

Where N_0 and N_t are the reference and survival number of bacteria in samples respectively.

3. Results and discussion

3.1. PVA stabilizer

It was observed from Fig. 1 that the optical density increased with decreasing Ag^+ concentration [Ag^+]. The maximum absorption wavelengths (λ_{max}) for the colloidal silver nanoparticles solution varied from 400 to 420 nm.

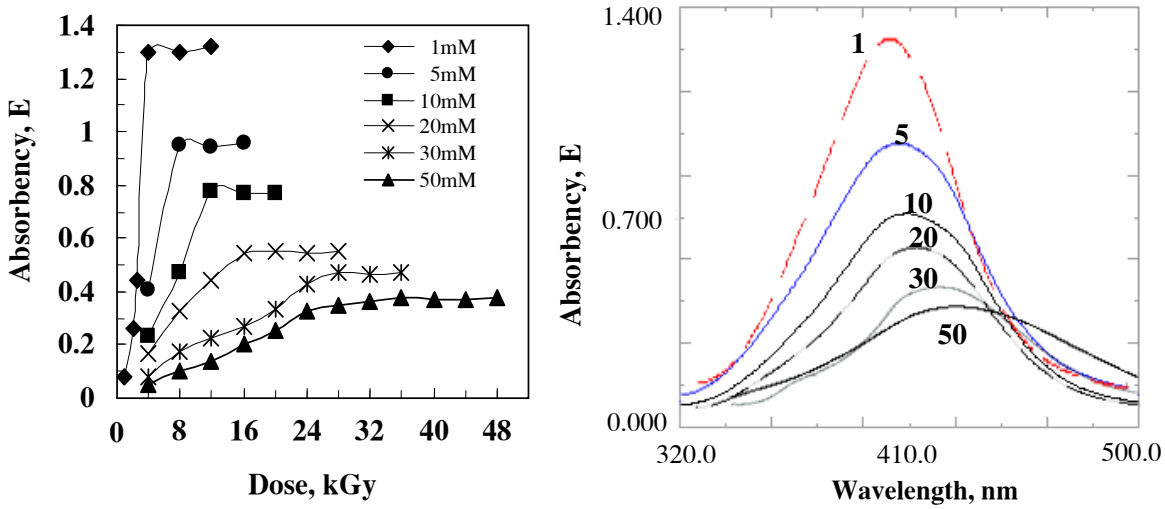

Fig. 1: The relationship of optical density of colloidal silver nanoparticles and dose

Table 1: The dependence of $[Ag^+]$ and average sizes (d) of colloidal silver (PVA 2 g, Ethanol 10 ml/100ml)

$[Ag^+]$, mM	1	5	10	20	50
d, nm	8.5 ± 1.4	9.7 ± 0.6	10.2 ± 0.7	10.7 ± 0.7	18.8 ± 2.3

The saturated conversion dose (D) varied from 4 to 36 kGy for Ag^+ concentration from 1 to 50 mM and it was fitted as: D (kGy) = $-0.0041\ [Ag^+]^2 + 0.8674[Ag^+] + 3.2262$ ($R^2 = 0.9799$)

The d of silver nanoparticles was calculated to be as: d (nm) = $0.0016[Ag^+]^2 + 0.136[Ag^+] + 7.068$ ($R^2 = 0.9736$). Results indicated the Ag nanoparticles size to be in the range of 9 - 19 nm for the Ag^+ concentration from 1 to 50 mM.

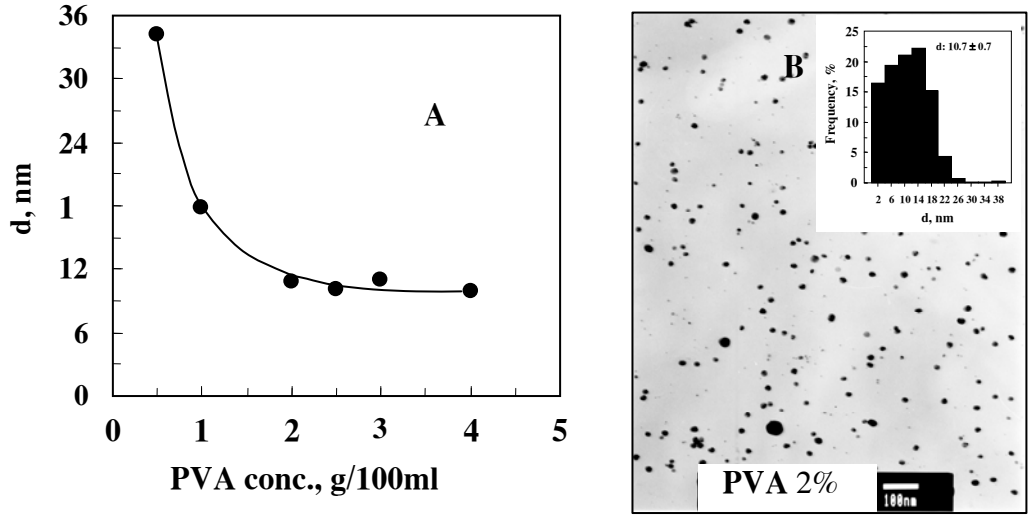

Fig. 2: The relationship of PVA conc. with d of colloidal silver nanoparticles 20 mM Ag^+

Fig. 2A showed the effect of PVA concentration on the size of Ag nanoparticles. It indicated that with the PVA concentration of 2 g/100ml are excellently selected. Fig. 2B showed a typical TEM image and size distribution of Ag nanoparticles from the sample of 20 mM Ag^+. It indicated that the Ag nanoparticles have spherical shape and Gaussian size distribution.

3.2. PVP stabilizer

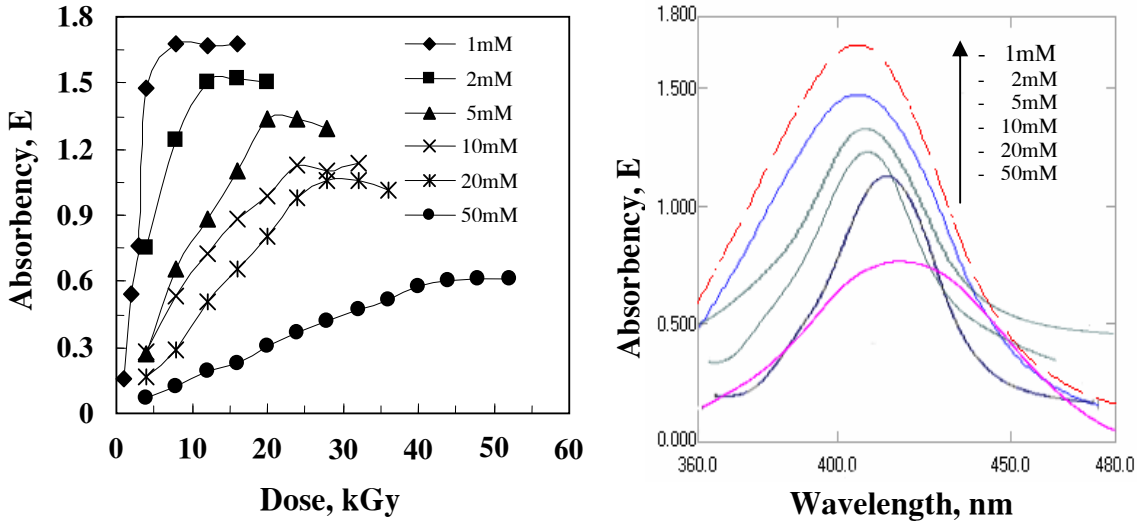

Fig. 3: The relationship of optical density of colloidal silver nanoparticles and doses

Table 2: The dependence of [Ag^+] on d of (PVP 2 g, ethanol 10 ml/100ml)

[Ag^+], mM	**1**	**2**	**5**	**10**	**20**	**50**
d, nm	5.1 ± 0.8	7.3 ± 1.0	9.5 ± 0.8	10.8 ± 1.1	12.2 ± 1.8	21.3 ± 2.4

Table 3: Effect of PVP molecular weight (MW) on colloidal silver nanoparticles

PVP- K90 $M_w = 10^6$Da		**PVP- K30** $M_w = 5\times10^4$Da		**[Ag^+]** (mM)	**D** (kGy)	**d** (nm)
E	$\lambda_{max.}$	E	$\lambda_{max.}$			
1.6806	405.5	-	-	**2**	**12**	**7.3 ± 1.0**
1.1279	409.5	-	-	**10**	**24**	**10.8 ± 1.1**
1.0574	411.0	-	-	**20**	**32**	**12.2 ± 1.8**
-	-	1.1974	407.0	2	12	14.1 ± 0.7
-	-	0.9232	412.5	10	24	17.0 ± 2.4
-	-	0.9000	417.0	20	32	21.7 ± 1.9

PVP K90 with high M_W showed good stabilization effect compared to that of K30 low M_W, particularly the size of silver nanoparticles was smaller in PVP K90.

The saturated conversion dose (D) varied from 8 to 48 kGy for Ag^+ concentration from 1 to 50 mM and it was fitted as: D (kGy) = – 0.0041 $[Ag^+]^2$ + 0.8674$[Ag^+]$ + 3.2262 (R^2 = 0.9799).

The d of silver nanoparticles was calculated to be as: d (nm) = 0.0016$[Ag^+]^2$ + 0.136$[Ag^+]$ + 7.068 (R^2 = 0.9736). Results indicated the Ag nanoparticles size to be in the range of 5 nm to 21 nm.

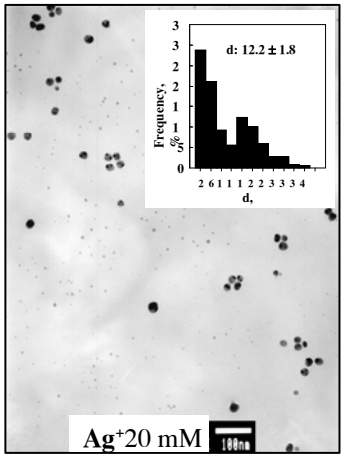

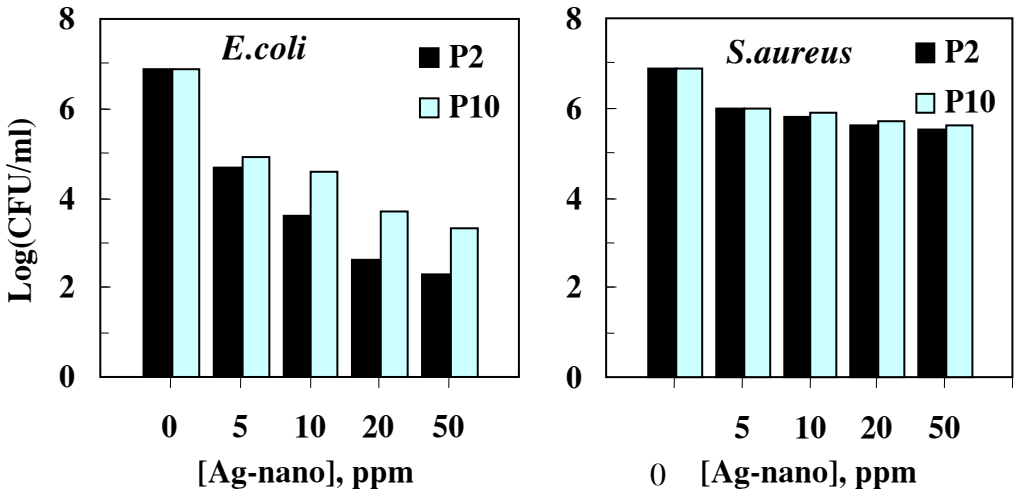

Fig. 4: Effect of silver nanoparticles on bacterial growth

Results in Fig. 4 indicated that silver nanoparticles with the size of 7.3 nm (P2) and 10.8 nm (P10) showed inhibition effect against *E.coli* and *S.aureus* more than 90% at 10 ppm and concentration dependence. The bactericidal property of silver nanoparticles was more effective against *E.coli* than *S.aureus*.

4. Conclusions

Colloidal silver nanoparticles were synthesized by gamma Co-60 irradiation of Ag^+ concentration from 1 to 50 mM using PVA and PVP as stabilizer.

Maximum absorption wavelengths (λ_{max}) of silver nanoparticles were from 400 nm to 420 nm.

The saturated conversion dose obtained from 4-36 kGy for PVA and from 8-48 kGy for PVP.

The suitable concentration of stabilizer was 2 g/100ml and high molecular weight exhibited good stabilization effect.

The average size of silver nanoparticles was in the range of 9-19 nm for PVA and 5-21 nm for PVP.

Silver nanoparticles with the size of about 10 nm showed strongly inhibition effect against *E.coli* and *S.aureus*.

REFERENCES

[1]. K.A. Bogle, S.D. Dhole, V.N. Bhoraskar, Silver nanoparticles: Synthesis and size control by electron irradiation, *Nanotechnology*, 17, pp.3204-3208, 2006.

[2]. http://lifesiver.com/

[3]. S. Silver, L.T. Phung, G. Silver, Silver as biocide in burn and wound dressings and bacterial resistance to silver compounds, *J. Ind. Microbiol. Biotechnol*, 33, pp.927-634, 2006.

[4]. Z. Zhang, B. Zhao, L. Hu, PVP protective mechanism of ultrafine silver powder synthesized by chemical reduction processes, *J. Solid State Chem.*, 121, pp.105-110, 1996.

[5]. T. Li, H.G. Park, S.H. Choi, γ-irradiation-induced preparation of Ag and Au nanoparticles and their characterizations, *Mater. Chem. Phys.*, 105, pp.325-330, 2007.

[6]. D. Meisel, Radiation effects on nanoparticles, *IAEA-TECHDOC-1438*, pp.125-136, 2005.

[7]. M. Kumar, L. Varshney, S. Francis, Radiolysis formation of Ag clusters in aqueous polyvinyl alcohol solution and hydrogel matrix, *Radiat. Phys. Chem.*, 73, pp.21-27, 2005.

[8]. B.D. Du, D.V. Phu, N. Trieu, N.Q. Hien, Synthesis of colloidal silver nanoparticles by γ-irradiation methods, J. Chem. Appl., (in Vietnamese), 3(63), pp.40-43, 2007.

[9]. K.S. Chou, C.Y. Ren, Synthesis of nanosized silver nanoparticles by chemical reduction method, *Marter. Chem. Phys.*, 64, pp.241-246, 2000.

[10]. Ministry of Health, Permit No: *09/2006/QĐ-BYT*.

PAPERS PUBLISHED IN RELATION TO THE PROJECT:

1. Nghiên cứu chế tạo bạc nano bằng phương pháp chiếu xạ, Tạp chí Hóa học và Ứng dụng, Số 3(63), Tr.40-43, 2007.
2. Synthesis of silver nanoparticles by γ-ray irradiation using PVA as stabilizer, Tạp chí Hóa học, Số ĐB(45), Tr.136-140, 2007.
3. Nghiên cứu chế tạo keo bạc nano bằng phương pháp chiếu xạ gamma Co-60 dùng PVP/chitosan làm chất ổn định, Hội nghị KH&CN Hạt nhân toàn quốc lần thứ 7, Đà Nẵng, 8/2007.
4. Hiệu ứng ức chế vi khuẩn hiếu khí trong nước cắm hoa của keo bạc nano chế tạo bằng phương pháp chiếu xạ, Hội nghị KH&CN Hạt nhân toàn quốc lần thứ 7, Đà Nẵng, 8/2007.
5. Preparation of colloidal silver nanoparticles in poly (N-vinylpyrolidone) by γ-Irradiation, Hội thảo Quốc tế lần thứ 1 về Công nghệ nano và ứng dụng, Vũng Tàu, 11/2007.

STUDY OF GAMMA RADIATION EFFECT ON NATURAL POLYMER OF EXTRACTED PEAT HUMIC/HUMATE TO APPLY IN AGRICULTURE

Le Huu Tu, Le Hai, Nguyen Tan Man, Tran Thi Tam, Tran Thu Hong
Pham Thi Sam, Nguyen Tuong Ly Lan and Le Van Toa

Nuclear Research Institute, VAEC, Vietnam.

ABSTRACT: Study of gamma radiation effects on the natural polymer such as humic/ humate, which was extracted from the peat, has been carried out. The parameters effect on the extraction yield of humic such as alkali concentration and ratio of NaOH and KOH mixture; dilution; extraction temperature and extraction time have been evaluated. The studied results indicated that the optimal parameters of extracting process of humic/humate have been investigated as follows: concentration of alkali is 2% with ratio of NaOH : KOH (1:1); at temperature 65^0C for 2hrs, extraction yield is 76%.

Under action of ionizing radiation like gamma Co-60, humic/humate is occurring crosslinking and degradation reactions in which depends on the absorbed dose and irradiation conditions. The optimal dose for degradation of humic in powder form was 500kGy while in 9% solution that was only 150kGy. The molecular weight of the original humic was 7,427 Da and after irradiation of 150kGy that was reduced and reached the value of 5,384 Da, the dissolubility of irradiated humic increases 1.8 times compared with the original. The other characters of product such as functional group exchange (IR spectra), the viscosity of solution of irradiated humic have been investigated as well. The product is promising in good application in future.

I. THE CONTENT OF PROJECT

1. The extracting process of humic/humate from the peat.

2. The effects of gamma radiation on humic/humate.

- The effect of gamma radiation on the dissolubility of humic acid.
- The effect of gamma radiation on the change of molecular weight of humic acid.
- The effect of gamma radiation on the change of viscosity of humic acid.

II. OBTAINED RESULTS

1. The optimal parameters of extracting process of humic/humate have been investigated as follows: concentration of alkali is 2% with ratio of NaOH : KOH (1:1); at temperature 65^0C for 2hrs, extraction yield is 76%.

2. The effects of gamma radiation on humic/humate.

- The dissolubility of irradiated humic acid increases 1.8 times compared with the original. The result is shown in figure 1.

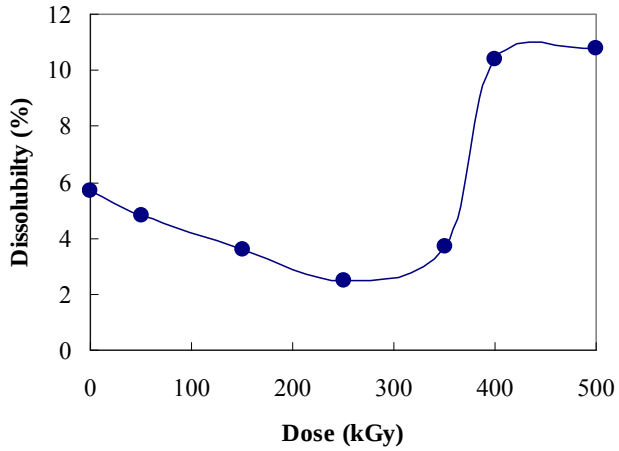

Fig. 1: The dependence of dissolubility of humic acid on dose

- The molecular weight of the original humic acid was 7,427 Da and after irradiation of 150 kGy that was reduced and reached the value of 5,384 Da. The results were presented in table I.

Table I: The dependence of molecular weight of humic acid on dose

Dose, kGy	0	20	30	50	70	100	150
[η]	0,28	0,31	0,36	0,33	0,29	0,26	0,22
$\overline{M_v}$	7.427	8.506	10.383	9.245	7.782	6.728	5.384

- The viscosity of humic acid increases from 22 Cps to 95 Cps in dose range from 0 kGy to 250 kGy and decreases from 95 Cps to 17 Cps in dose range from 250 kGy to 400 kGy. The result is shown in figure 2.

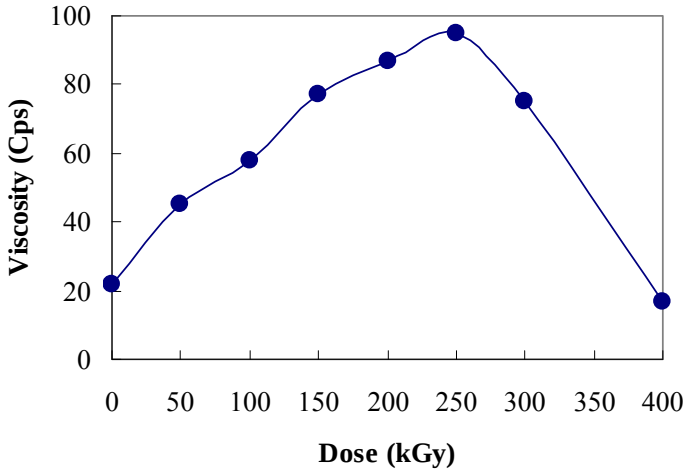

Fig. 2: The dependence of viscosity of humic acid on dose

III. CONCLUSION

1. The extracting process of humic/humate from the peat has been investigated.

2. The optimal dose for degradation of humic in powder form was 500kGy while in 9% solution that was only 150kGy.

3. By the method of irradiation could be produced the high concentration of humic acid solution but its viscosity is low. The product is stable in storage and promise in good application in future.

REFERENCE

[1]. Thổ nhưỡng học, Trường Đại học Nông nghiệp 1, Nhà xuất bản Nông thôn (1975), trang 64-68.

[2]. Nguyễn Quốc Hiến, Hóa học Bức xạ và các quá trình công nghệ bức xạ, Trường Đại học Đà Lạt (2000).

[3]. Nguyễn Hữu Đĩnh, Trần Thị Đà, Ứng dụng một số phương pháp phổ nghiên cứu cấu trúc phân tử, Nhà xuất bản Giáo dục (1999).

[4]. Lê Hải và các cộng sự, Nghiên cứu chế tạo gel nước bằng kỹ thuật bức xạ ứng dụng trong khai thác thu hồi dầu. Đề tài cấp cơ sở Viện Nghiên cứu hạt nhân, năm 2000.

[5]. Nguyen Quoc Hien et al., Growth-promotion of plants with depolymerized alginates by irradiation, Radiation Physis and Chemistry, Vol. 59, page 97-101 (2000).

[6]. Determination of humic acids in water samples.
http://en.wikipedia,org/wiki/humic acid.

[7]. Properties of humic substances.
http://www.ar.wroc.pl/~weber/kwasy2.htm.

[8]. Junping Zhang, Ruifeng Liu, An Li, and Aiqin Wang, Preparartion, Swelling Behaviors, and Slow-Release Properties of a Poly (actylic acid-co-acrylamide)/ Sodium humate Superabsorbent Composite. Center of Ecological and Green Chemistry. Lanzhou Institute of Chemical Physics, Beijing 100049, P.R. China.

[9]. Organic Solutions for Growth. http://www.australianhumates.com.

[10]. Humic aid and the Optimum Soil for Plants. http://www.sciencebuddies.org

1.9 - Radiochemistry and Materials Science

STUDY ON PREPARING POROUS HYDROXYAPATITE CERAMIC FOR BORN REPLACEMENT IN ANIMAL

Do Ngoc Lien, Nguyen Duc Kim, Dang Ngoc Thang, Cao Phuong Anh
Tran Thi Thanh Hien, Trinh Binh, Ngo Duy Thin and Luu Dinh Mui

Institute for Technology of Radioactive and Rare Elements, VAEC, Vietnam.

ABSTRACT: The present study describes synthesis of hydroxyapatite (HA) powders by using a wet chemical route with calcium nitrate and ammonium hydrogen phosphate.

The synthesized powders have been used for preparing porous ceramics in the block and the grain forms.

The block and grain porous ceramics have been tested for bone substitutes in animals such as dogs and rabbits.

The experimental results show that the prepared porous ceramic is a bioactive material having the potential and opportunity for development as bone substitutes.

On the other hand coatings of bioactive calcium phosphate prepared by electro deposition and by sol-gel technique have been introduced in this work.

Introduction

Synthetically produced calcium phosphate ceramics and implant have an important position among other biomaterials, because they are considered to be almost fully biocompatible with living bodies when replacing the hard bone tissues.

Calcium hydroxyapatite ($Ca_{10}(PO_4)_6$ $(OH)_2$) (HA) and tri-calcium phosphate (Ca_3 $(PO_4)_2$) (TCP) are currently recognized as ceramic materials that significantly simulate the mineralogical structure of bone.

HA and TCP powder can be synthesized by using techniques such as co-precipitation [1,2] or sol-gel methods [3-7] from aqueous solutions that contain calcium nitrate $Ca(NO_3)_2$ and diammonium hydrogen phosphate ($(NH_4)_2HPO_4$). The latest agents were selected as the starting materials in our studies.

As our knowledge, HA ceramic can be considered as bioactive and non-biodegradable bone replacement material. However, the HA grain having no biodegradability alveolar ridge augmentation is surrounded so it has no effect. As a result, β-TCP ceramics have been developed as a biodegradable bone replacement. However, the rate of biodegradation of β-TCP which has been shown is too fast. Biphasic calcium phosphate ceramic (i.e., composite ceramics) that consists of mixture of both HA and β-TCP phases has been used to slow the rate of biodegradation.

Experimental procedure

1. Preparing 0,1M $Ca(NO_3).4H_2O$ stock solution

Calcium nitrate tetra hydrate powder (23.40g) (99% Merck, Germany) was dissolved in 700 ml of distilled water at room temperature, and the solution was then stirred for a few minutes until the nitrate salt completely dissolved. The 10% ammonium solution was used to adjust to a pH value of 10. The working volume was later increased to 1000 ml via the addition of distilled water.

2. Preparing 0.06M $(NH_4)_2$ HPO_4 stock solution

Diammonium hydrogen phosphate (8.0g) (99 + % Merck) was placed into a 1000 ml beaker at room temperature. The powder was then readily dissolved by stirring in 700 ml of distilled water for a few minutes. The 10% ammonium solution on was used to adjust to a pH value of 10. The working volume was later increased to a lit via the addition of the required amount of distilled water.

3. Chemical precipitation

Calcium nitrate solutions of the proper concentration were added to the solutions of diammonium hydrogen phosphate at the rates of 2, 4, 6, 8, 10, 12, 14 and 16 ml/min under continuous stirring.

Results and discussion

1. Morphology of HA particles at various pH values

The Figure 1 shows the TEM micrographs of the HA powders at various pH values. It is reported that the morphology of HA particle changes from spheroid to needlelike with increasing pH values from 10 to 12.2. The precipitation of HA crystals can be to star at pH = 7.4 value. However, the growth rate at this value of pH is too small and the growth rate at pH = 12.5 value is too fast. Thus, the growth rate at a pH value of 10 is the most comfortable.

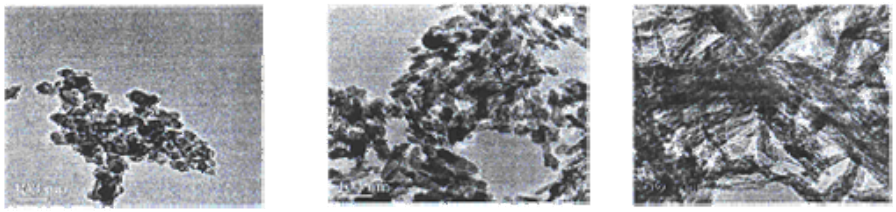

Fig. 1: Morphology of HA particles at various pH values

a. pH = 10 b. pH = 11.5 c. pH = 12.5

2. The relation bet ween addition rate of calcium nitrate and the Ca/P Ratio

Table 1: Influence of addition rate of calcium nitrate on Ca/P ratio

Samples	Addition rate ml/min	%Ca	%P	Ca/P ratio	Content
1	2	35.90	16.89	1.63	80% HA - 20% TCP
2	4	36.30	17.03	1.65	89% HA - 11% TCP
3	6	36.45	17.05	1.66	95% HA - 5% TCP
4	8	36.80	17.08	1.67	100% HA
5	10	37.45	17.30	1.68	Mixture of HA and CaO

From the table 1, it is reported that the addition rate of calcium nitrate can drive the content of hydroxyapatite powder. The addition rate of calcium nitrate has been chosen to be 4 - 6 ml/min. Thus, biphasic calcium phosphate powder that consist of mixture of both the HA and TCP phases have been reached.

3. The relation between the ripening time and crystal particle size

The table 2 that shows the crystal particle size decreased with increasing ripening time. It can be explained that rate of precipitation at the beginning time is too fast. Thus, the crystal particle size will be large and with increasing ripening time, the large crystal will be dissolved to create smaller crystal. It is reported that the morphology of the HA particles changes from needlelike to spheroid with increasing ripening time.

Table 2: Influence of ripening time on crystal particle size

Ripening time (hour)	6	12	24	48	72	100
Crystal particle size (nm)	53	47	42	40	38	37

4. Preparing hydropxyapatite coatings by electrochemical method

The electrochemical method has been used to activate stainless steel surface by synthesizing bioactive calcium phosphate coatings. Stainless steel serving as cathode was used in an electrochemical cell with a supersaturated calcium phosphate solution serving as electrolyte.

The experimental results have shown that the content of bioactive calcium phosphate (BCP) changed when electrode potential and temperature changed.

The table 3 and the table 4 show the experimental results.

Table 3: Influence electrode potential on content of BCP coating

Exp. Condition: Electrolysis at 65^0C, treatment temperature 700^0C

Samples	**Electrode potential (V)**	**% HA**	**% TCP**	**% $CaHPO_4$**
M_1	-1.05	21.50	56.30	22.20
M_2	-1.25	36.50	63.50	0
M_3	-1.45	100.00	0	0
M_4	-1.65	30.20	52.20	17.60
M_5	-1.85	36.40	63.60	0

Table 4: Influence of temperature of electrolysis on content of BCP coatings

Exp. Cond: Electrode potential – 1,45V, treatment temperature 700^0C

Sample	**Temperature**	**% HA**	**% TCP**	**% $CaHPO_4$**
M_6	45^0C	69.20	30.80	0
M_7	55^0C	100.00	0	0

M_8	65^0C	100.80	0	0
M_9	75^0C	100.00	0	0
M_{10}	85^0C	100.00	0	0

5. Substituting bone of animals by the block and grain porous ceramics

The experimental results show that the products of work can be used as bioactive and biocompatible materials for bone substitutes. The synthetic block and grain composite ceramics has excellent biocompatibility and promising bioactivity due to it resemble composition and structure of bone and tooth minerals.

Furthermore, the grain ceramic prepared by us is completely similar to the grain ceramic fabricated by fine ceramic commercial products of Italy.

Conclusions

1. Sub micrometer - sized calcium hydroxyapatite - tricalcium phosphate (HA-TCP) composite bioceramic powders have been synthesized.

It should be remembered that the HA phase represents the “bioinert” component and the TCP phase is the “bioresorbable” agent in these composite bioceramic.

2. The products of this work in block and grain ceramic have been tested for bone substitutes in animals such as dogs and rabbits .

The testing results showed that the porous ceramic prepared by this work is bioactive materials having the potential and opportunity for applications in both dentistry and medicine.

REFERENCES

[1]. A.C. Tas, F. Korkusuz, M.Timicin and N. Akkas "An investigation of the chemical synthesis and high temperature sintering behavior of calcium hydroxyuapatite (HA) and tricalcium phosphate (TCP) bioceramics" *J. Mater. SCi; Mater. Med. 8 91-96 (1997).*

[2]. S.H. Rhee and J. Tanaka, "hydroxyapatite coating on a collagen Membrane by a micro mimetic method" *J. Am. Ceram. Soc 81 3029 - 3031 (1998).*

[3]. P. Layrolle, A.Ito" Sol - gel synthesis of amorphous calcium phosphate and sintering into micro porous hydroxyapaptite Bioceramics" *J. Am. Ceram. Soc 81 1421 - 28 (1998).*

[4]. Jillavenkatesa and R. A. condrate "Sol-gel" processing of hydroxyapatite" J. Mater. SCi. 33 4111 - 19 (1998).

[5]. C. M. Lopatin, V. Pizziconi "Hydroxyapatite powder and thin films prepared by a sol-gel technique" *Thin Solid films 326 227 - 32 (1998).*

[6]. H. K. Verma, S.N. Kalkura - "polymeric precursor route for the preparation of calcium phosphate compounds" *Ceram. Int 24 467 - 470 (1998).*

[7]. G. Kordas, C. C. Trapalis "Fourier - Transfilm and multidimensional EPR spectroscopy for the characterization of sol-gel derived hydroxyapatite" *J. Sol-Gel Sci. Technol 9 characterization 17-24 (1997).*

PROCESSING PA LUA URANIUM ORE BY MIXING AND CURING WITH SULFURIC ACID ON A SCALE OF 500 KG/BATCH TO RECOVER YELLOWCAKE

Le Quang Thai, Cao Hung Thai, Le Thi Kim Dung, Phung Vu Phong, Tran Van Son Doan Thi Mo, Hoang Bich Ngoc, Nguyen Hong Ha, Vu Khac Tuan, Vu Hung Trieu Tran Van Hoa, Nguyen Duy Phap, Doan Thanh Son and Pham Quang Minh

Institute for Technology of Radioactive and Rare Elements, VAEC, Vietnam.

ABSTRACT: Uranium ore in Pa Lua area is sandstone with different levels of weathering. This kind of ore contains calcium and clay that may cause clogs during heap leaching. In this study, a technique of mixing and curing with strong acids is used and followed by washing to recover uranium. This study also focuses on study of ore processing issues such as crushing, regenerating particles in fine ores, mixing, curing and washing. The leach solution is treated by ion-exchange and precipitation of products by NH_4OH. The experiment results show that regenerating a portion of fine ores, mixing and curing help washing residues in the column more effectively. Flow rate of the input solution can be controllable and stable. Columns don't clog even when washing takes place in the ore column of 5 meters high. Efficiency of uranium recovery can reach to 85-90%. Products of technical uranium are obtained with high quality.

Key words: Uranium, uranium ore processing.

Introduction

Facing the risks of depletion of uranium sources and sharply rising price of uranium, besides, looking for solutions of renovating fuel cycle and producing new generation of reactors, many companies have strengthened exploration of new uranium ores and paid more attention to low-grade ores. Moreover, from the beginning of 2006, the Government has officially allowed to build the first nuclear power plant in Vietnam in order to put it into operation around the period of 2017 - 2020. In this context, continuing research for completion and selection of the most appropriate technology for uranium ore processing in Vietnam is extremely necessary and crucial. This is in line with the development trend in the world and at the same time helps gradually produce locally fuel for nuclear power plants.

The project entitled " *Processing Pa Lua Uranium by Technique of Mixing and Curing at a Scale of 500 kg/batch to Recover Technical Uranium*" was set up to conduct additional researches on several technical issues of mixing and curing with acid and washing to recover uranium from sandstone ores in Pa Lua area to complete a set of data in ore processing procedure, to develop an appropriate technological procedure for ore processing, calculating and designing several main equipments based on the data obtained from the study and previous ones.

Basics of the method

In water, sulfuric acid is dissociated into sulfate, bisulfate and hydrogen ions. These ions react with uranium (VI) in ores to create sulfate uranyl and complexes of sulfate uranyl. Depending on concentrations of acid and uranium, temperature and other complexes in the system, there may be any type of uranium in the solution. Uranium in

the ore under the form of U (IV) must be oxidized before the dissolution takes place. It is Fe^{3+} ion that is oxidant in the oxidation reaction of U (IV) in leaching precess by sulfuric acid. Iron is always present because the ore contains iron. In addition, during crushing and grinding ores, iron is also added due to abrasion of the equipment. However, to maintain Fe^{3+}, a certain amount of oxidants is needed.

Acid consumption is a function of constituents in the ores. Calcite, dolomite, magnetite and siderite react with acid right at the zone of low acid concentration and normal temperature. Sulfide, metal iron, several types of phosphate, molybdate, vanadate, oxides, flouride etc. consume acid and contaminate solutions when temperature or acid concentration increases.

In the process of mixing and curing with acid, most reaction of acid with minerals complete. Washing solution through the next layer is just simply to rinse residues to recover uranium. In the void of ore layer, there is air together with solution; therefore, leaching is an unsaturated system. Thus, to control leaching, it is necessary to pay attention to the conditions of complicated flow for hydraulics of unsaturated area. Two key issues of hydraulics are sufficient flow and (or) uniform flow through the ore heap. Sufficient flow is necessary so that the ore heap is percolated in an appropriate duration (cost effective) while uniform flow is necessary to allow the whole ore body is well leached. Leaching and washing require the ore body to have relatively well infiltration and the materials need to be uniform to avoid channels in the flow. Any portion of the ore body if not contacted well to the solution, will not be leached or rinsed.

Concerned ores

Sandstone ores used in the research have different weathering degrees. Sizes of non-weathered and semi-weathered ores are pretty large, mostly over 20 cm. Weathered ore is under the powder forms.

Main minerals of this sandstone ore are quartz (SiO_2), albite ($NaAlSi_3O_8$), glauconite ($(K,Na)(Fe^{+3},Al,Mg)_2(Si,Al)_4O_{10}(OH)_2$), calcite ($CaCO_3$), kaolinite ($Al_2Si_2O_5(OH)_4$), sericite ($K_2O.3Al_2O_3.6SiO_2.2H_2O$), illite ($(KH_3O)Al_2Si_3AlO_{10}(OH)_2$), siderite ($FeCO_3$), sphene ($CaO.SiO_2.TiO_2$). Mineral containing uranium is mainly Nasturan ($(U,Th)O_2.(O_{0,5\text{-}3})UO_3.xPbO$).

Uranium content in the ore is about 0.053–0.058%. The most abundant impurities are silica (average 75%), aluminum (>5%), iron (1%), potassium, sodium and alkaline metals (calcium in the non-weathered ores even reaches >0.9%) and many other impurities. Distribution of uranium based on particle sizes is relatively uniform.

Non-weathered and semi-weathered ores need to be crushed into particle sizes appropriate for chemical treatment.

Results and discussion

1. Crushing ores and calculating energy for crushing

For crude pieces of ores (>10 cm), it is needed to crush according to two levels (using crusher). In the first level, size is decreased to <10 cm, then in the second level, the size is decreased to appropriate size for mixing and curing stage.

When comparing grinding features of non-weathered and semi-weathered ores, it is shown that porosity of non-weathered ore is larger than that of semi-weathered one. In addition, non-weathered ores have less hardness. Most ore particles after crushing have their size bigger than 0.6 mm. Portion of fine particles that can cause clog in the ore column accounts for relatively low, less than 10%. Therefore this portion needs to be aggregated into bigger size depends on their impacts to the further treatment stages. The smaller width of the voids is, the higher fine portion is. It is possible to reduce the amount of fine ore by selecting an appropriate crushing condition that is without adjustment of the width of crushing gap to a certain value and with circulation of crude ore portion. However, it is also needed to pay attention to energy consumption and any raised issue.

For non-weathered and semi-weathered ores, to produce ore particles appropriate to heap leaching, using jaw crushing is the most appropriate. In order to get the ore with appropriate size for mixing and washing, appropriate width of the gaps between crushing bars in the second level is 20 mm.

In terms of energy, BOND formula has been used. For sandstone ore with average hardness, energy consumption for crushing 1 tone of ore with sizes reduced from 20 cm to 2cm is 0.46kW. However, in reality, depending on productivity of the equipment and operation, the real energy consumption may increase in comparison to the above calculated values. Results of calculation of consumed crushing energy will be used as basis for calculating capacity and productivity of crusher.

2. Recreating fine ores

The purpose of this process is to make ore portion of fine particles become particles with size large enough to ensure that washing process is not disturbed due to clogging or blocking the flow of solution. In addition, particles need to remain stable in leaching medium of acid. Uranium leaching efficiency needs to be at an acceptable degree without considerable impacts to the total efficiency of uranium recovery from the ores.

When investigating factors impacting to the process of recreation of particles, it is shown that necessary moisture content is 15 - 16% and duration of 14 - 16 minutes are needed. For the ore with size of -300 μm, the amount of liquid glass as adhesive appropriate for each type of non-weathered, semi-weathered and weathered ores are 6.9%; 6% and 4%, respectively. To strengthen ability of solidifying of the obtained pellets, Na_2SiF_6 is added with the rate of 1%. These agents mixture is selected for research because it creates pellets with certain stability after mixing and curing with strong acid while other agents do not have these characteristics. Results of trial of immersing in acid, ore pellets obtained in appropriate condition are as follows.

Table 1: Efficiency of uranium leaching and degree of particle broken down when creating particle in appropriate conditions

Ores	Efficiency of U recovery (%)	Degree of particle broken down (%)
Non-weathered	78.32	12.6
Semi-weathered	66.67	2.8
Weathered	63.86	13.7

Thus, after pelletizing, efficiency of uranium recovery partly reduces while acid consumption considerably increases (e.g. ordinary non-weathered ore when mixed and cured just consumes 50 kg acid/ ton of ore, but after pelletizing, this figure increases to 95 kg/ton of ore to reach uranium recovery over 75%. For semi-weathered ores: 35 kg/ton of ore, 80 kg/ton of ore and 66%, respectively). Degree of complete breaking down of pellets is in the acceptable range. The bigger initial ore particle size is, the more cost of agents is and the more difficult palletizing is.

Based on the above research results, in case it is necessary to pelletize, only portion of ore with particle sizes less than 0.3 mm needs to be pelletized. In that case, it is acceptable that acid consumption increase not much while efficiency of uranium recovery decreases a bit. If the ore contains a large portion of fine particles, the use of this method needs to be reconsidered because the efficiency of uranium recovery is impacted considerably. Moreover, high acid consumption and high operational cost can cause the increase of production price.

3. Mixing and curing

Several parameters related to ore mixing, curing and washing processes such as capability of water retention, void volume of the heap etc. are paid attention. In the ore body, water can be in the capillaries of ore particles, in the gap among ore particles and stick on the surface of particles and the wall of columns. For each ore particle size, the following parameters are determined (table 2). According to the results, the larger ore particles, the less water retention; therefore, it is very difficult to carry out mixing and curing process.

Table2: Capability of remaining water and void volume of all types of ores according to sizes of ore particles

Particle size (mm)	**Moisture content (%)**		**Total void volume (%)**	
	CPH	*BPH*	*CPH*	*BPH*
+ 20	1.4	2.0	59.2	58.5
- 20 + 10	3.7	6.0	57.5	57.8
-10 + 5	6.9	8.6	58.8	57.6
- 5	19.0	20.0	46.0	44.7

However, if ore body consists of many degrees of particle size with a certain ratio, due to the mixing of different ore sizes, degree of water retention and bulk density change (table 3), creating a favorable condition for reaction.

Table3: Distribution of particle size

TT	**Particle size (mm)**	**Weight ratio (%)**		
		Non-weathered	*Semi-weathered*	*Weathered*
1	+20		7.72	
2	+10 - 20	11.72	39.27	
3	+5 - 10	46.32	12.72	12.0

4	+2.36 - 5	13.62	5.83	5.6
5	+1.18 - 2.36	7.41	8.03	13.6
6	+0.6 - 1.18	6.91	8.24	30.4
7	+0.3 - 0.6	7.09	10.30	23.8
8	-0.3	6.93	7.90	14.6

Table 4: Degree of water retention and void volume of ores with many degrees of particle sizes

Ore type	Moisture content (%)	Total void volume (%)	Bulk density
Non-weathered	10.3	49.6	1.51
Semi-weathered	12.1	50.6	1.33
Weathered	20.2		

Determining water retention of ores allows us to calculate necessary amount of water during mixing and curing with strong acids.

During mixing and curing process, only a small part of acid is used to dissolve minerals containing uranium while most part of the acid is consumed by other minerals in the ore, especially carbonate (as in the case of non-weathered ore). Specific acid consumptions for each type of ores are as follows: non-weathered - 50 kg/ton, semi-weathered - 35 kg/ton and weathered ore - 30 kg/ton. If ore contains different minerals, acid consumption will be higher than the average value calculated according to the certain ratio. For example, acid consumption of 46 kg/ton is needed for the ore containing non-weathered and semi-weathered parts with a ratio of 1/1.

After mixing and curing with strong acid, initial ore particles are broken down into smaller sizes, especially for non-weathered ore. Degree of breaking down depends on initial particle size, acid concentration, duration of curing and degree of weathering. Therefore, degree of water retention as well as other parameters of ore residues changes a lot. Now, different levels of particle size stick together leading to the increase of water retention and the decrease void volume (see table 5).

Table5: Some features of ore tailings

Type of tailings	Moisture content (%)	Total void volume (%)	Bulk density
Non-weathered	16.2	37.9	1.55
Semi-weathered	14.3	39.0	1.47

However, the ratio of fine particles (<0.3 mm) almost does not increase. Obviously, when reacting with strong acid during mixing and curing, some products from reaction under the form of precipitant such as calcium sulfate, SiO_2, etc. aggregate fine particles together or with larger particles. This is an advantage for washing uranium in the next stage.

When investigating affect of oxidants to the efficiency of uranium dissolution, it is found that in non-weathered and semi-weathered ores, a part of uranium existing under the form of U (IV) cannot dissolve in acid solution. Therefore, an amount of oxidant to maintain iron concentration (Fe III) to supply for oxidizing reaction of U (IV) is required (around 3 kg/ton).

After being mixed with acid, the mixture is cured for 3 days. It is important that only after curing process is completed, the whole ore body is moved to columns or heaps to rinse for uranium recovery. If the ore is placed into the column right after completion of curing, the ore body will be pressed; therefore, fine particles will cause clog during washing process.

4. Washing for uranium recovery

After trials of options for washing ores that are mixed and cured with acid, it is found that the technique using batch washing should be used in combination with leaching. Based on this technique, at several initial washing times, the solution has pH value of 1. When each washing time is completed, the solution appears at the bottom of the column. When the solution mostly doesn't flow, it is the time to continue washing. Solutions with higher pH or clean water are used for washing residues. In the first washing times, total amount of solution released from the column will be smaller than the total amount of solution provided to the column because a part of solution is remained to maintain moisture content (the moisture content of residues increases) and time for the solution to break through the column will be longer than that of the further times of washing. This technique allows saving retention time of solution in the ore body so that reaction continues and amount of water needed is reduced. Efficiency of uranium recovery increases. For example, for non-weathered ore and semi-weathered ore, efficiency of uranium recovery can be 78% and 84.3% respectively while if solution with pH 2 is continuously rinsed, efficiencies can be 73.1% and 81.6%, respectively. The rate of washing is controllable.

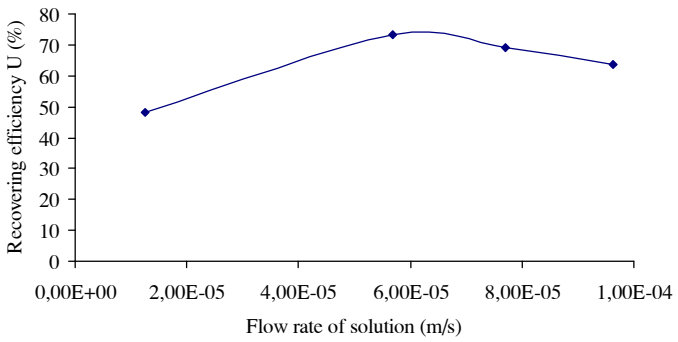

Ficgure 1. Effect of washing flow rate on uraium recovering efficiency (non-weathered ore)

Although after mixing and curing, all levels of particle sizes are more distributed than that of direct leaching on the column, it is unavoidable that there is a phenomenon in which

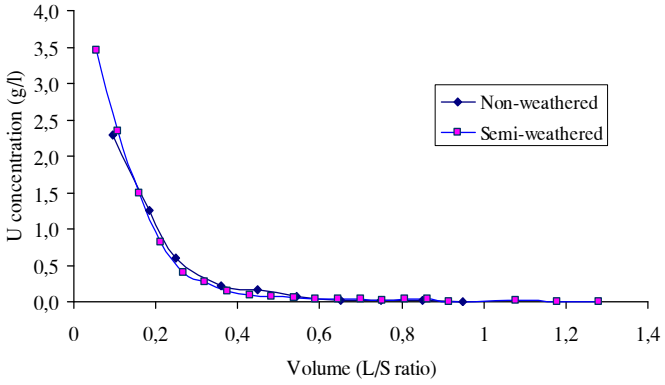

Ficgure 2. Washing curve for uranium recovery

residues of crude ore stick together in one place and fine particles stick together in another place causing inconsistence. In the primary study, if the flow rate of washing is getting higher, solution is getting more priority to go through ore body with large size and vice versa. Only when the flow rate is in a certain range, flow of solution will be likely consistent in the ore body. Therefore, the flow rate of washing is the most affecting factor in washing process. When trying with non-weathered ore which is mixed and cured as well as continuous rinsed with the total volume of solution reaches a ratio of L/R = 1/1v (L/R = liquid/solid). Diagram in the Figure 1 shows that only in a certain appropriate flow rates (around 6.00E-05 m/s); efficiency of uranium recovery reaches the highest value at 73.1%.

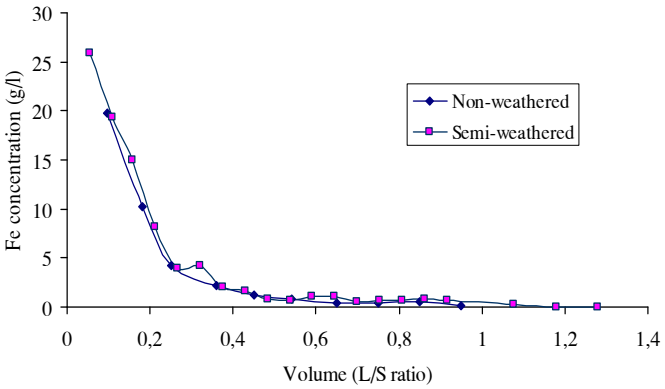

Ficgure 3. Iron washing curve

Flow rate depends on particle size. The finer ore particles size is, the lower flow rate is. For instance, for mixed ores consisting of 3 types of non-weathered, semi-weathered and weathered ores with a ratio of 1/1/1 in the first washing time, flow rate from outlet of the column just reaches 1.9E-05 m/s, and then increases more and more in the next washing times. For such fine ores like the above ones, flow rate also depends on the height of ore layer. The higher height, the more pressed the ore. Because void space is very small, the flow of solution is also blocked. Therefore, flow rate also is much decreased (for the height of 5 meters, the flow rate of the first washing time only reaches 7.78E-06 m/s). Time for washing also increases considerably when the height of ore layer increases.

During washing process, uranium and dissolved substances are rinsed right in the first time (see Figure 2. 3 and 4). Results show that the change of concentration and amount of dissolved substances almost takes place with a total volume of solution at the L/R ratio of 1/3. After that, though more amount of solution is needed, the amount of dissolved uranium obtained is only some percentages. Therefore, to decrease solution consumption and increase uranium concentration, the part of dilute solution needs to be circulated in the next columns. The part of high concentration is moved to the next treatment stage as ion exchange and consequently, precipitation to get technical uranium products.

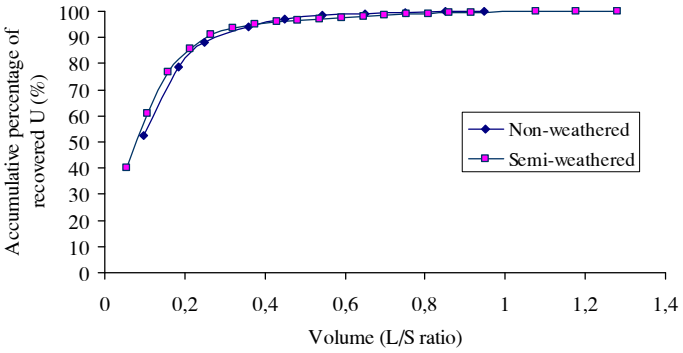

Ficgure 4. Accumulative percentage of recovered uranium with solution volume

Trial of processing ore on a scale of 500 kg/batch with mixture of non-weathered, semi-weathered and weathered ores at the ratio of 1/1/1 (height of ore layers in the washing column is up to 500 kg/batch) took place in a completely favorable condition. Washing is carried out with two stages, 6 times of washing without clogs of the column. Consumption of water when washing is just 1/3 of the weight of treated ores. Efficiency of uranium recovery reaches 85-90 %. Obtained solution contains around 1.2 g U/L.

After processing, the result obtained by using Amberlte IRA-420 resin in static column system, then followed by precipitation by agents H_2O_2 and NH_4OH, technical uranium with high quality (80% U_3O_8 and low contents of other metal impurities).

Conclusions

1. Using option of crushing at 2 levels in which the width of crushing gap at the second level of 20 mm is appropriate, can reduce the amount of fine ores. Energy consumption for this stage is 0.46 KW/ton of ore.

2. Regenerating particles in the portion of fine sizes which creates relatively stable particles in acid medium will have an ability to avoid clogging in the column when washing. However, this will cause the increase of acid consumption and partly decrease efficiency of uranium recovery, especially for semi-weathered and weathered ores. The larger initial size of ore particles, the higher degree of this change. This stage should only be applied for weathered ores with fine particles less than 0.3 mm on a scale in which the column is high.

3. During mixing and curing, ore is broken down too much, especially non-weathered ore. However, the portion of fine residues (less than 0.3 mm) mostly doesn't increase considerable, not causing any difficulty for the further process like washing to recover uranium. An appropriate mechanism for the stage is acid consumption of 30-55 kg/ton of ore; moisture content of 10-13%, oxidant 2-3 kg/ton of ore and curing duration of 3 days. After curing for 3 days, the ore needs to be cured before being placed in the washing column.

4. In the stage of washing, it is recommended that batch washing be applied and several initial washing times be used with pH 1 so that efficiency of uranium recovery can increase and the amount of washing water can be reduced. After mixing and curing process, flow rate of washing solution in washing stage can be controllable and stable in the whole process, avoiding column from being clogged. Appropriate flow rate of washing is around 6.0E-0.5 m/s. However, for weathered ores, the flow rate decreases considerably. Circulation of washing solution (2 stages) leads to the increase of concentration of uranium in the solution and reduction of water used.

When trying processing ores by mixing and curing, then washing on a scale of 500 kg/batch of ores, a solution containing 1.2gU/l was obtained. Amount of water consumed is equal to 1/3 ore weight. Duration for ore processing needs only 12 days. Efficiency of uranium recovery can reach up to 85-90%. Treatment of leaching solution by ion-exchange with amberlite IRA-420 resin is conducted and followed by precipitation to obtain product with concentration higher than 80% U_3O_8.

REFERENCE

[1]. Cao Hung Thai. Study on processing Pa Lua uranium ore in scale of 2tons/batch to recover technical uranium products. Report of Ministrial project 2001-2002, code BO/01/03/02. 2003.

[2]. Durupt Nicolas. Heap leaching of low grade uranium ores at Somair. Technical Meeting on Uranium Small-Scale and Special mining and Processing Technologies. Vienna. 19-22 June 2007.

[3]. IAEA. Recent Developments in Uranium Resources and Production with Emphasis on in situ Leach Mining. Proceedings of technical meeting organized by the IAEA in co-operation with the OECD Nuclear Energy Agency, The Bureau of Geology and China National Nuclear Corporation held in Beijing. 18-23 September 2002. IAEA-TECDOC-1396. 6/2004.

[4]. Merritt R.C. The Extractive Metallurgy of Uranium. First printing. Library of Congress Catalog Card No. 71-157076. p. 209. 417 - 490. USA. 1971.

[5]. O'Kane Consultants Inc., Demonstration of the Application of Unsaturated Zone Hydrology for Heap Leach Optimization. Industrial Research Assistance Program Contract #332407. Report No. 628-1. SK. 11/2000.

STUDY ON PRECIPITATION OF AMONI DIURANATE - $(NH_4)_3U_2O_7$ FROM UO_2F_2 - HF SOLUTION FOR FUEL CERAMIC UO_2 POWDER PREPARATION

Dang Ngoc Thang, Pham Danh Khanh, Ha Dinh Khai, Nguyen Van Doan
Tran Thi Hong Thai and Pham Hung Vuong

Institute for Technology of Radioactive and Rare Elements, VAEC, Vietnam.

ABSTRACT: Precipitation of ammonium diuranate (ADU) with ammonia solution was carried out at different flow rates of UO_2F_2- HF solution and at different mole ratio NH_4^+/UO_2^{2+}. Their effects on the characteristics of ADU and uranium content of mother liquors have also been studied. Mole ratio NH_4^+/UO_2^{2+}, precipitation rate and aging time are essential parameters to control the characteristics of ADU such as distribution of particle size, specific surface area and settling nature of precipitate. By concurrently dropping UO_2F_2- HF solution and concentrated ammonia solution into a NH_3 solution with mole ratio NH_4^+/UO_2^{2+} controlled and further aging after precipitating, ADU precipitate with large specific surface area, narrow distributions of particle size and low fluorine content has been obtained.

Keywords: Ammonumi diuranate; precipitation; aging; Ammonium uranyl fluoride.

Introduction

Uranium dioxide UO_2 for manufacturing fuel of light water reactor is currently produced from uranium hexafluoride UF_6. In this process, UF_6 is hydrolyzed with water to form an aqueous UO_2F_2-HF solution, from which ADU is precipitated with ammonia solution. The precipitation of ADU from uranyl fluoride solution after hydrolyzing UF_6 is an primary step in the process of ceramic UO_2 production.

Our work is concerned with precipitation of ADU for producing ceramic UO_2 from UO_2F_2-HF solution, which is similar to hydrolyzed UF_6 solution in chemical composition.

Research Results

1. Precipitation of ADU

ADU is precipitated from UO_2F_2- HF solution with ammonia solution [3]

$$HF + NH_3 + H_2O = NH_4F + H_2O$$

$$2UO_2F_2 + 6NH_3 + 6H_2O = (NH_4)_2U_2O_7 \downarrow + 4NH_4F + 3H_2O$$

An UO_2F_2- HF solution containing about 70gU/l and an 12M NH_3 solution are concurrently added to an 3M NH_3 solution which is being rapidly stirred. The flow rate of addition of UO_2F_2 solution and of ammonia solution is 10ml/min. and 5.5ml/min., respectively. The temperature in the precipitation vessel is maintained at around 25^0C. Precipitate is subsequently aged for about 5 hours and then washed with water to remove fluorides.

As being precipitated under these conditions, the ammoni diuranate slurry contains about 4% fluorides and has a surface area of only 4 - 10 m^2/g. However, when the ADU cake is washed with water and refiltered, the fluoride content decreases to less

than 1% and the surface area increases to above 20 m^2/g. The particle size distribution and morphology of ADU precipitate is shown in the figures 1 and 2.

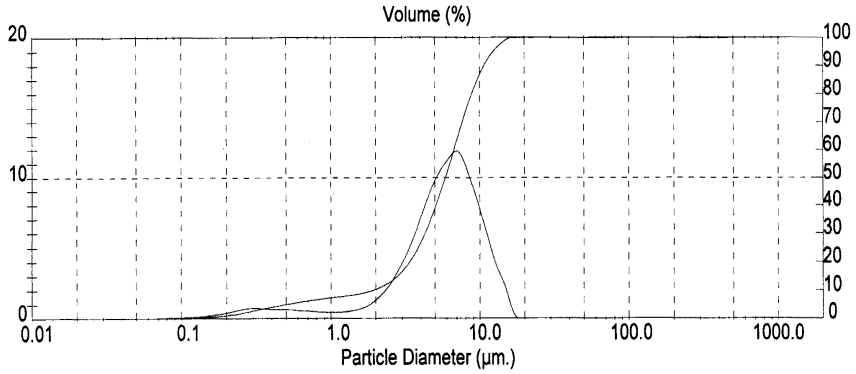

$\bar{D}$, µm	$D_{0.1}$, µm	$D_{0.5}$, µm	$D_{0.9}$, µm
6.09	2.04	5.84	10.46

Fig. 1: Particle size distribution of ADU precipitate after aging.

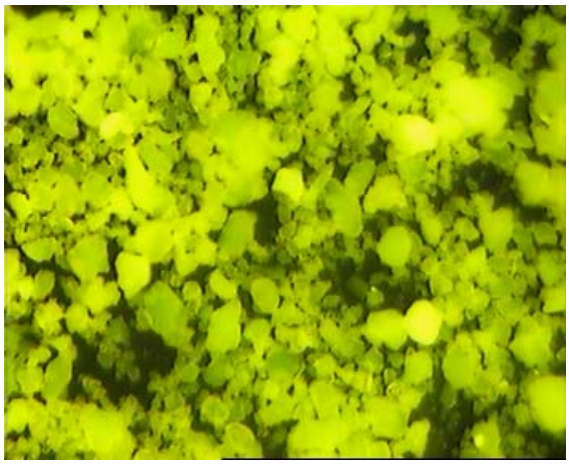

Fig. 2: Morphology of ADU precipitate after aging.

After washing, ADU is dried at about 90^0C. ADU product is porous, mainly in crystal form as shown in the figure 3 and 4.

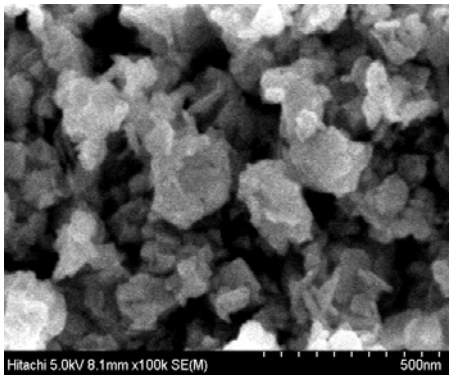

Fig. 3: The micrograph of ADU powder.

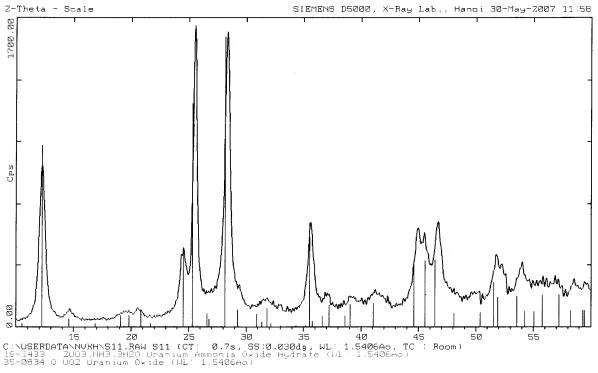

Fig. 4: The diagram XRD of ADU powder.

The ADU powder after drying has characteristics as follows:

- The surface area of 21.7 m^2/g
- The fluorine content of 0.83%.

2. Preparation of UO_2 powder

The ADU product is calcinated and then reduced to UO_2 powder at 700^0C for 4 hours. The UO_2 powder, prepared from this ADU precipitate has an average particle size of 2.78 μm and a surface area of $3.87m^2/g$. The morphology of UO_2 powder is shown in the figure 5.

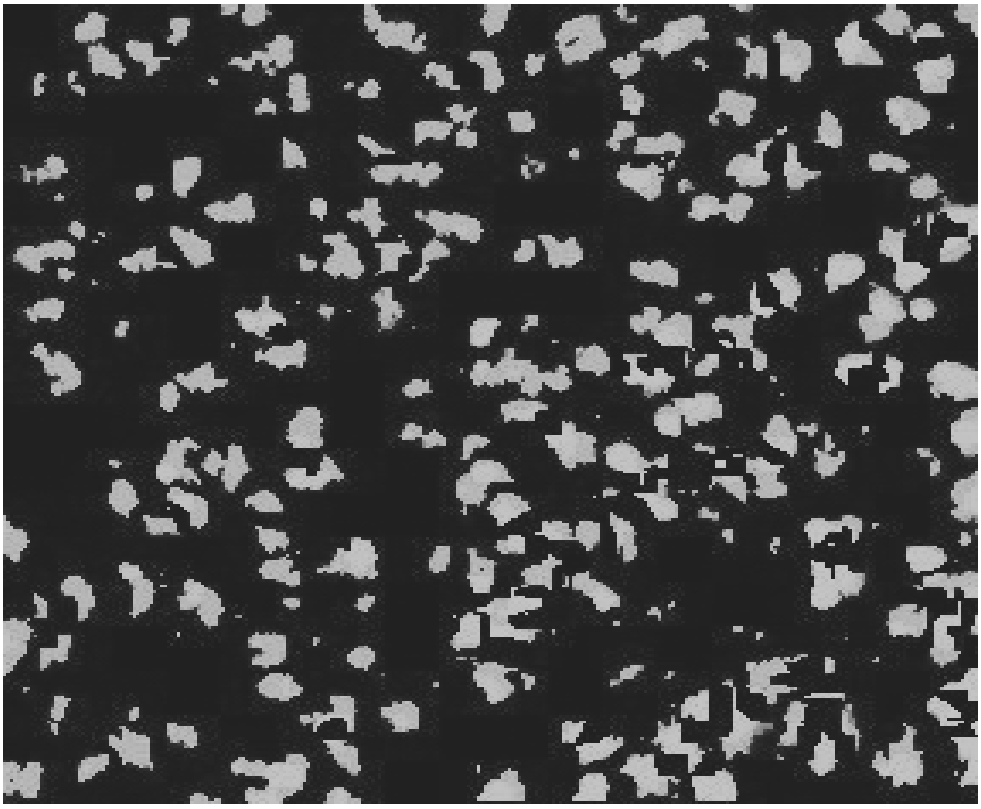

Fig. 5: The morphology of UO_2 powder reduced at 700^0C.

REFERENCES

[1]. John M. Googin, "Enriched Uranium Processing", Union Carbide Nuclear Company–USA,1963, p.29 – 32, 47-58, 130 -132.

[2]. А. А. Майоров, «Технология Получения Порошов Керамической Двуокиси Урана», Энергоатомиздат, Москва, 1985.

[3]. Н. П. Галкин, "Химия и Технология Фтористых Соединений Урана", Государсвенное Издательство Литературы в Области Атомной Науки и Техники, Москва, 1961.

[4]. G. V. S. R. K. Somayajulu, "Fabrication of Fuel for Light Water Reactors", Material Science Forum 1989, p. 1705 -1714.

STUDY ON THE SYNTHESIS OF DISIDA DERIVATIVES FOR LABELING WITH ^{99m}Tc

Pham Ngoc Dien, Duong Van Dong, Nguyen Thi Thu
Bui Van Cuong, Mai Phuoc Tho and Vo Cam Hoa

Nuclear Research Institute, VAEC, Vietnam.

ABSTRACT: This study describes the synthesis method and characterization of 2,6-Diisopropyl acetanilide iminodiacetic acid (DISIDA).

DISIDA is synthesized by replacement reaction of two Clo atoms in chloroacetyl chloride molecule. The synthesis process has two steps:

Step1: The synthesis of 2,6-diisopropylacetanilide

Step 2: The synthesis of DISIDA

The good result obtained in the step 1 reaction, it was carried out in the low pH i.e acid medium. The synthesis reacction achieved high performance at room temperature for 2 hours. The product was crystallized completly while adding in mixture reaction amount sodium acetate by drop wise and stir slowly.

The step 2 reaction was carried out in medium of alkali (pH = 10-12), reaction temperature was 50^0C-60^0C, reaction time during 8 hours.

After that EtOH was evaperated by vaccum and compound was crystalized with pH = 2-3, in cool medium (<10^0C).
Raw material was recrystalized many time by cool EtOH.

Pure product (DISIDA) was characterized by IR, LC/MS, HPLC spectroscopy, melting point, crystal picture.

Synthesized DISIDA, when tagged with diagnostic radionuclids such as ^{99m}Tc are quite good, ^{99m}Tc-DISIDA Complexes with RC purity and labeling efficency >98% and above could be prepared by ordinary reaction condition, that reason can apply for valuation of posibility and reality on different purposes.

I. INTRODUCTION

Within the last decade, there has been an increasing interest in developing new radiopharmaceuticals for Diagnostic techniques and therapy, especially Diagnostic techniques in nuclear medicine use radioactive tracers which emit gamma rays from within the body, for example, Hepatobiliary imaging with Tc-99m-labeled derivatives of iminodiacetic acid (IDA) has become a clinically useful procedure since its introduction in 1976.

The synthesis process has two steps according to the general scheme given below.

Step1: The synthesis of 2,6-diisopropylacetanilide by using reaction between 2,6-diisopropylaniline and chloroacetyl chloride.

Step 2: The synthesis of DISIDA by using reaction between step 1 production.

(2,6-diisopropylacetanilide) and iminodiacetic acid.

II. MATERIALS AND METHODS

A. Chemicals and tools

Chemicals

- Diisopropyllaniline (FW = 177.29, d = 0.940).
- Chloroacetyl chloride (FW = 112.94, d = 1.42, 96%).
- Sodium acetate (FW = 82.03), $CH_3COONa.3H_2O$ (FW = 136,08).
- Glacial acetic acid; Distilled water; Ethanol.
- Iminodiacetate acid, disodium salt (FW = 195.08).
- 2,6-diisopropyl acetanilide (step I production, FW = 254).
- HCl; NaOH; Diethyl ether; Distilled water; Ethanol.

Tools

1000ml Round flask (2 or 3 neck); Hot plate; Electric stirrer; Beaker; Icebath; Melting point; 1000ml evaporation flask; Rotary evaporation; Condenser; Dropping Funnel; Extracting Funnel; Filtering Funnel; Hot plate; Electric stirrer; Beaker; Melting point; Syringe (Glass); Stirring bar; Stopper; Septum; Needle; Spatula; pH paper.

B. Preparation

Step I (Synthesis of 2,6-Diisopropyl Acetanilide).

- 2,6-diisopropylaniline, 56.58ml (0.3 mol); glacial acetic acid 300ml, condition: ice bath, electric stirrer setting 10'.

- Use Syringe (glass) dropwise chloroacetyl chloride (FW 112.94, d = 1.42, 96%) 27.4ml (0.33mol = 27.345ml), time 45'-1hrs.

- Stirring for 0.5-2hrs at room temperature.

- Sodiumacetate (0.72mol) FW 82.03 = 59.06g (0.72mol) or Sodiumacetate threehydrate FW = 136.08 net = 97.92 (0.72mol).

- Fixed limite into 420ml by H_2O. 100ml/every 15'.

- Filtration and dry vaccum.

- Recrytalization using Abs EtOH (several time).

Step II (Synthesis of 2,6-Diisopropyl acetanilido iminodiacetic acid).

- 2,6-diisopropylacetanilide 40g (FW 254.23, 157.62mmol) step I production) plus 400ml ethanol in 1000ml three neck round flask.

- 31g (158.9 mmol) iminodiacetic acid disodium salt is dissolved in 200ml distilled water.

- 10% NaOH 100ml dropwise (to meet pH 10-12) Reaction condition: Heating, Stirring, and reaction time: 8 hours.

- After that remove ethanol by rotary eveporator and vaccum pump.

- The production is extracted three time by Diethylether (Reservoir, Starting, Impurities).
- Conc. HCl dropwise until pH 2-3 (using ice bath, and stirring).
- Filter drying.
- Recrystalization by ethanol.
- Vaccum pump condition for drying.

C. Quality control

Final production is characterized by checking the melting point, Microscopic Crystal Picture, IR spectrum, HPLC, LC/M, Labelling efficiency of ^{99m}Tc.

III. RESULT AND DISCUSION

DISIDA could be synthesized easily by replacement reaction of two Clo atoms in chloroacetyl chloride molecule, Final production is high purity and similar in standart sample, productivity synthesis is more than 40%.

Quality control result

The Quality control is carried out on three samples.

D1: Import sample.

D2: Synthesized production (first batch).

D3: Synthesized production (second batch).

1. M.p: 198^{o}C-200^{o}C
2. Microscopic Crystal Picture.

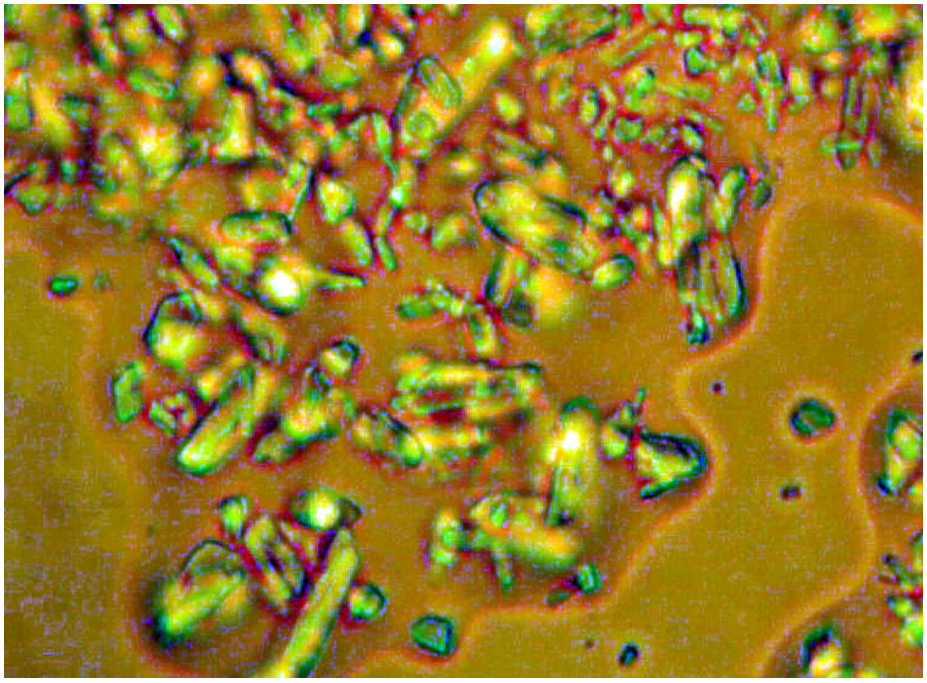

Fig. 1: DISIDA crystal picture

3. Comparison of IR absortion spectrum (cm^{-1})

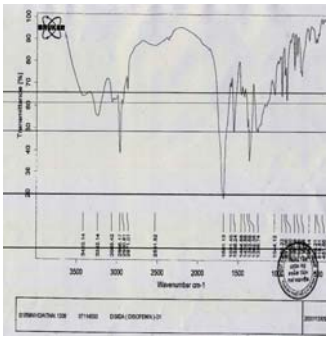

Fig. 2a: IR spectrum D1

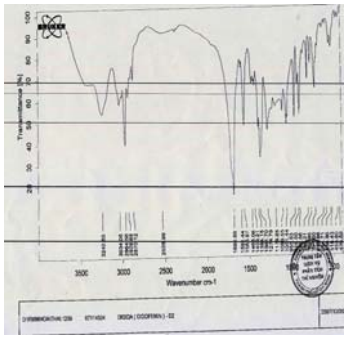

Fig. 2b: IR spectrum D2

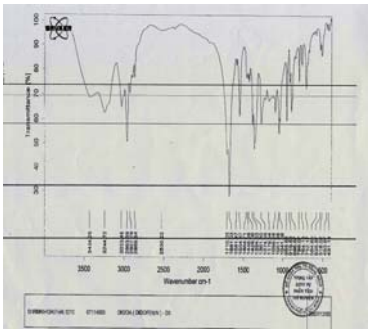

Fig. 2c: IR spectrum D3

Table 1: Comparison of IR absortion spectrum (cm^{-1})

Functional group	D1	D2	D3
-OH	3242	3242	3242
Cyclic hydrocarbon	2966	2964	2964
C = O	1681	1680	1681
C-N-H	1556	1555	1555
Deformated hydrocarbon	1383	1383	1383
CH alkan	400-1051	400-1050	1050

4. As results shown the specification of LC/MS method

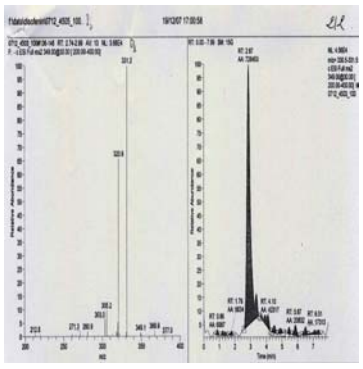

Fig. 3a: LC/MS spectrum D1

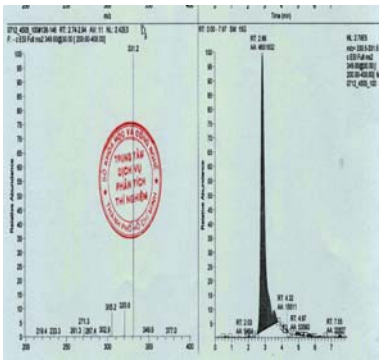

Fig. 3b: LC/MS spectrum D2

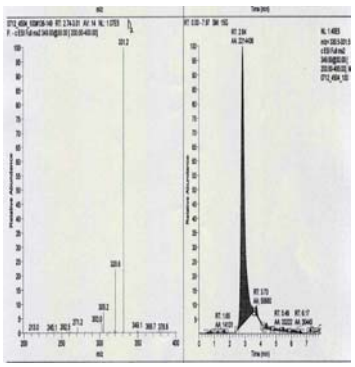

Fig. 3c: LC/MS spectrum D3

- Molcular weigth calculated: m/z = (MW + nH^+)/n = 340.

Purity production (in accordance with peaks) D1 = 88.65%; D2 = 94.50%; D3 = 98.10%

5. As results shown HPLC

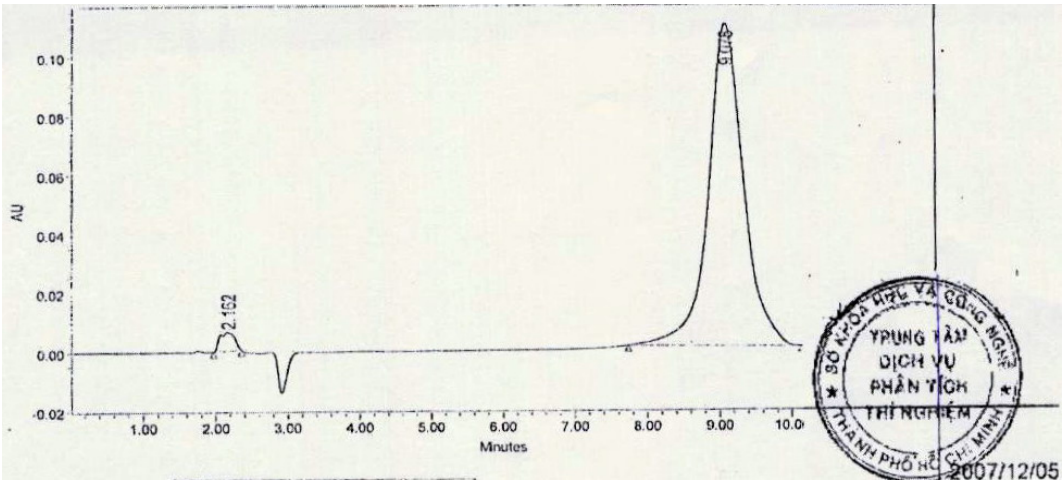

Fig. 4: HPLC spectrum- D3

Table 2: Results of HPLC

	Retention time	**Peak area**	**% Peak area**
1	2.162	91641	2.42
2	9.076	3693283	97.58

5. As results shown labeling DISIDA - ^{99m}Tc

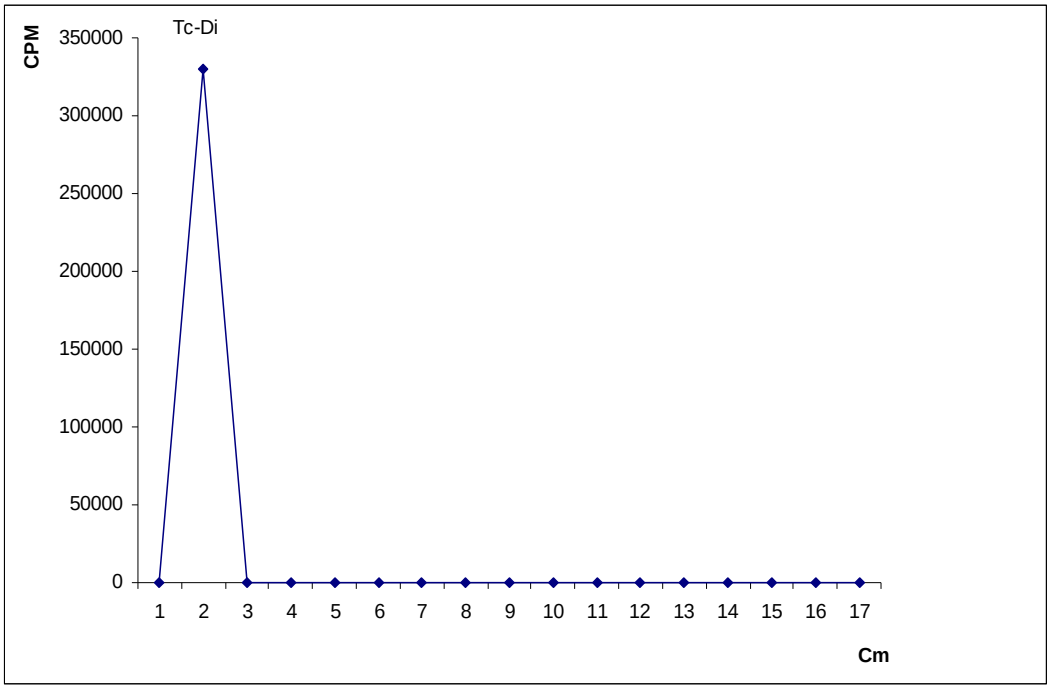

Fig. 5a: Paper chromatography Scheme of D1

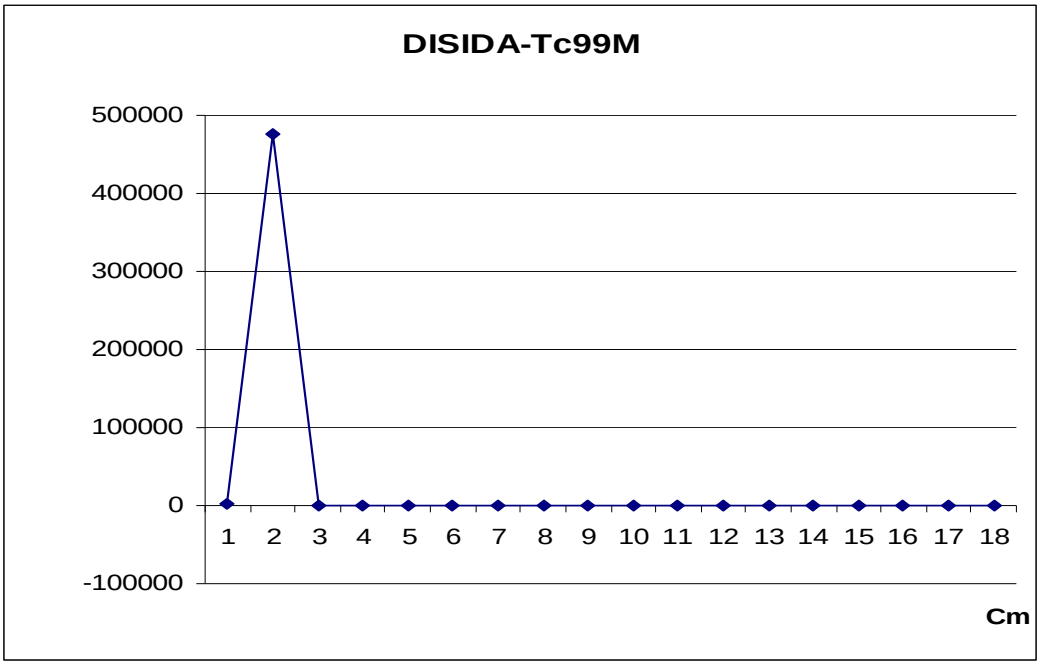

Fig. 5b: Paper chromatography Scheme D3

Labelling effiency of D1 =98.2%, D2 = 99%.

IV. CONCLUSION

DISIDA could be easily synthesized by the replacement reaction of two Clo atoms in chloroacetyl chloride molecule. The synthesis process has two steps. The product was found to be pure as results shown above.

Basing on the results obtained the following conclusion were outdrawn:

The methods of DISIDA synthesis are quite good and applicable for production of radiopharmaceuticals used in labeling with radionuclide ^{99m}Tc

The quality of synthesized DISIDA products is suitable for purpose of labeling and clinical application.

REFERENCE

[1]. International Journal of Nuclear and biology, Vol . 7, pp 1 to 7 (1980).

[2]. Journal of Medicial Chemistry, Vol . 19. No. 7, 962-964 (1974).

[3]. Technical Facilities, Vol .8, No.3, 0971- 4413, June 2000.

[4]. Xavier Calvet, Francesca Pons, Jordi Bruix,... Technetium-99m DISIDA Hepotobiliary Agent in Diagnosis of Hepatocellular Carcinoma: Relationship Between Detebility and Tumor Diffrentiation. J. Nucl Med. 29: 1916-1920, 1988.

[5]. Aibert E. Ament, M.D, Ronald J. Bick, M.D, Floro D. Miraldi, M.D, Sc.D,…Sclerrosing Cholagitis: Cholescintigraphy with Tc-99m-labeled DISIDA. Radiology, 151, 197-121, 1984.

[6]. Y. Cao and M. R. Sures. A simple And Efficient Method For Radiolabeling of

preformed Liposomes. J. Pharmaceut. Sci. 1(1): 31-37, 1998.

[7]. Margaret M. Coleman, Philip W. Peng, Joaan M. Regan, Quantitative Comparsion of Leakage Under the Tourniquet in Forearm Versus. Conventional Intravenous Regional Anesthesia. Anesth Analg . 89, 1482-1486, 1999.

[8]. Mahesh K . N. Anand, David A . Nicholson,…

Cholagiocarcinoma . January 19, 2007. Medicine World Medical Library.

[9]. IAEA-TECDOC-1114, September 1999. Optimization of production and quality control of therapeutic radionuclides and radiopharmaceuticals.

[10]. W. F. GOECKELER et al. Nucl. Med. Biol. Vol. 13, No. 4, pp. 479-482, 1986.

[11]. Regional workshop (RCA) on production of TherapeuticRadiopharmaceuticals. Beijing, China, Sept. 22-Oct.3 1997.

[12]. Regional workshop (RCA) on production of Therapeutic Radiopharmaceuticals Daejon, Korea, Oct.4-8 1999.

[13]. Azuwuike Owunwanne, Mohan Patel, Samy Sadek. The Handbook of Radiopharmaceuticals, 1992.

[14]. IAEA. Quality assurance manual for radiopharmaceuticals - 2002.

DESIGNING, MAKING APPARATUS AND STUDY ON TECHNOLOGY OF FORMING CERAMICS BY EXTRUSION METHOD

Dao Truong Giang, Nguyen Duc Kim, Ngo Quang Hien
Cao Phuong Anh and Ha Dinh Khai

Institute for Technology of Radioactive and Rare Element, VAEC, Vietnam.

ABSTRACT: Extrusion apparatus of cylinder-piston having inner diameter of 60 mm and length of 250 mm, die of ϕ5 for producing thermal couple and dies of ϕ10, ϕ30 for processing specimens were fabricated. A mixture of aluminum oxide suitable for extrusion was prepared. It comprised Al_2O_3 of 3.0μm particle size, additives: 7.0 %W of dibutyl phtalate as a plasticizer, 4.0 %W of glycerin as lubricant, 1.5 %W PVA as a binder.

The ϕ5-core of thermal couple having two ϕ1 holes was linear and well compacted (92-93% TD).

Keyword: Extrusion, apparatus.

1. Introduction

The considerable advantage of extrusion is ability of making species having thin wall (long multi-hole tube, etc.) with high productivity. Extrusion apparatus comprises force making part, holding part and cutting part. For study on forming ceramics by extrusion, it is necessary to make an appropriate apparatus and suitable material mixture. Dies have to meet requirement of smoothness, polish and regularly material release ability. Extrusion material mixture must satisfy requirement of engineering characteristics such as plasticity, lubricity, and strength of green products.

To setup a method for extrusion to form ceramics, the main objectives are studying on designing, making extrusion apparatus, composition of extrusion material mixture and finding suitable extrusion conditions for fabricating Al_2O_3 thermal couple.

2. Theory

There are lots of different forming methods. They are press, casting, plastic forming and other methods [1]. Each of them has requirement of apparatus, technology and technological performances of material for their own.

Extrusion is the process of forcing a plastic mass through a die having designed shape and dimension to produce green parts with a constant cross section and unlimited length. The extrusion apparatus in generally has two types, the horizontal and the vertical ones.

Extrusion material mixture must satisfy requirements of engineering characteristics such as plasticity, lubricity and strength of green products. Extrusion processing normally includes some steps: mixing materials in appropriate proportions of each, treating the obtained plastic mixture and extruding.

The extruded products often have defects such as cracks, laminar occurring, swelling and peeling off on the surface of products, curving products during drying

process, etc. It is possible to eliminate these defects by strictly controlling parameters of the extrusion process, adjudging composition of the extrusion mixture.

Die is a part that determines the form and dimension of the products. Die was made of abrasion resistance material having high hardness (60-62 HRC) and mirror polish.

The extrusion mixture must have sufficient plasticity, lubricity and binding ability, as a result of this, it is necessary to supply some certain additives of suitable quality and quantity. The plasticizers normally are polyethylene glycol, dibutyl phthalate, etc. The binders are polyvinyl alcohol, polyvinyl butyral, and methylcellulose. Typical binders are glycerin, stearate, silicone, graphite gel, etc. The humidity of the mixture is also an important factor [2].

3. Experiment and result

3.1. Design and fabricate apparatus

The apparatus must satisfy the requirements of accuracy, strength, simplicity for making, assemble and operation, and materials used for making apparatus must be easily to get and not expensive.

The cylinder-piston extrusion apparatus that was chosen suited thermal couple fabrication on a scale of laboratory. The cylinder had inner diameter of 60 mm and length of 250 mm, the hardness of 50-55 HRC, polish of ∇7 and high abrasion resistance.

The die had outer diameter of 5 mm, and two rods insides to make the product as a tube with two holes along its length. All the parts of the die were made of high abrasion resistance material (60-62 HRC). The hole for releasing material had high polish of ∇9 and an appropriate flow angle.

Force making system, a capstan screw fixed on a steel frame structure having the dimension of 400 x 400 x 1300 mm. The capstan screw had 30 mm moving interval.

3.2. Preparing material mixture for extrusion

The material mixture must be soft enough to move easily through the die, and it must have sufficient plasticity, lubricity and binding to obtain expected green products. The softness of the material is defined by the content of water that is in the material. The plasticity, lubricity and binding depend on the nature and content of different additives. So the accepted limits (upper and lower) of water' amount and the additives' content have been studied and found.

Plasticity is defined as ratio (%) of sag of the green product under a weight and initiated length [3]. At the content of dibutyl phthalate of 7-8 %W, the plasticity was satisfied, the extrusion process went easily, and obtained green products were strong enough.

Lubricity is determined through press force. The result denoted that in the glycerin content range of 3-5%W, the extrusion mixture had appropriate lubricity, and obtained green products are accepted.

Binding ability is determined through dried specimen destroying force. The result of experiments denotes that at the content of 1.5 %W of PVA in extrusion mixture the green products have sufficient strength for moving around and roughly processing.

The water content affected the plasticity of the extrusion mixture. At water content of 8-9%, the extrusion had satisfied the requirement for plasticity and other engineering requirements.

3.3. Sapling extrusion engineering and appreciating products' quality

The suitable parameters for extrusion technology were determined by experiments using the die having diameter of 8 mm, the extrusion mixture of Al_2O_3 of 3.0 μm mean particle size, which contained 7% dibutyl phthalate as a plasticizer, 1.5% glycerin as a lubricant and 1.5 %W PVA as a binder.

Density of the products obtained by extrusion gained the value of 92-93% TD.

The homogeneity in size of the products mainly depended on the skill manipulations during processing green product and sintering.

4. Conclusion

1. A complete instrument of cylinder-piston with inner diameter of 60 mm, length of 250 mm, and the dies of ϕ5, 10, and 30 for making thermal couple (core) and processing specimens were made. These instruments have worked well.

2. An appropriate mixture of Al_2O_3 having particle size of 3.0 μm for extrusion, which contained 7% dibutyl phthalate as a plasticizer, 4% glycerin as lubricant, 1.5% PVA as a binder, was found.

3. Thermal couple prototype, which is homogeneous linear and has density as high as 92-93 % TD was made.

REFERENCES

[1]. David W. Richerson, Modern ceramic engineering, Marcel Dekker, inc., New York, 1982.

[2]. M. Bengisu, Engineering Ceramics, Springer, Verglag Berlin, Heidelberg, 2001.

[3]. Do Minh Dao, Plasticity of ceramics material, Information of Construction porcelain and ceramics.

STUDY ON TECHNOLOGY FOR MANUFACTURING ALLOY (LEAD - TIN - BISMUTH - CADMIUM) HAVING LOW MELTING TEMPERATURE ($\leq 80^0$C) USED TO SHIELD RADIOACTIVE RAYS FOR TREATING CANCER

Ngo Xuan Hung, Pham Duc Thai, Nguyen The Khanh
Vu Quang Chat and Nguyen Huu Quyet

Institute for Technology of Radioactive and Rare Elements, VAEC, Vietnam.

ABSTRACT: Up to now, hospitals in Vietnam have mostly imported radioactive equipments from America, German, France, England to treat cancer. Accompany with those equipments, alloy, namely Cyroben having low melting temperature ($\leq 80^0$C) is used to cover patients' good tissues in order to protect them against harmful rays and help radioactive rays get through the cast hole to kill cancer cells. This project is carried out for determining chemical compositions and melting temperatures of researched alloy to create alloy having low melting temperature ($\leq 80^0$C) to meet demand for treating cancer in Vietnam.

Key words: Processing flow sheet, name element: Lead (Pb); Tin (Sn); Bismuth (Bi); Cadmium (Cd).

INTRODUCTION

The Cyroben alloy (Pb – Sn – Bi – Cd) used to cover the cancer has to meet 3 basic demands:

- Meet technique characters of radioactive treating: can cover 92-95% of radioactive rays (compared with open radiation source) in order to keep those harmful rays out of patients' good tissues as few as possible.

- Have low melting temperature ($\leq 80^0$C), easy to melt and to cast in complex shapes.

- Prevent workers, patients and doctors from harmful rays.

EXPERIMENT RESULTS AND DISCUSSION

After analyzing chemical compositions, measuring melting temperatures of imported alloy samples, we have received following technique parameters. We have used these parameters as well as studied foreign reference documents for carrying out experiments. The results are shown on the table 1.

Table 1: Chemical compositions of imported alloy samples

No	Composition,%				Melting temperature ^{0}C	Ability to cover radioactive rays
	Bi	Pb	Sn	Cd		
1	51.5	28	10	10.32	80	95%

Table 2: Chemical compositions and characters of some alloy having low melting temperature

LOW 117	Typical End Use	**Melt Temp: 117°F (47°C)**	**Density: 0.3200 lb/in^3**
	Bismuth 44.7%, Lead 22.6%, Tin 8.3%, Cadmium 5.3% , Indium 19.1%		
LOW 136	Typical End Use	**Melt Temp: 136°F (58°C)**	**Density: 0.3253 lb/in^3**
	Bismuth 49%, Lead 16%, Tin 12%, Indium 21%		
LOW 158	Typical End Use	**Melt Temp: 158°F (70°C)**	**Density: 0.3390 lb/in^3**
	Bismuth 50%, Lead 26.7%, Tin 13.3%, Cadmium 10%		
LOW 158-190	Typical End Use	**Melt Temp: 158-190°F (70-88°C)**	**Density: 0.3541 lb/in^3**
	Bismuth 42.5%, Lead 37.7%, Tin 11.3%, Cadmium 8.5%		
LOW 203	Typical End Use	**Melt Temp: 203°F (95°C)**	**Density: 0.3502 lb/in^3**
	Bismuth 52.5%, Lead 32%, Tin 15.5%		
LOW 217-440	Typical End Use	**Melt Temp: 217-440°F (103-227°C)**	**Density: 0.3660 lb/in^3**
	Bismuth 48%, Lead 28.5%, Cadmium 14.5%, Antimony 9%		

1. Materials and equipments

- A small well stove has capacity of 5 kg/batch and temperature control. Maximal temperature is 1000^{0}C.

- A refractory glass has capacity from 100g to 2000g/batch. A Hg thermometer can measure temperature to 500^{0}C, trays made of stainless steel, glass or plastic are used to contain products.

The results of analyzing materials are shown on the table 3.

Table 3: The first material compositions

No	Signs of samples	Norms of anlysis(%)				
		Pb	***Sn***	***Bi***	***Cd***	***Others***
1	M01	99.85	-	-	-	-
2	M02	99.87	-	-	-	-
3	M03	-	99.94	-	-	-
4	M04	-	-	99.95	-	-
5	M05	-	-	-	99.86	-

2. Research on alloying process of metals (Pb-Sn-Bi-Cd)

The 1st experiment: Use mixture of 500 gram of metals (Pb-Sn-Bi-Cd). The first ratio of mixing is shown on the table 4.

Table 4: The first ratio of mixing

Element	Bi	Pb	Sn	Cd	Others
Ratio %	50	30	10	10	-

Melt mixture of Pb and Sn first, when temperature of mixture increases to 270^0C, it melts completely. Continue increasing temperature to 300^0C (average increasing speed: 12^0C/ minute), add Bi and Cd to the mixture slowly, keep stirring to avoid Bi and Cd to float on the surface of the liquid mixture. Melting process of Bi and Cd makes temperature of the mixture (Pb-Sn-Bi-Cd) decrease, so we can obtain alloy having low melting temperature. After melting Bi and Cd completely, maintain melting temperature in 5 minutes, keep stirring the mixture and skim slag out of the stove.

Pour the mixture in to the clean stainless steel tray, let hot mixture cool, we obtain alloy (Pb-Sn-Bi-Cd).

The experiment results:

Cut this alloy sample and analyze its chemical compositions. The results are shown on the table 5.

Table 5: The result of analyzing chemical compositions of alloy sample

No	Alloy	Chemical composition, (%)			
		Pb	***Sn***	***Bi***	***Cd***
1	Pb – Sn – Bi – Cd	31.6	9.5	48.3	9.2

Measure density of the alloy, then melt it again to check its melting temperature. Use the Hg thermometer. The results are shown on the table 6.

Table 6: The result of checking alloy sample

No	Alloy	Melting temperature, ^{o}C	Density, g/cm^3
1	Pb – Sn – Bi – Cd	78	9.90

3. Research on influence of experiment temperature on recover efficiency and melting temperature of alloy (Pb-Sn-Bi-Cd)

The 2nd experiment:

- Choose the ratio of metals: 50% Bi – 30% Pb – 10% Sn – 10% Cd

- Carry out 3 experiments with 3 samples having the same weight: 200g.

When temperature of the mixture increases to 270^0C, Pb and Sn melt completely, keep on increasing temperature to 300^0C and add a half of Bi and Cd to the mixture, stir it continuously. After 5 minutes, the mixture becomes liquid. Skim slag out of the stove and add the rest of Bi and Cd to the mixture. Wait for 4 minutes, the mixture melts completely, skim slag out of the stove and maintain melting temperature

in 5 minutes, turn of the stove. Pour the mixture into the clean stainless steel tray to let it cool, we obtain alloy (Pb-Sn-Bi-Cd).

- Carry out 2 experiments with 2 other samples having the same weight: increase temperature to 350^0C and 400^0C, then add Bi and Cd to.

Let the hot mixture cool, weigh products for checking their recovery efficiency, then bake them for checking melting temperature of alloy. The results are shown on the table 7.

Table 7: Check melting temperature and recover efficiency of alloy samples

No	**Alloy**	**Experiment temperature, ^{o}C**	**Melting temperature,^{o}C**	**Recovery efficiency (%)**
1	Pb – Sn – Bi – Cd	300	78	95
2	Pb – Sn – Bi – Cd	350	80	92
3	Pb – Sn – Bi – Cd	400	85	90

The results show that experiment temperature affects recover efficiency and melting temperature of alloy obviously. The higher experiment temperature is, the lower recovery efficiency is. At high temperature, Bi and Cd are oxygenized easily to create oxide, so amount of Bi and Cd diminishes, this makes melting temperature of alloy increase. Therefore, Bi and Cd play an important role in the experiments, they decide low melting temperature of the alloy.

4. Research on influence of time on melting temperature of alloy(Pb-Sn-Bi-Cd):

The 3rd experiment:

Ratio of mixture: 50% Bi – 30% Pb – 10% Sn – 10% Cd. Melt completely mixture of Pb and Sn. Add Cd and Bi to the mixture, stir it continuously. Then maintain temperature of the stove at 330^0C. After 15 minutes without stirring, a layer of black slag creates and floats on the surface of the mixture. Skim all of slag out of the stove, it weighs 22 g, accounts for 11% in total of alloy. Pour alloy into the cool tray. Cut this alloy sample and analyze its chemical compositions, measure its melting temperature. The results are shown on the table 8.

Table 8: Chemical compositions and melting temperature of alloy sample

No	**Keeping temperature time, minute**	**Melting temperature, ^{o}C**	**Chemical composition, %**			
			Pb	***Sn***	***Bi***	***Cd***
1	15	87	40.8	10.3	41.5	7.3

The results show that: melting time affects melting temperature of alloy. The longer melting time lasts, the higher melting temperature is.

The 4th experiment:

Carry out the same experiment with keeping temperature time is 30 minutes without stirring. After 30 minutes, a layer of black slag creates much more and floats on the surface of the mixture. It weighs 32 grams and accounts for 16% in total of alloy.

Table 9: Chemical composition and melting temperature of alloy

No	Keeping temperature time, minute	Melting temperature, ^oC	Chemical composition, %			
			Pb	***Sn***	***Bi***	***Cd***
1	30	116	41.8	14.2	37.7	6.2

Conclusion: We should stop carrying experiment when the mixture melts completely, the most appropriate melting time is from 5-7 minutes with stirring continuously to alloy metals in the mixture completely.

5. Research on co-additional order of alloying process (Pb –Sn –Bi -Cd)

The 5th experiment:

Use 300 grams of mixture (150 grams Pb; 130 grams Sn; 10 grams Bi; 10 grams Cd) to carry out this experiment. After melting bismuth, add tin, lead and cadmium to the mixture. This process is carried out in the well stove without guard air. After 26 minutes, temperature of the stove increases to 290^0C, all of 150 grams Bi changes into brown oxide bismuth completely. So, when Bi is a member metal of the research alloy, it is impossible to melt it first.

The 6th experiment:

Use 300 grams of mixture (150 grams Pb; 130 grams Sn; 10 grams Bi; 10 grams Cd). Melt Cadmium first, then add Tin, Lead and Cadmium to the mixture. This process is carried out in the well stove without guard air. Cadmium becomes liquid at 325^0C, but a part of it is changed into Oxide. So, if we maintain stove's temperature at $\geq$ 325^0C, Cadmium slowly changes into Oxide Cadmium. This experiment shows that: if we melt Cadmium first, recovery efficiency is low because cadmium is lost during melting. Low content of Cadmium makes temperature of the alloy higher.

6. Analysis results: Analysis results are shown on the table 10.

Table 10: Result of analyzing alloy's chemical compositions

Order	Sample sign	Chemical composition, %				
		Pb	***Sn***	***Bi***	***Cd***	***Others***
1	SP01	30.1	19.4	49.2	-	-
2	SP02	31.6	9.5	48.3	9.2	-
3	SP03	40.8	10.3	41.5	7.3	-
4	SP04	41.8	14.2	37.7	6.2	-
5	SP05	35.17	5.08	49.17	9.27	-

6	SP06	30.28	10.49	44.53	14.68	-
7	SP07	40.49	9.32	45.28	4.73	-
8	SP08	39.73	5.26	39.61	9.71	-

7. Use Cyroben alloy to measure parameters and check its ability to cover radioactive rays of on the radiation source of Center for radioactive safety and environment-Institute for nuclear science and techniques

Use 2 kilograms of alloy (melting temperature: 78^0C) from the 2nd experiment. Melt and then cast it with thickness of 10 mm. Stick alloy sample on the plastic tray and set it in front of the radiation source to check the ability to cover radioactive rays at Center for radioactive safety and environment.

* Measure coefficient transmit of the tray: Measure R_{tray} and R_{open} in the water, use the plastic tray, standard radiation field (10x10 cm)

- The 1st measure: Use open resource without covering, coefficient transmit of the tray

R_{open}= 573.3. Then we use a transparent plastic tray to cover the radioation source, coefficient transmit of the source R_{tray}= 541.3. So, coefficient transmit of the source decreases from 573.3 to 541.3 if we use the tray. We have a result: only 95.4% radioactive rays of the source can go through the tray, it means the transparent plastic tray can cover 4.6% of radioactive rays.

- The 2nd and 3rd measure are carried out in the same way as the 1st: 96.2% of the radioactive rays go through the tray, it means the transparent plastic stray can cover 3.8 % of the radioactive rays .

The results are shown on the table 11.

Table 11: Coefficient transmit of the tray

Order	**Result**	**R_{open}**	**R_{tray}**
1	95.4%	573.3	541.3
2	96.2%	573.3	551.4
3	96.2%	556.1	535.1

*Measure the coefficient transmit of the block: Measure R_{tray} and $R_{tray + block}$ in the water, we use Cyroben with radiation field 8 x 8 mm.

- The 1st measure: use a transparent plastic tray to cover the source, coefficient transmit of the source R_{tray} = 534.6. Then we use a plastic tray with Cyroben alloy to cover radioactive source in the small radiation field 8 x 8 mm, the source's coefficient transmit decreases to 42.82 accounts for 6.0% of the source going through. So, if we use the plastic tray with Cyroben alloy, it can cover 94% of radiation source (compared with open radiation source).

The 2nd and the 3rd measure: the plastic tray with alloy Cyroben can cover 94% of the radiation source. The results are shown on the table 12.

Table 12: The coefficient transmit of the block

Order	Result	$R_{tray + block}$	R_{tray}
1	6.0%	42.82	534.6
2	6.0%	42.84	535.1
3	6.0%	42.81	535.4

8. Result and discussion

- Alloy meets the best quality when it contains 20-30% Pb, 10-15% Sn, 50-55% Bi, 10-12 %Cd. With those contents, alloy has low melting temperature and can cover 94-95% of radiation source (compared with open radiation source).

- We have obtained the first results: making alloy having low melting temperature ($\leq 80^0$C) to meet the requirements of treating cancer.

- Alloy newly created can cover 94-95% of radiation source (compared with open radiation source) to save good tissues from damaging.

9. Conclusion

- Using materials and equipments in Vietnam, we have succeeded in melting alloy which has low melting temperature ($\leq 80^0$C) and are similar to imported alloy used to cover radioactive for treating cancer. So, hospitals in Vietnam don't have to import this alloy.

- This project has advertised on the newspapers of Vietnam foundry and metallurgy science and technology association (VFMSTA).

REFERENCE

[1]. Nguyen Khac Xuong. "metal of materials".

[2]. Phung Viet Ngu, Pham Kim Dinh, Nguyen Kim Thiet, melting metal alloy, 11/1997.

[3]. B. N. ARZAMAXOV, metal alloy, 2000.

[4]. Crystal Structure of phases of binary alloy Systems, compiled by Donald. T. Hawkisc information scientist, bell laboratories, murray hill, N.J.

[5]. Pro. Y. LAKHTIN, ENGINEERING PHYSICAL METALLURGY, translated from the Russian alloy Nicholas Weinstein, MIR PUBLISHERS, MOSCOW. 1968.

[6]. D.A. Porter Rautaruukki Oy Research Centre Raahe Finland, Phase transformations in Metals and alloys, second edition. London-Glasgow-New York-Tokyo-Melbourne-Madras.

RESEARCH ON THE RECOVERY OF NEODYMIUM AND IRON FROM NDFEB PERMANENT MAGNET SCRAPS

Hoang Nhuan, Tran Ngoc Ha, Nguyen Thuc Phuong
Hoang Van Duc and Nguyen Thi Thanh Thuy

Institute for Technology of Radioactive and Rare Elements, VAEC, Vietnam.

ABSTRACT: There are many new kinds of material in the world created with Rare Earth Elements by modern technology. Among them NdFeB magnet gains the most popularity in the area of high magnetic field and permanent magnet. The research is aiming at investigating possibilities of separation of iron and neodymium, which is a Rare Earth Element of high value and applicability in technology, from NdFeB magnet scraps that can be collected in large quantity in manufacture of NdFeB magnets (about thousands of tones). It is necessary to carry out a research on recovery as much as 20 percent of neodymium from magnet compound. A focus was also on gaining iron (accounting for 75%) from the substance for environmental sanitation and high efficiency. During the experiment, NdFeB permanent magnets were demagnetized, grinded to enlarge surface area. It was followed by oxidization baking to change metal into oxide, facilitating dissolving process. Then the mixture of oxides was dissolved by H_2SO_4. Neodymium was separated from iron by double sulphate neodymium precipitation. Iron was recovered in form of Fe_2O_3 (to protect environment and provide high efficiency) by precipitated iron hydroxide in excess Na_2CO_3 medium. The experiment showed the possibility of simultaneous recovery of both Nd and Fe from NdFeB permanent magnets wastes.1.

Experimental and Results

1. Research on the chemical composition of NdFeB samples

To evaluate the dissolution ability of NdFeB permanent magnet sample there should be information on chemical composition and compound forms of metals in the sample. The results of powder X-ray diffraction spectrogram for the NdFeB magnet scrap sample indicated: the compound consists of metal Fe, oxidized Fe including α-hematite Fe_2O_3 and magnetite Fe_3O_4, neodymium presented in $NdFeO_3$. The unusual compound of NdFeB (presence of metal oxide) is due to that sample provided by Meiwa Company was not permanent magnet, which also included other metal oxides.

Quantitative analysis showed that powder NdFeB compound consisted of 15.77% of neodymium, 50.95% of Fr, 0.834% of Bo (Table1). Other rare earth elements accounted for small amount of 3.92%, of which Dy accounted for about 2.95%.

Table 1: Composition of NdFeB alloy samples

Composition / Sample	Metal (%)			Conversion into metal oxide (%)		
	Nd	***Fe***	***B***	***Nd_2O_3***	***Fe_2O_3***	***B_2O_3***
Meiwa (Japan)	15.77	50.95	0.834	18.40	72.86	2.69
China	5.44	64.80	-	6.35	92.66	-

The results of structure composition analysis by powder X-ray diffraction spectrograph indicated that Chinese NdFeB permanent magnet sample had high amorphousness. Compounds could only be identified after oxidization baking with 2 main components: neodymium in $NdFeO_3$ and Fe in Fe_2O_3. Results of quantitative analysis presented in Table 2 includes: 5.44% of neodymium, 64.08% of iron. The Nd content was much lower than that of Japanese. Although the physical characteristics of Chinese magnets, it can be estimated that Chinese cost is lower than that of Japanese. Moreover, considering some experiences of using Chinese permanent magnets that showed some properties such as durability, strength of magnetic field, etc. all indicated effectiveness of such magnets. That commercially manufactured material should be taken into account.

2. Determination of the oxidation roasting temperature for NdFeB scraps

Main reactions of oxidization baking of NdFeB magnets are presented as follows:

$$2\,Nd + 3/2\,O_2 \longrightarrow Nd_2O_3 \quad (3.1)$$

$$2\,Fe + 3/2\,O_2 \longrightarrow Fe_2O_3 \quad (3.2)$$

$$Nd_2O_3 + Fe_2O_3 \longrightarrow 2\,NdFeO_3 \quad (3.3)$$

The oxidization baking of magnet aimed at breaking the chemical composition, facilitating dissolution of the compound.

The experiment showed that dissolution effect of NdFeB scrap was increased in direct ratio to temperature range from 500^0C up to 800^0C. In the higher temperature, dissolution output strongly decreased. Examination of powder X-ray diffraction spectrogram showed that the creation of Fe compounds in form of magnetite Fe_3O_4 was not in favor for dissolution process.

Results of examination of impacts of temperature on separation of metals by acid are presented in Figure 1.

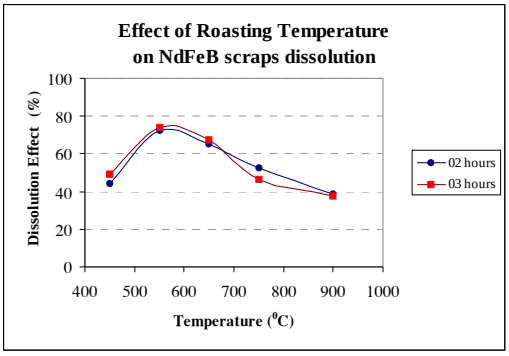

Fig. 1: Effect of Roasting Temperature on NdFeB scraps dissolution ceramic bone.

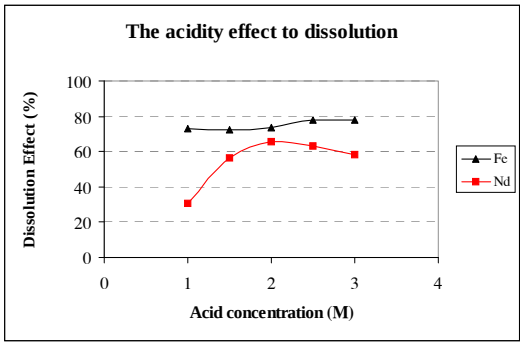

Fig. 2: Impact of acid concentration on NdFeB scrap dissolution.

3. Research on the impacts of acid concentration for dissolution process

The main chemical reactions during dissolution by acid are presented as follows:

$$Nd_2O_3 + 3\,H_2SO_4 \longrightarrow Nd_2(SO_4)_3 + 3\,H_2O \quad (3.4)$$

$$Fe_2O_3 + 3\,H_2SO_4 \longrightarrow Fe_2(SO_4)_3 + 3\,H_2O \quad (3.5)$$

Results of experiment showed in Table 1 indicate that the amount of dissolved neodymium and iron increased with the increasing concentration of H_2SO_4 within 1.5÷2.5M with temperature of 50°C reaction maintaining in duration for 1.5 hours. At acid concentration of more than 3M, dissolution coefficient decreases. It was due to the decrease of dissolubility of $Nd_2(SO_4)_3$ salts in the excess medium of SO_4^{2-} ion, resulting in dissolution restriction of neodymium into solution and decrease of dissolution efficiency for alloy powder. The acid concentration of H_2SO_4 = 2.5M (and within 1.5-2.5M) was also used for the experiment of dissolution conditions in the next coming parts.

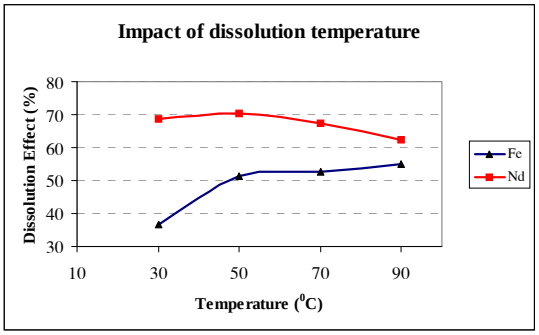

Fig. 3: Impact of Temperature on NdFeB scraps dissolution. ceramic bone.

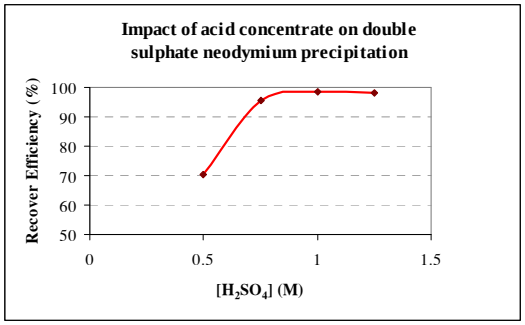

Fig. 4: Impact of H_2SO_4 concentration on the neodymium recover efficiency ceramic bone.

4. Research on the impacts of temperature on dissolution efficiency of metals

An experiment to investigate the impact of temperature of the dissolution reactions on neodymium and iron separation was conducted in the conditions: concentration of acid H_2SO_4 2.5M; NdFeB sample was baked at 650°C, sample weight was 100g/sample and time of dissolution lasted for 2 hours. Results presented in Figure 3 showed that dissolved efficiency reached maximum at 50°C and this was also the temperature for the highest effective separation of Nd and Fe. This temperature was used for further experiments on separation condition of Nd and Fe.

5. Separation and purification of neodymium from dissolved solution

The neodymium separation process from solution of sulphates including $Nd_2(SO_4)_3$ and $Fe_2(SO_4)_3$ was carried out based on the double sulphate precipitation of trivalent rare earth elements (it is Nd in this case), by precipitant in excess of Na_2SO_4. Neodymium could create a precipitated complex compound in form of sodium bi-sulphate neodymium and iron was in solution in form of soluble salt. The main reactions were as follows:

$$Nd_2(SO_4)_3 + Na_2SO_4 = 2\,Na[Nd(SO_4)_2]\downarrow$$

$$Fe_2(SO_4)_3 \xrightarrow{+\,Na_2SO_4} Fe_2(SO_4)_3\ (Sol.)$$

Experiments for investigating impacts of sulfuric acid concentration on precipitation of double sulphate neodymium were conducted in the conditions of rare

earth element content of 50g/L, weight ratio of $m_{Na_2SO_4} / m_{Nd_2O_3} = 2$, temperature T = 60°C (Figure 4).

Results from experiments showed that neodymium could be obtained with 95.6% in condition of 0.75M acidity. The pureness of neodymium reached 99.99% (in comparison with iron) and more with iron content less than 0.005%

6. Research on iron recovery in form of Fe_2O_3

Powder NdFeB permanent magnet sample was baked at temperature of 550°C for 2 hours. The powder compound of metal oxides afterwards was dissolved in sulfuric acid for 1.5 hours. The concentration of H_2SO_4 of 1.5M was maintained until the end of reaction. Undissolveable parts were filtered, washed by dilute H_2SO_4, giving a sulphate mixture of Fe and Nd. After double sulphate precipitation of rare earth elements (mainly neodymium), a mixture of Na_2CO_3 and air-oxygen was used to obtain precipitate of trivalent iron hydroxide from $Fe_2(SO_4)_3$ solution. Filtering and washing the precipitate by $NaHCO_3$ of 5%, drying at 90°C, calcined at 450°C for 2 hours, then Fe_2O_3 could be obtained. The undissolvable parts of the acid extraction process (mostly Fe) were dried, grinded, and baked at 550°C for 2 hours. NdFeB scrap dissolution by H_2SO_4 gave sulphates solution, precipitate of double sulphate Nd, precipitate of $Fe(OH)_3$ were repeated in the same conditions. To obtain iron recovery of high efficiency there should be continuous uninterrupted process.

7. Separation of Nd and Fe from NdFeB magnets

Process of recovery of Nd took place simultaneously with the above described Fe separation process. The second phase of separation obtained Nd_2O_3 with coefficient of 68.5%. The total coefficient of separation of neodymium of the two stages reached 88.12%. The pureness of Nd was more than 99.99%. To recover neodymium completely there should be the third stage: using all undissolvable parts after dissolution reaction of the two prior stages, filtering, washing, drying and baking at temperature of 750°C for 2.5 hours. Continue to separate Nd by acid, precipitate double sulphate neodymium. The separation coefficient of Nd in the third stage reached 98.5%. The average coefficient was 99.83%.

8. Procedure of separation and recovery of neodymium and iron from NdFeB

Segmental procedure (NdFeB scrap recycle): NdFeB alloy was demagnetized, crushed and baked at 550°C for 2 hours; dissolution by 2M of H_2SO_4 in 50°C for 1.5 hours. Obtained solution included $Fe_2(SO_4)_3$ and $Nd_2(SO_4)_3$. Undissolvable NdFeB part was about 32÷35% that could be mixed with new powder of NdFeB scrap, baked at 550°C again and continuous Nd and Fe recovery as presented above.

Interruptive procedure (direct neodymium recover): NdFeB scraps were baked at 750°C for 2 hours, dissolved by H_2SO_4, etc. and recovery of Nd and Fe was done in the same way as above mentioned experiments. This process is applied in case of neodymium recovery only, with iron separation below 50%.

REFERENCE

[1]. Yu Zongsen, Chen Minbo (1995), *Rare Earth Element and Their Applications*, Metallurgical Industry Press, Beijing.

[2]. B. K. Sharma (2000), *Industrial Chemistry*, Goel Publishing House, India.

[3]. Technical Information (1997), *Chemical Safety Training Modules*, IARC.

[4]. Alexei A. Minaev *, Dimitri G. Kuznetsov, Boris F. Gulev (2000); *Synthesis and properties of some insoluble high-temperature neodymium ceramic compounds*, Institute of Physical Chemistry, Russian Academy of Science, Moscow, Russia, Journal of Alloys and Compounds 303-304, p. 426-431.

[5]. Mei-Ling Feng, Jang-Gao Mao* (2005), *Synthesis and crystal structure of a new neodymium(III) selenate-selenite:* $Nd_2(SeO_4)(SeO_3)_2(H_2O)_2$; Elsvier Publisher, Journal of Alloys and Compounds 388, p. 23-27.

[6]. Sung-Don Kim, Ho-Sung Yoon, Chul-Joo Kim, Hoo-In Lee (2004); *Preparation of neodymium hydroxide from NdFeB Magnet scrap*, Proceedings of the first Vietnam-Korea Symposium on rare earths development and applications, p. 163-172.

[7]. Le Ba Thuan, Vu Dang Do, Hoang Nhuan, Luu Xuan Dinh (2004), "*Cerium separation from Dong Pao bastnazite ore by double sulphate precipitation method*", Journal of Chemistry, S. 42 (4), P. 483-487.

STUDY ON PREPARATION OF ZINC OXIDE CATALYST FOR REMOVING HYDROGEN SULFIDE FROM GAS MATERIAL OF UREA PLANT

Vu Thanh Quang, Ngo Van Tuyen, Trinh Giang Huong and Vuong Huu Anh

Institute for Technology of Radioactive and Rare Elements, VAEC, Vietnam.

ABSTRACT: Zinc oxide is widely used to remove H_2S from feed gas material of urea production process. Rate and capacity of hydrogen sulfide absorption depend on physic-chemical behaviors of zinc oxide such as the surface acid/base properties (pH), specific surface area (SSA), porosity and particle size, etc. These typical properties can be modified by using the different synthesis methods or introducing changes into the procedure of its chemical preparation. Ammonia-ammonium carbonate method which is the simple and effective one for preparing active zinc oxide with H_2S adsorption capacity achieved up to 30g of H_2S/100g of ZnO is introduced in this paper. A technical procedure for preparing desulphurization absorbent in form of two hole extrusive pellet with the adsorption capacity of more than 20 g H_2S/100 g of material have also been introduced here.

Key words: Zinc oxide active, AAC method, remove H_2S, ZnO catalyst, desulphurization absorbent, extrusion pellet.

Introduction

Zinc oxide (ZnO) has been used in various technologies as varistor, gas-sensor, catalyst, pigment, etc. These various applications of ZnO are due to the specific chemical, surface and microstructure properties of ZnO. In the catalytic applications of ZnO the surface acid/base properties and the adsorption capacity are the most important functional parameters.

Preparation of desulphurization absorbent based on zinc oxide catalyst consists of two stages:

1) Preparation of ZnO catalyst as initial material of the next stage.

2) Preparation of the desulphurization absorbent in a desired form.

The first stage is performed by different synthesis methods as precipitation, hydrolysis of urea, co-precipitation of ZnO-TiO_2, ZnO-Al_2O_3, sol-gen, ammonia-ammonium carbonate (AAC), matrix-assisted method, etc. The physic-chemical properties of obtained zinc oxide depend on the preparing methods [1, 2, 3, 4, 5, and 6].

The second stage is to make the initial material form that has not only mechanical crushing strength but also the H_2S adsorption rate and capacity in accordance with the required level of producers. At present, extrusive method is widely used in urea manufacture.

The technique procedure for preparing zinc oxide catalyst and desulphurization absorbent in form of two holes extrusive are introduced as below.

Experimental, Results and Discussion

1. Preparation of ZnO catalyst by using AAC method.

In principle, the AAC method consist of three stages.

1) Dissolve material as ZnO or $Zn(OH)_2$ or $ZnCl_2$ into solution of NH_4OH + $(NH_4)_2CO_3$ (AAC Sol.) at temperature 40-50^{0}C.

2) Precipitate Zinc Basic Carbonate ZBC by removing NH_3 vμ CO_2 from the AAC solution at temperature 80-100^{0}C.

3) Convert ZBC to ZnO catalyst by thermal decomposition at 300-800^{0}C.

Experimental procedure for preparing ZnO catalyst by using AAC method

a) Experimental procedure

Dissolving 200 grams of $(NH_4)_2CO_3$ into 500 ml NH_4OH 25% and adding distillation water until to 1 liter volume. The solution is transferred into a 3-5 liter vessel having mechanical agitator and heater. About 150 grams of ZnO raw material is added slowly into the vessel while stirring and heating up to 45 **± 5** ^{0}C. Adding ZnO continuously until its weight reaches to 200 grams. As usual, white slurry precipitate of ZBC has appeared at this moment. The agitation and the temperature are maintained constantly for 2 hrs. The ZBC is precipitated and aged at temperature 85 **± 5** ^{0}C for 4-5hrs. The precipitate is filtered, washed, dried and calcined to convert to ZnO catalyst at temperature 300-600^{0}C for 3-8 hrs.

b) Effect of calcined temperature and time on properties of ZnO catalyst

Temperature and time for converting ZBC to ZnO catalyst effect very sensitively on appearance, particle size, specific surface area and bulk density of final product. In general, in low temperature and short time conditions, ZnO product has color, smaller size, higher surface area and lighter density in comparison with those in case of the higher temperature and the longer time. Data in the table 1 show the effects on physical properties of ZnO catalyst. The properties control the rate and H_2S adsorption capacity of ZnO catalyst.

Table 1: Effects of calcined temperature and time on several typical properties of ZnO

Samples	**T_Calc., 0C**	**t, hr**	**Appearance/ color**	**d_apparent, um**	**BD, g/cc**	**SSA, m2/g**
ZnO-1	300 - 350	3	grey	~ 0.5-1	0.124	42.3
ZnO-2	300 - 350	5	off-white	~ 1-1.5	0.176	36.7
ZnO-3	400-450	6	white	~ 2.5-3.2	0.225	27.6
ZnO-4	500-550	6	lemon-white	~ 5	0.58	22.9

c. Determining the rate and H_2S adsorption Capacity and Rate of ZnO catalyst.

Before preparing of desulphurization absorbent, the raw material ZnO catalyst should be determined perfectly its physical properties as particle size, bulk density, SSA and adsorption rate as well as maximum capacity. Because, suitable raw material for making the absorbent having good ability for resisting mechanical clash and high adsorption capacity is a mixture of several kinds of the ZnO catalyst.

Determination of adsorption capacity (C mgH_2S/g ZnO) bases on increase of ZnO mass after H_2S absorption. Adsorption reaction occurs as below:

ZnO Catalyst + H_2S = ZnS + H_2O

$$C, mgH_2S / gZnO = \frac{M_t - M_0}{M_0} x2.125x1000$$

Where: M_0 is mass of ZnO free H_2S, M_t is mass of ZnO saturated H_2S.

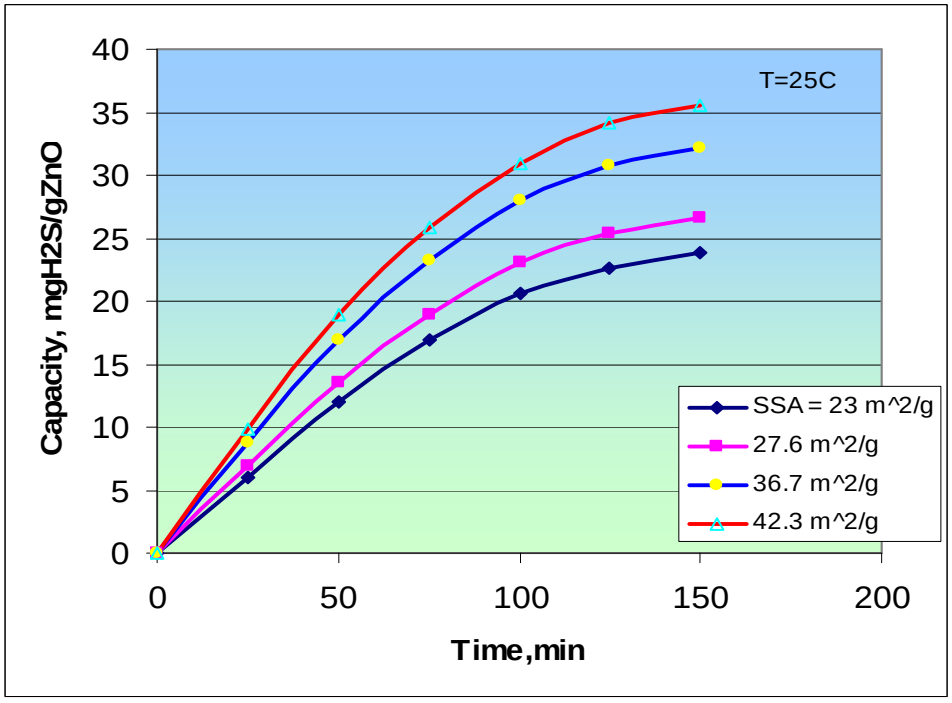

Fig. 1: Dependent of capacity on adsorption time and SSA of ZnO

The figure shows that the higher SSA ZnO powder has, the higher adsorption and rate of capacity are. The catalyst with SSA in a range of 23-43 m^2/g can absorb 25-25g of H_2S/100 g of ZnO and absorption rate is 2.5-3.5 mg of H_2S/g.min. at room temperature during the first 60 min of the absorption.

2. Preparation of desulphurization absorbent in form of two-hole extrusive pellet

It is necessary to create sufficient pliable, homogeneous and non gluey paste for preparing the absorbent by using extrusion technique. ZnO is good smooth substance so using lubricant is not necessary. As usual, active bentonite is used as a binder. Table 2 shows component of two kinds of paste extrusion-1 and extrusion-2 from ZnO-1 to ZnO-4 of the table 1.

Table 2: Component of paste: Extrus-1 and Extrus-2.

Samples	ZnO-1,g	ZnO-2,g	ZnO-3,g	ZnO-4,g	Bentonite,g
Extrus-1	50	100	100	250	40
Extrus-2	250	100	100	50	40

The components are mixed in a mill without grinding ball for 24 hrs. After that bulk density of the mixture always increases to 30%. The best choice of the components is the density in a range of 0.9 – 1.0 g/cc. The raw paste is created by slowly adding 60±10 ml of water for each 100g of the mixture and then it is kneaded perfectly. The paste is extruded using a laboratory scale extruder having a ϕ - 6mm diameter die with 2 holes ϕ - 0.2mm. The extrudate was then cut into pellets of about 2-3 cm in length. After being dried at 50-80^{0}C for 24 hrs in the oven in slowly flowing air, these pellets were cut into pellets of about 0.5-1 cm in length and heat treated at 700^{0}C for 5 hours in a muffle furnace. The figure 2 is a picture of the two hole extrusive pellets and ZnO catalyst. The properties of these materials are illustrated in the table 3.

Fig. 2: ZnO catalyst and two holes desulphurization extruder

Table 3: Typical properties of the two hole desulphurization extrusive pellet

Desulphurization extrusive pellets

Appearance: white or light-gray extrusions

Size: 5.7 Mm Dia

Shape: Two hole extruders

Bulk Density: 1. 3 + / -0. 1 KG/L

Crush Strength (Min.): 50 N/cm

ZnO Content (Wt%) : 90 + / -2%

LOI at 540^{0}C: 5. 0% Max

Breakthrough sulfur capacity, %: 19.1-21.2(25-30^{0}C).

Data in the table 1 & 3 show that adsorption capacity and rate of the extruders achieve about 80% those of raw powder materials.

Conclusion

Above results indicate that AAC method is simple and effective for preparing ZnO catalyst having a H_2S adsorption capacity of 25-35%. Preparation of the extrusive pellets having the capacity of 19-21% is a promised success at the first step, however there are lots of problems that must have to research and modify more detail. Procedure for preparing the extrusive pellets need more experimental data for optimizing, the components of the paste should be optimized by using more perfectly experimental matrix.

REFERENCES

[1]. Liyu Li and David L. King. Sulfur Removal to Produce Ultra Clean Fuel H_2S removal with ZnO during fuel processing for PEM fuel cell applications, Catalysis Today, Volume 116, Issue 4 , 15 September 2006, Pages 537-541.

[2]. Svetozar Musić, Đurđica Dragčević, Miroslava Maljković, and Stanko Popović. Influence of chemical synthesis on the crystallization and properties of **zinc** oxide. Materials Chemistry and Physics, Volume 77, Issue 2 , 15 January 2003, Pages 521-530.

[3]. T. Zaki, M. Riad, L. Saad and S. Mikhail. Selected oxide materials for sulfur removal. Chemical Engineering Journal, Volume 113, Issue 1 , 1 October 2005, Pages 41-46.

[4]. United States Patent 20030152508 Kind Code: A1, Method of preparing zinc ammonia carbonate solution.

[5]. No-Kuk Park, Jong Dae Lee, Tae Jin Lee, Si Ok Ryumand Chih Hung Chang. A high surface area metal oxide prepared by a matrix-assisted method for hot gas desulphurization. Fuel Volume 84, Issue 17 , December 2005, Pages 2165-2171. The 5th European Conference on Coal Research and its Applications.

[6]. United States Patent 4977123. Preparation of extrusions of bulk mixed oxide compounds with high macroporosity and mechanical strength.

STUDY ON THE PREPARATION OF TITANIUM DIOXIDE POWDER FOR PRODUCING PIGMENT FROM 85% SYNTHETIC RUTILE (TiO_2)

Tran Van Son, Cao Hung Thai, Than Van Lien
Nguyen Dinh Van, Doan Thi Mo and Hoang Bich Ngoc

Institute for Technology of Radioactive and Rare Elements, VAEC, Vietnam.

ABSTRACT: Our project has elucidated factors that influence hydrolytic process of titanisulfat solution and bleaching products after hydrolyzing. Appropriate conditions for hydrolyzing such as: concentration of TiO_2 230gTiO_2/l; temperature of hydrolytic process 100^0C; and nucleating solution: 1.31% compared with weight of titanium dioxide in the solution has been determined. Appropriate conditions for bleaching process: concentration of sulfuric acid in the solution: 8%; bleaching time: 35 minutes; and temperature of the solution: 80^0C have also been chosen.

After hydrolyzing and bleaching, the sample is dried, calcined at 900^0C for 2 hours and ground into TiO_2 powder containing 97-98% TiO_2; 0.012-0.017% Fe_2O_3; < 0.001% Cr; 0.8-1.44% SiO_2 ; <0.01% Al_2O_3.

Key words: 85% TiO_2 synthetic rutile, titanium dioxide powder 92-98% TiO_2

Introduction

Titanium dioxide is used in many fields such as paper, rubber and consumer's goods industries. Besides, it is used for producing paint, coating oil, printing ink, plastics, glass fiber, condensers, ceramics, welding flux, cosmetics, catalyst, soap, toothpaste and so on.

Titanium ore in Vietnam has abundant reserves (about 35 million tons). In 2005, output of raw titanium ore was 415.200 tons, 90% of which was exported. However, our current demand for titanium pigment is increasing; we have to import powder of titanium from France and Korea, which has high price. Therefore, it is very necessary to study on producing titanium dioxide powder from 85% synthetic rutile.

Experiments and results

I. Initial materials

Research sample containing 85% TiO_2 synthetic rutile is produced from ilmenite beach sands from Ha Tinh by reducing and removing iron from reduced ilmenite by Becher process, the characteristics of the synthetic rutile are shown in the table 1.

Table 1: The characteristics of the synthetic rutile

Component	TiO_2	Fe	Cr	Particle size
Content, %	85.07	5.15	0.19	< 40 μm

The synthetic rutile sample is digested in sulfuric acid, the digested cake is dissolved in 10% sulfuric acid solution. Liquor for hydrolyzing may contain 160 g of TiO_2, 10 g of Fe and 0.1 g of Cr per liter.

2. Study on hydrolytic process

2.1. Effect of hydrolytic temperature

TiO_2 solution 210.97g/l is hydrolyzed by heating to 90, 95 and 100^0C, adding 10ml of nucleus 0.96% compared with weight of titanium dioxide in the solution. After hydrolysis is completed, precipitated hydrolysate is filtered, washed, dried and calcined. The results of experiments are shown in the table 2.

Table 2: Effect of temperature on the hydrolytic process

Temp, ^{0}C	90	95	100
TiO_2, %	95.52	95.67	95.78
Fe, %	0.25	0.22	0.15
Cr, %	0.021	0.018	0.014
TiO_2 recovery, %	89.54	89.76	90.47

The experimental results showed that appropriate temperature for hydrolyzing is 100^o C.

2.2. Effect of TiO_2 concentration

TiO_2 solutions 171.15; 191.34; 210.97; 230.25 and 249.57g/l are hydrolyzed by heating to 100^0C, adding 10 ml of nucleus 1.18; 1.05; 0.96; 0.88 and 0.81%, respectively (compared with weight of titanium dioxide in the solution). After hydrolysis is completed, that precipitated hydrolysates are filtered, washed, dried and calcined. The results of experiments are shown in the table 3.

Table 3: Effect of TiO_2 concentration on the hydrolytic process

TiO_2 conc., g/l	171.15	191.34	210.97	230.25	249.57
TiO_2, %	94.64	94.97	95.78	96.58	96.02
Fe, %	0.35	0.28	0.15	0.09	0.13
Cr, %	0.032	0.027	0.014	0.011	0.013
TiO_2 recovery, %	88.57	89.73	90.47	92.61	95.58

The experimental results show that appropriate concentration of TiO_2 is 230g/l.

II.3. Effect of nucleus

TiO_2 solutions 230.47g/l is hydrolyzed by heating the solution to 100^0C, with 0.5, 10, 15, 20 ml of nucleus (corresponding with 0; 0.44; 0.88; 1.31; 1.75% titanium dioxide in the solution). After hydrolysis is completed, that precipitated hydrolysates are filtered, washed, dried and calcined. The results of experiments are shown in the table 4.

Table 4: Effect of nucleus on the hydrolytic process

Nucleus, %	0	0.44	0.88	1.31	1.75
TiO_2, %	94.14	95.37	96.58	97.85	97.17

Fe, %	0.21	0.12	0.09	0.07	0.082
Cr, %	0.028	0.017	0.011	0.009	0.01
TiO_2 recovery, %	88.56	90.62	92.61	94.24	93.67

The experimental results showed that appropriate amount of nucleus is 15 ml (corresponding with 1.31% titanium dioxide in the solution).

3. Study on bleaching process

3.1. Experimental sample

Experimental sample is prepared by hydrolyzing solution TiO_2 230.47g/l at 100^0C, with nucleus 1.31% (compared with weight of titanium dioxide in the solution). Hydrolytic time is 4 hours. After hydrolysis is completed, the precipitated hydrolysates are filtered and washed to obtain products for bleaching process. The results are shown in the table 5.

Table 5: The composition of the sample for bleaching process

Component	TiO_2	Fe	Cr
Content, %	97.76	0.07	0.01

3.2. Effect of bleaching acid concentration

Experimental samples are washed by 4, 6, 8, 10 and 12% sulfuric acid solution, concentration of TiO_2 200 g/l, temperature 50^0C, and then add 2g of zinc powder for 1 kg TiO_2, bleaching time is 30 minutes. After bleaching, the sample is filtered, dried and calcined at 900^0C for 2 hours and ground into TiO_2 powder. The experimental results are shown in the table 6.

Table 6: Effect of bleaching acid concentration

Acid conc., %	4	6	8	10	12
TiO_2, %	97.87	97.89	97.92	97.95	97.97
Fe, %	0.032	0.030	0.024	0.024	0.022
Cr, %	0.007	0.006	0.005	0.005	0.005
TiO_2 recovery, %	96.32	96.07	95.86	95.54	94.79

The experimental results showed that appropriate acid concentration is 8%.

3.3. Effect of bleaching time

Experimental sample is washed by sulfuric acid solution 8%, concentration of TiO_2 200g/l, temperature 50^0C, add 2g of zinc powder for 1kg TiO_2, bleaching time is 20, 25, 30, 35 and 40 minutes. After bleaching, the samples are dried, calcined at 900^0C for 2 hours and ground into TiO_2 powder. The experimental results are shown in the table 7.

Table 7: Effect of bleaching time

Time, minute	20	25	30	35	40
TiO_2, %	97.86	97.90	97.92	97.96	97.98
Fe, %	0.035	0.028	0.024	0.021	0.021
Cr, %	0.0073	0.0064	0.005	0.0042	0.0042
TiO_2 recovery, %	96.30	96.02	95.86	94.81	94.77

The experimental results showed that appropriate bleaching time is 35 minutes.

3.4. Effect of bleaching temperature

Experimental sample is washed by sulfuric acid solution 8%, concentration of TiO_2 200g/l, temperature 50 60, 70, 80 and 90 ^{0}C , add 2g of zinc powder for 1kg TiO_2, bleaching time is 35 minutes. After bleaching, the samples are dried, calcined at 900^{0}C for 2 hours and ground into TiO_2 powder. The experimental results are shown in the table 8.

Table 8: Effect of bleaching temperature

Temp., ^{0}C	50	60	70	80	90
TiO_2, %	97.96	97.99	98.04	98.09	98.12
Fe, %	0.021	0.019	0.014	0.012	0.012
Cr, %	0.0042	0.0038	0.0024	0.0014	0.0014
TiO_2 recovery, %	94.81	94.67	94.39	94.26	94.32

The experimental results showed that appropriate bleaching temperature is 80^{0}C.

4. Proposing a flow sheet for preparation TiO_2 powder from 85% TiO_2 synthetic rutile

According to above experimental results, we have proposed the following flow sheet for preparation of TiO_2 powder from 85% TiO_2 synthetic rutile (figure).

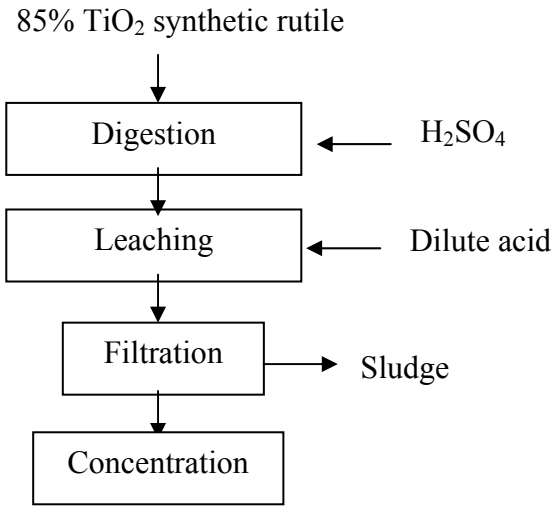

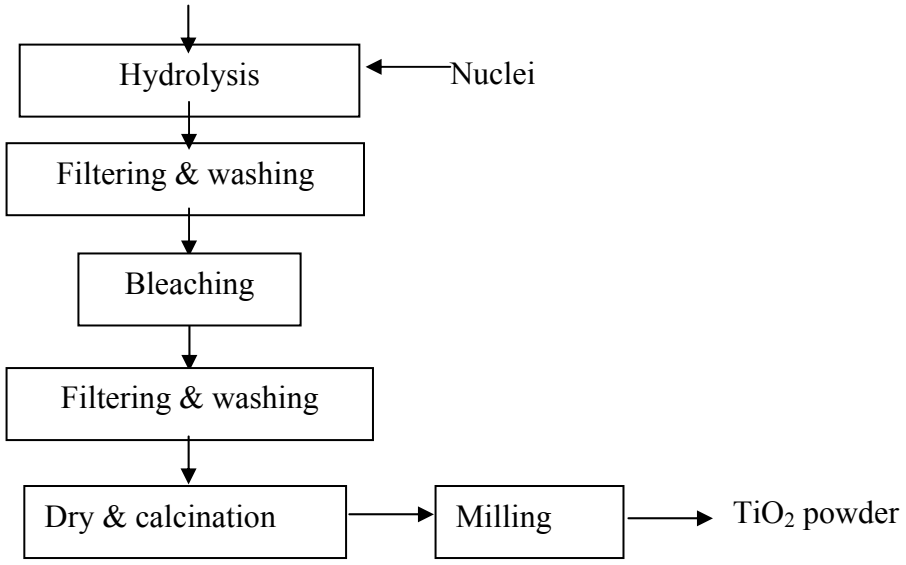

Fig. 1: Flow sheet for preparation TiO_2 powder

Conclusion

1. The theme has researched factors influencing on hydrolytic process, the experimental results showed that appropriate conditions for hydrolytic process are as follows: concentration of TiO_2 in the solution is 230g TiO_2/l; temperature of the solution is 100^0C; nnucleating the solution with 1.31% compared with weight of titanium dioxide in the solution.

2. Factors affecting bleaching process were also researched. Appropriate conditions were determined as follows: concentration of sulfuric acid in the solution is 8%; the bleaching time is 35 minutes; and temperature of the solution is 80^0C.

3. We have proposed a flow sheet for preparation TiO_2 powder using 1 kg TiO_2 powder containing 97-98% TiO_2, 0.012-0.017% Fe_2O_3, < 0.001% Cr; 0.8-1.44% SiO_2 , <0.01% Al_2O_3.

REFERENCES

[1]. Cao Hùng Thái, Nguyễn Đức Hưng, Tổng quan về các hoạt động khoa học công nghệ trong lĩnh vực sa khoáng ven biển. Viện Công nghệ xạ hiếm, Tuyển tập công trình khoa học 1985-2000.

[2]. Cao Hùng Thái, Xây dựng quy trình công nghệ nung khử Ilmenit và tách sắt kim loại để thu sản phẩm titandioxit 92-94% TiO_2. Đề tài cấp bộ mã số BO/05/03-01.

[3]. Cao Văn Hồng, Viện Nghiên cứu Mỏ và Luyện kim: Định hướng phát triển công nghệ luyện kim, chế biến sâu quặng Titan Việt Nam trong giai đoạn 2006-2010 và những năm tiếp theo. Tuyển tập báo cáo khoa học, Hội nghị khoa học kỹ thuật Mỏ toàn quốc lần thứ XVII.

[4]. Hoàng Nhâm, Hoá học vô cơ, Nhà xuất bản Giáo dục.

[5]. Nguyễn Đức Vận, Hoá học vô cơ, Nhà xuất bản Khoa học và Kỹ thuật.

[6]. Nguyễn Mạnh Khôi, Xây dựng cơ sở sản xuất bột màu TiO_2 200 tấn/năm. Viện Công nghệ xạ hiếm, 1990.

[7]. Nguyễn Văn May, thiết bị truyền nhiệt và chuyển khối, Nhà xuất bản Khoa học và Kỹ thuật.

[8]. Altairnano.com/documents/A2003-02-25 Verhulst.pdf.

[9]. T.K MukherJee, Mining and processing of titanium minerals in India, Metals Materials and processing, 1998, Vol. 10, pp. 85-98.

[10]. Ullman's Encyclopedia of Industrial Chemistry, Pigments, inorganic, Vol. A20.

[11]. Tidco.com/images%255CTITANIUM%2520DIOXIDE.doc+DU+pont+ Pigment+tio2+kolmak+chemicals+ltd.,+calcutta&hl=fr&ct=clnk&cd=1&gl=vn

INVESTIGATING THE APPLICATION OF THE ISP TECHNOLOGY FOR PRODUCING ZINC METAL FROM GALVANIZING ZINC DUST

Pham Quang Trung, Pham Minh Tuan, Le Minh Tuan
Tuong Duy Nhan, Ngo Trong Hiep and Tran The Dinh

Institute for Technology of Radioactive and Rare Elements, VAEC, Vietnam.

ABSTRACT: ISP (Imperial Smelting Process) is a zinc metal production method from zinc concentrates that has been applied in the world for a long time. Capability of the thermal process to produce high quality zinc metal (Zn 99% and Pb<1%) directly from zinc concentrates and dust on an industrial scale is outstanding character of the ISP.

Nowadays, in Vietnam, a lot of zinc dust from galvanization factories can be used as raw materials for ISP zinc production.

Project "Investigating the application of the ISP technology for producing zinc metal from galvanizing zinc duct" is carried out for initial technological experiments and to review application capability in practice.

We has designed and manufactured an imitative experiment apparatus according to the ISP principles. This apparatus consists of two main parts: zinc reduction and condensation of zinc into lead. It was operated on a scale of 5 kg raw materials per batch. This zinc reduction process occurred well at 1100-1250^{0}C with ratio of coke/zinc dust: 0.6/1.0. Zinc vapor is condensed into stirred smelting lead obviously. However, the oxidation process of zinc vapor backing to zinc oxide wasn't controlled so zinc recovery efficiency decreases. The zinc-lead condensation apparatus wasn't designed reasonably. It is the reason why recovery efficiency is low. Final results show that the ISP is a prosperous technology method which needs to be researched more thoroughly.

Introduction

In Vietnam, there have recently been many factories for plating steel details and tubes with zinc meeting the demand for developing mechanics and construction branch. Up to 2007, according to the statistic, there are ten galvanization factories, with consumption about 10,000 ton of zinc metal per year. These factories discard a lot of zinc dust, mainly in three kinds:

1. Zinc powder recovered from zinc vapor of galvanizing pot or from cleaning air in the steel tube.

2. Zinc dust recovered from surface of the galvanizing pot by creating zinc oxide and impurities.

3. Zinc alloy recovered from the bottom of the galvanizing pot because of agglomeration of zinc and other metals.

If these galvanization factories use 10,000 ton of zinc metal for a year, they will discard about 3,000 ton of zinc dust. This industrial waste containing zinc has high economic value if it is used for recycling or producing zinc products.

Project "Investigating the application of the ISP technology for producing zinc metal from galvanizing zinc dust" is carried out for initial research on ISP technology

which was applied all over the world with material is rich zinc-lead ore. From this, it is possible to apply for material that is zinc dust recovered from galvanization factories in Vietnam in order to increase practical efficiency of recovering, recycling zinc from industry waste.

Contents of project

1. Gathering reference documents about ISP method.
2. Analyzing, selecting appropriate zinc dust which is recovered from galvanization process is raw material for producing zinc by ISP method.
3. Research on reduction process of zinc.
4. Designing, manufacturing experiment apparatus followed by ISP method.
5. Experimenting ISP method on the produced apparatus.
6. Evaluating results and ability of applying ISP method.

Overview

Based on the combination of some zinc production methods by pyro-metallurgy on the cross-fired and cupola furnace, ISP method is used. The first ISP factory was built in Avonmouth (England) in 1967-1968, since then it has always been improved and perfected, especially on environment issue. Nowadays, there are about twelve ISP factories in the world, among which there are four ISP in Europe. In 1994, those factories produced 867,000 ton of zinc and 364,000 ton of lead (approximate 12% and 7% of the total production of the world, respectively).

Nowadays, ISP is a special method used to treat ore with high content of zinc and lead; it has replaced almost other fire metallurgy methods and is used on a large scale in many countries.

Research results

1. Researching, designing, manufacturing experimental apparatus

Based on the reference designs, we have built a system of apparatus according to the following principle diagram:

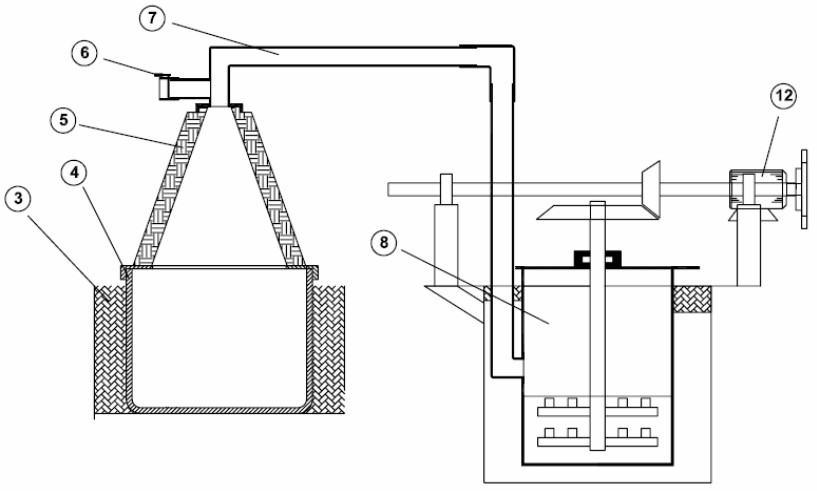

Fig. 1: A system for testing ISP method

Coke coal is grinded, mixed with zinc dust and then put into reduction pot (4) for each batch. Reduction process is carried out in coal furnace by supplying heat to the pot. The lid of pot is made of refractory ceramics and is assembled tightly with the mouth of reduction pot.

The tube system conducting CO air and zinc vapor (7) is made of heat- resisting steel with heat- retaining by fiber ceramics. After being heated through the valve (6), heat air is led to the reduction pot. The condenser (8) is made of stainless steel. The stirrer is used to create lead vapor in the condenser turned by a motor (12) with capacity 1,0kW. Rotational speed of wing is 120 rounds /minute. The pot for condensing zinc is heated by coal furnace. The temperature in condenser is adjusted by gas cooker.

2- Experiment results

Reduction process occurs well, zinc evaporates rapidly. Lead liquid is stirred well. Metal sample on the face of lead block is taken out after the experiment stopped. There is a little powder of zinc oxide. Therefore, oxidized zinc vapor is limited. Condensation process of zinc in lead appears rather clearly. Because amount of lead compared with zinc is high (ratio of Zn/Pb: 0.04, accounting all of reduced and absorbed zinc), it is difficult to take out and analyze alloy samples. The analysis results of four alloy samples are shown on the table 1.

Table 1: The analysis results of four alloy samples

Number of the sample	**1**	**2**	**3**	**4**
Pb	98.32	97.61	98.25	97.18
Zn	1.15	1.64	0.01	1.06

Remark: Because experiment apparatus are still simple, recovered zinc metal product isn't as much as initial expectation. There have been two dissolved problems:

1. Controlling oxidation of zinc vapor backing to zinc oxide.
2. Creating vapor of lead liquid to absorb zinc vapor.

In practice, this is a very hard problem that is solved only when experiment apparatuses are fabricated more perfectly and technologically.

Conclusion

1. We have gathered lots of reference documents connecting with ISP method and production of zinc in the world. It is very useful for our work and development of producing zinc which is carried out in ITRRE.

2. Some science problems relating to technology for treating and recovering zinc from industrial waste are clarified though researching. For example, study on reduction process of zinc dust in the medium frequency furnace helps to develop production of zinc output from zinc dust in ITRRE. Besides some parameters such as temperature, pressure, ratio of reducer, adding appropriate air to strengthen reduction process but not to oxidize zinc vapor backing to zinc oxide is a complex problem in practice.

3. We have designed and fabricated a system of apparatus following ISP method, which consists of two main parts: the first for reducing zinc and the second for condensing zinc in lead. Although those apparatus are simple but they are the first model in ITRRE for researching, producing zinc metal by fire metallurgy method. From this, researchers can have more knowledge and experience when making those apparatus.

4. We have operated self-made apparatus on a scale of 3kg of raw material per batch. Zinc reduction process occurred well at 1100-1250^{0}C, with ratio of coke coal/ material is 0.6/1.0. Zinc vapor is condensed into stirred smelting lead obviously. However, the oxidation process of zinc vapor backing to zinc oxide wasn't controlled so zinc recovery efficiency decreases. The zinc-lead condensation apparatus wasn't designed reasonably. It is the reason why recovery efficiency is low.

5. Final results show that the ISP is a promising technology method which needs to be researched more thoroughly.

REFERENCE

[1]. Secondary Zinc Source/ Imperial Smelting Process.

[2]. Prof. Dr. O. Rentz, et al, Report on Best Available Techniques (BAT) in German Zinc and Lead Production (Final Draft), Karlsruhe, February 1999.

[3]. BSC. Milo Sjardin, CO_2 Estimation Factor for Non -Energy Use in the Non - Ferrous Metal, Ferroalloy and Inorganic Industry, Utrecht, June 2003.

[4]. ISP Zinc Production.

[5]. Imperial Smelting Process.

[6]. A. Cox.; D.J.Fray, Zinc Reoxidation in the Shaft of a Zinc-Lead Imperial Smelting Furnace-1: Zinc-Carbon-Oxygen System with Deposition Initiated on a Quartz Substrate and Subsequent Propagation on Zinc Oxide, Maney Publishing.

SYNTHESIS AND STUDY ON COMPLEXES OF SOME LANTHANIDES TO L-ISOLEUCINE

Le Minh Tuan, Pham Minh Tuan and Tran The Dinh

Institute for Technology of Radioactive and Rare Elements, VAEC, Vietnam.

ABSTRACT: The formation of lanthanide (La, Pr and Nd) complexes with L-isoleucine have been studied as a function of pH values. The titrations were performed at 25 degrees C, and the ionic strength of the medium was maintained at 0.10 M by using potassium nitrate. The formation curves of their complexes (n-p[L]) were obtained by means of the titration data. Then the stability constants were determined in relation to these curves.

The complexes were synthesized in the mixture of water-ethanol. The coordination of the complexes were determined by elements analysis, ^{13}C-NMR, ^{1}H-NMR and IR methods. These complexes are formulated as $Ln(HIle)_3.(NO_3)_3.3H_2O$; (Ln: La, Pr and Nd,; L-Ile: L-isoleucine). Comparision of the IR, ^{13}C-NMR and ^{1}H-NMR spectra of the ligand with those of their complexes shows that isoleucine acts as a bidentate ligand bonding the lanthanide ions through the amino and carboxylate groups.

Key words: Complex, coordination, lanthanide, L-isoleucine.

Introduction

For a long time, lanthanides and their compounds are widely used in many industries especially in agriculture and biotechnology industry based on bioactivities of lanthanide compounds including lanthanide amino acid chelates.

Survey of the literature shows that studies on the lanthanide complex formation with amino acids need to be paid attention for solving the disagreements on the coordination modes between lanthanides and amino acids. In this report, the formation of some lanthanide (III) isoleucine complexes will be studied as a function of pH and the coordination of lanthanides with L-isoleucine will be clarified by using IR, 1H-NMR and 13C-NMR spectrometries.

Results and disscussion

1. Stability constant calculations

It is well known that amino acids exist in the “zwitter” ionic form (figure 1). L-isoleucine possesses two different functional groups, e.g. carboxyl and amino groups that can be used for complexation with lanthanides.[3, 4].

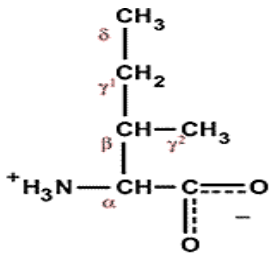

Fig. 1: The “zwitter” ionic form of L-isoleucine.

In acid medium, L-isoleucine (H_2Ile^+) dissociated following equations

$$H_2Ile^+ = H^+ + Hile \qquad K_1 = \frac{[H^+].[HIle]}{[H_2Ile^+]} \qquad (1)$$

$$HIle = H^+ + Ile^- \qquad K_2 = \frac{[H^+].[Ile^-]}{[HIle]} \qquad (2)$$

From the pH titration of a 2:1 mixture of the ligand and lanthanide ions and L-isoleucine alone, complex formation carried out following these reactions:

$$Ln^{3+} + HIle = LnIle^{2+} + H^+$$

$$LnIle^{2+} + HIle = LnIle_2^+ + H^+$$

The stability constants of complexes was calculated by using Bjerrum method relying on the ralations between n values (the average number of ligand molecules bound per metal ion) and Ile^- concentration. From experimental standpoint, n may be expressed in terms of the total isoleucine concentration (C_{H2Ile}+), the concentration of Ile^- and the total Ln^{3+}concentration (C_{Ln}3+):

$$\bar{n} = \frac{C_{H_2Ile^+} - X.[Ile^-]}{C_{Ln^{3+}}} \qquad (3)$$

In which:

$$X = \frac{[H^+]^2}{K_1.K_2} + \frac{[H^+]}{K_2} + 1 \qquad (4)$$

$$[Ile^-] = \frac{(2-a).C_{H2IL}}{\frac{[H^+]}{K_1}} \qquad (5)$$

n and [Ile^-] values can be calculated from the experiment data. If n versus p[Ile^-] is plotted (figure 2), then approximate values of the stepwise formation constants, k_1 and k_2 are obtained at n = 0.5 and n = 1.5.

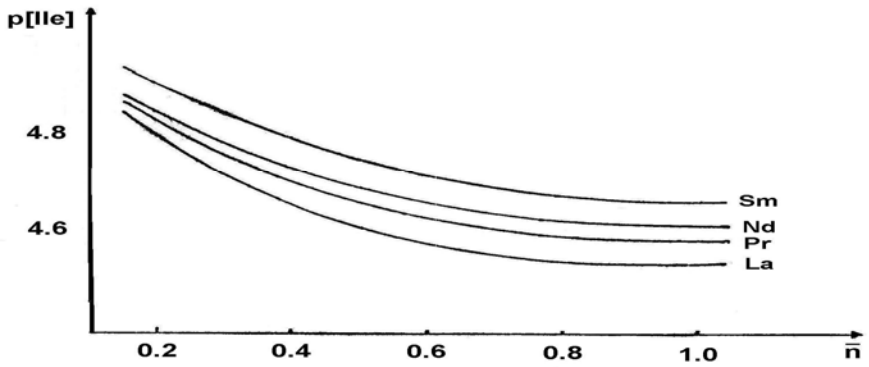

Fig. 2: Dependence of the average number (n) on p[Ile^-]

The results from experiment showed that the end point (n > 0,6) was indicated by the incipient formation of precipitates, presumably of lanthanide hidroxides. So that, only first stability constant k_1 was calculated at n = 0,5 following the equation (6) and showed in table 1.

$$k_1 = \frac{1}{[Ile^-]} \rightarrow \lg k_1 = -\lg[Ile^-] = p[Ile^-] \quad (6)$$

Table 1: Stability constants k_1 of lanthanide complexes

Lanthanides (Ln)	La	Pr	Nd
Lg k_1	4.65	4.69	4.72

2. Synthesis and determine the coordination modes between lanthanides and L-isoleucine in complexes

Lanthanide nitrates and L-isoleucine dissolved separately in mixture of H_2O & C_2H_5OH (volume ratio 1:1) were mixed together and the resuling solution was kept at 50-60^oC in about 6 hours on a water bath. The complexes were obtained following the reaction:

$$Ln(NO_3)_3 + 3HIle \rightarrow Ln(HIle)_3(NO_3)_3.nH_2O$$

The coordination compounds of lanthanides and the ligand were concentrated by solvent evaporation and the water contents reduced by successive additions of absolute etanol. After cooling, crystals of complex that were separated from solution are filtered, washed by absolute ethanol and stored in exsiccator.

The lanthanide, nitrogen and nitrate contents in isolated complex were determined and the obtained results were showed in table 2. The results showed that Ln, N and NO_3^- contents that have been determined by experiments agreed with calculated data from proposed formula $Ln(HIle)_3(NO_3)_3.nH_2O$.

Table 2: Elemental analysis of lanthanide complexes

Proposed formula	**Ln (%)**		**N (%)**		**NO_3^- (%)**	
	Cal.	*Found*	*Cal.*	*Found*	*Cal.*	*Found*
$La(HIle)_3(NO_3)_3.3H_2O$	17.99	18.24	10.87	10.62	24.08	24.87
$Pr(HIle)_3(NO_3)_3.3H_2O$	18.19	17.95	10.85	11.63	24.02	23.86
$Nd(HIle)_3(NO_3)_3.3H_2O$	18.54	18.22	10.80	10.58	23.92	24.55

IR spectra of L-isoleucine and its complex with Ln^{3+} were obtained in KBr pellets on a Magna-IR 760 Nicolet infrared Spectrophotometer in the range of 400-4000 cm^{-1}. The obtained results were showed in table 3 belows.

Table 3: Band assignment of the IR bands of ligand and lanthanide complexes

Compound	$\sqrt{}_{as}^{COO-}$	$\sqrt{}_{s}^{COO-}$	$\sqrt{}^{NH_3^+}$	$\sqrt{}^{NH_2}$	$\sqrt{}_{1}^{NO3}$	$\sqrt{}_{2}^{NO3}$	$\sqrt{}_{3}^{NO3}$	$\sqrt{}^{O-H}$
L-isoloxin	1571	1418	2961	-	-	-	-	-
$La(HIle)_3(NO_3)_3.3H_2O$	1581	1387	-	2930	1031	1331	1495	3373
$Pr(HIle)_3(NO_3)_3.3H_2O$	1586	1385	-	2931	1020	1320	1487	3372
$Nd(HIle)_3(NO_3)_3.3H_2O$	1585	1387	-	2935	1024	1332	1489	3374

IR spectra of complexes and ligand not only had differing shape but also position of specific bands. They demonstrated the complex formation between Ln^{3+} and L-isoleucine.

The IR spectrum of L-isoleucine exhibited a band at 2961 cm^{-1}, which was assigned to vibration of the $^{+}NH_3$ group. The ν NH_3 band appears at a region lower than that expected for ν NH_3 band (3400 cm^{-1}), probably due to strong interaction between NH_3 and COO groups in the zwitter ion.

In the spectrum of the ligand, the bands corresponding to ν_a COO and ν_s COO vibrations were observed at 1571 cm^{-1} and 1418 cm^{-1}. In IR spectrum of complex, the band due to ν_a COO and ν_s COO vibrations were shifted to lower wave number appearing at about 1585-1586 cm^{-1} and 1384-1387 cm^{-1} . Besides, the position of ν NH_2 band was at a lower region than that normally observed, and hence NH_2 group of L-isoleucine was coordinated to the lanthanide ions.

Three additional bands at 1408.82 cm^{-1}, 1234.71 cm^{-1} and 1029.87 cm^{-1} in the spectra of complex were assigned respectively to ν_3, ν_2 and ν_1 modes of coordinated nitrate ions.

Besides, in the spectra of complex, The new broad band appears near 3400 cm^{-1} was assigned to vibration of OH^- group in crystalized water molecules. This agreed with results obtaining from thermal analysis of complex.

These shifts indicated that L-isoleucine was coordinated to Y^{3+} ion through amino and cacboxylate groups.

To confirm results obtaining from analysis of IR spectrums, ^{13}C-NMR, ^{1}H-NMR of ligand and complexes have been recorded to determine the changes of chemical shifts of all positions in ligand and complexes that indicate the evidence of functional groups in binding with lanthanide ions.

Data obtaining from ^{1}H-NMR spectrum of L-isoleucine and complexes (table 4) showed that, except fixed signal of D_2O (4,7 ppm), The signals of all H atoms (from α to δ) were shifted to lower field with significant change at H-α and gradually decreased from H-β to H-γ^2 after complexation with Ln^{3+}. This result was compatible with the lanthanide complexation by the amino (-NH_2), since it caused a highly decrease of the electron density around the H-α and a lower level decrease ones at remaining H atoms, and this decreased in shielding displaces the NMR signals toward a lower field.

Table 4: ^{1}H-NMR data for L-isoleucine and lanthanide isoleucine complexes

Coumpound	Peak position (ppm)						
	D_2O	H-α	H-β	H-γ^1		H-γ^2	H-δ
L-isoleucine	4.700	3.624	1.938	1.424	1.218	0.895	0.967
$La(HIle)_3(NO_3)_3$	4.700	4.450	2.509	1.881	1.540	1.276	1.046
$Pr(HIle)_3(NO_3)_3$	4.700	3.749	2.035	1.475	1.255	0.916	1.009
$Nd(HIle)_3(NO_3)_3$	4.700	3.741	2.025	1.464	1.258	0.910	1.005

^{13}C-NMR spectrum (table 5) of L-isoleucine and complexes showed the changes of resonance signal positions (chemical shift) of L-isoleucine after complexation with Ln^{3+}. We can see that, resonance signal of the cacboxyl C was slightly shifted downfield because of the insignificant affect of ionic bonding between lanthanide ions and cacboxyl group causes little decrease of electron density of cacboxyl-C.

Table 5: ^{13}C-NMR data for L-isoleucine and lanthanide isoleucine complexes

Coumpound	Peak position (ppm)					
	$C_{caboxyl}$	C-α	C-β	C-γ^1	C-γ^2	C-δ
L-isoleucine	174.535	59.993	36.294	24.875	15.102	11.509
$La(HIle)_3(NO_3)_3$	174.629	62.595	36.537	25.096	15.300	11.597
$Pr(HIle)_3(NO_3)_3$	174.773	64.349	36.736	25.300	15.482	11.704
$Nd(HIle)_3(NO_3)_3$	174.830	66.021	36.859	25.071	15.279	11.592

While, resonance signal of C-α adjacent both cacboxyl and amin groups was shifted significantly to lower field (from 59.993 ppm to 62.595 - 66.021 ppm). This change are due to the interaction between lanthanide ions to amin ($-NH_2$) group caused decrease in electron density at C-α. Besides, coordination between Ln^{3+} and amin group ($-NH_2$) caused much enough effect to pull electron density of the remaining carbon atoms at lower level and this effect was gradually decreased following the distances between respectively carbon and C-α.

The changes of resonance signals in ^{13}C-NMR, ^{1}H-NMR spectrums confirmed the assessment on coordination mode of lanthanide and L-isoleucine.

Conclusions

1. The complexation between Ln^{3+} and L-isoleucine have been investigated. In aqueous solution, $LnIle^{2+}$ complex (Ln: La, Pr and Nd) formed and stability constants k_1 were calculated by J. Bjerrum method.

2. Solid complexes of some lanthanides and L-isoleucine have been synthesized and isolated. From the analysis of IR, 1H-NMR and 13C-NMR spectrums of ligand and complexes, the complexes were formulated as $Ln(HIle)_3(NO_3)_3.3H_2O$. In obtained complexes, L-isoleucine acted as a bidentate ligand bonding Ln^{3+} ion through the amino and cacboxylate groups. The anion NO_3^-, acted as additional ligand occupies a coordinated position.

REFFERENCES

[1]. Niu chunji, Ni Jiazuan (1994), *Advances in bioinogranic chemistry of rare earth in China Programme and abstracts of the international symporium on Appied bioinogranic chemistry (ISABC-3)*, Australia C24.

[2]. Спицин В.И. Мартыненко Л.И (1979), *Координационная химия редкоземельных элементов*, Изд.Москвого университетта.

[3]. Яцинмирский К.Б (1996), *Химия комплексных соединений редкоземельных элементов*, АН Укр. СССР, Киев.

[4]. Holleman A.F., Wiberg Egon (1995), *Inorganic Chemistry*, 34th Edition, ACADEMIC PRESS, New York.

[5]. Phan Tong Son, Tran Quoc Son, Dang Nhu Tai (1980), Basics of Organic Chemistry, Vol.II, Publishing House of University and Professional College, Hanoi, Page. 416 – 434.

[6]. Tran Ich (1979), *Boichemistry*, Publishing House of Education, Hanoi, Page. 6 - 71.

[7]. Vickery R.C. (1950), *Separation of Lanthanons by means of complexes with amino acids*, J. Chem, Soc, 2058.

[8]. Katzin L.I., Gulyas E. (1968), *Absorption and circular dichroism spectral studies of chelate of praseodymium with α-amino acids, Inorganic Chemistry*, pp 2442-2446.

[9]. Celia R Carubelli, Ana MG.Massabni and sergio R.deA.leite (1997), *Study of the binding of Eu^{3+} and Tb^{3+} to L- phenylalanine and L- triptophan. J Brazil*, Chem.soc, vol 8 , $N^0$6, Brazil, ,pp 597-602.

[10]. Indrasenan P, Lakshmy M. *Indian Jornal of Chemistry*. Vol. 36A, pp 998-1000 (1997).

[11]. Nguyen Trong Uyen, Le Huu Thieng, Le Minh Tuan, Du Dinh Dong. Journal of Chemistry, Vol.44 (3), Page 311-316 (2006).

[12]. Nguyen Trong Uyen, Le Huu Thieng, Le Minh Tuan, Du Dinh Dong. Journal of Chemistry, Vol. 45 (3), page.315-318 (2007).

PREPARATION OF HIGH QUALITY ZIRCONIUM OXYCHLORIDE FROM ZIRCON OF VIETNAM

Ngo Van Tuyen, Vu Thanh Quang, Trinh Giang Huong and Vuong Huu Anh

Institute for Technology of Radioactive and Rare Element, VAEC, Vietnam.

ABSTRACT: This paper introduces a sodium hydroxide decomposition method for zirconium oxychloride production from zircon sand of Vietnam such as Ha Tinh, Hue, Binh Thuan seaside. Techniques for separation of impurities in ZOC final product such as SiO_2, Fe_2O_3, TiO_2, rare earths, uranium, and thorium have also been introduced. Content of uranium and thorium in the final product of ZOC is less than 1 ppm.

Key words: Zircon oxyclorua, zirconium silicate, uranium, thorium.

Introduction

Zirconium oxychloride is a very important precursor for preparation of many other zirconium compounds. At present, the zirconium oxychloride is widely used in various fields such as textile dyeing; oil-field acidizing; antiperspirants, water repellents and TiO_2 pigment coating. In addition, it is also applied in ceramic, electronic and nano material technology...

Zircon sand is initial material for producing zirconium oxychloride. This technology consists of three stages:

- Decomposition of zircon sand with sodium hydroxide at 600-700^{0}C.

- Precipitation of base sulfate of zirconium for removing unwanted impurities such as Fe, Ti, Al, U, Th, etc.

- Crystallization of the final product of zirconium oxychloride.

Experiment, Results and discussion

1. Preparation of zirconium oxychloride having high quality by decomposition method with sodium hydroxide

1.1. Chemical composition of samples and chemical for experiment

Table 1 shows composition of zircon sands used as initial material. Chemicals for experiments include NaOH, HCl, $(NH_4)_2SO_4$ in industrial grade and HCl, NH_4OH are in analytical grade.

Composition of Zircon sands

No	Samples	Component content (%)							
		TiO_2	*Fe_2O_3*	*Cr*	*SiO_2*	*ZrO_2*	*U*	*Th*	*Al_2O_3*
1	$ZrSiO_4$ Hue	0.28	0.081	0.002	33.34	63.1	0.0659	0.0631	0.52
2	$ZrSiO_4$ Ha Tinh	0.12	0.071	0.0016	34.21	62.6	0.070	0.028	0.55

3	$ZrSiO_4$ BinhThuan	0.56	0.118	0.0018	34.32	61.9	0.064	0.039	0.59
4	$ZrSiO_4$ Ti west US	0.15	0.14	0.0014	34.23	62.1	0.025	0.019	0.48
5	$ZrSiO_4$ Iluka China	0.21	0.14	0.0013	34.31	61.5	0.027	0.018	0.53

1.2. Flow chart of ZOC preparation

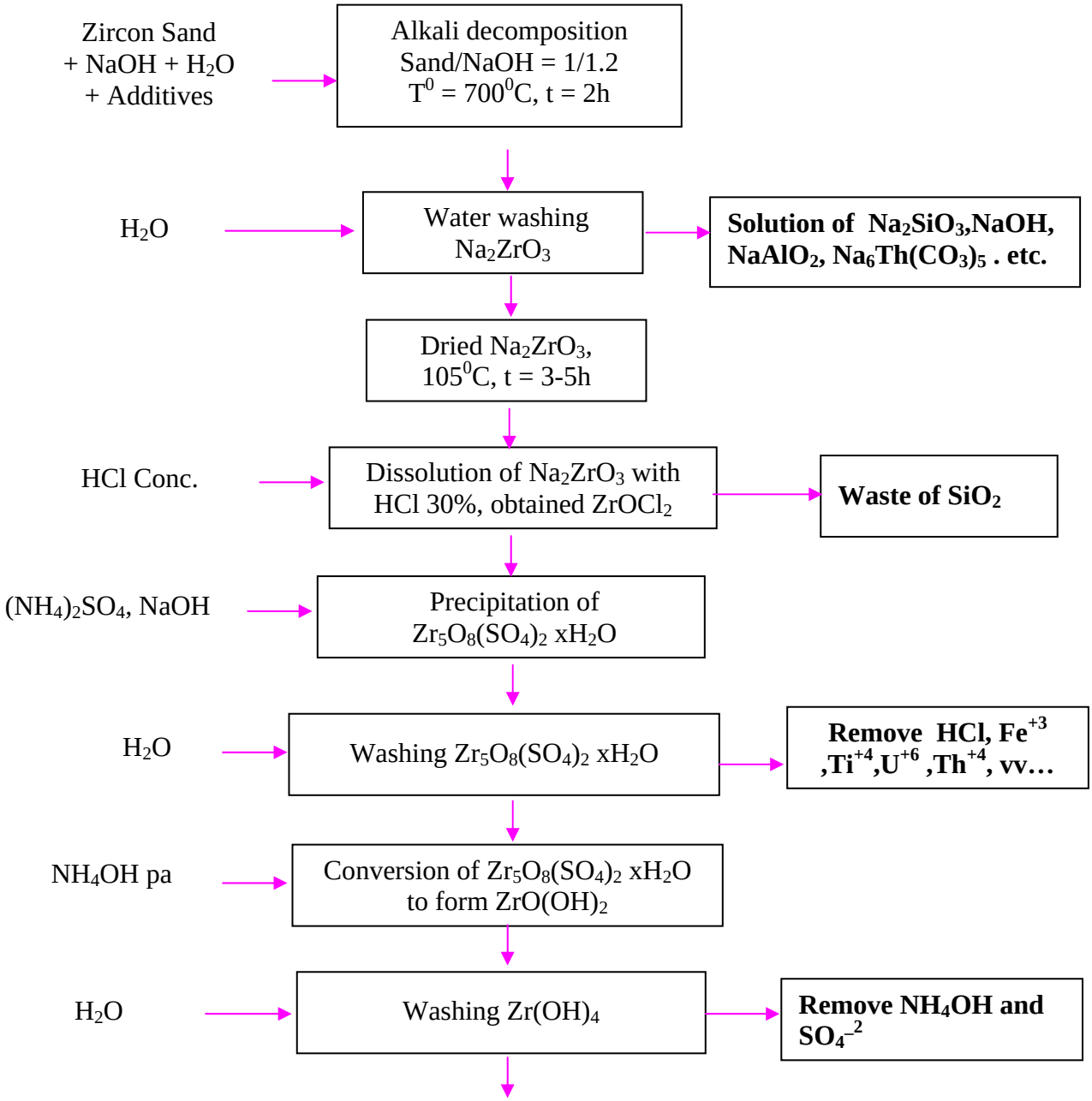

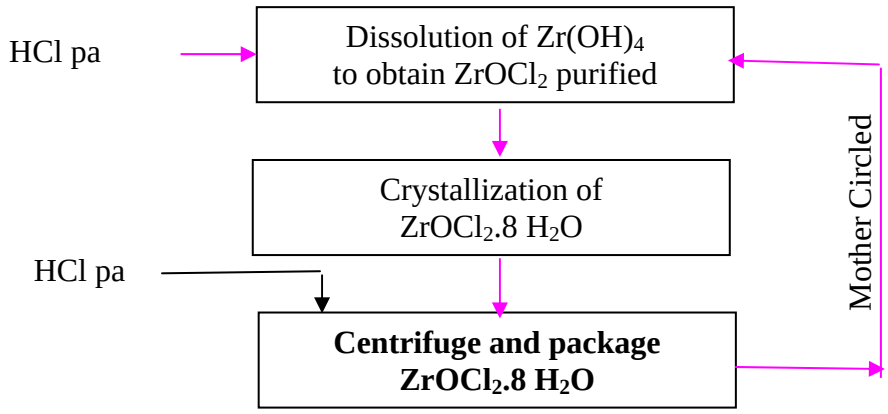

2. Experiment Procedure

- Decomposition of zircon sand by alkali NaOH

All experiments are carried out in a steel pipe furnace with volume of 2 liters. For each experiment, 500 grams of zircon sand is perfectly mixed with NaOH, NaF, Na_2CO_3 and H_2O in a ratio of $NaOH/ZrSiO_4/H_2O/NaF/Na_2CO_3$ is 1.2:1:0.1:0. 015:0.015. The mixture is heated to 400^0C and continuously stirred for 35 min. At the moment, the reaction occurs drastically and the mixture becomes liquid that is easy to overflow. After that, the temperature is increased to 670-700^0C for 3hrs. Decomposition yield of the process achieves up to 93%. The final product is a fine soft powder that is easy to take out of the furnace. The powder is leached with water in a ratio of solid/liquid equal 1/8. After 5 times of the leaching, about 80% of SiO_2 and 75% of total of U, Th is removed from the final product named sodium zirconate.

- Dry sodium zirconate for getting para SiO_2

Obtained sodium zirconate from alkali decomposition and water leaching of zircon sand consists of ZrO_2 (80.4%), SiO_2 (6.21%), TiO_2 (1.76%), Fe_2O_3 (0.31%), Al_2O_3 (0.25%), CaO (0.27%), Cr_2O_3 (<0.015), P_2O_5 (<0.01%). The sodium zirconate is dried at 105^0C for 4hrs to fix silicon compounds in para SiO_2 that is difficult to dissolve by acids.

- Acid leaching

The sodium zirconate is dissolved by HCl of 20-30% at temperature of 90-100^0C. The acid addition is about 35% higher than theoretical requirement. Obtained solution is zirconium oxychloride consisting of ZrO_2 (65-70g/l) ; Fe (0,8-1g/l); TiO_2 (0,6-0,8g/l); SiO_2(1,2-1,5g/l) and solid waste containing a small amount of origin starting material and silicon colloid. Then the next step is precipitating base sulfate of zirconium.

- Precipitation of zirconium base sulfate

Precipitating zirconium base sulfate is a characteristic and high selective method for removing unwanted impurities to get the pure zirconium compounds. The precipitation is carried out as bellows: Adding $(NH_4)_2SO_4$ or Na_2SO_4 in ratio of SO_4^{-2}/ZrO_2 = 0.5 /1 (M) to zirconium oxychloride solution then stirring it in 150 rpm and heating it up to 80 - 90^0C. The pH of the solution is controlled in a range of 1.8-2.0 using 10% NaOH solution. Zirconium base sulfate precipitates ($4\ ZrO_2.3SO_3.14H_2O$) formed and has some

characteristic properties as filterable, well form, solid and thus it is easy to remove impurities of Ti, Fe, Si, U, Th, etc. by 5 times of washing.

- Conversion of $ZrO_2.3SO_3.14H_2O$ to $ZrO(OH)_2$ form

Obtained zirconium base sulfate in slime form is converted to zirconium hydroxide, NH_4OH 10% is used as precipitation agent. Reaction conditions include as below:

Temperature is of about 70-80^{0}C.

Stirring speed is of 150 rpm.

Reaction time is of 1.5hrs.

Velocity of NH_4OH is 3 liters/min.

Final pH is of 10.

Then the zirconium hydroxide is washed by water in 5 times to remove all SO_4^{-2}.

- Dissolution of resulted $ZrO(OH)_2$

A slury in ratio of $ZrO(OH)_2/H_2O$ = 1/1 is dissolved used HCl concentrate in analytical grade. Dissolution conditions are below:

Temperature is about 70-80^{0}C.

Stirring speed is of 150 rpm.

Reaction time is of 30 min.

Ratio of HCl/ZrO_2 = 5/1 (M)

C_{HCl} odd: 4-6M

C_{ZrO2} : 1.5 M.

The last step is filtration and waste of SiO_2 gel and to obtain clarified and pure solution of zirconium oxychloride.

- Crystallization of ZOC

The obtained ZOC solution is concentrated to get C_{ZrO2} : 2 M, C_{HCl} : >6 M. Then cooling to room temperature and maintain for 24hrs for perfect crystallization.

- Centrifuge washing ZOC crystal and packing

Separation of resulted ZOC crystal and mother solution is performed in centrifuge machine. After that the crystal is washed by used HCl 5.5 M with ratio of L/S= 1/10. Recovery yield is more than 60%. The mother solution contains C_{HCl} : 6 M, C_{ZrO2} :1.1 M and reused in the dissolution of zirconium hydroxide.

The last stage is packing in PVC.

Table 2: Composition of final zirconium oxyclorua determined by MeiWa, Japan.

No	Name of Product	Composition of components							
		$Zr(Hf)O_2$ (%)	*Fe_2O_3 (ppm)*	*Na_2O (ppm)*	*SiO_2 (ppm)*	*TiO_2 (ppm)*	*Al_2O_3 (ppm)*	*U (ppm)*	*Th (ppm)*
1	ZOC1	≥ 32.7	≤ 10	≤ 10	35.78	51	≤ 36	≤ 0.133	2.97
2	ZOC2	≥ 26	≤ 10	≤ 10	0.15	≤ 5	≤ 36	≤ 0.133	0.84
3	ZOC3	≥ 29.5	≤ 10	≤ 10	2.85	68	≤ 36	≤ 0.133	0.72
4	ZOC4	≥ 28	≤ 10	≤ 10	2.33	6	≤ 36	≤ 0.133	0.35
5	ZOC5	≥ 28	≤ 10	≤ 10	2.18	≤ 5	≤ 36	≤ 0.133	0.33

ZOC1 : ZOC from zircon sand Hue

ZOC2 : ZOC from zircon sand Ha Tinh

ZOC3 : ZOC from zircon sand Binh Thuan

ZOC4 : ZOC from zircon sand ILuka (china)

ZOC4 : ZOC from zircon sand TiWest (US)

Conclusion

Preparation of high quality zirconium oxychloride $ZrOCl_2 8H_2O$ contained U, Th < 5 pap from zircon sand of Binh Thuan, Ha Tinh, Vietnam is possible.

Alkali decomposition method with additives of NaF, Na_2CO_3 and H_2O have been applied for ZOC preparation in this paper that is not only achievement of a fine soft reaction mass with a high yield of more than 93% but also easy to remove > 80% SiO_2 and > 75% total of U,Th of starting material by water washing.

The sodium zirconate is dried at temperature of 105^0C for 4hrs to fix silicon compounds in para SiO_2 . That is difficult to dissolve by acids and easy to separate from ZOC solution.

It is possible to separate perfectly impurities of Fe, Ti, Al, U, Th, etc. from Zr by application of zirconium base sulfate precipitation method at acid medium and temperature of 90-100^0C. The method can achieve a recovery yield of more than 98% and able to develop up to large scale.

Zirconium base sulfate is easy to convert to zirconium hydroxide by using NH_4OH at room temperature. Removal of SO_4^{-2} from $ZrO(OH)_2$ is very simple. Dissolution of $ZrO(OH)_2$ by means of HCl at temperature of 70-80^0C occurs very fast.

Crystallization of ZOC from purified solution of zirconium oxychloride is carried out in a strong acid medium and washing the product with HCl pure 5.5M hence preparation of high quality ZOC contained total of U, Th less than 1ppm is possible.

REFERENCES

[1]. Phan Dinh Tuan, Do Quy Son, Ngo Van Tuyen, Le Thi Kim Dung, Hoang Van Sinh, Study on technology for removal of Si during process of zirconia technique grade. ITRRE, 2001.

[2]. Cao Dinh Thanh, Ngo Van Tuyen, Vu Thang Quang. Final report of project: Development of production line of Zirconia stabilized by CaO and CeO_2. ITRRE 2005 -2006.

[3]. Zelikman A. N, Krein O.E, Samsonob G. B, *Metallurgy of Rare Metals*, Metallurgy, Moscow, 1978.

[4]. Miller, Technology of ziconia, New York, 1975.

[5]. United States Patent 4822575. Process for the purification of zirconium compounds.

[6]. United States Patent 5160482. Zirconium-hafnium separation and purification process.

1.10 - Computation and Other Related Topics

DEVELOPMENT OF A GRAPHICAL INTERFACE COMPUTER CODE FOR REACTOR FUEL RELOADING OPTIMIZATION

Do Quang Binh, Nguyen Phuoc Lan and Bui Xuan Huy

Centre for Nuclear Techniques, VAEC, Vietnam.

ABSTRACT: This report represents the results of an institute project performed in 2007. The aim of this project is to develop a graphical interface computer code that allows refueling engineers to design fuel reloading patterns for research reactor using simulated graphical model of reactor core. Besides, this code can perform refueling optimization calculations based on genetic algorithms as well as simulated annealing. The computer code was verified based on a sample problem, which relies on operational and experimental data of Dalat research reactor. This code can play a significant role in in-core fuel management practice at nuclear research reactor centers and in training.

1. Introduction

After a time of operation, a reactor must be refueled. Because of the unsymmetrical distribution of fuel burnup over the reactor core, a decision on how many fuel bundles and what fuel bundles to be refueled must be based on the solution of the problem of in-core fuel management optimization.

For a very long time after the first nuclear power reactor was launched into critical and put into operation, only two traditional methods of fuel reloading having been adopted were those of 'out-in' pattern and checkerboard pattern [1]. These initial reloading methods are assured to give the flat radial power distribution over the reactor core. The existence of only a few of methods for fuel reloading for a long time reflects somewhat the complexity and difficulty of this typical problem in reactor area. Since 1980 researches into this problem have increasingly developed, resulting in much optimistic progress in the process of this matter. An apparent consequence resulting from the past researches is a change in the fuel reloading strategy from following the out-in scheme to adopting the low-leakage patterns. The out-in scheme, by which fresh fuels are loaded into outermost core positions, flattens the radial power density distribution while the low-leakage patterns allow the arrangement of fresh fuels into non-periphery positions to extend the cycle length.

For nearly four decades research into the problem of in-core fuel management optimization has increasingly developed, resulting in a perspective progress [2-14]. Recent research works have been usually based on stochastic methods like GA [5-12], simulated annealing method [2-5,13,14], etc. as well as combinations of these methods with heuristic rules [5]. Turinsky [15] overviewed the development of nuclear fuel management optimization capabilities for PWRs and BWRs ranging from the employment of experience-based rules to the usage of mathematical approaches.

Besides, development of graphical interface reactor calculation programs combined with heuristic rules also allows the more convenient manual preparation of fuel LPs at many centers. This approach is of great interest to fuel managers because of its intuitive, concrete and easy to understand features. Furthermore, stochastic methods often reach near global optimal solutions but not exact optimum, so graphical interface

reactor calculation programs can be used to move towards better solutions from the solutions of stochastic methods.

2. Orientation of works

Principal characteristics of a reactor such as k_{eff}, neutron flux distribution can be determined by solving the following multigroup neutron diffusion theory equations:

$$-D_{r,g}\Delta\Phi_{r,g} + (\Sigma_{a,r,g} + \sum_{g'}\Sigma_{s,r,g\to g'})\Phi_{r,g} = \sum_{g'}(\Sigma_{s,r,g'\to g} + \frac{\chi_g(\nu\Sigma)_{f,r,g'}}{k_{eff}})\Phi_{r,g'}$$

Power peaking factor PPF is determined based on the neutron flux distribution. Each global reactor calculation provides neutron parameters needed for optimal calculations. Graphical representation of reactor on computer screen together with its neutron parameters can help refueling engineers perform simulated fuel exchanges in computer model to find out optimal fuel reloading patterns according to their experience. A graphical interface computer code has been developed in this project to make the above idea become practical. It means that this program can help a refueling engineer to design manually refueling patterns using simulated model of the reactor.

The code includes programme modules written independently in languages Visual Fortran and Visual Basic, running on PCs. This version of the code can perform global reactor calculation, automatically searching fuel reloading patterns that maximize the effective multiplication factor and minimize the power peaking factor within rigorous constrains and design manually optimal refueling configurations using graphical representation of reactor in two-dimensional geometry. The reactor calculation involves the finite difference diffusion theory representation of neutron transport theory [16], treating three space dimensions with arbitrary groups. The radial geometric mesh options in reactor calculation include slab, cylinder, hexagonal and triangular. The flowchart of the code, named REFUELOP, is shown in fig. 1. The code includes three principal modules CITALIB, OPTIVN and SIMULATE and an additional. CITALIB is modified based on the CITATION reactor calculation code [16], module OPTIVN written in Visual Fortran is an optimization programme, and SIMULATE written in Visual Basic and module RECONFIG written in Visual Fortran is graphical interface modules.

3. Results and discussion

Calculations were performed to verify the computer program. The program was used to design optimal refueling patterns of the Dalat reactor for its second cycle. At that time, all the 89 existing fuel bundles in the core were unchanged; only 11 beryllium rods, which have the same shape and size as the fuel bundles, at the core periphery were replaced by 11 fresh fuel bundles. fig. 2 presents the arrangement of 100 fuel bundles in the core after 11 beryllium rods were replaced by fresh fuel bundles. This core configuration defines the base LP, in which the fuel bundles are assigned by the same number as the core positions. The number on the upper line in a cell indicates core position. Fuel burn-up BU = $\Delta m^5/m^5_0$ (where Δm^5 is spent amount of fuel U^{235} and m^5_0 initial amount in a fuel bundle) in units of percentage is indicated by the number on the lower line.

From the base configuration, refueling calculations were carried out by using the simulated models of the reactor core on computer screen. Exchanges of fuel bundles on the simulated models were done by clicking mouse on the **Fuel shuffle** menu. After a fuel exchange, a global reactor calculation was performed by clicking on the **Preinput** and **Estimate** menus. Calculated results are presented on computer screen. Adapted to the result of genetic algorithm optimization [11], calculations with 11 fuel exchanges compared to the base configuration were performed using the simulated model of the reactor and the results are presented in table1.

After 11 fuel exchanges, the optimal fuel pattern has k_{eff} = 1.061468 and PPF = 1.361876. This is the optimal fuel pattern found out by genetic algorithm optimization with the 11 limited numbers of fuel shuffles [11].

Because genetic algorithm is a stochastic search, it likely find out near global optimum but not exact optimum solution in almost cases. So, in this case we proposed 3 binary exchanges more in order to move towards better solution. This proposal is based on the inherent advance of the symmetry of fuel burnup distribution over the reactor core. Results are presented on the last three rows of table 1. It can be seen that the parameters of the final optimal pattern are better (with k_{eff} = 1.065086 and PPF = 1.331527). A significant decrease in PPF through the last three exchanges is due to the final fuel configuration (fig. 3) has a more symmetrical distribution of fuel burnup than the optimal genetic algorithm solution.

4. Conclusion

This is a computer code for refueling optimization based on modern methods taking advance on the development of computer science. This code runs on PCs with XP Windows. This code can apply to research reactors and helps refueling engineers to establish refueling patterns, analyze reactor core configurations directly using graphical representative of the reactor on computer screen.

REFERENCES

[1]. Bell, G. I., Glasstone, S. - Nuclear Reactor Theory. Robert E. Kreiger Publishing Co., Malabar, Florida, 1979.

[2]. Stevens, J. G., Smith, K. S., Rempe, K. R., Downar, T. J. - Optimization of Pressurized Water Reactor Shuffling by Simulated Annealing with Heuristics. Nucl. Sci. Eng., 121, 67-80, 1995.

[3]. Kropaczek, D. J., Turinsky, P. J. - In-core Nuclear Fuel Management for Pressurized Water Reactors Utilizing Simulated Annealing. Nucl. Technol., 95, 9-32, 1991.

[4]. Lee, H. C., Shim, H. J., Kim, C. H. - Parallel Computing Adaptive Simulated Annealing Scheme for Fuel Assembly Loading Pattern Optimization in PWRs. Nucl. Technol., 135, 39-50, 2001.

[5]. Yamamoto, A. - A Quantitative Comparison of Loading Pattern Optimization Methods for In-core Fuel Management of PWR. Journal of Nucl. Sci. and Technol., 34 (4), 339-347, 1997.

[6]. Do Q. B., H. Choi - A genetic algorithm to search for the optimal loading patterns of a research reactor. Trans. KNS 2005, Korea, Vol. 2, Oct. 2005.

[7]. Do Q. B., H. Choi, G. ROH - A comparative study on the refueling simulation methods for a CANDU reactor. Trans. KNS 2006, Korea, May 2006.

[8]. Do Q. B., H. Choi, G. ROH - Optimization of a refueling simulation for a CANDU reactor by using an evolutionary algorithm. Proc. ANS 2006, USA, Vol. 94, June 2006.

[9]. Do Q. B., H. Choi, G. ROH - Optimal refueling pattern search for a CANDU reactor using a genetic algorithm. Proc. ICAPP'06, USA, June 2006.

[10]. Q. B. Do, H. Choi, G. Roh - An evolutionary optimization of the refueling simulation for a CANDU reactor. IEEE TNS, USA, Vol. 53, No. 5, Oct. 2006.

[11]. Q. B. Do and P. L. Nguyen - Application of a genetic algorithm to the fuel reload optimization for a research reactor. Applied Mathematics and Computation, USA, Vol. 187, 2007, 977-988.

[12]. Do Quang Binh, Nguyen Phuoc Lan and Nguyen Van Quoc - Development of a computer code for reactor fuel reloading optimization using genetic algotirhms and related techniques. Institute Project CS/04/02-05.

[13]. Do Quang Binh, Nguyen Phuoc Lan and Bui Xuan Huy - Development of a computer code for reactor fuel reloading optimization using genetic algotirhms and simulated annealing. Institute Project CS/05/02-02.

[14]. Do Quang Binh, Nguyen Phuoc Lan and Bui Xuan Huy - Design of optimal fuel reloading patterns for a research reactor using simulated annealing method. Procs. 7th Nucl. Sci. Technol. Danang - 2007.

[15]. P.J. Turinsky, Nuclear fuel management optimization: a work in progress, Nucl. Technol. 151 (2005) 3-8.

[16]. Fowler, T. B., Vondy, D. R., Kemshell, F. B. - Nuclear Reactor Core Analysis Code: CITATION. ORNL-TM-2496, RSICC, 1971.

Table 1: K_{eff} and PPF in refueling process

No.	Fuel exchange	K_{eff}	PPF
	0	1.060453	1.374156
1	1 ↔ 50	1.060828	1.374205
2	2 ↔ 33	1.061212	1.372689
3	3 ↔ 58	1.061664	1.375163
4	4 ↔ 68	1.062037	1.374655
5	5 ↔ 34	1.062558	1.375359
6	12 ↔ 51	1.062948	1.377114
7	67 ↔ 89	1.063486	1.364327
8	44 ↔ 96	1.063994	1.363218
9	32 ↔ 97	1.064245	1.363708
10	28 ↔ 99	1.064249	1.363613
11	57 ↔ 100	1.064768	1.361876
Sum		Δρ (%) = 3.82	ΔPPF (%) = 0.01228
12	35 ↔ 99	1.064788	1.363209
13	43 ↔ 97	1.064974	1.331632
14	20 ↔ 66	1.065086	1.331527
		Δρ (%) = 0.028	ΔPPF (%) = 0.030349

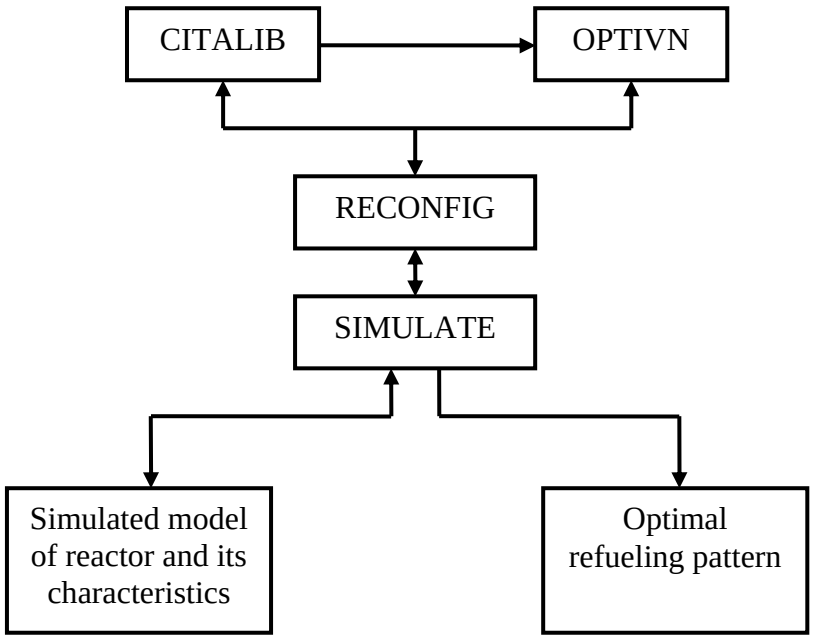

Fig. 1: Flowchart of the computer code REFUELOP

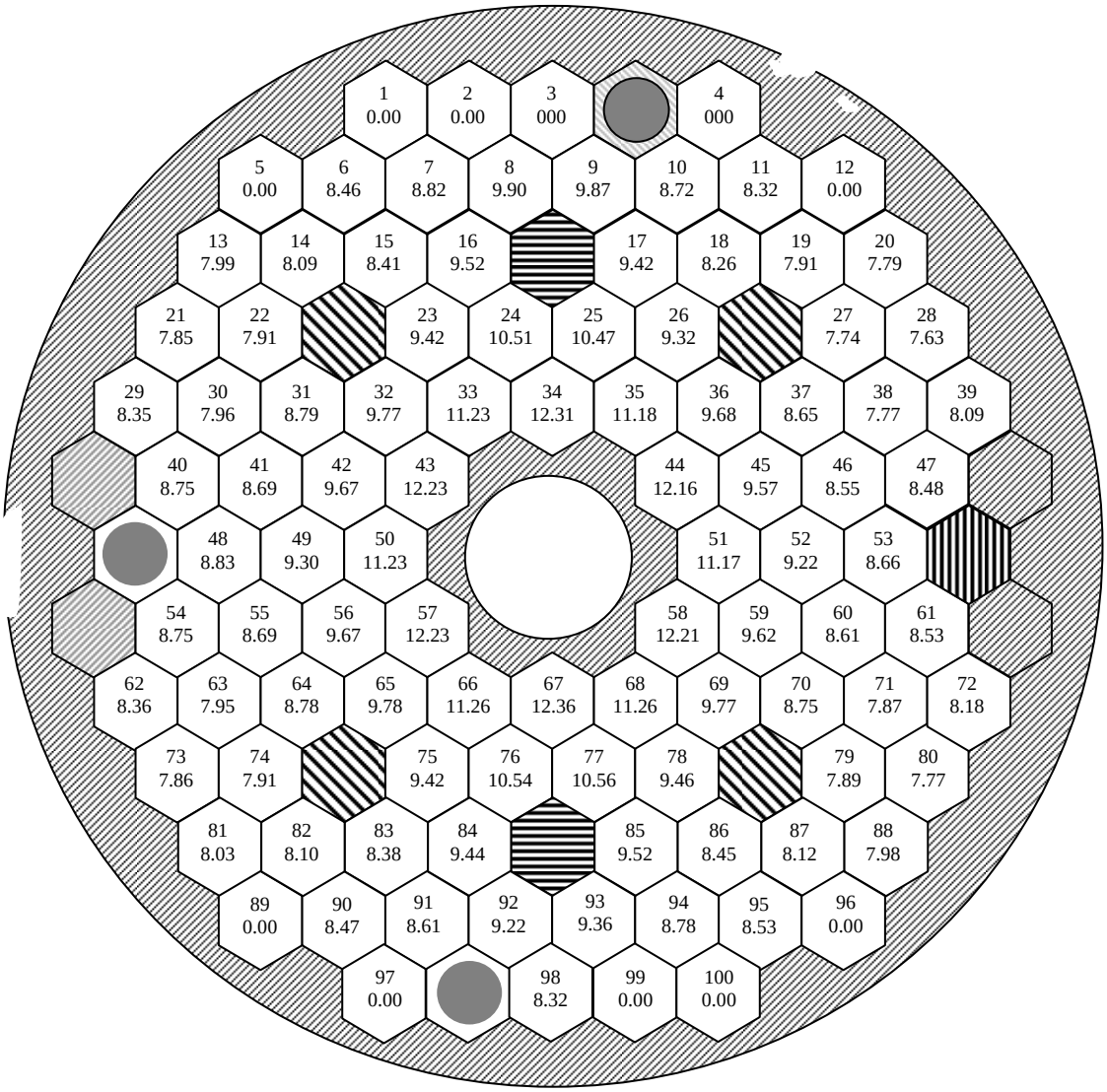

Fig. 2: Arrangement of fuel bundles in the sample problem.

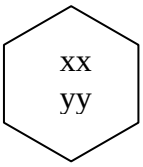

xx: Bundle index
yy: Fuel burnup in dimension %

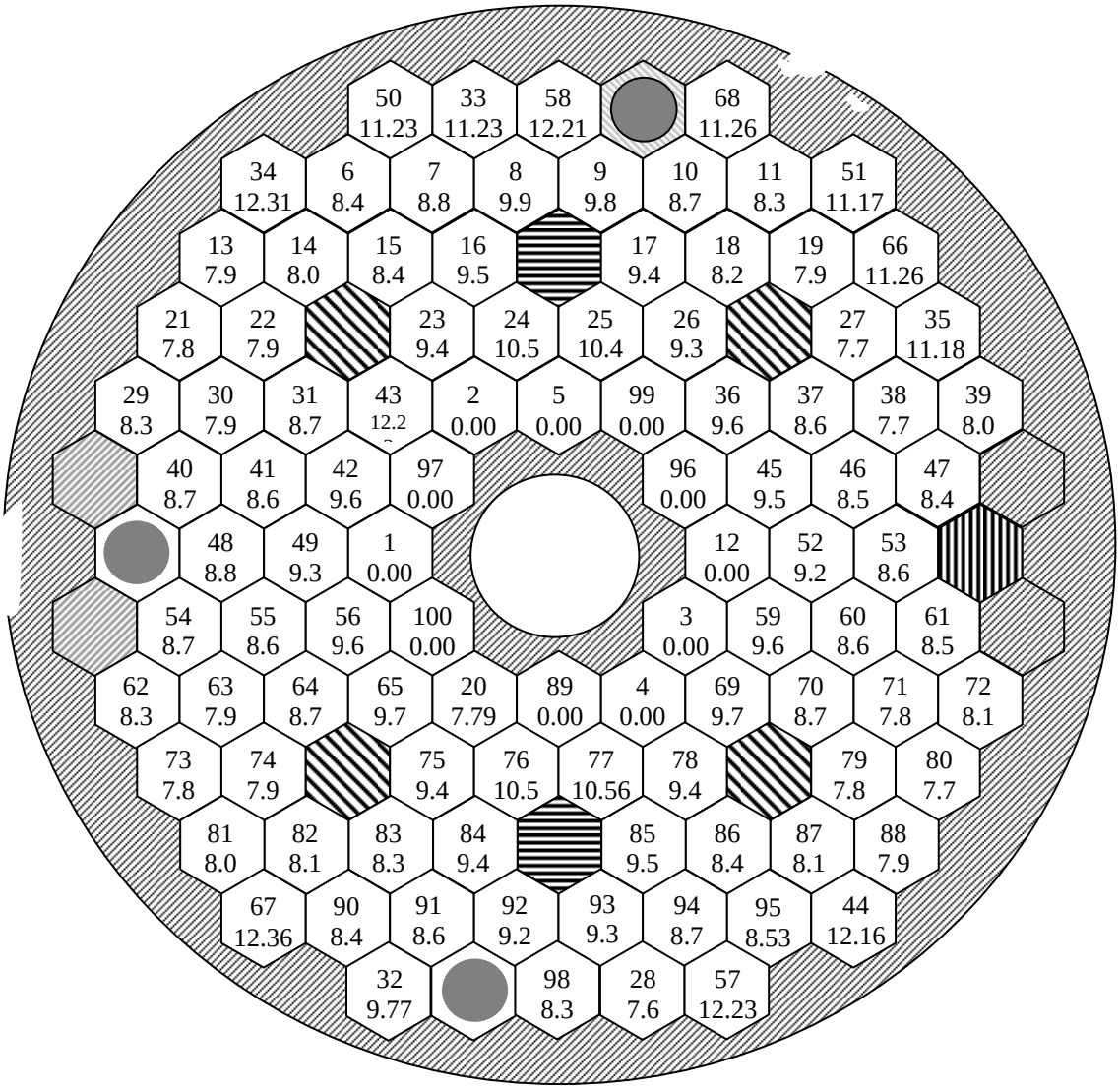

Fig. 3: Optimal refueling patterns with k_{eff} = 1.065 and PPF = 1.332.

2. TC Projects and Resaerch Contracts

2.1-LIST OF VIE Projects Implementing in 2007

	Code	Project (in English)	Project (in Vietnamese)	Counterpart	Implementing Institute	Budget (USD)
1	VIE0008	Human Resource Development and Nuclear Technology Support	Phát triển nhân lực và trợ giúp công nghệ hạt nhân	Nguyen Tien Nguyen, Tran Huu Phat	VAEC	1,202,262
2	VIE0010	Technical Support for Training in Nuclear Engineering at the Hanoi University of Technology	Hỗ trợ kỹ thuật để đào tạo kỹ sư về công nghệ hạt nhân	Phung Van Duan	Hanoi Technology Univ.	213,840
3	VIE0011	Human Resource Development and Nuclear Technology Support*	Phát triển nhân lực và trợ giúp công nghệ hạt nhân	Vuong Huu Tan	VAEC	988,620
4	VIE4014	Modification of the Dalat Reactor Control System*	Đổi mới hệ điều khiển lò PƯ Đà Lạt	Nguyen Nhi Dien	NRI	243,220
5	VIE5014	Rice Mutant Varieties for Saline Land	Tạo giống lúa cho vùng nước mặn	Nguyen Huu Dong	Agri. Ministry	731,725
6	VIE5015	Enhancement of Quality and Yield of Rice Mutants Using Nuclear and Related Techniques, Phase II*	Nâng cao năng suất và chất lượng lúa bằng kỹ thuật hạt nhân và các kỹ thuật liên quan	Le Xuan Tham	CNT	323,845
7	VIE6021	Application of Accelerator Technique for Medical Treatment	Ứng dung kỹ thuật LINAC trong điều trị bệnh	Vo Van Thuan	INST	351,660
8	VIE6023	Establishment of National Cyclotron Facilities and Centres for Medical and Research*	Xây dựng Trung tâm Pet-Cyclotron quốc gia phục vụ cho nghiên cứu và y tế	Pham Minh Bao	Health Ministry	548,661
9	VIE8014	Upgrading the Irradiation Facility at Hanoi Irradiation Centre	Nâng cấp Trung tâm Chiếu xạ Hà Nội	Ho Minh Duc	INST	34,300

10	VIE8016	Isotope and Nuclear Techniques for Better Management of Groundwater	Ứng dụng kỹ thuật hạt nhân và đồng vị trong quản lý nước ngầm	Dang Duc Nhan, Nguyen Kien Chinh	INST+CNT	283,370
11	VIE8017	Upgrading the Irradiation Facility at Hanoi Irradiation Centre*	Nâng cấp Trung tâm Chiếu xạ Hà Nội	Ho Minh Duc	Hanoi Irradiation Center	424,950
12	VIE8018	Applying Electron Beam Technology for Processing Biomaterials*	Ứng dụng công nghệ EB trong xử lý các vật liệu sinh hoc	Tran Khac An	VINAGAMMA	352,650
13	VIE9008	Establishment of a National Radiation Safety Training Centre	Xây dựng Trung tâm quốc gia Đào tạo về An toàn bức xạ	Dang Thanh Luong, Nguyen Nhi Dien	NRI	154,666
14	VIE9009	Formulation of Atomic Law	Xây dựng luật hạt nhân	Vuong Huu Tan	VAEC	88,410
15	VIE/2/008	Development of Nuclear Analytical Techniques for Application and Research Purpose	Phát triển kỹ thuật hạt nhân phục vụ mục đích nghiên cứu và ứng dụng	Nguyen Duc Thanh	CNT	380,552
16	VIE/8019	Establishment of Tracer Technique to Study Processes in the Gas Industry	Thiết lập kỹ thuật đánh dấu trong khảo sát quá trình công nghiệp khí	Nguyen Huu Quang	Center of Nucl. Tech. for Industrial Applications	123,362
17	VIE/3/005	Upgrading Capacity of Waste Processing and an Interim Storage Facility for Low and Intermediate Level Radioactive Waste	Nâng cấp cơ sở lưu giữ tạm thời xử lý chất thải phóng xạ có hoạt độ thấp và trung bình.	Le Ba Thuan	ITRRE	239,351
18	VIE/9/010	Strengthening the Technical Capacity of the Regulatory Body for Radiation and Nuclear Safety	Tăng cường năng lực kỹ thuật cho cơ quan quản lý nhà nước về an toàn bức xạ, hạt nhân	Ngo Dang Nhan	VARANSAC	312,588

2.2- List of RAS Projects Implementing in 2007

	Code	Project	Kind of project	Year of commencement	Implementing Institute
1.	RAS5043	Sustainable Land Use and Management Strategies for Controlling Soil Erosion and Improving Soil and Water Quality (RCA).	RCA	2007 Continuation	NISF
2.	RAS5045	Improvement of Crop Quality and Stress Tolerance in for sustainable crop production using mutation Selected Crops by Mutation Techniques and Biotechnology.	RCA	2007	CNT
3.	RAS5046	Novel application of Food Irradiation Technology for Improving Socia-Economic Development.	RCA	2007	VINAGAMMA
4.	RAS6040	Improvement in QA for Brachytherapy of Frequent Cancers in the Region.	RCA	2007 Continuation	NCI
5.	RAS6041	Prevention of Osteoporosis and Promotion of Bone Mass in Asian Populations using a Food-based Approach.	RCA	2007 Continuation	NIN
6.	RAS6042	Tumor Imaging Using Radioisotopes.	RCA	2007 Continuation	Tran Hung Dao Hospital
7.	RAS6038	Strengthening Medical Physics through Education and Training Phase II.	RCA	2007 Extention	Bach mai Hospital
8.	RAS6029	Upgrading Nuclear Medicine Technologist Training.	RCA	2007 Extention	HMU
9.	RAS6049	Upgrading of Sustainability of PET technology in RCA Member States.	RCA	2007	Tran Hung Dao Hospital
10.	RAS6048	Application of 3D conformal radiotherapy for predominant cancers in the RCA region.	RCA	2007	NCI
11.	RAS7015	Characterization and source identification of Air Particulate Pollution in the Asian Region.	RCA	2007	INST

12.	RAS8104	Assessment of trends in freshwater quality using environmental isotopes and chemical techniques for improved resource management.	RCA	2007	CNT
13.	RAS7016	Establishment of a benchmark for assessing the radiological impact of nuclear power activities on the marine environment in the Asia-Pacific region.	RCA	2007	NRI
14.	RAS8105	Improvement of production quality and safety in steel, petrochemical and civil industries using Advanced Industrial Radiography and Tomography Techniques.	RCA	2007	NEAD
15.	RAS8106	Consolidation of Radiation Processing Applications for Health and Environment.	RCA	2007	INST
16.	RAS8107	Intensification of Productivity in Coal, Minerals and Petrochemical Industries using Nucleonic Analysis Systems (NAS) and Radiotracers.	RCA	2007	Center of Nucl. Tech. for Industrial Applications
17.	RAS0045	Evaluation of Sustainable Energy Development Strategies for Addressing Climate Change Issue.	RCA	2007	VAEC
18.	RAS4026	Increasing material value by neutron irradiation.	RCA	2007	NRI
19.	RAS9042	Sustainability of Regional Radiation Protection Infrastructure.	RCA	2007	VARANSAC
20.	RAS0048	Management of TCDC.	RCA	2007	VAEC
21.	RAS/6/034	Quality Assurance Programme for Molecular-Based Diagnosis of Infectious Diseases.	NON-RCA	2001	NIHE
22.	RAS/7/014	Monitoring of Food Fortification Programmes Using Nuclear Techniques.	NON-RCA	2003	CRRI
23.	RAS/0/046	Support towards Self-Reliance and Sustainability of National Nuclear Institutions.	NON-RCA	2007	VAEC
24.	RAS/0/047	Supporting Web-Based Nuclear Education and Training through	NON-RCA	2007	VAEC

		Regional Networking.			
25.	RAS/2/013	Good Radiopharmacy Practice and Good Manufacturing Practice	NON-RCA	2007	NRI
26.	RAS/3/009	Strengthening Infrastructure for Radioactive Waste Management.	NON-RCA	2007	ITRRE
27.	RAS/4/028	Integrated Management Systems for Expanding Nuclear Power Programmes.	NON-RCA	2007	VAEC
28.	RAS/4/029	Strengthening Nuclear Power Infrastructure and Planning.	NON-RCA	2007	VAEC
29.	RAS/5/049	Sharing Regional Knowledge on the Use of the Sterile Insect Technique within Integrated Area-Wide Fruit Fly Pest Management Programmes.	NON-RCA	2007	FCRI
30.	RAS/6/034	Quality Assurance Programme for Molecular-Based Diagnosis of Infectious Diseases.	NON-RCA	2007	NIHE
31.	RAS/6/043	Regional Screening Network for Neonatal Hypothyroidism.	NON-RCA	2007	Nat. Hospital of Pediatics
32.	RAS/6/051	Supporting Education and Training in Medical Physics.	NON-RCA	2007	INST
33.	RAS/9/046	Strengthening Technical Capacities for Occupational Exposure Control.	NON-RCA	2007	VARANSAC
34.	RAS/9/048	Strengthening National Capabilities for Public Exposure Control.	NON-RCA	2007	VARANSAC
35.	RAS/9/049	Establishment of National Capabilities for Response to Radiological and Nuclear Emergencies.	NON-RCA	2007	VARANSAC
36.	RAS/9/050	Education and Training in Support of Radiation Protection Infrastructure.	NON-RCA	2007	INST
37.	RAS/9/051	Awereness Raifsing and training for Nuclear Security.	NON-RCA	2007	VARANSAC, VAEC

2.3- International Research Contracts in 2007

TT	Code	RC tittle	Year	Start date	End dade	Budget	Chief Investigator	Institutions
1.	12331/R4/RB	Estimation of soil erosion and redistribution on the cofee and tea crop land using 137Cs, 210Pb and 7Be tracer	2007	15/2/2007	14/2/2008	6700	Phan Son Hai	NRI
2.	12951/R2/RB	Tracers in hight temperature and fractured basement rock reservoir	2007	1/12/2006	30/11/2007	4000	Nguyen Huu Quang	CANTI
3.	12951/R2/RB	Interaction between water from Red River and groundwater in catchment of the rever.	2007	1/12/2006	30/11/2007	4500	Bui Hoc	Hanoi University of Mining and Geology
4.	12959/R2/RB	Devlopment of an intergrated computer code for in-core fuel management based on modern methods	2007	1/12/2006	30/11/2007	4500	Do Quang Binh	NRI
5.	13013/R2/RB	Determination of genetic diversity in Vietnamese indigenous goat breed based on molecular marker	2007	15/12/2006	14/12/2007	8000	Le Thi Thuy	National Inst. of Animal Husbandry
6.	13003/R2/RB	Validation and pyramiding of drought resistants/genes	2007	1/12/2006	30/11/2007	8400	Nguyen Thanh D.	Inst of Biology

7.	13027/R2/RB	Development of rearing techniques for Bactrocera pyrifoliae in Vietnam	2007	15/10/2006	14/10/2007	5000	Le Duc Khanh	Plant Protection Research Insitute (PPRI)
8.	13429/R0/RB	Comparision of the various calibration methods of diagnostic kVp meters	2007	1/12/2006	30/11/2007	4500	Tran Ngoc Toan	INST
9.	13850/R0/RB	Assessment of Source and Release to the Environment for Research Reactor	2007	15/4/2007	15/4/2008	2300	Luong Ba Vien	NRI
10.	14077/R0/RB	Role of ECG-gated Tc-99m MIBI SPECT imaging in evaluation of asymptomatic diabete patients	2007	15/12/2006	14/12/2007	5000	Le Ngoc Ha	108 Hospital
11.	14/78/R0/RB	Value ofECG-gated TC-99m MIBI SPECT imaging in patients with acute chest pain	2007	15/12/2006	14/12/2007	5000	Vu Dien Bien	108 Hospital
12.	14074/R0/RB	Using radiation-induced mutation to obtain superior rice varieties that enhance nutrient use efficiency	2007	1/12/2006	30/11/2007	5000	Le Van Nha	Agricutural Genetics Institute
13.	14085/R0	Application and evaluation of real time PCR in diagnosis on avian influenza	2007	15/12/2006	14/12/2007	5000	Nguyen Tien Dung	Veterinary Institute

3. Scientific Parpers Published Abroad and in Vietnam

3.1- INTERNATIONAL JOURNAL

1. **VATLY Group.**

   Correlation of The Highest-Energy Cosmic Rays with Nearby Extragalactic Objects. Science 318 (2007) 938.

2. **Vatly Group.**

   Anisotropy Studies around The Galactic Center at Eve Energies with The Auger Observatory. Astropart. Phys 27 (2007) 244.

3. **VATLY Group.**

   An Upper Limit to The Photon Fraction in Cosmic Rays above 1019 Ev from The Pierre Auger Observatory. Astroparticle Physics 27 (2007) 155.

4. **D.T. Khoa, W. Von Oertzen, H.g. Bohlen and S. Ohkubo.**

   Nuclear Rainbow Scattering and Nucleus-nucleus Potential.- *Journal of Physics G*, 2007, **37**, R111 (topical Review).

5. **D.T. Khoa, H.s. Than and D.c. Cuong.**

   Folding Model Study of The Isobaric Analog Excitation: Isovector Density Dependence, Lane Potential and Nuclear Symmetry Energy.- *Physical Review*, 2007, **C76**, 014603 (15 Pages).

6. **D.E.Groh, J.s. Pinter, P.f. Mantica, T.j. Mertzimekis, A.e. Stuchbery and D.T Khoa.**

   Nuclear Spin Polarization Following Intermediate-Energy Heavy-Ion Reactions.- *Physical Review*, 2007, **C76**, 054608 (10 Pages).

7. **Tran Dai Nghiep, Khuong Thanh Tuan and Ngo Danh Du.**

   The Positron Annihilation Rates in Materials. To Be Published in International Journal of Nuclear Energy Science and Technology, Vol. 3, No. 4, 2007.

8. **Ha Van Thong, Farhang Sefidvash, Do Thi Nguyet Minh.**

   Some Advantages of Nuclear Fuel Under Spherical Form for Nuclear Power Plants. International Journal of Nuclear Energy Science and Technology (IJNEST), Vol. 3, No. 4, (2007**).**

9. **V.T.Bac and P.D.Hien.**

   Urban and Rural Sources of PM_{10} in The Red River Delta, Northern Vietnam. *Atmospheric Environment Journal* in March 2007, Revised in August 2007.

10. **Norrman, J., Sparrenpom, S. J., Rosqvist, H., Gunnar, J., P. Q. Nhan, Berg, M., D. D. Nhan, E. Sigvardson, Baric, D., and Moreskog.**

    Arsenic Mobilisation in A New Well-Field along The Red River, Nam Du, Hanoi. *Appl. Hydrogeol*., 58: 129-138, 2007.

11. **Tateda, Y., D. D. Nhan.**

    Carbon Sequestration for The Mitigation of The Global Warming Effect by Mangrove Planting along The Coastal Zone of South-East Asian Countries. *The Ecology*, 72:417-434, 2007 (Japanese).

12 **Tran Huu Phat, Nguyen Tuan Anh, Nguyen Van Long and Le Viet Hoa.**

Phase Transition of Nuclear Amtter Beyond Mean Field Theorym Phys.Rev. C 76, 045202 (2007).

13 **Tran Huu Phat, Le Viet Hoa, Nguyen Tuan Anh and Nguyen Van Long.**

High Temperature Symmetry Nonrestoration and Inverse Symmetry Breaking in The Cornwall-Jackiw-Tomboulis Formalism, Phys.Rev. D 76, 125027 (2007).

14 **Tran Huu Phat, Nguyen Tuan Anh and Nguyen Van Long.**

Determination of Nuclear Symmetry Energy Beyond Mean Field Theory, Submitted To Phys.Rev. C.

3.2 - DOMESTIC JOURNAL

1. **Le Hong Minh, Tran Tu Hieu, Nguyen Viet Thuc.**

Determination of Trace of Some Heavy Metals in Shell Fishes in West Lake Using ICP-MS Method. Journal of Science and Technology, Vol. 45, No. 1B, 2007.

2. **Nguyen Xuan Chien, Huynh Van Trung, Tran Kim Hung.**

Determination of Rare Earth Elements in Tea, Soybean, Vegetables and Environmental Samples by Using ICP-MS. Journal of Chemical, Physical and Biological Analysis (Accepted).

3. **Le Ba Thuan, Luu Xuan Dinh, Nguyen Trong Hung.**

Synthesis of Cerium Dioxide in Nano Dimension from Cerium Carbonate. Journal of Chemical, Physical and Boilogical Analysis, Vol. 12, No.4, Page: 47-51 (2007).

4. **Le Ba Thuan, Luu Xuan Dinh.**

Synthesis of Cerium Dioxide in Nano Dimension by Decomposition Reaction of Cerium Hydroxide Carbonate Journal of Chemical, Physical and Biological Analysis, Vol. 12, No.3, Page: 48-53 (2007).

5. **Cao Hung Thai, Than Van Lien, Bui Dang Hanh, Le Kim Dung, Dinh Manh Thang.**

Study on Treatment of Radioactive Waste after Leaching Process by Sulfuric Acid. Journal of Chemistry, Vol.45, 1/2007, Page. 1-4.

6. **Cao Hung Thai.**

Study on Determination of Impurities: Cr, V, Ta, Nb, Th, U in Products of Artificial Rutile Production Process from Vietnamese Ilmenite Ore. Journal of Chemistry (Accepted).

7. **Tran Danh Tuan, Cao Hung Thai, Dang Van Duong.**

Statistical Model for Description of Fe Dissolution in Reprocessing Non-Weathered Uranium Ore. Journal of Science and Technique, Military Technique Academy, No 119, Page 19-24.

8. **Cao Hung Thai, Than Van Lien, Bui Dang Hanh, Le Thi Kim Dung.**

Study on Treatment of Solid Waste after Technical Uranium Precipitation. Journal of Mining Technology. 21st Year, No 4/2007.

9. **Ngo Sy Luong, Nguyen Hung Huy, Hoang Nhuan.**

Synthesis and Study Some Iridium (III) β-Dixetonate Complexes. Journal of Chemical, Physical and Biological Analysis, No 10/2007.

10. **Le Minh Tuan, et al.**

Synthesis and Study Complexes of Some Rare Earth Elements (Pr, Nd, Eu and Gd) with L-Isoleusin, Journal of Chemistry (Accepted).

11. **Le Minh Tuan, Nguyen Trong Uyen.**

Synthesis and Study Complexes of Prazeodim and Leusin, Journal of Chemistry Vol.45, Page 315-318, 2007.

12. **Vu Thanh Quang, Pham Quang Minh, Cao Dinh Thanh, Vu Thanh Tuan, Nguyen Duc Tuan, Nguyen Xuan Phuc.**

Determination of Kinetic Functionof Stirring Leaching Process of Non-Weathered Uranium Ore. Journal of Science and Technology, Vol. 45, No. 1B, 2007.

13. **Nguyen Trong Hung, Le Ba Thuan, Tran Ngoc Ha, Le Thi Bang, Nguyen Thi Thanh Thuy (2007).**

Summary of Study on Refining Uranium of Nuclear Grade by Liquid-Liquid Extraction Technique Using TBP Extractant, Nuclear Science and Technology, Vol.5, No.1, (2007) PP.33-45.

14. **Vuong Thu Bac, A. Mihara, O. Maita.**

Determining Tritium Concentration in The Atmosphere Using HTO/HT Discriminating Air Sampler. *Nuclear Science and Technology*. V.5, N.1, P. 52-56 (2007).

15. **P.N.Diep et al.**

Research at VATLY: Main Themes and Recent Results. To Appear in Proc. INSPUN07, Vietnam, 2007.

16. **Pham Quy Nhan, Nguyen Van Hoan, etc.**

Discussion on Sucking Water Sample from Endosmose Water Stratum. *Journal of Mining and Geology Science, No* 20, 10/2007, Page 54-60. Hanoi.

17. **Tran Dai Nghiep, Nguyen Thanh Cong, Le Van Minh, Tran Manh Toan, Nguyen Thi Cam Ha and Nguyen Thi Ha Thu.**

Differential Incoherent Scattering Cross Sections for Bound Electrons at 662 Kev Gamma Rays in Some Metals. *Nuclear Science and Technology,* ISSN 1810-5408, Vol. 5, No. 1, 2007, PP. 21-26.

18. **Le Van Ngoc, Nguyen Thi Thanh Huyen, Nguyen Hao Quang.**

Study on Monte Carlo Calculation of Peak Efficiencies of The Super Pure HpGe Detector (GMS) in Environmental Spectrometry with Using MCNP4C2. Science Journal, VNU, Hanoi, Vol 23, No 2, 2007.

19. **Mai Van Nhon, Le Van Ngoc, Truong Hong Loan et al.**

    Spectrum Simulation and True Coincidence Factor Calculation with Using MCNP Code. Journal of Communication in Physics (Vietnam), Vol 17, No 2, 2007.

20. **P.N.Diep et al.**

    Extensive Air Shower in Hanoi. Submitted to Com. Phys. Vietnam (2007).

21. **Bui Duy Du, Dang Van Phu, Nguyen Trieu, Nguyen Quoc Hien.**

    Study on Production of Nano Silver by Using Irradiation Method. Journal of Chemistry and Application. No 3 (63) Pager. 40-43, 2007.

3.3 - OVERSEA WORSHOP

1. **Le Ba Thuan, Luu Xuan Dinh.**

   Study on Preparation of Cerium Oxide Nanoparticle from Cerium Carbonate, Proceeding of The 2nd Korea-Vietnam Joint Symposium on Rare Earths Development and Application, April 3-6, 2007 Gyeongju Commodore Hotel, Korea, P.22-28.

2. **Le Ba Thuan, Le Thi Bang, Luu Xuan Dinh, Nguyen Trong Hung, Doan Thi Mo, Nguyen Duy Phap.**

   Removal Arsenics from Water Using Rare Earths Based Materials, Proceeding of The 2nd Korea- Vietnam Joint Symposium on Rare Earths Development and Application, April 3-6, 2007 Gyeongju Commodore Hotel, Korea P.49.

3. **Nguyen Van Hai, Le Ba Thuan, Pham Duc Roan, Nguyen Duc Vuong, Tran Ngoc Ha.**

   Features of Extraction Chemistry of Rare Earths Gd, Sm, Dy, Y with Extractant PC88A, Proceeding of The 2nd Korea-Vietnam Joint Symposium on Rare Earths Development and Application, April 3-6, 2007 Gyeongju Commodore Hotel, Korea, P.65.

4. **Nguyen Van Hai, Le Ba Thuan, Pham Duc Roan, Nguyen Duc Vuong, Tran Ngoc Ha.**

   The Parameters of Solvent Extraction Process on The Base of Neutral Networks Approach, Proceeding of The 2nd Korea-Vietnam Joint Symposium on Rare Earths Development and Application, April 3-6, 2007 Gyeongju Commodore Hotel, Korea, P. 80.

5. **Nguyen Xuan Chien, Le Hong Minh, Le Ba Thuan.**

   The Determination of Rare Earth Elements in Environmental Samples by ICP-MS, Proceeding of The 2nd Korea-Vietnam Joint Symposium on Rare Earths Development and Application, April 3-6, 2007 Gyeongju Commodore Hotel, Korea, P. 86.

6. **Le Ba Thuan, Nguyen Duc Vuong, Luu Xuan Dinh, Nguyen Trong Hung.**

   Study on Preparation of Light-convertible Polyethylene Film Containing Europium Coordination Compound, Proceeding of The 2nd Korea-Vietnam Joint Symposium on Rare Earths Development and Application, April 3-6, 2007 Gyeongju Commodore Hotel, Korea, P.106.

7. **Ludwig, R.,Nguyen, T.K.D., Traving,M.,Baecker,W.,Gutknecht,W.**

A Calixarence-Based Ion Exchanger in Solvent Extraction Processes, CIGP'07, Benjaia, Algeria.

8. **Nguyen,T.K.D., Ludwig.R.**

"Kinetics of Interfacial Transport during Solvent Extraction: Experiment with Cr(VI), Mo(VI), Ag(I) and Modeling With FDM", Une Conference Internationale Sur Le Genie Des Procedes, Oct. 28-30, 2007 Algieria

9. **Huynh Van Trung, Nguyen Xuan Chien, Le Hong Minh.**

Application of X-Ray Fluorescence Spectrometry for The Determination of Some Elements in Alloys, 12th Asian Chemical Congress, August 23 - 25, 2007.

10. **Flemming Larsen, Nguyen Van Hoan, et al.**

Geological and Hydrogeological Control on The Distribution of Arsenic in A Holocene Aquifer, Red River Plain, Vietnam. Int. Workshop on Arsenic Contamination, Manchester City, England , Nov., 2007.

11. **Pham Quy Nhan, Jenny Norrman, Nguyen Van Hoan, et al.**

Sources and Distribution of Ammonia in The Nam Du Area, Vietnam. International Workshop on The Security and Sustainability of Water Supply Systems. May, 2007, Taiwan. Page: C1-5-C1-8.

12. **Vuong Thu Bac.**

Vietnam Country Report for The IAEA/RCA/RAS/7/013 Project Final Progress Assessment and Planning Meeting. Lower Hutt, New Zealand, 26-30 March 2007.

13. **V.T.Bac and P.D.Hien.**

Urban and Rural Sources of PM10in The Red River Delta, Northern Vietnam. Symposium on Nuclear Analytical Techniques Applications in Air Pollution Studies. Quezon City, Philippines, 25 May 2007.

14. **Vuong Thu Bac.**

Vietnam Country Report for The IAEA/RCA/RAS/7/015 Project Planning Meeting. Goa, India, Goa, India, 21-24 August 2007.

15. **David Cohen, Ed Stelcer and Vuong Thu Bac.**

Quantification of Fine Particle Composition, Sources and Tran Boundary Transport in Hanoi, Vietnam from 2001-06, IUAPPA World Clean Air and Environmental. Protection Congress in Brisbane, Australia, 9-13 Sep 2007.

16. **Yoichiro Shimazu, Takashi Hirayama, Lhossine L.Erradi, Evegeny Grishanin, Farhang Seffidvash, Georgi Tsiklauri, Ha Van Thong.**

Benchmark Results of Various Particle Fuels For Small Reactors without on Site Refueling. Proceedings of Conference on Nuclear Science and Technology, 21-25/3/2007 (Morocco).

17. **Tran Khac An, Nguyen Quoc Hien.**

Radiation Processing in Vietnam, FNCA Workshop HCM City, Vietnam 22-26 Oct. 2007.

18. **Nguyen Quoc Hien et al.**

    Polymer Electrolyte for Fuel Cells, 10th Pacific Conference, Kobe, Japan, 5-8 Dec. 2007.

3.4 - DOMESTIC WORSHOP

1. **Huynh Van Trung, Nguyen Xuan Chien.**

   Skill Test, Conference of Vietnam Testing Laboratory Society Hanoi, 8-2007.

2. **Pham Quang Minh, Vu Thanh Quang, Cao Dinh Thanh, Ngo Van Tuyen.**

   Model of Percolation Leaching Process of Uranium Ore for Transferring from Laboratory Scale to Large Scale Testing Equipment . The 7th National Conference of Nuclear Science and Technology, Da Nang 30-31/8/2007.

3. **Than Van Lien, Cao Hung Thai, Tran Van Son, Nguyen Dinh Van, Doan Thi Mo, Hoang Bich Ngoc, Nguyen Hong Ha.**

   Application and Increasing Value of Bentonite in National Economy. The 7th National Conference of Nuclear Science and Technology, Da Nang 30-31/8/2007.

4. **Than Van Lien, Cao Hung Thai, Bui Van Thang, Ngo Sy Luong.**

   Study on Production of Nano Material from Domestic Natural Minerals. The 7th National Conference of Nuclear Science and Technology, Da Nang 30-31/8/2007.

5. **Than Van Lien, Do Quy Son, Le Thi Kim Dung.**

   Utilization of Bentonite in Atomic Energy Field and Results of Study on Uranium Adsorption on Vietnam Natural Bentonite. The 7th National Conference of Nuclear Science and Technology, Da Nang 30-31/8/2007.

6. **Cao Hung Thai, Than Van Lien, Tran Van Son, Nguyen Nu Hoai Vi, Le Quang Thai.**

   Study on Technology of Producing Artificial Rutile from Vietnam Ilmenite Ore. The 7th National Conference of Nuclear Science and Technology, Da Nang 30-31/8/2007.

7. **Nguyen Duy Phap, et al.**

   Results of Study on Sifting and Testing The Dac Lac Feldspar For Producing Body and Graze of Advanced Ceramic. The 7th National Conference of Nuclear Science and Technology, Da Nang 30-31/8/2007.

8. **Nguyen Ba Tien.**

   5 Year Summary of Study on Application of Rare Earth Fertilizer in Agriculture The 7th National Conference of Nuclear Science and Technology, Da Nang 30-31/8/2007.

9. **Nguyen Ba Tien.**

   Radioactive Waste Management, Status and Challenge. The 7th National Conference of Nuclear Science and Technology, Da Nang 30-31/8/2007.

10. **Nguyen Minh Thu, Nguyen Thi Phuong Nam, et al.**

    Study on Absorption Ability of Some Heavy Metal Ions (Ni, Cu, Zn, etc.) on Soft

Polymer Synthesized in Center for Purification Technology, ITRRE The 7th National Conference of Nuclear Science and Technology, Da Nang 30-31/8/2007.

11. **Nguyen Trong Hung, Le Ba Thuan, Tran Ngoc Ha, Vu Dang Do, Le Thi Bang, Nguyen Thanh Chung, Luu Xuan Dinh, Nguyen Thi Thanh Thuy, Hoang Van Duc.**

    Study on Influence of Precipitated Salt and Impurities on Uranium Extraction by TBP. The 7th National Conference of Nuclear Science and Technology, Da Nang 30-31/8/2007.

12. **Nguyen Van Sinh.**

    Study on Technology for Preparation of $ZrCl_4$ by Chlorination ZrO_2 in Laboratory Scale. The 7th National Conference of Nuclear Science and Technology, Da Nang 30-31/8/2007.

13. **Dang Ngoc Thang, Pham Danh Khanh, Ha Dinh Khai, Nguyen Van Doan.**

    Precipitation of Amoni Diuranate from UO_2F_2 Solution for UO_2 Fuel Ceramic Production. The 7th National Conference of Nuclear Science and Technology, Da Nang 30-31/8/2007.

14. **Le Minh Tuan, Pham Quang Trung, Pham Minh Tuan, Tuong Duy Nhan, Tran The Dinh.**

    Study on Technology of Preparing Active Zno 35% as Rubber Activators. The 7th National Conference of Nuclear Science and Technology, Da Nang 30-31/8/2007.

15. **Nguyen Trung Son, et al.**

    Study on Application of Barite Mineral for Producing Roughen Radiation Protection Material. The 18th National Conference of Mining Science and Technique, 2007.

16. **Huynh Van Trung, Nguyen Xuan Chien.**

    Certified Reference Materials and Stand Ardization Process. Conference of Vietnam Testing Laboratories Hanoi 8-2007.

17. **Le Thi Dinh, et al.**

    Study on Quarantine of Poisoned Flour Rye Grass Lolium L. In Some Imported Agricultural Products by Using Gamma Irradiation Method. The 7th National Conference of Nuclear Science and Technology, Da Nang 30-31/8/2007.

18. **Le Thi Dinh, et al.**

    Establishment of Gamma Irradiation Procedure for Quarantine of Poisoned Flour Rye Grass Lolium Temulentum L**.** Containing in Imported Wheat. The 7th National Conference of Nuclear Science and Technology, Da Nang 30-31/8/2007.

19. **Vuong Thu Bac.**

    Technical Support for The Governmental Management Activities on Atomic Energy, Radiation Protection, Nuclear Safety, Preparedness and Monitoring of Environmental Radioactivity. *Vietnam-French Workshop on Towards to The First Nuclear Power Plant in Vietnam. Ha Noi* 10/ 7/2007.

20. **Vuong Thu Bac.**

    Pollution of Respiration Dust in Super Fine Dimension. The Vietnam Society of Science and Technique on Labor Safety and Hygiene. Ha Noi, 16/8/2007.

21. **Bui Hoc, Dang Duc Nhan, and Nguyen Chi Nghia.**

    Preliminary Results of The Estimation for The Base Flow in The Red River Plain Using Isotopes Techniques. Proc. of The National Workshop on Geocology and Environmental Technology. Ministry of Education and Training and Hanoi Univ. of Mining and Geology. Ha Noi, Oct 25-27, 2007. PP. 35-43.

22. **Dang Duc Nhan, Dang Anh Minh, Nguyen Van Hoan, Nguyen Thi Hong Thinh, Dinh Thi Bich Lieu, Vo Thi Anh, Ha Thi Lan Anh.**

    Mobilization of Arsenic in Groundwater in The Southern Hanoi City as Studied by Isotopic and Related Techniques. The 7th National Conference of Nuclear Science and Technology, Da Nang 30-31/8/2007.

23. **Tran Thu Ha.**

    Study on Application of New Technology Solution for Treatment of Low Level Radioactive Waste in Vietnam. The 7th National Conference of Nuclear Science and Technology, Da Nang 30-31/8/2007.

24. **Nguyen Quang Long.**

    Analytical Procedure Po-210 in Water and Urine Samples, Results Obtained from The International Comparison Series (PT) IAEA-CU-2007-09". The 7th National Conference of Nuclear Science and Technology, Da Nang 30-31/8/2007.

25. **Nguyen Quang Long.**

    Result of Global Examination on Ability of Determining Gamma-Radiated Radioactive Nuclei IAEA-CU-2006-03. The 7th National Conference of Nuclear Science and Technology, Da Nang 30-31/8/2007.

26. **Nguyen Thanh Cong, Tran Dai Nghiep.**

    Study on In-Coherent Gamma Scattering in Materials with Different Atomic Number Z. The 7th National Conference of Nuclear Science and Technology, Da Nang 30-31/8/2007.

27. **Tran Huu Phat, Nguyen Tuan Anh, Nguyen Van Long, Le Viet Hoa.**

    On The Phase Transition in Stable Quark Model. The 7th National Conference of Nuclear Science and Technology, Da Nang 30-31/8/2007.

28. **Hoang Sy Than, Do Cong Cuong, Dao Tien Khoa.**

    Microcosmic Study of The Isobaric Analog Excitations and Its Astrophysical Implication. The 7th National Conference of Nuclear Science and Technology, Da Nang 30-31/8/2007.

29. **Vuong Huu Tan, Tran Tuan Anh, Nguyen Canh Hai, Pham Ngoc Son, Tokyo Fukahori.**

    Measurement of Neutron Captures Cross Sections of ^{139}La, ^{152}Sm and ^{191,193}Ir at 54 Kev and 148.3 Kev. The 7th National Conference of Nuclear Science and Technology, Da Nang 30-31/8/2007.

30. **Vuong Huu Tan, Pham Ngoc Son, Tran Tuan Anh, Nguyen Canh Hai, Trinh Tu Anh, Mai Xuan Trung.**

    Analysis of Correction Factors in Measurement of Neutron Radiative Capture Cross Sections on Filtered Neutron Beam. The 7th National Conference of Nuclear Science and Technology, Da Nang 30-31/8/2007.

31. **Vuong Huu Tan, Pham Dinh Khang, Nguyen Xuan Hai.**

    Exploitation of Gamma Two-Step Cascade of ^{153}Sm and ^{172}Yb in Reaction with Thermal Neutron. The 7th National Conference of Nuclear Science and Technology, Da Nang 30-31/8/2007.

32. **Ngo Quang Huy, Vo Xuan An, Do Quang Binh.**

    Investigation into The Impact of Detector Parameters on Its Efficiency for The HpGe Using The MCNP4C2 Code. The 7th National Conference of Nuclear Science and Technology, Da Nang 30-31/8/2007.

33. **Tran Quoc Dung, Nguyen Duc Thanh, Luu Anh Tuyen, Lo Thai Son, Nguyen Canh Hai, Ngo Minh Triet.**

    Experimental Evaluation of Systematic Errors of Gamma Technique for Assay of Radioactive Waste Drums. The 7th National Conference of Nuclear Science and Technology, Da Nang 30-31/8/2007.

34. **Tran Khac An, Cao Van Chung, Tran Van Hung.**

    Determination of The Minimum Dose' Position in The Tote Box with Various Densities of Product by Using MCNP4C Code for Operation of STSV-Co60/B Irradiators at The Center for Research and Development of Radiation Technology. The 7th National Conference of Nuclear Science and Technology, Da Nang 30-31/8/2007.

35. **Nguyen Van Hung.**

    Training and Development of Nuclear Manpower in 2005-2007 at Training Center, Nuclear Research Institute. The 7th National Conference of Nuclear Science and Technology, Da Nang 30-31/8/2007.

36. **Do Quang Binh, Nguyen Phuoc Lan, Bui Xuan Huy.**

    Design of Optimal Fuel Reloading Partners for Research Reactor Using Simulated Annealing Method The 7th National Conference of Nuclear Science and Technology, Da Nang 30-31/8/2007.

37. **Nguyen Minh Tuan.**

    Analysis of Physical Experiments Being Based for Modifying Sub Cooled Flow Boiling Models in TRAC-BF1Code in order to Predict Void-Fraction in Transient Boiling Experiments Simulating BWR RIA Condition. The 7th National Conference of Nuclear Science and Technology, Da Nang 30-31/8/2007.

38. **Pham Van Lam, Le Vinh Vinh, Huynh Ton Nghiem, Nguyen Kien Cuong, Luong Ba Vien, Nguyen Manh Hung, Nguyen Minh Tuan, Trang Cao Su, Pham Quang Huy, Pham Hong Son, Tran Quoc Duong, Le Quang Trung, Vo Doan Hai Dang.**

Study of Core Conversion to A Mixed Core of Heu and Leu for The Dalat Nuclear Research Reactor. The 7th National Conference of Nuclear Science and Technology, Da Nang 30-31/8/2007.

39. **Le Dai Dien.**

Investigation of The Buckling-Reactivity Conversion Coefficient Using SRAC and MVP Code for UO_2 Lattice in TCA Experiments**.** The 7th National Conference of Nuclear Science and Technology, Da Nang 30-31/8/2007.

40. **Tran Quoc Duong, Eric Dumonteil, Jean Michel Do, Yi-Kang Lee, Huynh Tan Dat.**

Modeling and Neutron Calculation of VVR-M2 Fuel Assembly and Dalat Nuclear Research Reactor (DNRR) with Tripoli4 Monte Carlo Code and Apollo2 Assembly Code. The 7th National Conference of Nuclear Science and Technology, Da Nang 30-31/8/2007.

41. **Ha Van Thong, Do Thi Nguyet Minh.**

Lengthening of Fuel Cycles by Operation without Burn-Up Poison for The Fixed Bed Nuclear Reactor. The 7th National Conference of Nuclear Science and Technology, Da Nang 30-31/8/2007.

42. **Nguyen Kien Cuong, M. Q. Huda.**

Benchmark Analysis of The High Temperature Gas Cooled Reactors Using Monte Carlo Technique. The 7th National Conference of Nuclear Science and Technology, Da Nang 30-31/8/2007.

43. **Ha Van Thong, Do Thi Nguyet Minh.**

Some Advantages of Nuclear Fuel under Spherical Form for Nuclear Power Plant. The 7th National Conference of Nuclear Science and Technology, Da Nang 30-31/8/2007.

44. **Do Cong Cuong, Dao Tien Khoa, Nguyen Ngoc Quynh.**

Complex Nucleon-Nucleon Interaction from Brueckner Hartree–Fock Calculation. The 7th National Conference of Nuclear Science and Technology, Da Nang 30-31/8/2007.

45. **Vuong Huu Tan, Pham Ngoc Son, Tran Tuan Anh, Ho Huu Thang, Nguyen Canh Hai.**

Calculation of Specific Parameters for Development of New Filtered Neutron Beams at Dalat Reactor. The 7th National Conference of Nuclear Science and Technology, Da Nang 30-31/8/2007.

46. **Nguyen Canh Hai, Ho Huu Thang, Nguyen Thi Thuy Nham.**

Accessing of Nuclear Data from Nuclear Data Bank The 7th National Conference of Nuclear Science and Technology, Da Nang 30-31/8/2007.

47. **Luu Anh Tuan, Tran Van Hien, Trinh Cuong, Hoang Duc Huynh.**

Investigation of The Maximal Values of The Fuel Surface Temperatures in The Active Zone of The Dalat Research Reactor for Operating Core Configuration of 89 Fuels Assembles and Fundamental Core Configuration of 94 Fuels Assembles

at Limited Power Level of 550kw. The 7th National Conference of Nuclear Science and Technology, Da Nang 30-31/8/2007.

48. **Luong Ba Vien, Le Vinh Vinh, Huynh Ton Nghiem, Nguyen Kien Cuong.**

Calculation of Photon Dose for The Dalat Research Reactor in Case of Loss of Reactor Tank Water. The 7th National Conference of Nuclear Science and Technology, Da Nang 30-31/8/2007.

49. **Vo Xuan An, Ngo Quang Huy, Do Quang Binh.**

Estimation of Decrease in Efficiency of The High Purity Germanium Detector after A Long Time Operation The 7th National Conference of Nuclear Science and Technology, Da Nang 30-31/8/2007.

50. **Nguyen Thi Thuy Nham, Pham Dinh Khang, Nguyen Xuan Hai, Ho Huu Thang, Pham Ngoc Son.**

Some Matters of Nuclear Level Density for ^{36}Cl. The 7th National Conference of Nuclear Science and Technology, Da Nang 30-31/8/2007.

51. **Nguyen Xuan Hai, Pham Dinh Khang, Pham Ngoc Tuan, Nguyen Duc Tuan, Vu Xuan Cach, Nguyen Thi Thuy Nham, Ho Huu Thang, Pham Duy Tung.**

Development of An Interface Card for Data Acquisition System for Two-Step Cascade Method. The 7th National Conference of Nuclear Science and Technology, Da Nang 30-31/8/2007.

52. **Do Thi Nguyet Minh, Tran Dai Nghiep, Ha Van Thong, Dao Duy Dung, Le Van Minh.**

The Energy Amplifier System. The 7th National Conference of Nuclear Science and Technology, Da Nang 30-31/8/2007.

53. **Nguyen Dinh Lam, Nguyen Kien Cuong, Nguyen Tan Man.**

Research on MCNP4C2 Code for Calculation of Gamma Dose Distribution for Dalat ^{60}Co Unit. The 7th National Conference of Nuclear Science and Technology, Da Nang 30-31/8/2007.

54. **Hoang Hoa Mai, Le Van Ngoc, Nguyen Dinh Duong.**

Investigation of Gamma Dose Field of Irradiation Facility at Hanoi Irradiation Center Using MCNP Code and Monte Carlo Method. The 7th National Conference of Nuclear Science and Technology, Da Nang 30-31/8/2007.

55. **Tran Quoc Dung, Bui Xuan Huy, Lo Thai Son.**

Simulation of Assay of Radwaste Drums by 3DSMAX Software. The 7th National Conference of Nuclear Science and Technology, Da Nang 30-31/8/2007.

56. **Nguyen Ngoc Duy, Vuong Huu Tan, Nguyen Nhi Dien, Pham Dinh Khang, Nguyen Xuan Hai, Ho Huu Thang, Nguyen Thi Thuy Nha.**

Study on Reaction of Two-Step Cascade Gamma Ray From ^{27}Al(n,2g) ^{28}Al with Thermal Neutron. The 7th National Conference of Nuclear Science and Technology, Da Nang 30-31/8/2007.

57. **Nguyen Kien Chinh, Huynh Long, Le Danh Chuan, Nguyen Van Nhien, Tran Thi Bich Lien.**

    Isotope Compositions of Mekong River Flow Water in The South of Vietnam. The 7th National Conference of Nuclear Science and Technology, Da Nang 30-31/8/2007.

58. **Luu Anh Tuyen, Nguyen Duc Thanh, Tran Quoc Dung, Lo Thai Son, Bui Xuan Huy.**

    Positron Annihilation Method for Analyzing Porosity of Materials and Application Studied Results at Center for Nuclear Technique in Ho Chi Minh City. The 7th National Conference of Nuclear Science and Technology, Da Nang 30-31/8/2007.

59. **Nguyen Huu Quang, Pham Hoang Ha, Huynh Thai Kim Ngan.**

    Study on Determination of The Origins of Produced Water in Black Lion Basement Oil Reservoir. The 7th National Conference of Nuclear Science and Technology, Da Nang 30-31/8/2007.

60. **Nguyen Thanh Tuy, Tran Dai Nghiep, Vo Van Thuan, Nguyen Phuc, Dang Quang Thieu, Nguyen Tien Dung, Khuong Thanh Tuan, Vu Van Tien.**

    Design and Manufacture Edxrf for Powder Cement Analyzer. The 7th National Conference of Nuclear Science and Technology, Da Nang 30-31/8/2007.

61. **Trinh Cong Tu, Phan Son Hai.**

    Utilization of Isotopic Technique for Surveying Soil Erosion in Highlands. The 7th National Conference of Nuclear Science and Technology, Da Nang 30-31/8/2007.

62. **Bui Dac Dung.**

    Evaluating Origins and Water Seepage Rate at The Sub Dam A of The Dong Mo Reservoir Using Environmental Isotope Technique. The 7th National Conference of Nuclear Science and Technology, Da Nang 30-31/8/2007.

63. **Nguyen Van Hung, Hoang Sy Minh Phuong, Pham Xuan Hai.**

    Application of Scattering Gamma Technique Using Scintillation Detector of YAP (Ce) and Source of Am-241 in Some of Practices on Non-Destructive Testing. The 7th National Conference of Nuclear Science and Technology, Da Nang 30-31/8/2007.

64. **Doan Binh, Tran Thu Hong, Tran Khac An.**

    Study on Effects of The Gamma and Electron Beam Radiation on Physico-Chemical Characteristics of Polyvinylpirrolidone Nanogel. The 7th National Conference of Nuclear Science and Technology, Da Nang 30-31/8/2007.

65. **Hoang Hoa Mai, Noriaki Seko, Masao Tamada.**

    Development of Adsorbent by Radiation Graft Used for Selective Collecting of Metallic Ions in Environmental Water. The 7th National Conference of Nuclear Science and Technology, Da Nang 30-31/8/2007.

66. **Tran Thu Hong, Le Hai, Naotsugu Nagasawa, Akihiro Hiroki, Masao Tamada.**

Adsorption Capacities of Metal Ions onto CMC/CMCTS Blend Hydrogels. The 7th National Conference of Nuclear Science and Technology, Da Nang 30-31/8/2007.

67. **Dang Van Phu, Bui Duy Du, Nguyen Trieu, Vo Thi Kim Lang, Nguyen Quoc Hien.**

Radiation Induced Synthesis of Colloidal Silver Nanoparticles Stabilized by PVP/Chitosan. The 7th National Conference of Nuclear Science and Technology, Da Nang 30-31/8/2007.

68. **Le Hai, Le Huu Tu, Tran Thu Hong, Nguyen Tuong Ly Lan, Le Van Toan, Pham Thi Sam, Tran Thi Tam, Nguyen Duc Hieu, Le Dinh Lang, Nguyen Minh Toan, Pham Anh Tuan.**

Application of Radiation Grafted Copolymers to Enhance Oil Recovery in The White Tiger Field. The 7th National Conference of Nuclear Science and Technology, Da Nang 30-31/8/2007.

69. **Doan Thi The.**

Hydrogel Dressing Prepared from PVA/PVP/KC/CMC by Gamma Irradiation and Some Results of Pre-Clinical Trial. The 7th National Conference of Nuclear Science and Technology, Da Nang 30-31/8/2007.

70. **Nguyen Huu Quang, Trinh Van Giap.**

Overview of R&D in Application of Nuclear Techniques in The Period of 2005-2007. The 7th National Conference of Nuclear Science and Technology, Da Nang 30-31/8/2007.

71. **Tran Khac An, Nguyen Quoc Hien.**

Overview of R&D in Radiation Technology in The Period of 2005-2007. The 7th National Conference of Nuclear Science and Technology, Da Nang 30-31/8/2007.

72. **Bui Quang Tri, Nguyen Huu Quang, Dang Nguyen The Duy, Tran Tri Hai, Tran Thanh Minh.**

Investigation of Abnormal of Condensate Stabilizer in South of Con Son Gas Processing Plant by Radioisotope Technique. The 7th National Conference of Nuclear Science and Technology, Da Nang 30-31/8/2007.

73. **Tran Van Luyen, Trinh Hoai Vinh, Thai Khac Dinh.**

Distribution of Natural Radioactivity On Soil Particle Sizes. The 7th National Conference of Nuclear Science and Technology, Da Nang 30-31/8/2007.

74. **Nguyen Thanh Tuy, Luong Duc Long.**

Design and Manufacture of X-Ray Analyzer of CaO, Fe_2O_3, SiO_2, and Al_2O_3, A Investment Opportunity of Vietnam Cement Factories. The 7th National Conference of Nuclear Science and Technology, Da Nang 30-31/8/2007.

75. **Bui Duy Du, Dang Van Phu, Bui Duy Cam, Nguyen Quoc Hien.**

Study on Effect of Radiation Degradation of Water Soluble Chitosan by Gamma Co-60. The 7th National Conference of Nuclear Science and Technology, Da Nang 30-31/8/2007.

76. **Doan Binh, Tran Khac An, Pham Thi Thu Hong, Nguyen Nguyen Hy, Trinh Thuy Lieu.**

Study on Rate of The Water Attraction and Contraction of Water Super Absorbent Gel Named Gamsorb under Free-Substrate Condition. The 7th National Conference of Nuclear Science and Technology, Da Nang 30-31/8/2007.

77. **Vo Thi Kim Lang, Dang Van Phu, Nguyen Quoc Hien, Bui Duy Du.**

Inhibitory Effect of Aerobic Bacteria in Water of Flower Vase by Silver by Nanoparticle Prepared by Gamma ^{60}Co Radiation. The 7th National Conference of Nuclear Science and Technology, Da Nang 30-31/8/2007.

78. **Dang Nguyen The Duy, Nguyen Huu Quang, Nguyen Huy Thuc, To Ba Cuong.**

Determination of Ra^{226} and Rn^{222} in Aqueous Samples by Liquid Scintillation Counting. The 7th National Conference of Nuclear Science and Technology, Da Nang 30-31/8/2007.

79. **Trinh Van Giap.**

Utilization of Isotope Techniques to Determine Groundwater Origin Producing in Hanoi Area. The 7th National Conference of Nuclear Science and Technology, Da Nang 30-31/8/2007.

80. **Nguyen Quang Long, Tran Tuyet Mai.**

Results Participated on The IAEA-CU-2006-03 World Wide Open Proficiency Test on The Determination of Gamma Emitting Radionuclide. The 7th National Conference of Nuclear Science and Technology, Da Nang 30-31/8/2007.

81. **Pham Thi Kim Loan, Tran Van Luyen, Thai Khac Dinh.**

Investigation of Natural Background Radioactivity at Tan Long, Lagi, Binh Thuan Residential Area on Ilmenite Deposit Location. The 7th National Conference of Nuclear Science and Technology, Da Nang 30-31/8/2007.

82. **Le Quang Luan, Vo Thi Thu Ha, Naotsugu Nagasawa.**

Plant Growth Stimulation Activity of Radiation-Degraded Alginate Fraction. The 7th National Conference of Nuclear Science and Technology, Da Nang 30-31/8/2007.

83. **Hoang Thi My Linh, Phan Dinh Thai Son, Doan Pham Ngoc Nga, Nguyen Thi Vang, Le Xuan Tham, Lou De Filippis.**

Estimation of Genetic Changes in Rice Mutants after Gamma Irradiation Using RAPD and Micro Satellite Markers. The 7th National Conference of Nuclear Science and Technology, Da Nang 30-31/8/2007.

84. **Nguyen Thi Thu Hien, Ho Quang Cua, Le Xuan Tham.**

Ability of Developing BDS1 Rice Variety. The 7th National Conference of Nuclear Science and Technology, Da Nang 30-31/8/2007.

85. **Do Khac Thinh, Le Xuan Tham.**

Study and Application of Nuclear Technique in Agriculture and Biology in South of Vietnam in 2005-2007. The 7th National Conference of Nuclear Science and Technology, Da Nang 30-31/8/2007.

86. **Le Xuan Tham, Nguyen Giang, Nguyen Thi Dieu Hanh, Bui Quang Trung.**

Study on Selenium Accumulation in Turkey Tail Fungus (*Trametes Versicolor*) by Using Instrumental Neutron Activation Analysis. The 7th National Conference of Nuclear Science and Technology, Da Nang 30-31/8/2007.

87. **Phan Phuoc Hien, Le Xuan Tham, Ho Dang Vang, Dang Van Chung.**

Testing Results of The New Rice Lines in Winter-Spring Crops in 2006-2007. The 7th National Conference of Nuclear Science and Technology, Da Nang 30-31/8/2007.

88. **Nguyen Thi Thu, Vu Thi Bich Huong, Le Quang Huan, Duong Van Dong, Vo Thi Cam Hoa, Bui Van Cuong, Chu Van Khoa.**

Making Recombinant Monoclonal Antibody and Radiolabelling for Medical Purpose. The 7th National Conference of Nuclear Science and Technology, Da Nang 30-31/8/2007.

89. **Nguyen Manh Hung, Tran Ngoc Toan, Duong Van Vinh, Vu Manh Khoi, Nguyen Van Ngoc, Nguyen Huu Quyet, Vu Van Cam, Chu Vu Long, Dang Duc Nhan.**

QA/QC Program for X-Ray Machine Used in Medical from 2001-2004 in Northern of Vietnam. The 7th National Conference of Nuclear Science and Technology, Da Nang 30-31/8/2007.

90. **Tran Ngoc Toan, Chu Vu Long.**

Establishment of The Diagnostic Radiology Calibration at SSDL -Vietnam. The 7th National Conference of Nuclear Science and Technology, Da Nang 30-31/8/2007.

91. **Nguyen Huu Quyet.**

Advantages of C-Band and X-Band Medical Linear Accelerator. The 7th National Conference of Nuclear Science and Technology, Da Nang 30-31/8/2007.

92. **Tran Van Quy.**

Demand and Prospect of Application of Radioisotopes and Radiopharmaceur in Medicine in Vietnam. The 7th National Conference of Nuclear Science and Technology, Da Nang 30-31/8/2007.

93. **Tran Van Quy.**

Production and Application of Radioisotopes and Radiopharmaceur ^{18}F-FDG; ^{11}C; ^{67}Ga and ^{201}Tl in The World. The 7th National Conference of Nuclear Science and Technology, Da Nang 30-31/8/2007.

94. **Duong Van Dong, Pham Ngoc Dien, Bui Van Cuong, Nguyen Thi Thu, Mai Phuoc Tho, Vo Cam Hoa.**

Study on Synthesis of AMP Derivatives as Tracer with ^{153}Sm and ^{166}Ho. The 7th National Conference of Nuclear Science and Technology, Da Nang 30-31/8/2007.

95. **Dang Duc Nhan, Dang Anh Minh, Nguyen Van Hoan, Dinh Thi Bich Lieu, Nguyen Thi Hong Thinh, Vo Thi Anh, Nguyen Thi Lan Anh.**

A Possible Mechanism of The Mobilization of Arsenic in Groundwater in The South Area in Hanoi. The 7th National Conference of Nuclear Science and Technology, Da Nang 30-31/8/2007.

96. **Tran Thu Ha.**

Study on Application of A New Technology Solution for Treatment of Low-Level Solid Radioactive Waste. The 7th National Conference of Nuclear Science and Technology, Da Nang 30-31/8/2007.

97. **Truong Thi Hanh, et al.**

Preparation of Polyme Electrolyte Membranes for Application Infuel Cell by Radiation Grafting of Binary Monomer Mixtures onto Etfe Films. The 7th National Conference of Nuclear Science and Technology, Danang 30-31/8/2007.

98. **Nguyen Quoc Hien et al.**

Degradation Of-Chitosan by Combine Treatment with Hydroperoxide and Gamma Co-60 Radiation. The 7th National Conference of Nuclear Science and Technology, Da Nang 30-31/8/2007.

99. **Tran Khac An, Pham Huu Chuong, Cao Van Chung, Tran Van Hung, Nguyen Nguyen Hy, Nguyen Thi Kieu Trang, Bui Thi Nguyen Thuy, Nguyen Truong Duc Tuan.**

Study and Estimation of X-Ray Converter Using RT-Office Software. The 7th National Conference of Nuclear Science and Technology, Da Nang 30-31/8/2007.

VIỆN NĂNG LƯỢNG NGUYÊN TỬ VIỆT NAM

TUYỂN TẬP
BÁO CÁO CÁC CÔNG TRÌNH KHOA HỌC
NĂM 2007

Người chịu trách nhiệm xuất bản: **Ts. Phạm Văn Diễn**

Biên tập: **Viện Năng lượng nguyên tử Việt Nam**

Trình bày bìa: **Trịnh Đăng Hiệu**

NHÀ XUẤT BẢN KHOA HỌC VÀ KỸ THUẬT
70 Trần Hưng Đạo, Hà Nội.

In 100 cuốn, khổ 20,5 x 290 cm, tại Công ty in Ba Đình.
Số đăng ký kế hoạch xuất bản: 82-2008/CXB/143-02/KHKT, cấp ngày 14.1.2008
Quyết định xuất bản số: 322/QĐXB-NXBKHKT ngày 20.11.2008
In xong và nộp lưu chiểu tháng 12.2008.